



If you have discovered material in AURA which is unlawful e.g. breaches copyright, (either yours or that of a third party) or any other law, including but not limited to those relating to patent, trademark, confidentiality, data protection, obscenity, defamation, libel, then please read our [Takedown Policy](#) and [contact the service](#) immediately

THEORETICAL AND EMPIRICAL EVALUATION OF PHAKIC
AND PSEUDOPHAKIC ACCOMMODATION

GEORGE ANTHONY GIBSON

Doctor of Philosophy

ASTON UNIVERSITY

November 2008

This copy of the thesis has been supplied on condition that anyone who consults it is understood to recognise that its copyright rests with its author and that no quotation from the thesis and no information derived from it may be published without proper acknowledgement.

ASTON UNIVERSITY

**THEORETICAL AND EMPIRICAL EVALUATION OF PHAKIC AND
PSEUDOPHAKIC ACCOMMODATION**

GEORGE ANTHONY GIBSON

Doctor of Philosophy

November 2008

Summary

The binding theme of this thesis is the examination of both phakic and pseudophakic accommodation by means of theoretical modelling and the application of a new biometric measuring technique.

A modern schematic eye was utilised, which was derived from several studies that measured intraocular spacings and surface curvatures, by means of corrected Scheimpflug images, in a large number of subjects at several levels of accommodation. These relations were built into a schematic eye with aspheric surfaces (Norrby, 2005). Using this schematic eye, the study of accommodation with regard to vergence change with reverse ray-tracing, was possible. The same model was used to derive biometric, vergence and vergence contribution changes from each ocular interface with variation in age and accommodative stimulus.

Traditional methods of studying biometric change include considering physical movements, changes in dimension, radius or axial separation of ocular components. Considering accommodative changes in terms of the vergence contribution each interface has on outcome refractive status, provides more information on the role each component plays in the process of accommodation. In the phakic eye with a fixed axial length, all changes in ocular spacing resulted in a reduction in vergence with accommodation; the crystalline lens surface radii are solely responsible for positive accommodative vergence changes. The use of a Vergence Contribution Factor (VCF; D/mm) alludes to the ability each interface has to affect vergence change with accommodation; this is a novel method of quantifying vergence changes with accommodation.

Alteration of the model axial length allows the investigation of accommodative vergence changes with ametropia. The model confirms the hyperopic shift with age. The damping effect first described by Erickson (1984), accounts for a reduction in myopic ametropia. It also accounts for the increased dioptric output with accommodation in myopes, as the negative effects of intraocular spacings previously described, are also damped. The pseudophakic eye was also modelled using the same schematic. It confirms the focus-shift principle of accommodating intraocular lenses (AIOL), but emphasises that magnitude of accommodative output is dependant on axial length and the power of the AIOL implanted; shorter eyes with higher powered lenses produce greater accommodative outcomes.

Anterior Segment Optical Coherence Tomography (AS-OCT) was used to assess phakic accommodative changes in 30 young subjects (19.4 ± 2.0 years; range, 18 to 25 years). A new method of assessing curvature change with this technique was employed with limited success. Changes in axial accommodative spacing, however, proved to be very similar to those of the Scheimpflug-based data. A unique biphasic trend in the position of the posterior crystalline lens surface during accommodation was discovered, which has not been alluded to in the literature. All axial changes with accommodation were statistically significant ($p < 0.01$) with the exception of corneal thickness ($p = 0.81$).

A two-year follow-up study was undertaken for a cohort of subjects previously implanted with a new AIOL (LensteC *Tetraflex KH3500*). All measures of best corrected distance visual acuity (BCDVA; $+0.04 \pm 0.24$ logMAR), distance corrected near visual acuity (DCNVA; $+0.61 \pm 0.17$ logMAR) and contrast sensitivity ($+1.35 \pm 0.21$ log units) were good. The subjective accommodation response quantified with the push-up technique (1.53 ± 0.64 D) and defocus curves (0.77 ± 0.29 D) was greater than the objective stimulus response (0.21 ± 0.19 D). AS-OCT measures with accommodation stimulus revealed a small mean posterior movement of the AIOLs (0.02 ± 0.03 mm for a 4.0 D stimulus); this is contrary to proposed mechanism of the anterior focus-shift principle.

The investigations discussed explore the role of the accommodative system in terms of vergence power, and provides an empirical assessment of human phakic and pseudophakic accommodation using new techniques.

Key words: Accommodation, Optical Coherence Tomography, ray-tracing, schematic eyes, intraocular lens.

In dedication to my grandfather

George Nicholas Gibson

1916 - 2008

ACKNOWLEDGEMENTS

Firstly, I would like to thank my supervisors, Dr Leon Davies and Professor James Wolffsohn for their help and guidance over the last three years. Special thanks go to Dr Davies for not only professional and academic support, but also for his continuing friendship, advice and encouragement.

Thanks also to the Engineering and Physical Sciences Research Council (EPSRC) and Bausch and Lomb, USA, for the award of a three-year CASE scholarship to support my postgraduate studies.

I would like to extend my warmest thanks to the staff and students at Aston University for happily participating in many of my studies. I would also like to thank my postgraduate colleagues, in particular, Mr Navneet Gupta and Miss Amy Sheppard, who have helped and collaborated in a number of studies.

I would especially like express my gratitude to Dr Mark Dunne, who has sacrificed a great deal of his time to the benefit of my knowledge and understanding.

Finally, I am eternally indebted to my parents and Lisa, without whom none of this would be possible.

CONTENTS

	Page
SUMMARY	2
DEDICATION	3
ACKNOWLEDGEMENTS	4
CONTENTS	5
LIST OF TABLES	8
LIST OF FIGURES	10
CHAPTER 1 PHAKIC AND PSEUDOPHAKIC ACCOMMODATION	
1.1	General introduction. 13
1.2	Anatomical structures of ocular accommodation. 14
1.3	Theories of accommodation. 17
1.4	Accommodative biometric changes. 20
1.5	Neurophysiology of accommodation. 20
1.6	Components of accommodation. 21
1.7	Accuracy of focus. 23
1.8	Presbyopia. 24
1.9	Schematic eyes. 29
1.10	Cataract. 31
1.11	Accommodating intraocular lenses. 37
1.12	General summary. 45
1.13	Aims of the thesis. 46
CHAPTER 2 COMPONENT VERGENCE CHANGES WITH ACCOMMODATION	
2.1	Introduction. 47
2.2	Methods. 52
2.3	Results. 57
2.4	Discussion. 68
2.5	Conclusions. 71

**CHAPTER 3 AMETROPIA: VERGENCE CHANGES WITH
ACCOMMODATION**

3.1	Introduction.	74
3.2	Methods.	76
3.3	Results.	80
3.4	Discussion.	93
3.5	Conclusions.	95

**CHAPTER 4 MODELLING THE ACCOMMODATING
INTRAOCULAR LENS**

4.1	Introduction.	97
4.2	Methods.	100
4.3	Results.	104
4.4	Discussion.	110
4.5	Conclusions.	114

**CHAPTER 5 ANALYSIS OF PHAKIC ACCOMMODATION WITH
ANTERIOR SEGMENT OPTICAL COHERENCE
TOMOGRAPHY**

5.1	Introduction.	116
5.2	Methods.	121
5.3	Results.	130
5.4	Discussion.	144
5.5	Conclusions.	149

**CHAPTER 6 ACCOMMODATING INTRAOCULAR LENSES:
A 2 YEAR FOLLOW-UP**

6.1	Introduction.	151
6.2	Methods.	158
6.3	Results.	163
6.4	Discussion.	167
6.5	Conclusions.	170

CHAPTER 7 GENERAL CONCLUSIONS

7.1	General conclusions.	172
7.2	Analysis of experimental work: suggestions for improvement.	177
7.3	Concluding statement.	178

REFERENCES		179
-------------------	--	-----

APPENDICES

A1	Human Sciences Ethical Committee submission.	220
A2	Information and consent forms for experimental participants.	227
A3	Solihull NHS Ethical Committee submission.	230
A4	Solihull NHS information and consent forms.	252
A5	Individual stimulus-response curves.	257
A6	Submitted abstracts.	264
A7	Bausch & Lomb report: UV+ Tinted Intraocular Lens.	270

SUPPORTING PUBLICATIONS		341
--------------------------------	--	-----

LIST OF TABLES

Table	Page(s)
1.1 A selection of studies which have examined the amplitude of accommodation in accommodating intraocular lenses.	41-42
2.1 Formulae used to calculate the ocular component characteristics for the Dubbelman model eye.	50
2.2 Refractive indices used in the Dubbelman model eye.	50
2.3 Ocular component changes for model eyes aged 20 to 50 years in decade increments, as a function of accommodation demand.	60
2.4 Ocular component vergence changes for model eyes aged 20 to 50 years, in decade increments, as a function of accommodation demand.	61
2.5 Summary of surface radii and axial distance vergence contributions to outcome refractive status, as a function of age and accommodation.	63
2.6 Ocular component vergence contribution changes for model eyes aged 20 to 50 years in decade increments, as a function of age and accommodation.	65
3.1 Level of ametropia, normalised ametropia and refractive status (accommodation output) as a function of age, ametropia, axial length and accommodation stimulus.	82
3.2 Total vergence variations for both surface radii and axial distance changes for three levels of ametropia as a function of accommodation stimulus.	83
3.3 Component vergence change at each level of ametropia, with a 2.0 and 4.0 D accommodation stimulus.	84
3.4 Vergence contribution factors for all ocular components at each level of ametropia, at 2.0 and 4.0 D of accommodation stimulus.	89
4.1 A selection of studies which have evaluated single-piece intraocular lenses and their accommodative function using modelling techniques.	98
4.2 Refractive status (pseudophakic accommodation) with anterior IOL shift of 0.5, 1.0 and 1.5 mm; in models with three axial lengths.	105
4.3 Vergence changes for each ocular component with anterior IOL shift of 0.5, 1.0 and 1.5 mm; in models with three axial lengths.	107

4.4	Vergence Contribution Factor changes for each ocular component with anterior IOL shift of 0.5, 1.0 and 1.5 mm; in models with three axial lengths.	107
5.1	Corneal thickness, anterior chamber depth and lens thickness measures for each level of accommodation stimulus corrected for <i>Visante</i> instrument and optical distortion.	131
5.2	Corrected ocular surface apical radii and conic constants for each level of accommodation stimulus, corrected for <i>Visante</i> instrument and optical distortion.	131
5.3	Errors remaining after correction for optical distortion for crystalline lens thickness and the posterior lens surface <i>x</i> -coordinate error for a specific <i>y</i> -coordinate value; using the original and modified equations.	136
5.4a	Anterior eye axial distances and their variation with accommodation demand measured with the <i>Visante</i> , compared to the Dubbelman model eye data (<i>n</i> = 30). The ACD is the distance between the posterior corneal surface and the anterior corneal surface.	138
5.4b	Anterior eye axial distances and their variation with accommodation demand measured with the <i>Visante</i> , compared to the Dubbelman model eye data (<i>n</i> = 30). The ACD is the distance between the anterior corneal surface and the anterior corneal surface.	139
5.5	Anterior eye relative axial distance changes with accommodation demand measured with the <i>Visante</i> , compared to the Dubbelman model eye data (<i>n</i> = 30).	142
6.1	A selection of studies which have measured intraocular lens shift with either physiological or pharmacological stimulation of accommodation.	153-154
6.2	Comparison of binocular and monocular measures of visual function of the <i>Tetraflex KH3500</i> accommodating intraocular lens.	165
6.3	Change in ocular measures from 1 and 6 months to 2 years in patients implanted with the <i>Tetraflex KH3500</i> accommodating intraocular lens.	165

LIST OF FIGURES

Figure	Page(s)
1.1 <i>Visante</i> AS-OCT image: cross sectional view of the anterior segment of the eye.	14
1.2 <i>Visante</i> AS-OCT image: crystalline lens and gradient index structure.	15
1.3 <i>Visante</i> AS-OCT image: magnified view of the ciliary body, anterior chamber angle and iris.	16
1.4 Schematic diagram of the accommodative mechanism originally described by Helmholtz.	18
1.5 A typical human accommodative stimulus response curve.	24
1.6 Mean monocular subjective amplitude of accommodation, as a function of age (based on Duane [1922]).	26
2.1 Comparison of paraxial and aspheric model refractive output, with variation in age, accommodative demand and pupil size.	58
2.2 Ocular vergence changes as a function of accommodation demand for eyes aged 20 to 50, in decade increments.	62
2.3 Axial distances: Normalised change in vergence for a 20 year old eye, for 4.0 D of accommodation demand.	66
2.4 Crystalline lens surface radii: Normalised changes in vergence for a 20 year old eye, for 4.0 D of accommodation demand.	67
3.1 Outcome refractive status (accommodation) variations with age for an axial myope, hyperope and emmetrope with a 4.0 D accommodation stimulus.	81
3.2 Variations in vergence change with age for a 4.0 D accommodation stimulus.	85
3.3 Variations in vergence change with ametropia for a 4.0 D accommodation stimulus.	86
3.4 Individual ocular component variations in vergence change with ametropia, at ages 20 to 50 years in decade increments.	87
3.5 Variation in Vergence Contribution Factor (VCF) with age, for a 4.0 D accommodative stimulus.	90

3.6	Variations in Vergence Contribution Factor (VCF) with ametropia, for a 4.0 D accommodative stimulus.	91
3.7	Individual ocular component variations in Vergence Contribution Factor (VCF) ametropia at ages 20 to 50 years in decade increments, for a 4.0 D accommodative stimulus.	92
4.1	Refractive status (pseudophakic accommodation) as a function of anterior shift in IOL position (50 year old eye).	106
4.2	Vergence changes for each ocular component with anterior IOL shift (50 year old eye).	108
4.3	Vergence Contribution Factor changes for each ocular component with anterior IOL shift (50 year old eye).	109
5.1	The <i>Visante</i> AS-OCT screen displaying the anterior segment image of a phakic eye with the measuring callipers <i>in situ</i> .	123
5.2	Flow chart showing the theory and methods in deducing a correction factor for <i>Visante</i> instrument distortion.	133
5.3	The dependence of correction factor on uncorrected lens thickness measurements made using the <i>Visante</i> .	134
5.4	Anterior eye axial distances and their variation with accommodation demand measured with the <i>Visante</i> , compared to the Dubbelman model eye data.	137
5.5	Anterior eye relative changes in axial distance with accommodation demand measured with the <i>Visante</i> , compared to the Dubbelman model eye data.	140
5.6	Relative movements of the various lens parameters as a function of accommodative demand or response.	143
6.1	The <i>Visante</i> AS-OCT screen displaying the anterior segment image of a pseudophakic eye with the measuring callipers <i>in situ</i> .	160
6.2	Defocus curves for monocular right and left eyes.	163
6.3	Objective accommodation, as measured using the Shin-Nippon <i>SRW-5000</i> and a +5.0 D Badal optical system, for monocular right eyes (6.3A) and monocular left eyes (6.3B).	163
6.4	Mean shift in intraocular lens position with accommodative demand (n = 14 eyes).	166
A5.1	Individual stimulus-response curves (right eyes; Chapter 6).	258-260

A5.2 Individual stimulus-response curves (left eyes; Chapter 6).

261-263

CHAPTER 1

PHAKIC AND PSEUDOPHAKIC ACCOMMODATION

1.1 General introduction

Accommodation is defined as a dioptric change in the power of the eye (Millodot, 1997). Its primary function is to change the refractive power of the eye to bring objects of regard at different distances into focus (Atchison, 1995). It is primarily driven and controlled by the retinal blur element of a visual stimulus (Ong and Ciuffreda, 1997). The loss of accommodative ability with age is well known (Donders, 1864). Presbyopia has been the subject of many studies, with its exact mechanism still equivocal (Charman, 2008). The goal of accommodation restoration is not only to provide functional static near vision as can be achieved with spectacles, but to supply a true, dynamic and continuous range of focussing ability of the eye without the need for an external appliance.

The remit and aim of this thesis is to investigate the subtleties of the phakic accommodative mechanism by examining theoretical schematic eyes, and to extend this theory to the practical application and measurement of real human accommodation. Further, the correction of presbyopia by Accommodating Intraocular Lenses (AIOLs) will be studied using the same approach.

The use of a recently produced schematic eye which allows modification for age and accommodative demand, gives a unique opportunity to examine in detail, the exact biometric and dioptric changes which occur during human accommodation. A contemporary method of imaging the eye (i.e. anterior segment Optical Coherence Tomography; AS-OCT) allows an insight into real life application of human phakic and pseudophakic accommodation.

This chapter reviews the literature covering the plethora of topics associated with the ocular accommodative system, describes its anatomy, function and components, paying particular attention to the areas pertinent to the thesis. Discrete topics have been omitted to allow a more focussed approach to the subject, in the chapter to which it relates.

1.2 Anatomical structures of ocular accommodation

1.2.1 The crystalline lens

The crystalline lens is an optically clear structure located behind the iris but in front of the vitreous body and retina (Johns *et al.*, 2003). It is a transparent, biconvex structure, the purpose of which is, along with the cornea, to refract light to focus on the retina. The diameter of the lens is approximately 9-10 mm with a thickness of 3.6 mm in its unaccommodated state (Millodot, 1997). The lens is made of transparent proteins called crystallins. The proteins are arranged in approximately 20,000 thin concentric layers (Cook *et al.*, 1994), with a refractive index (for visible wavelengths) varying from approximately 1.406 in the central layers down to 1.386 in less dense cortex of the lens (Hecht, 1987). The lens, therefore, has a gradient index structure (Nakao *et al.*, 1968; Nakao *et al.*, 1969; Pierscionek, 1989; Figure 1.2). This refractive index gradient enhances the optical power of the lens and is thought to lessen the spherical aberration of the eye (Bennett and Rabbetts, 2007).

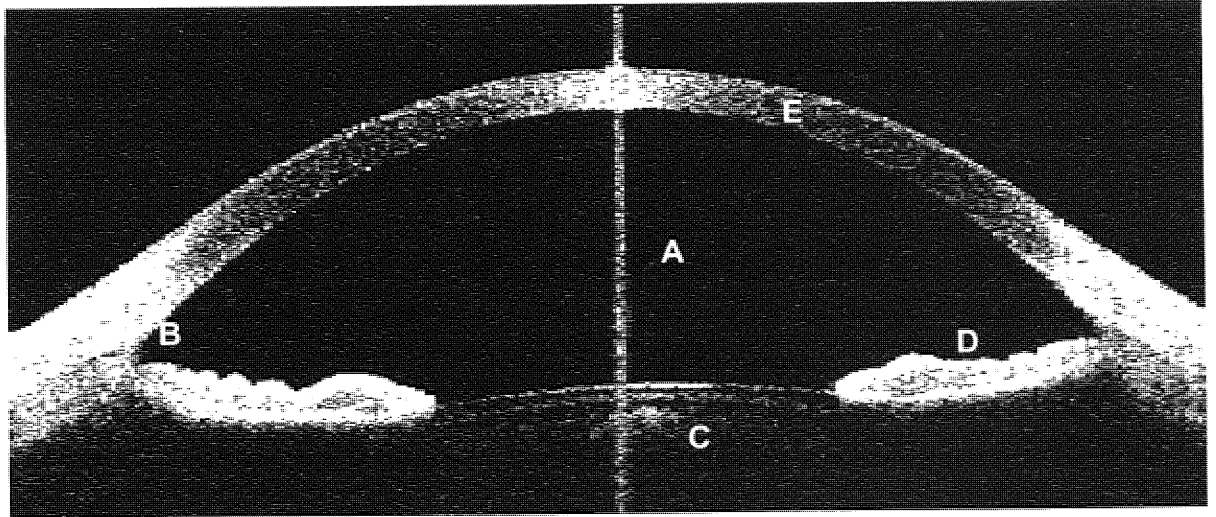


Figure 1.1 Cross sectional view of the anterior segment of the eye. The image is taken on the *Visante* anterior segment Optical Coherence Tomographer. A = The anterior chamber, B = the anterior chamber angle, C = the crystalline lens, D = the iris, E = the cornea.

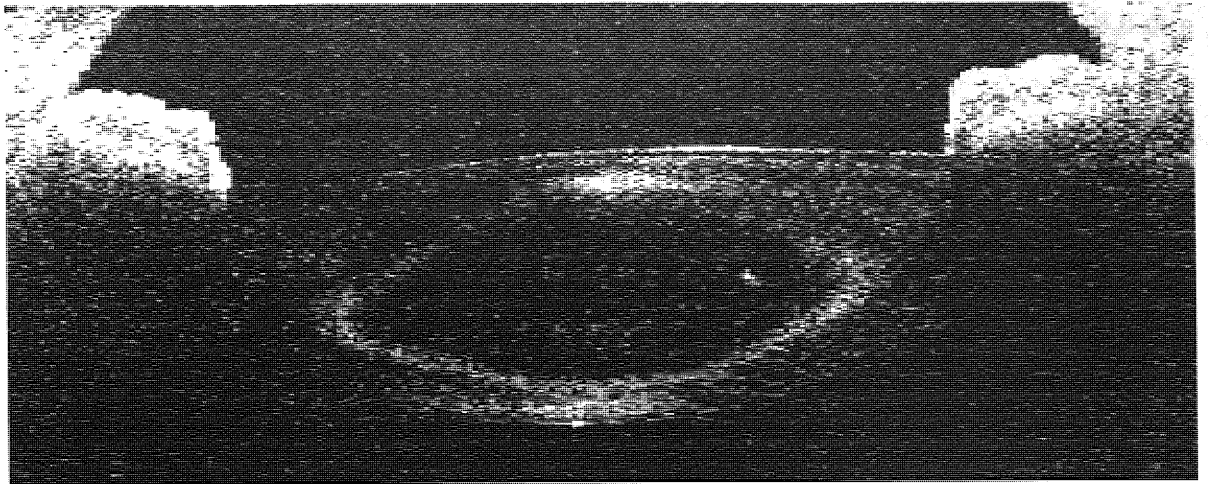


Figure 1.2 The crystalline lens in situ. The image is taken on the *Visante* Anterior Segment Optical Coherence Tomographer (AS-OCT). The nucleus and gradient index structure is highlighted here.

The lens is incorporated into the capsular bag, which is suspended from the surrounding ciliary body by the zonular fibres (zonules of Zinn) attached to the equator of the lens. The zonules of Zinn consist of a series of radially arranged fibres connecting the ciliary processes to the lens capsule. They are divided into three groups; two sets are attached to both the anterior and posterior of the capsule, the third is attached to the equator of the crystalline lens (Snell and Lemp, 1998). In the young eye, the lens is flexible, and its curvature is controlled by the ciliary body. The lens is therefore used to supply some of the eye's refractive power (approximately 20%, the cornea providing 80%; Hecht, 1987) and to instigate an increase in power to focus on objects at different distances; the process of accommodation.

1.2.2 The ciliary body

The ciliary body is a ring of tissue inside the globe, just behind the origin of the cornea (limbus). It gives rise to the iris, secretes the aqueous humour into the anterior chamber, provides attachment for the zonules of the lens, and contains the ciliary muscle. The shape of the ciliary body is roughly triangular in cross section, with the short anterior side facing the anterior of the eye being almost perpendicular to its scleral surface. The iris arises at the approximate mid-point between the corneo-scleral spur (a ridge of the sclera at the level of the limbus) and the trabeculum. The length of the ciliary body varies with each individual. It is always longest infero-temporally and shortest nasally. Typically, it

measures 5.6 to 6.3 mm temporally and 4.6 to 5.2 mm nasally, but it can be up to 10.0 mm long in abnormally enlarged eyes (Streeten, 1982).

The ciliary body comprises two distinct parts. The anterior part is known as the pars plicata. This is made up of seventy to eighty ciliary folds or processes which are approximately 0.5 mm wide and 1.0 mm high (in adults). These processes are vascular structures and do not contain ciliary muscle. These processes become enlarged and more convoluted with age (Streeten, 1982). The crystalline lens lies 1.0 to 1.5 mm centrally to the ciliary processes. The area of ciliary body posterior to the pars plicata is known as the pars plana (obicularis ciliaris). It is about 4.0 mm long temporally and approximately 3.5 mm long nasally (Young, 1801). The pars plana is in close relation to the zonular fibres and is attached to the vitreous in its posterior 2.0 mm. The anterior majority of the ciliary body contains ciliary muscle. This smooth muscle takes up most of the anterior two-thirds of the ciliary body. Most of the fibres of the ciliary muscle take their origin from the scleral spur (Wobig *et al.*, 1981), whilst some may arise from the trabecular meshwork. The action of the ciliary muscle is to move the ciliary body forward and inward.

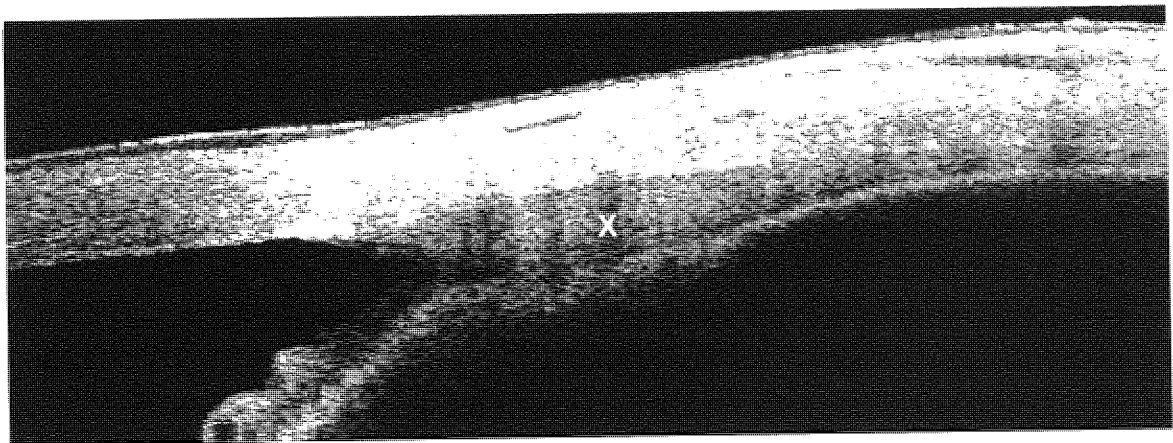


Figure 1.3 Magnified view of the ciliary body (X), anterior chamber angle and iris. The image is taken on the *Visante* anterior segment Optical Coherence Tomographer (AS-OCT).

The ciliary muscle also has an important role in the outflow of aqueous humour. The ciliary muscle, trabecular meshwork and Schlemm's canal are intimately connected. Consequently, on accommodation and contraction of the ciliary muscle, the fenestrations in the meshwork widen and the canal opens, facilitating outflow. Therefore intra-ocular pressure (IOP) reduces during accommodation (Whiteacre and Stein, 1993). Armaly and

Rubin found that four dioptres of accommodation sustained for one minute produced a mean reduction of 0.69 mmHg in five patients aged 45 to 55 years (Armaly and Rubin, 1961). More recent work by Rai and colleagues has identified a dose dependant relationship between IOP and accommodation (Rai *et al.*, 2006).

1.3 Theories of accommodation

The theories of accommodation have evolved over the past 300 years, and have been reviewed extensively by a number of authors (Cramer, 1853; Helmholtz, 1855, 1924; Fincham, 1937; Weale, 1992; Atchison, 1995; Schneider *et al.*, 2001; Strenk *et al.*, 2005; Charman, 2008, Glasser, 2008). As such, a full discourse of topics is too extensive for this thesis; however, the key historical events are outlined here.

In 1677, Descartes (cited by Fincham, 1937) suggested accommodation was caused by changes in lens shape and curvature in order to allow clear visualization of near objects. He assumed these changes were caused by the tendons which suspend the lens. Young (1801) stated that it was the crystalline lens that was responsible for accommodation. Disregarding the ciliary muscle, he assumed the lens itself was muscular. Following more accurate methods of observing accommodation (Purkinje, 1823), experimental evidence for Descartes' hypothesis was provided by Cramer (1853). He described an increase in anterior lens curvature during the process of accommodation by observing Purkinje images. He suggested that the ciliary muscle and iris were responsible for the observed changes in the anterior lens; the ciliary muscle acting upon the choroid, and therefore the vitreous, and the iris acting upon the anterior lens directly (Fincham, 1937).

Helmholtz (1855, 1924) attributed the accommodative response to the contraction of the ciliary muscle reducing zonular tension, allowing the crystalline lens to increase its curvature, as described above. He showed this by utilizing Purkinje images in a similar manner to Cramer, and supported his theory with evidence and mathematical formulae. Our present understanding of the mechanism of accommodation is based upon this theory. It follows that, when the eye accommodates, contraction of the ciliary muscle releases the resting tension on the zonular fibres that span the circumlental space extending between the ciliary body and the lens equator. This releases the outward-directed equatorial tension on the lens capsule and allows the elasticity of the capsule to "round up" the lens

substance. This causes a decrease in the circumferential lens diameter and increases the curvature of the anterior and posterior lens surfaces. When the ciliary muscle relaxes after the accommodative effort ceases, the zonular tension on the lens equator is again increased. This pulls the capsule at the lens equator and causes a flattening of the lens and a decrease in the curvature of the anterior and posterior lens surfaces. The movement of the equatorial edge of the lens is thus away from the sclera during accommodation and towards the sclera during disaccommodation (Glasser and Kaufman, 1999).

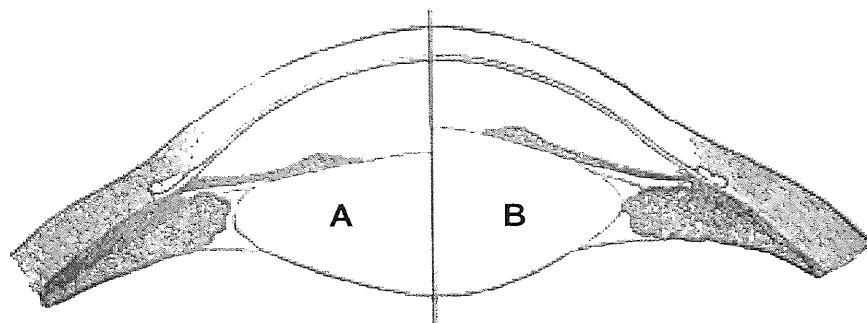


Figure 1.4 Schematic diagram of the accommodative mechanism originally described by Helmholtz who believed the posterior lens surface was stationary during accommodation. A = during disaccommodation, B = during accommodation. After Charman (2008).

Tscherning (1909; cited by Fincham, 1937), and more recently Schachar and Anderson (1995), have suggested that, contrary to the classic Helmholtz theory, ciliary contraction causes an increase in zonular tension. They believe that the equatorial zonule inserts to the anterior aspect of the ciliary muscle at the root of the iris, and that the posterior zonule inserts into the posterior ciliary body. Schachar and Anderson (1995) suggested that contraction of the ciliary muscle causes a posterior-outward movement of the anterior ciliary muscle toward the sclera at the iris root. This movement, it is proposed, increases tension on the equatorial zonular fibres, while releasing the tension on the anterior and posterior zonular bundles. The subsequent force created by the equatorial fibres would pull the equator towards the sclera during accommodation, and in conjunction with the concurrent relaxation of the anterior and posterior zonular bundles, would cause a flattening of the peripheral lens surfaces while increasing the central anterior and posterior lens surfaces (Fincham, 1937; Schachar and Anderson, 1995; Schachar *et al.*, 1996; Schneider *et al.*, 2001). Tscherning later modified his theory suggesting that the contraction of the ciliary muscle exerts tension on the choroid, compressing the vitreous body against

the peripheral parts of the posterior lens; the anterior lens surface being fixed at its periphery by the zonules (Fincham, 1937; Atchison, 1995). Pflugk also utilised Tscherning's theory, but suggested that the vitreous, iris and anterior chamber pressure must also play a role in accounting for increasing zonular tension causing accommodative increases in lens curvature (Pflugk, 1932; Fincham, 1937; Schneider *et al.*, 2001). The elasticity of the lens capsule and its role in accommodation was described by Fincham in 1937. In 1970, Coleman's hydraulic suspension theory described the force applied by the vitreous in producing changes in posterior lens curvature, and subsequently, anterior lens curvature (Coleman, 1970).

Support for the Helmholtz theory of accommodation has been difficult to achieve due to the difficulty in gathering direct, *in vivo* experimental evidence from human subjects; particularly hampered by the presence of the iris. Fincham published findings from a slit-lamp study in 1937, where he observed the accommodative changes in the lens periphery and ciliary processes in a 22 year old man with traumatic aniridia. He noted that accommodation produced a decrease in lens equatorial diameter and the diameter of the ciliary processes, as well as an increase in lens thickness. Further, more recent studies have used retro-illumination infrared video photography (Wilson, 1997), animal studies using gonio-videography and ultrasound biomicroscopy (Glasser and Kaufman, 1999) and Optical Coherence Tomography (OCT; Baikoff *et al.*, 2004) and finite element modelling (Martin *et al.*, 2005) to show similar changes. Evidence from fresh human tissues (Glasser and Campbell, 1998), and from scanning electron microscopy (Rohen, 1979), discount the Tscherning-Pflugk theory by showing no insertion of equatorial bundles or any other zonular fibres at the iris root and anterior ciliary muscle. Strenk and co-workers (1999, 2004, 2005) have conducted a number of studies on *in-vivo* human accommodation using high resolution Magnetic Resonance Imaging (MRI). This technique is unique in its representation of the accommodation process, in that it allows direct and simultaneous visualization of the ciliary body, ciliary muscle and entire crystalline lens *in situ*. Strenk and colleagues demonstrated that Helmholtz' theory was correct (Strenk *et al.*, 1999, 2004, 2005).

1.4 Accommodative biometric changes

The main changes which occur in the human eye have been the subject of many investigations. Many studies have employed a variety of techniques to quantify ocular biometric changes with accommodation (Drexler *et al.*, 1997; Garner and Yap, 1997; Koretz *et al.*, 1997b; Dubbelman *et al.*, 2001; Dubbelman and van der Heijde, 2001; Koretz *et al.*, 2002; Dubbelman *et al.*, 2002; Kirschcamp *et al.*, 2004; Strenk *et al.*, 2004; Baikoff *et al.*, 2004; 2005a; 2005b; Dubbelman *et al.*, 2005; Mallen *et al.*, 2006; Jones *et al.*, 2007; Tsorbatzoglou *et al.*, 2007). A more complete review and discussion is included in Chapters 2 and 5 of this thesis.

1.5 Neurophysiology of accommodation

Fundamentally, the nature of the retinal image governs the afferent accommodative pathway (Campbell, 1954). When retinal cone cells are stimulated by defocus, a summated blur signal is transmitted through the magnocellular layer of the lateral geniculate nucleus (LGN) to visual cortex area 17. The signal is then passed onto the parieto-temporal areas for further processing and dissemination (Ohtsuka *et al.*, 1988). Once at the midbrain, the signal moves to the oculomotor nucleus complex/Edinger-Westphal nucleus where a motor command is generated (Jumblatt, 1999). Efferent accommodative pathways involve the oculomotor nerve (III cranial nerve), the ciliary ganglion and the short ciliary nerve culminating in the innervation of the ciliary muscle resulting in the accommodative response. The ciliary muscle is innervated by the antagonistic action of the autonomic nervous system (Cogan, 1937; Morgan, 1944; Gilmartin, 1986; Gilmartin *et al.*, 1992; Gilmartin, 1998). The autonomic nervous system is composed of two main branches; the parasympathetic (primary) and sympathetic divisions (supplementary; Gilmartin *et al.*, 1992).

1.5.1 Parasympathetic innervation

Accommodative control in humans is achieved principally by the action of the neurotransmitter acetylcholine on post-synaptic muscarinic (M3) receptors on ciliary smooth muscle (Woldemussie, Feldmann, & Chen, 1993). Activation of the parasympathetic system increases the accommodative response. The action of acetylcholine is blocked by anti-muscarinic drugs such as atropine, cyclopentolate and

tropicamide, which concurrently decrease accommodative output. Cholinesterase inhibitors (e.g. physostigmine) accentuate the effect of acetylcholine.

1.5.2 Sympathetic innervation

The sympathetic division is mediated by the neurotransmitter noradrenaline (also known as norepinephrine). Adrenergic receptors are divided into alpha (α) and beta (β) types. These sympathetic receptors are further broken down into α_1 , α_2 , β_1 and β_2 depending on the relative effects noted with adrenergic drugs. α_1 and β_1 are generally excitatory, whilst α_2 and β_2 are generally inhibitory. Accommodation appears to be mediated by α_1 and β_2 receptors; both have an inhibitory effect (Van Alphen, 1976; Wax and Molinoff, 1987; Zetterstöm and Hahnenberger, 1988). Although there still remains a degree of controversy around the pathway of the sympathetic fibres, some authors propose that they originate from the superior cervical ganglion and join the long and short posterior ciliary nerves (Kaufman, 1992). Controversy exists over whether the sympathetic nervous system plays a role in accommodation. Gilmartin (1986) concluded that sympathetic inhibition of accommodation is relatively small and slow, and is a function of the concurrent level of parasympathetic activity. It has been suggested that modifications to the accommodative response with mental effort are achieved by altering the balance of autonomic innervation to the ciliary muscle (Malmstrom *et al.*, 1980; Bullimore and Gilmartin, 1987; 1988; Davies *et al.*, 2005); this ability is present in as much as 29 % of the population (Mallen *et al.*, 2005).

1.6 Components of accommodation

It was suggested by Heath (1956) that it is possible to distinguish several components of accommodation.

1.6.1 Reflex accommodation

This is a quasi-automatic adjustment of the refractive state to maintain a sharply defined retinal image of the object of regard. However, a number of studies have shown that some normal subjects fail to accommodate to clear stimuli which are modestly blurred (Heron *et al.*, 1999; Chen *et al.*, 2006).

1.6.2 Proximal accommodation

Here, the accommodative response is triggered by knowledge (or a belief of knowledge) of the object distance (Hung *et al.*, 1996). In addition, the accommodative response may also be conditioned by the knowledge of surroundings and their proximity to the subject (i.e. surround propinquity; Rosenfield and Ciuffreda, 1991).

1.6.3 Tonic accommodation

Tonic accommodation refers to an intermediate accommodative state in the absence of an adequate visual stimulus such as darkness (dark focus; Leibowitz and Owens, 1975), ganzfield (structure-less/empty field; Schor *et al.*, 1984), low contrast targets (Luckiesh and Moss, 1937) and reduced visual acuity (Heath, 1956), a low spatial frequency target (Kotulak and Schor, 1987), or pinhole (open-loop condition; Rosenfield and Ciuffreda, 1991). It is influenced by a variety of factors including age (Whitefoot and Charman, 1992; Mordi and Ciuffreda, 1998), duration of open-loop state (Rosenfield and Gilmartin, 1989), cognitive demand (Malmstrom *et al.*, 1980; Bullimore and Gilmartin, 1987; Jaschinski-Kruza and Toenies, 1988), or proximity of visual and non-visual stimuli (McLin and Schor, 1988; Rosenfield and Gilmartin, 1990; Rosenfield and Ciuffreda, 1991; Winn *et al.*, 1991; Rosenfield *et al.*, 1993; 1994).

1.6.4 Convergence accommodation

When we shift our gaze from a distant to a near target, we execute at least three related motor acts: the eyes converge to minimize binocular disparity (convergence), we accommodate to focus on the near object (accommodation), and the pupils constrict (pupil miosis), which increases depth of focus. These three responses have been termed the 'near-response' or 'near triad' (Myers and Stark, 1990) and is due to the neural connections between the systems. As such, all vergence movements are accompanied by an accommodative change (Ong and Ciuffreda, 1997). The magnitude of this response will depend on the subjects' convergence accommodation to convergence ratio (CA/C); the greater the ratio, the larger the accommodative response will be.

1.7 Accuracy of focus

Changes in focus are not achieved instantaneously. There is a finite reaction time or latency of about 300 ms, followed by an interval or response time of up to about 1000 ms during which accommodation is changing before stabilising at its new level (Campbell and Westheimer, 1960; Phillips *et al.*, 1972; Tucker and Charman, 1979; Beers and van der Heijde, 1994; Kasthurirangan *et al.*, 2003; Kasthurirangan and Glasser, 2005). Small fluctuations in accommodative amplitude are noted when observing a constant stimulus over time (Charman and Heron, 1988); these may help to maintain the steady-state response (Charman, 2000). Figure 1.5 illustrates the mean steady-state response level achieved compared to the stimulus level over the available range of accommodation (Bennett and Rabbetts, 2007; Charman, 2008). There is an over-accommodation (accommodative lead) for distant objects, and an under-accommodation (accommodative lag) for near objects. The lead at distance is often attributed to conventional refractive techniques of utilising the best visual acuity with the most positive/least negative spherical lens. This is said to leave the true refraction of the eye slightly myopic at six metres (conventional testing distance).

The central semi-linear slope of the stimulus-response curve varies with the individual (e.g. age and visual acuity), the nature of the target (e.g. its form, contrast and colour) and other conditions (e.g. luminance; Charman, 1986; Charman, 2008). The cross over point, where the stimulus response curve crosses the unity line, is said to be equal to the individuals' level of tonic accommodation (Ramsdale and Charman, 1989); other studies have dismissed this theory (Ciuffreda *et al.*, 1984; Ong *et al.*, 1993). Large accommodative lags have been found in children, particularly in myopes (Gwiazda *et al.*, 1983).

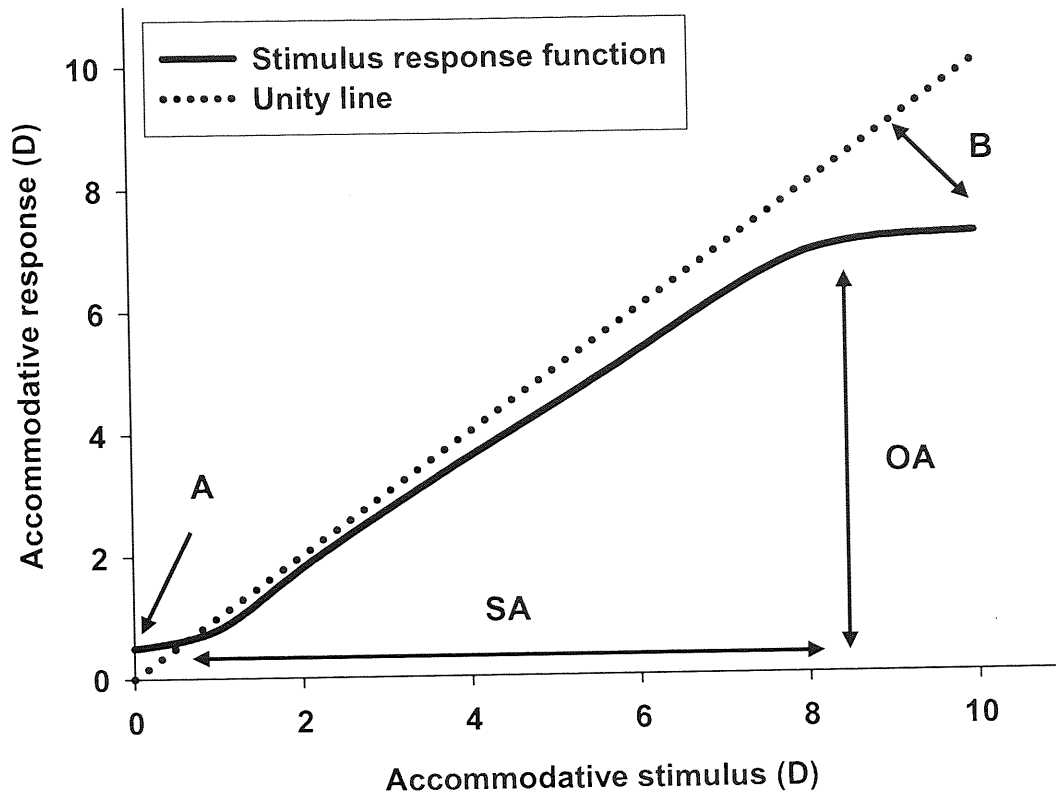


Figure 1.5 Typical stimulus response curve (after Bennett and Rabbetts [2007] and Charman [2008]). A = accommodative lead, B = accommodative lag, OA = range of objective accommodation, SA = range of subjective accommodation. The unity line corresponds to equal response and stimulus values.

1.8 Presbyopia

Presbyopia is a large and varied topic, and has been studied for a great number of years. The theories of presbyopia have been comprehensively reviewed in a number of publications (Stark, 1988; Atchison, 1995; Gilmartin, 1995; Charman, 2008). A full review is beyond the remit of this thesis, a summary, however, is provided below.

Helmholtz' theory of presbyopia did not receive the same support as his theory of accommodation. He suggested that mechanical changes in the lens (or "lens sclerosis" as he termed it) was the cause of presbyopia (Helmholtz, 1855). It is more likely that there are a number of lenticular and extra-lenticular changes which are the causal factors leading to an age-related accommodative loss we call presbyopia.

There have been a number of theories within the field of presbyopia. Donders (1864) suggested that an inability of the ciliary muscle to shorten with advancing age was the basis. In a similar vein as their theory of accommodation, Tsherning (1909) and Pflugk (1932) attributed accommodative loss to reduced movement and fluidisation of the vitreous (Fincham, 1937; Schneider *et al.*, 2001). A number of authors have categorised the theories of presbyopia into lenticular and extra-lenticular theories. Lenticular theories are further subdivided into mechanical changes in the lens and capsule and a geometric theory, whilst extra-lenticular theories comprise changes in the ciliary muscle and changes in the elastic components of zonule and/or ciliary body.

1.8.1 Lenticular theories

The mechanical theory is based upon the assumption that the lens hardens and becomes more rigid with age, and therefore is increasingly resistant to the elastic forces upon it (Atchison, 1995). The Hess-Gullstrand lenticular mechanism theory purports that there is a lifelong consistency in the amount of ciliary muscle contraction required for a given change of accommodation (Hess, 1901; Gullstrand, 1924). It is predicted that the ciliary muscle contraction will become more latent with age; i.e. it will have less effect on accommodation. To support this theory, the authors would need to show increasing ciliary contraction at stimulus levels beyond which the accommodative response is static. Evidence of this has come from studies assuming electrical impedance across the equatorial region of the lens reflects ciliary muscle activity and/or blood flow (Swegmark and Olsson, 1968; Saladin *et al.*, 1974; Saladin and Stark, 1975), studies showing iris sphincter innervation and pupil miosis in the absence of continuing accommodative response (Alpern and David, 1958), and demonstrations of retinal stretching with accommodative stimulus being equal in pre- and presbyopic cohorts (Hollins, 1974). The Hess-Gullstrand theory, if true, would show signs of zonular slackness in older subjects as they attempt to accommodate beyond their amplitude limit. Neider *et al.* (1990) noted that the opposite was true in aniridic rhesus monkey eyes as a function of accommodation and age.

The Duane-Fincham theory claims that the ciliary muscle is maximally contracted at the amplitude of accommodation, in contradiction to the Hess-Gullstrand theory. Although both authors assert the same outcome, their methods of arriving at this are very different.

Duane (1922, 1925) suggested that the ciliary muscle weakens with age, having noticed reduced amplitudes of accommodation in older patients upon instillation of diluted atropine drops. Fincham's theory was that the lens requires greater pressure from the capsule to mould it into shape during accommodation with increasing age. This, Fincham suggests, can only be achieved by further release of zonular tension, thereby requiring increasing ciliary contraction for a given change in accommodation throughout life (Fincham, 1937). Support for this theory comes from studies of age and drug effects on the AC/A ratio (convergence induced by an accommodative stimulus which also induces a unit accommodation response) and CA/C ratio (accommodation induced by a convergence stimulus which also induces a unit convergence response). The former increases whilst the latter decreases with age, contradicting the Hess-Gullstrand model, which predicts that the accommodation-convergence relationship remains equal throughout life (Fincham and Walton, 1957; Fry, 1959; Breinin and Chin, 1973; Eskridge, 1983; Bruce *et al.*, 1995).

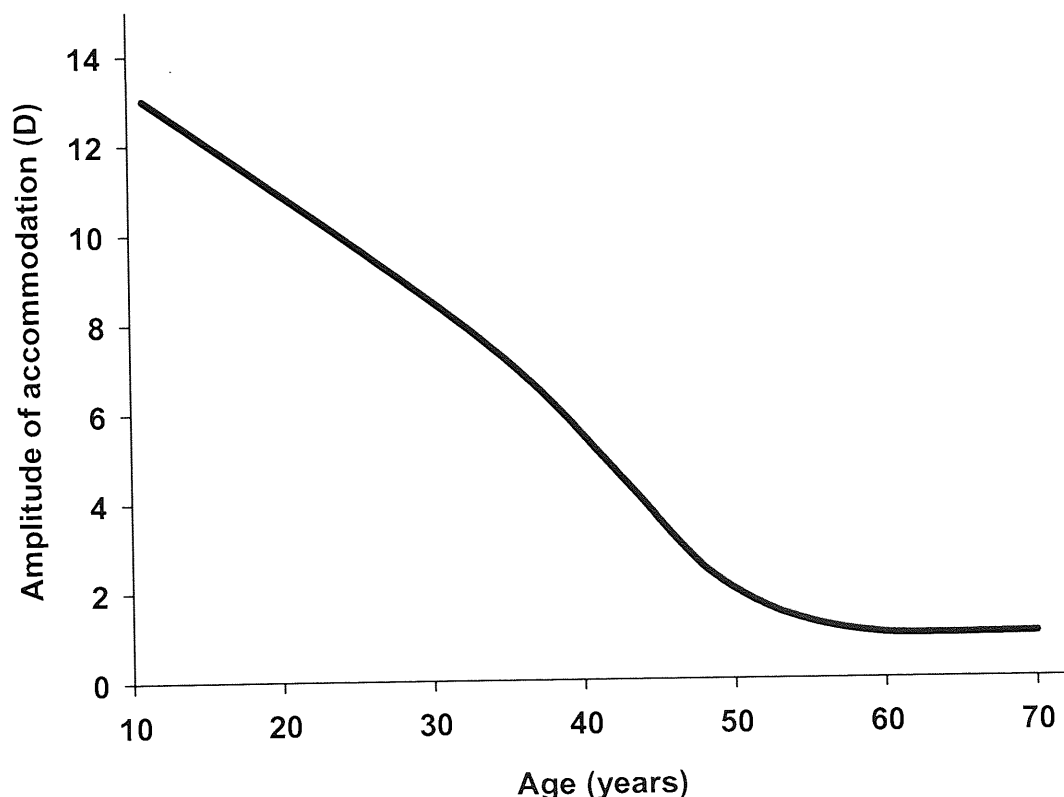


Figure 1.6 Mean monocular subjective amplitude of accommodation, as a function of age (based on Duane [1922]; after Charman [2008]).

The geometric theory of presbyopia is concerned with age-related changes in size and shape of the lens and its relationship with the surrounding accommodative structures. The lens increases in size with age mostly as a result of increasing cortical thickness; the dimensions of the lens nucleus appear to remain constant throughout life (Strenk *et al.*, 1999, 2004). The human anterior segment length is constant with age, thus increasing lens thickness causes a decrease in anterior chamber depth and an anterior displacement of the lens centre of mass (Brown, 1973; Koretz *et al.*, 1989, 2001, 2004; Cook *et al.*, 1994; Strenk *et al.*, 1999, 2004). These changes fail to produce increasing myopia due to compensatory changes in the refractive index gradient of the lens (Pierscionek, 1990; Smith *et al.*, 1992; Hemenger *et al.*, 1995).

The crystalline lens is biconvex with the anterior surface being less curved than the posterior surface. With age, there is a linear reduction in the central anterior lens radius of curvature in emmetropic un-accommodated eyes (Brown, 1974; Koretz *et al.*, 2004); changes in radius of the posterior surface with age are less marked (Cook *et al.*, 1991; Koretz *et al.*, 1984; Strenk *et al.*, 2004). The result of these changes is that the insertional area of the zonules is widened, with fewer equatorial insertions and a concurrent increase in the distance between the anterior and posterior zonular insertions (Brown, 1974; Farnsworth and Shyne, 1979). Increasing lens curvature and shifting zonule insertions as a function of age, are likely to result in the zonules applying more tension parallel to the surface of the capsule; relaxation may therefore lead to smaller effects on lens shape (Koretz and Handelman, 1988). It is also noted that as lens curvature increases with advancing age, the ability to effect an additional accommodative increase in curvature diminishes, as there is an intrinsic limit to how far the lens can “round up” (Strenk *et al.*, 2005). Schachar and co-workers believe that accommodation is caused by *increased* tension on the zonules and attribute presbyopia to equatorial growth of the lens reducing this tension (Schachar, 1992; Schachar *et al.*, 1994; Schachar and Anderson, 1995). Subsequent to his theory, Schachar developed scleral expansion bands; made of polymethylmethacrylate and designed to increase the diameter of the sclera, thus restoring zonular tension. There is, however, no evidence to support this theory (Rohen, 1979; Glasser and Campbell, 1998; Glasser and Kaufman, 1999).

1.8.2 Extralenticular theories

Extralenticular theories are concerned with accommodative loss due to weakening of the ciliary muscle or loss of elasticity of zonules or ciliary body components. A weakening of the ciliary muscle was proposed by Duane (1922, 1925). From the work of Fisher (1977), it would appear that the contractile force of the ciliary muscle reaches a maximum at around 45 years of age. Other studies have shown no statistically significant age-related change in ciliary muscle contraction. Confirmation appears in the form of investigations into the contraction of older rhesus monkey eyes (Poyer *et al.*, 1993; Lütjen-Drecoll *et al.*, 1988a; 1988b), high-resolution MRI studies on human subjects (Strenk *et al.*, 1999), and indirectly by human impedance cyclography *in vivo* (Saladin and Stark, 1975). Microscopy based studies have shown increasing levels of connective tissue in the human ciliary muscle with age (Tamm *et al.*, 1992a; Pardue and Sivak, 2000). These studies also suggest post-presbyopic atrophy of the ciliary muscle may occur. Strenk and co-workers (2005) propose that this is likely to be an effect of presbyopia, rather than its cause, as increases in connective tissue do not appear to occur in subjects still capable of accommodation (Strenk *et al.*, 2005)

Since loss of ciliary muscle contractile ability appears to be insignificant, it leads to the possibility that deterioration of elastic components of ciliary body and choroid might be responsible for decline in accommodation with age. Tamm and colleagues concluded that the decline in ciliary muscle response was likely to be due to decreasing choroidal compliance rather than the inability of the muscle to contract. This was shown in rhesus monkeys, where muscle mobility was restored when the attachment to the choroid is disrupted (Tamm *et al.*, 1991; 1992b).

Bitto and Miranda (1989) proposed that presbyopia was actually a loss of disaccommodative ability (the ability to relax accommodation) resulting from a reduction in choroidal elasticity, thus preventing the ciliary muscle from returning to its resting state. This theory would account for the increasing curvature of the lens for zero accommodation with progressing age, and would rely on a change in lens refractive index distribution to maintain the refractive error as mentioned above (Pierscionek, 1990; Smith *et al.*, 1992; Hemenger *et al.*, 1995). Recent MRI studies provide evidence that the human ciliary muscle maintains its mobility throughout life (Strenk *et al.*, 1999), indicating that the

choroid has the ability to return the ciliary muscle to its resting state. Proof of this can also be found by removing the presbyopic human lens and inserting an intraocular lens (IOL) during routine cataract surgery. Lifelong lens growth causes an anterior shift in the lens centre of mass, a decrease in the anterior chamber depth and an anterior displacement of the uveal tract (Strenk *et al.*, 1999). The removal of this age-enlarged lens allows the choroid to bring the ciliary muscle and iris back to their more youthful locations.

1.8.3 Modified geometric theory

Further MRI imaging studies conducted by Strenk and co-workers have proposed a modified geometric theory of accommodation (Strenk *et al.*, 2005). These studies suggest that the human uveal tract acts as a unit in response to lens growth and accommodation, suggesting an alternate theory by which lens growth acts upon the ciliary muscle and result in accommodative loss (Strenk *et al.*, 2004). It appears that the ciliary muscle and iris root are anteriorly displaced at the same rate as the age related increase in lens thickness; thus preserving the antero-posterior relationship between ciliary muscle and zonular insertion on the lens. The latter has been calculated to remain a fixed distance from the anterior pole of the lens with advancement of age (Weale, 2000). The circumlental space decreases with age due to the ciliary muscle's inward movement; the lens equatorial length remaining constant (Strenk *et al.*, 1999). The iris root and pupillary margin also move inward at the same rate as the inward movement of the ciliary muscle. The decrease in circumlental space is likely to cause a decrease in zonular tension during resting accommodation, leading to both increased lens curvature and a reduction in lens accommodative response. (Strenk *et al.*, 2005).

1.9 Schematic eyes

Anatomically close, schematic, model eyes that can reproduce the properties of the human eye are extremely useful. These models stimulate the real world performance of a human eye, and can therefore be used for a full range of research and development purposes. These include predicting the outcome of IOL implantation and studying the features of the optical component systems (Bakaraju *et al.*, 2008). Research into the production and use of schematic eyes still seeks to arrive at a schematic eye which mimics the properties of the natural human eye in all its various aspects. Several models have been produced over the

past two centuries. They range from those considering only single refracting surfaces (reduced eyes) to models with refractive index variation within the lens and conicoidal, rather than spherical, retinal surfaces.

Paraxial schematic eyes only consider the first order (Gaussian) properties of the optical system, with small apertures and at small field angles. The most popular of these is the Gullstrand (1909) schematic eye which is based on the work of Listing in 1851 (after Helmholtz, 1909). This model was later modified by Le Grand and El Hage (1980), and is still considered the standard for retrieving Gaussian ocular properties. Other paraxial models include those of Emsley (1952), Drasdo and Fowler (1974), Blaker (1980) and Bennett (1988). Gullstrand's model eye addressed the variation in lenticular refractive index by using a two-shell structure for the crystalline lens. Recently, more elaborate representations of the lens gradient index have been attempted by introducing a series of shells; up to 602 in some cases (Pomerantzeff *et al.*, 1971; Al-Ahdali and El-Messiery, 1995; Popiolek-Masajada, 1999; Liu *et al.*, 2005). Kasprzak (2000) proposed an approximation of the profile of the crystalline lens using mathematical hyperbolic cosines.

Shell structured lenses have largely been replaced by ray tracing through gradient refractive indices bound by aspheric surfaces. Many of these finite, or wide angle, designs have been suggested to offer good predictions for both on- and off-axis aberrations. Popular examples of these include the schematic eyes of Lotmar (1971), Kooijman (1983), Navarro *et al.* (1985), Liou and Brennan (1997) and Escudero-Sanz and Navarro (1999).

Spherical and chromatic aberrations have been accurately predicted with a simplified, single reduced surface model proposed by Thibos and colleagues (1992). However, the reduced eye still suffers from the lack of natural variation in refracting surfaces, so cannot truly represent real vision (Le Grand and El Hage, 1980). In order to better represent the behaviour of the natural human eye, models have been designed to incorporate accommodative changes at near (Gullstrand, 1909; Le Grand and El Hage, 1980; Navarro *et al.*, 1985; Norrby, 2005; Goncharov and Dainty, 2007), lenticular gradient refractive index changes with age (Smith *et al.*, 1992; Bennett and Rabbetts, 1998; Popiolek-Masajada and Kasprzak, 2002; Zadnik *et al.*, 2003; Norrby, 2005; Goncharov and Dainty, 2007), and changing refractive error in a generic adult model (Atchison, 2006).

Further, Goncharov and Dainty (2007) incorporated a mathematical model for the gradient index lens (GRIN), and reproduced the properties of both the Navarro eye (Navarro *et al.*, 1985; Escudero-Sanz and Navarro, 1999) for off-axis aberrations and Thibos' chromatic on-axis model (the Indiana eye; Thibos *et al.*, 1992). Individual, personalised model eyes have recently been proposed by Navarro and colleagues (2006) to overcome problems in predicting visual outcomes in individual subjects. The method was limited due to the inability to accurately reproduce the correct lenticular gradient index profile and geometry. Rosales and Marcos (2007) have also utilised the individual approach with eyes fitted with IOLs, and have found good correspondence with *in vivo* data.

This thesis utilises the Norrby eye model (2005), which accounts for changes in age and accommodation. It is based on the work of Dubbelman and colleagues (Dubbelman and van der Heijde, 2001; Dubbelman *et al.*, 2001; 2002; 2005) who used corrected Scheimpflug images in a large number of subjects of different ages at several levels of accommodation. A fuller explanation of this model is given in Chapter 2.

1.10 Cataract

Johns and co-workers (2003) suggest that cataracts are the commonest cause of reversible loss of useful vision worldwide. The World Health Organisation (WHO) estimates 180 million people worldwide are visually disabled; 40 to 45 million of these are deemed to be without useful vision (WHO, 2000). Approximately 46% of these cases are thought to be the result of cataracts (WHO, 2000); it has been projected that this could increase to 50 million by 2020 (WHO, 2004).

The development of cataract can have a number of causational factors. These may include developmental abnormalities, trauma, metabolic disorders and drug-induced changes (Johns *et al.*, 2003). The main cause however is ageing. Age-related (senile) cataracts have an aetiology which is not fully understood; however, it is likely to be multi-factorial (Streeten, 2000, Johns *et al.*, 2003;). Age-related cataracts are defined mainly by their physical appearance, and are broadly classified as nuclear, cortical or posterior subcapsular. They can appear on their own, or in combination. Cataractous changes are typically bilateral but are often asymmetrical in density and/or progression.

1.10.1 Types of cataract

Nuclear cataract

The crystalline lens constantly grows throughout life (Weale, 1982). With age, the new fibre layers which are added to the lens compress the lens nucleus, which becomes harder (nuclear sclerosis). There is also an associated yellowing of the lens with age. These slowly progressing changes can affect vision, colour discrimination and often lead to a change in refraction (myopic shift or second sight; as often reading glasses can be discarded; Johns *et al.*, 2003).

Cortical cataract

The newest fibres of the lens make up the lens cortex. Fibres are not lost with age, with new fibres being added to the outside of the lens, under the outer coating or capsule. Discrete opacities (cortical spokes) can develop within this lens cortex. These opacities typically cause no disruption to vision unless they involve the visual axis (Johns *et al.*, 2003).

Posterior subcapsular cataract (PS)

These cataracts are commonly granular opacities which form centrally in the posterior cortex under the posterior capsule. They often present in younger patients, and are associated with symptoms such as glare and a reduction in vision biased to near versus distance acuity (Johns *et al.*, 2003).

1.10.2 Cataract surgical techniques

Currently, WHO estimates that the number of cataract operations performed worldwide is in the region of 12 million per annum. The World Health Organization also estimates that by 2010, this figure will have increased to 20 million per annum, and that this will increase again to 32 million annual surgeries by 2020 (WHO, 2004).

The first forms of cataract surgery involved primitive techniques used to move the hardened cataractous lens out of the line of sight and into the vitreous chamber. The procedure, known as couching (Saxena, 1965), was employed by ancient civilisations and is no longer in use other than in isolated tribal communities. In modern times, cataract surgery has become the most commonly performed intraocular procedure, with constantly

improving outcomes. The intracapsular technique had been popular until the 1980's (Apple *et al.*, 1984). Thereafter, planned extracapsular cataract extraction became more widespread (Apple *et al.*, 1984); which was further refined by phacoemulsification (Kelman, 1967; Linebarger *et al.*, 1999).

Intracapsular cataract extraction (ICCE)

This procedure involves the removal of the entire crystalline lens complex, including the lens capsule. The refractive function of the lens is then replaced by the insertion of an intraocular lens (IOL), usually into the anterior chamber, or a high hypermetropic prescription in aphakic spectacles or contact lenses. The advantages of this procedure include the ease and speed of surgery, avoidance of future posterior capsular opacification (PCO), and a vastly increased field of view when performing direct funduscopy.

Extracapsular cataract extraction (ECCE)

This technique was first employed over fifty years ago, but was subsequently abandoned in favour of ICCE. Extracapsular cataract extraction became more popular in the 1980s with the introduction of microsurgical techniques (Apple *et al.*, 1984). The technique involves removing the contents of the lens leaving the posterior lens capsule intact. This capsule then acts as a barrier between the anterior and posterior segments as well as forming the most useful site for replacement lens implantation. This form of surgery can be manual (Blumenthal *et al.*, 1992) or mechanical (Alio *et al.*, 2006; phacoemulsification). If the manual technique is employed, the lens nucleus is removed *en bloc*, and therefore requires a relatively large incision (Allen and Vasavada, 2006).

Phacoemulsification is used in modern extracapsular extractions and uses sophisticated machinery to break the lens nucleus into small pieces and emulsion which can be aspirated through an irrigation-aspiration dual lumen system (Allen and Vasavada, 2006). This technique has the added benefit of being performed through a small corneal incision (commonly 3.0 mm). Latest developments, however, have allowed removal through 2.0 mm incisions. Advantages of small incision surgery include reduction in the disruption to the shape of the cornea leading to improved unaided vision, and more control of intraocular pressure, for example (Minassian *et al.*, 2001).

Minassian and colleagues (2001) performed a randomised trial of manual ECCE with a rigid IOL compared to small incision phacoemulsification with foldable IOL. Their results agreed with current clinical consensus that small incision phacoemulsification is less invasive, has fewer complications, and results in quicker and more stable visual rehabilitation.

In phacoemulsification, a small incision is made in the edge of the cornea. A viscoelastic substance is then injected into the anterior chamber to maintain the depth of the chamber and protect the corneal endothelium. A round hole, known as the capsulorrhexis, is made in the anterior lens capsule, usually in the region of 5.0 or 6.0 mm in diameter. The contents of the lens are then emulsified and/or broken up and aspirated. The capsule is filled with more viscoelastic to maintain its shape whilst awaiting the IOL. Once the foldable IOL is injected into the capsule, the remaining viscoelastic is removed and the incision site is inspected; a suture is rarely required.

Complications of this form of surgery are rare but do occasionally occur. The most common complication is the rupture of the posterior capsule and the prolapse of the vitreous body into the anterior segment, which must be carefully removed. More serious complications include infected endophthalmitis (Kamalarajah *et al.*, 2006), cystoid macular oedema (Mentes *et al.*, 2003) and retinal detachment (Erie *et al.*, 2006).

1.10.3 Intraocular lens technology

The first intraocular lens

The first IOL operation took place at St Thomas' Hospital, London, on the 29th November 1949 (Rosen, 1984). Records suggest that the initial implantation rendered the patient highly myopic, and so on 8 February 1950 it was exchanged (Trivedi *et al.*, 2003). The surgeon, Sir Harold Ridley, inserted a 'lenticular graft' to correct the anisometropia of a 45 year old woman who had previously had an ECCE (Spalton, 1999). Original concerns regarding intraocular lenses stemmed from the fears of interactions *vis-à-vis* a foreign body within the eye. The valid use of IOLs came from the observation of wartime ocular injuries involving Royal Air Force personnel, who had suffered eye injuries with shattered cockpit canopies made of *Perspex*TM. The then Mr. Ridley observed that these plastic fragments were biologically inert and well-tolerated by the eye.

The original IOL was made of polymethylmethacrylate (PMMA; or *Perspex*TM). Named *Transpex 1*, it had a shape which roughly approximated the human crystalline lens. At approximately 100 mg in weight it was, however, much heavier than modern PMMA, acrylic or silicone IOLs and did not include a haptic portion. The lens was implanted behind the iris and in front of the capsular bag following ECCE. Complications were common, and of approximately one thousand Ridley lenses implanted, 15 % were explanted mainly due to dislocation, decentration, uveitis or secondary glaucoma. (Ridley, 1951; 1952; 1953)

Early anterior chamber intraocular lenses (1953-1962)

In 1953, the anterior chamber became the location of great interest with regard to the implantation of IOLs. Pioneered by Barton, anterior chamber IOLs (AC IOL) were designed and began to be implanted. The first IOL was plano convex, with the steep anterior surface in close proximity to the posterior cornea. Barton's work was closely followed, and later that same year an Italian surgeon named Stampelli, and a German named Danheim, developed their own anterior chamber IOLs. The Stampelli lens had three points of contact with the anterior chamber angle and was of rigid design. The Danheim lens was flexible, with a 5.0 mm optic and nylon loops. Ridley also designed his own anterior chamber IOL after abandoning his original posterior chamber intraocular lens (PC IOL; Davies *et al.*, 2006)

Due to the unstable nature of these lenses, a number of complications became common in patients with these implants. These stemmed from damaged corneal endothelium or from iris rubbing. The former often led to corneal decompensation, oedema and pseudophakic bullous keratopathy, with many patients requiring a corneal graft (Cheng and Tan, 1999). The latter frequently resulted in hyphaema, iris erosion and pupil block; making it necessary to undergo peripheral iridectomy at the time of implant. Secondary complications also included cystoid macular oedema (CMO), uveitis, uveitis-glaucoma-hyphaema syndrome (UGH) and IOL dislocation (Davies *et al.*, 2006).

Iris supported intraocular lenses (1957-1973)

To achieve better stability for these new IOLs, emphasis shifted from the anterior chamber to the iris to provide the much needed support. Binkhorst designed the first iris clip lens in

1957 which utilised the pupillary portion of the iris for fixation (Binkhorst, 1962). It had four fixation loops and was so-called because of its resemblance to a paper clip. In 1966, a Russian, Svyatoslav Fyodorov (Fedorov) used fibres for his external haptic loops drawn from the patient's own Achilles tendon. Epstein designed the collar stud lens, which also used the iris for support, at the same time as Binkhorst.

These lenses did reduce the rate of endothelial dystrophy but were subsequently associated with a large number of glaucoma cases due to pupillary occlusion. The lenses were modified to try and increase aqueous flow through the pupil, but pupillary fixed lenses soon became obsolete. Further developments of the iris supported IOL theme came in the form of iris-claw lenses, which captured a fold of iris tissue to maintain fixation, and lenses fixed to the iris via a suture (e.g. the Medallion IOL; Davies *et al.*, 2006).

Modern anterior chamber intraocular lenses (1970 to date)

Clinical findings from the early AC IOLs pointed out that for an AC IOL to be safe, it should be in minimal contact with and no movement in the drainage angle, have no endothelial touch and no iris chafing. Modern AC IOLs have flexible open loop haptics attached to a PMMA lens to attain these criteria and result in fewer corneal complications (Davies *et al.*, 2006). There is, however, a higher prevalence of CMO and compared to PC IOLs (Nikica *et al.*, 1992).

Advantages of AC IOLs include the fact that the posterior capsule need not be intact, and they can be implanted with the crystalline lens still in place (phakic intraocular lens; a form of refractive surgery; Solomon *et al.*, 2002).

Posterior chamber intraocular lenses (1975 to date)

The use of PC IOLs became routine in 1975; Dr. John Pearce was the first surgeon to use these lenses in a consistent manner (Pearce, 1977). Posterior chamber IOLs require the posterior capsule to remain following ECCE; the IOL being placed in the capsular bag or into the groove between the posterior root of the iris and the ciliary body; known as the sulcus (Vargas *et al.*, 2001). Initial problems with fixation arose from the uveal site chosen; where one or both haptics were outside of the capsular bag. This quite frequently led to IOL optic decentration (Tappin and Larkin, 2000).

Polymethylmethacrylate was commonly used as the optic material, with the haptics being constructed of PMMA, polypropylene or polyamide (Davies *et al.*, 2006). With PMMA being inflexible, the corneal incision was generally quite large (approximately 11.0 mm wide). Softer IOL materials began being used in the late 1970s. With the improvement of surgical techniques, including the use of viscoelastic agent (Alpar, 1986), continuous curvilinear capsulorhexis (Gimbel and Neuhann, 1990) and enhanced cortical clean-up (Fine, 1992), cataract surgery began to advance towards what we see today.

Today, most surgery consists of secure, in-the-bag (capsular) fixation of foldable silicone or acrylic IOLs. Phacoemulsification and the use of foldable lenses has reduced the size of the corneal incision required, largely negated the use of sutures, and improved visual recovery and unaided vision post-operatively (Minassian *et al.*, 2001). Ocular biometry is now applied to improve the end point refractive status of the patient.

More modern developments in IOL technology have led to the development of clear lens extraction as a form of refractive surgery (Solomon *et al.*, 2002; Sandoval *et al.*, 2005), refractive IOLs and lenses to restore ocular accommodation (Dick, 2005).

1.11 Accommodating intraocular lenses

The goal of today's cataract surgeon is to provide rapid visual rehabilitation with the fewest postoperative complications and refractive errors. Cataract surgery has become more and more refractive in nature. Providing good distance vision is no longer a problem, however, the missing element is the ability to deal with the loss of accommodation through the processes of presbyopia, which is then rendered complete with the removal of the crystalline lens. Modern posterior chamber intraocular lenses (PC IOLs) provide good visual acuity with biocompatibility, but provide almost no accommodation for pseudophakic eyes. This problem of remaining presbyopia has been addressed to some degree by various methods which include the use of bifocal and diffractive multifocal IOLs (Gray and Lyall, 1992; Lane *et al.*, 2006), refilling the capsular bag with an inflatable endocapsular balloon (Nishi *et al.*, 1991) or biocompatible silicone gel (Parel *et al.*, 1986), scleral expansion surgery (Schachar, 1992; Mathews, 1999), zonal photorefractive keratectomy (Vinciguerra *et al.*, 1998) and decentred laser *in situ* keratomileusis (LASIK; Bauerberg, 1999).

Multifocal IOLs have been noted to give effective distance and near vision (Gray & Lyall, 1992; Javitt and Steinert, 2000; Lane *et al.*, 2006), but can present significant symptoms such as reduced contrast sensitivity (Schmitz *et al.*, 2000; Kamlesh *et al.*, 2001), glare and haloes (Pieh *et al.*, 2001). Multifocal IOLs provide more than one focal length simultaneously; therefore, the quality of the retinal image is worse than that produced by a monofocal lens (Steinert *et al.*, 1999). As a result of this loss of image quality, there has been increased interest in producing pseudophakic accommodation.

AIOLs would normally be inserted following standard cataract surgery, including the production of a capsulorhexis, the removal of the crystalline lens and the insertion of the IOL into the empty capsular bag. The AIOL would then rely on some part of the eyes accommodative physiology to cause a change in refraction with accommodative effort; this may be in the form of ciliary muscle contraction, capsular bag elasticity or pressure from the vitreous. There exist a number of different AIOLs which have been designed to rely on a variety of different mechanisms of action (Dick, 2005; Findl, 2005; Glasser, 2006; Menapace *et al.*, 2007; Doane and Jackson, 2007; Glasser, 2008). They can be broadly classified as single-optic AIOLs which are designed to undergo anterior translation of the optic, dual-optic AIOLs that are designed to undergo an increase in separation of the two optics, or AIOLs which increase in curvature to produce and optical change in power with accommodative effort.

1.11.1 Single-optic AIOLs

Currently, there are a number of single-optic AIOLs which are either licensed for use in the United States (US) or Europe, or are still undergoing clinical trials. These lenses include the Eyeonics *Crystalens AT-45* and *AT-50* (with a 4.5 and 5.0 mm diameter optic, respectively; Aliso Viejo, California, USA), *Tetraflex KH3500* (Lenstec, St. Petersburg, Florida, USA), HumanOptics *ICU* (Erlangen, Germany), Bausch & Lomb *OPAL* (Rochester, New York, USA), Acuity *C-Well* (OrYehuda, Israel), AMO/Quest Vision lens (Santa Ana, California, USA) and Morcher *BioComFold 43E* (Stuttgart, Germany; Tonekaboni and Whitsett, 2005; Dick and Dell, 2006; Beiko, 2007; Doane and Jackson, 2007; Glasser, 2008). The *Crystalens AT-45* and *AT-50* are approved for clinical use in the USA by the Food and Drug Administration (FDA). The Lenstec *Tetraflex* is undergoing US FDA clinical trials. The Morcher *BioComFold 43E*, Human Optics *ICU* and Lenstec

Tetraflex have been, or are being used clinically in Europe. The other IOLs are in the research and development stage, or have had limited clinical use (Glasser, 2008).

Not all of these AIOLs are designed to work in the same manner. The *Crystalens* has hinged plate haptics and is intended to be implanted into the capsular bag in a posteriorly vaulted position with the optic against the anterior vitreous face. It is proposed that post-surgical capsular fibrosis seals the AIOL within the capsule, thus creating a single diaphragm against the vitreous face. The manufacturer advocates that an increase in vitreous pressure during accommodation (Coleman, 1970) causes a temporary forward movement of the optic. The *Tetraflex* utilises the same principal, but uses a flexible plate haptic (as opposed to hinged haptics) to facilitate forward movement of the AIOL. The other designs rely on a decrease in capsular bag diameter in accordance with the natural mechanism of accommodation. Such a decrease produces a lever action on the haptics, propelling the optic anteriorly (Glasser, 2008). The accommodative results for these lenses are outlined in Table 1.1.

1.11.2 Dual-optic AIOLs

Dual-optic AIOLs were first developed in the 1990s (Hara *et al.*, 1990). More recently, the Sarfarazi Elliptical Accommodative IOL (Sarfarazi, 2006) and the Synchrony Dual Optic Accommodative IOL (Visiogen, Irvine, California, USA) have been developed (McLeod *et al.*, 2003; McLeod, 2006; McLeod *et al.*, 2007; Ossma *et al.*, 2007). These AIOLs fill the capsular bag but retain a fluid space between the two optics. They have a high positive bi-convex anterior surface (approximately 32 D) and a weaker negative concave posterior optic (approximately 12 D) joined by sprung haptics (Sarfarazi, 2006; McLeod, 2006; McLeod *et al.*, 2007). These haptics are designed to keep the two optics separated and allow the optics to move with respect to each other from the capsular forces during accommodation. Implantation of such lenses is designed to follow standard cataract surgery, with the AIOL retaining the natural dimensions of the capsular bag.

Theoretical calculations indicate accommodative outcomes of 2.0 to 2.5 D for a change in axial separation of the optics from 0.5 to 1.0 mm (Sarfarazi, 2006; McLeod, 2006; McLeod *et al.*, 2007). The mode of action follows the natural process of accommodation, whereby zonular tension is released causing the equatorial diameter of the capsular bag to decrease

under its own elastic properties. The capsule acts on the spring haptics causing the anterior optic to translate forwards with respect to the relatively stationary posterior optic (McLeod *et al.*, 2007). Possible caveats to the success of these lenses include loss of capsular elasticity caused by fibrosis, lens epithelial cellular proliferation, capsular shrinkage and achieving the correct post-operative refraction. Nd:YAG laser capsulotomy may be contraindicated due to the detrimental effects it will have on the integrity of the capsular bag (Glasser, 2008).

Study	AIOL	Time point	N (eyes)	Methods	Accommodation (D)
Langenbucher <i>et al.</i> (2003)	1CU	23 months	23	PlusOptix PowerRefractor videorefractometry [Streak retinoscopy] Defocusing*	1.00 ± 0.44 (range 0.75 to 2.13) [0.99 ± 0.48 (range 0.13 to 2.00)] {1.60 ± 0.55 (range 0.50 to 2.56)} 1.46 ± 0.53 (range 1.00 to -2.50)*
Claoué (2004)	1CU	6 to 18 months	9	Dynamic retinoscopy	0.44
Dogru <i>et al.</i> (2005)	1CU	3 months	22	Nidek AA-2000 Accommodometer	0.50 ± 0.44 (range 0.50 ± 1.00)
Wang <i>et al.</i> (2005)	1CU	7 days 30 days 90 days	94	Subjective push-up [Defocusing]	1.96 ± 0.63 (range 0.75 to 4.50), [1.74 ± 0.59 (range 0.75 to 4.50)] 1.68 ± 0.47 (range 0.75 to 3.25), [1.89 ± 0.54 (range 0.75 to 3.25)] 1.77 ± 0.53 (range 0.75 to 2.75), [1.66 ± 0.50 (range 0.75 to 2.75)]
Wolffsohn <i>et al.</i> (2006a)	1CU	4 months 2 years	12	Stimulus response (SRW-5000 autorefractor; static* and dynamic**) [PlusOptix PowerRefractor] {Subjective push-up}	0.72 ± 0.38* (range 0.17 to 1.16) 0.71 ± 0.47** (range 0.31 to 1.56) [0.32 ± 0.23 (range 0.10 to 0.75)] {2.24 ± 0.42 (range 1.50 to 2.50)} Subjective decrease by -0.25 ± 0.59 (at 2 years)
Wolffsohn <i>et al.</i> (2006b)	Tetraflex	6 months	28	Stimulus response (SRW-5000 autorefractor) [Subjective push-up]	0.39 ± 0.53 (range 0.00 to 2.69) [3.10 ± 1.60 (range 1.00 to 6.40)]

Macasai <i>et al.</i> (2006)	Crystalens AT-45	6 months	112	Dynamic retinoscopy [Defocusing] {Near point of accommodation}	2.42 ± 0.39 [1.74 ± 0.48] {4.78}
Hancox <i>et al.</i> (2006)	1CU	18 to 24 months	20	Defocusing [Subjective push-up]	1.09 ± 0.58 [2.31]
Ossma <i>et al.</i> (2007)	Synchrony dual optic	6 months	24	Defocusing	3.22 ± 0.88 (range 1.00 to 5.00)
Sanders and Sanders (2007)	Tetraflex	6 months	74	Subjective push-up	>1.0 = 100%, >2.0 = 75.7%, >2.5 = 71.6%, >3.0 = 18.9%
Harman <i>et al.</i> (2008)	1CU	3 months	82	Near point of accommodation [Defocusing]	3.13 (range 2.50 to 4.00) [2.85 (range 2.40 to 4.00)]

Table 1.1 Studies which have measured amplitudes of accommodation in accommodating intraocular lenses, after implantation into human subjects. Shown are the investigators' name and year of each study, the AIOL assessed, the time post-implantation that the lenses were assessed, the number of eyes studied, the method of measuring amplitude of accommodation, and the amplitude of accommodation (mean ± standard deviation plus range, where applicable).

1.11.3 Curvature change AIOLs

The changes in curvature of the crystalline lens surfaces are the primary correlates in the accommodative response (Garner and Yap, 1997; Bennett and Rabbetts, 2007). They incite relatively large dioptric changes for small physical alterations (Glasser *et al.*, 2006). It follows, that any AIOL that can employ this technique of changing curvature will provide a very efficient accommodative system. A number of different designs are currently under development, or have seen limited animal or human trials. A recent review by Glasser (2008) gives a detailed account of these new designs. A brief review is given here.

The PowerVision *FluidVision* IOL (Belmont, California, USA) is a fluid filled IOL with hollow haptics. It is designed to sit inside the capsular bag following standard cataract surgery. During accommodation, release of zonular tension results in the elastic forces of the capsular bag applying pressure to the hollow haptics of the IOL. This in turn displaces fluid from the haptics into the optic causing an increase in the anterior surface curvature.

The Medennium *SmartLens* (Irvine, California, USA) was developed a number of years ago. It adheres to the basic principle of the crystalline lens in terms of its dimensions and biconvex surfaces. It is manufactured from a soft thermoplastic hydrophobic acrylic material, with properties (refractive index, surface curvature and thickness) that can be altered during the moulding process. The lens can be rolled into a 2.0 mm rod at room temperature and subsequently chilled to maintain this shape. On injection into the capsular bag, it quickly returns to its natural shape, and in theory, should respond to the accommodative forces of the eye in a similar manor to the natural lens.

Capsular refilling has been the subject of a number of studies. The crystalline lens is removed through a small (1.0 to 2.0 mm) peripheral capsulorhexis which is subsequently plugged and filled with a clear liquid polymer. Work has been done on rabbits (Kessler, 1964; 1966; Agarwal, 1967; Gindi *et al.*, 1985; Nishi, 2003; Norrby *et al.*, 2006), primates (Gindi *et al.*, 1985), dogs (Gindi *et al.*, 1985), human cadaver eyes, enucleated pig, rabbit and cat eyes (Parel *et al.*, 1986; Nishi *et al.*, 1997; 1998) and in monkeys eyes (Haefliger *et al.*, 1987; Haefliger and Parel, 1994; Nishi and Nishi, 1998; Koopmans *et al.*, 2006). Refilling of the capsule with an endocapsular balloon, and filling the balloon with a silicone polymer, is a variation on this method (Nishi *et al.*, 1992; 1993; Nishi and Nishi,

1998). Results are limited due to the high incidence of post-operative capsular opacification (Haefliger *et al.*, 1987; Haefliger and Parel, 1994). Some monkey studies have reported as little as 20 to 40 % of accommodative ability being restored after this technique (Nishi *et al.*, 1993; Nishi and Nishi, 1998; Koopmans *et al.*, 2006).

The *NuLens* (Herzliya, Pituah, Israel; Ben-Nun and Alió, 2005; Ben-Nun, 2006) is based on the accommodative mechanism of the cormorant eye, where constriction of the muscular iris sphincter causes anterior lenticonus (Levy and Sivak, 1980). The optic of the IOL consists of a transparent annulus, behind which, is a soft gel. The arrangement is completed with a piston-like solid base behind the gel. Pressure from this piston causes the gel to 'balloon' through the anterior annulus, causing a change in anterior curvature. The lens is held outside the capsule, with haptics attaching it to the ciliary sulcus. The empty capsular bag, post-cataract extraction, is collapsed to form a single diaphragm; this is placed against the posterior piston. The IOL works in opposition to the normal method of natural accommodation. In the normally relaxed state, zonular tension holds the capsule taught, applying pressure to the piston and causing the previously described curvature change. The opposite is true for ciliary muscle contraction under 'normal' accommodative effort. This *modus operandi* presents significant challenges to the patient, not only in learning to accommodate in opposition to natural intuitive processes, but also to overcome the near vision triad, which includes convergence with accommodation. It has been suggested that humans are capable of overcoming these neurological processes (Ben-Nun and Alió, 2005).

1.12 General summary

The processes of both accommodation and presbyopia remain the subject of much research and debate. The exact mechanism of each remains equivocal, with some authors purporting theories in opposition to those which are widely held (Schachar *et al.*, 1996).

Hitherto, the biometric analysis of accommodation has been limited to quantifying physical distances and component changes (Drexler *et al.*, 1997; Garner and Yap, 1997; Koretz *et al.*, 1997b; Dubbleman *et al.*, 2001; Dubbelman and van der Heijde, 2001; Dubbelman *et al.*, 2002; Kirschcamp *et al.*, 2004; Koretz *et al.*, 2004; Strenk *et al.*, 2004; Baikoff *et al.*, 2004; 2005a; 2005b; Dubbelman *et al.*, 2005; Mallen *et al.*, 2006; Jones *et al.*, 2007; Tsorbatzoglou *et al.*, 2007). A recent study by Kirshcamp and colleagues (2004) utilised the assessment of component contribution to vergence change with accommodation; a method originally enunciated by Leary (1981) and Erickson (1984).

Recent studies into the biometric changes associated with age and accommodation have provided a new schematic eye, which is acquiescent to alterations with age and accommodation (Norrby, 2005). Based on corrected Scheimpflug images from a large cohort (Dubbelman and van der Heijde, 2001; Dubbelman *et al.*, 2001; 2002; 2005), it provides an ideal opportunity to assess the accommodative vergence contribution for each component in the visual system. Assessment of accommodation in this way will provide a new appreciation of the role each component plays in the accommodative reflex. Further, the introduction and use of AIOLs in recent years has become the focus of many studies (Table 1.1). These lenses have seen variable success with regard to accommodative output. The use of the schematic eye allows investigation into the exact mechanism of the focus shift principle.

The use of Optical Coherence Tomography (OCT) in the study of phakic and pseudophakic accommodation is new and relatively limited (Baikoff *et al.*, 2004; 2005a; 2005b; Richdale *et al.*, 2008). The application of this technique to both phakic and pseudophakic patients will qualify its use in a clinical setting, and add further evidence as to the exact mechanism of accommodation.

This chapter gives an introduction to the themes of this thesis. Each subsequent chapter will give a fuller appreciation of the literature pertinent to the topic in question.

1.13 Aims of the thesis

The main aim of this thesis is to investigate both phakic and pseudophakic accommodation. In particular, the examination of ocular component contributions to changes in vergence with accommodation. This will be approached using schematic modelling to reveal the role of each component in human ocular accommodation under a variety of conditions, and to extend the biometric analysis of human phakic accommodation by employing a new imaging technique (Anterior Segment OCT).

Further, the correction of presbyopia is a prominent area of current research. The use of AIOLs in this process is relatively new and has shown limited success. This study aims to examine the process of accommodation using both schematic modelling and AS-OCT, and to present theories as to why their success is attenuated at this time.

Ultimately, this research will provide information to allow a greater understanding of the mechanism of accommodation, and which may influence the manufacturers' of AIOLs, so that they may approach the ultimate goal of effective pseudophakic accommodation.

CHAPTER 2

COMPONENT VERGENCE CHANGES WITH ACCOMMODATION

2.1 Introduction

Refractive errors are essentially the expression of a dysfunction in a system of light vergences. Historically, vergence ray tracing has considered the nature of the surfaces within an optical system and expressed them as a dioptric value (Bennett and Rabbetts, 2007). The system outlined does not describe satisfactorily the function of these surfaces under any condition other than when receiving plane, parallel light. It is also true, that in considering secondary and tertiary surfaces within the same system, the first surface receiving plane, parallel light, will express its dioptric value as a product of the vergence of the incident light; it being brought to the principal focus. Any other surfaces in the optical system will modify these secondary rays. Surface powers under these conditions will not express the vergence of the emergent light from any given surface.

Leary (1981) proposed that the optical system could be evaluated in terms of the vergence contributions at each surface within the model, stating that the whole optical system can be described in terms of the dioptries of vergence taking place within it. Such a suggestion is contrary to the original method of listing dioptric powers and surface positions (Ledley *et al.*, 1966). The major advantage of Leary's technique was to show unequivocally, the contribution that each component makes to the final vergence; the back vertex power of the system. Leary suggested the expression of these component vergences as percentage contributions to the final back vertex power, to allow a fuller understanding of the working of the system.

Erickson (1984) subsequently modified Leary's method, which had hitherto considered back vertex power by tracing the vergence changes through the eye, beginning with parallel incident light at the anterior corneal surface. The vergence of light exiting the posterior lens surface and travelling towards the plane of the retina was there upon, equal to the back vertex power of the anterior segment. Erickson suggested that this method was

flawed, as it failed to account for the optical effects of the vitreous chamber; this being a major contributor to refractive status. Erickson proposed that this could be overcome in two ways. Firstly, if the refractive status of the eye is known, light can be traced from the far point of the eye instead of from optical infinity, as suggested by Leary. The second method is to assign a divergent dioptric value to the vitreous chamber and perform a reverse ray trace, finishing at the anterior plane of the eye. Erickson gives the calculation used to assign this vitreous chamber vergence (V_V):

$$V_V = n_V / d_V, \quad (2.1)$$

where n_V and d_V are the refractive index and the depth of the vitreous chamber, respectively (Erickson, 1984). The vergence exiting the cornea in Erickson's method is equivalent to the refractive status of the eye.

There appears to have been only one study which has considered reverse ray tracing with regard to changes in accommodation by employing the method advocated by Erickson. Kirschcamp and co-workers conducted a study into ocular surface radii of curvature, axial separations and alignment in accommodated and disaccommodated (relaxed) eyes using phakometric techniques (Kirschcamp *et al.*, 2004). Kirschcamp and colleagues utilised the ocular component data found using these methods, and performed vergence ray tracing. Differences in vergence contributions of each ocular component were compared in eyes observing a sharp edge placed 25.0 cm from the subject (representing a 4.0 D accommodative stimulus) and eyes under cycloplegia (0.5 % cyclopentolate), to determine what effects accommodation had on the system.

The authors subtracted the vergence contributions found in accommodated eyes from those found in relaxed eyes to provide a measure of the change in vergence contribution that took place with accommodation. The study showed that the anterior chamber depth and crystalline lens thickness decreased and increased, respectively, by the same statistically significant amount (0.2 mm; $p < 0.01$). However, the decrease in the anterior chamber depth brought about a statistically significant decrease in vergence (-1.5 D; $p < 0.01$), whilst the increase crystalline lens thickness elicited a non-significant reduction of -0.2 D ($p = 0.09$). The major correlates in vergence change with accommodation were shown to

be the crystalline surface radii. The anterior crystalline lens surface induced a positive vergence change of 3.1 D, the posterior surface 2.1 D; both of which were statistically significant. Both the cornea and vitreous produced minimal non-significant changes in vergence contribution.

2.1.1 Schematic eyes

The principal reasoning behind schematic eyes is to allow theoretical studies into the function of the eye as an optical instrument (Bennett and Rabbetts, 2007). Historically, there have been a number of schematic eye models which have been adapted and improved on over time (Bakaraju *et al.*, 2008). Swaine (1921) gives a good account of early schematic eyes and more recently, Popiolek-Masajada and Kasprzak (2002) and Bakaraju *et al.* (2008) have produced comprehensive reviews of many others. A more complete account of these schematic eyes can be found in Chapter 1 of this thesis.

Recent studies by Dubbelman and co-workers have determined intraocular spacings and surface shapes by means of corrected Scheimpflug images in a large number of subjects of different ages at several levels of accommodation (Dubbelman and van der Heijde, 2001; Dubbleman *et al.*, 2001; 2002; 2005). Norrby (2005) compiled an eye model from these studies. Interestingly, the resultant Dubbelman eye model contains mathematical corrections for a number of optical components as a function of both age and accommodation. The appropriate values for the Dubbelman eye model derived by Norrby are summarised in Table 2.1. The model also contains a spectacle lens with a vertex distance of 12.0 mm, central thickness of 2.0 mm, refractive index of 1.5 and a posterior surface power of -6.0 D in air (refractive index 1.0). To focus the ray being traced, the anterior lens surface power is varied to give the refractive correction.

Element	Radius or thickness (mm)	Reference
Anterior corneal surface	7.87	Dubbelman <i>et al.</i> , (2002)
Corneal thickness	0.574	Dubbelman <i>et al.</i> , (2002)
Posterior corneal surface	6.40	Dubbelman <i>et al.</i> , (2002)
Anterior chamber depth	$3.87 - 0.010A - D(0.048 - 0.0004A)$	Dubbelman <i>et al.</i> , (2001)
Anterior lens surface (at the apex)	$1/[1/(12.7 - 0.058A + 0.0077D)]$	Dubbelman <i>et al.</i> , (2005)
Lens thickness	$2.93 + 0.0236A + D(0.058 - 0.0005A)$	Dubbelman <i>et al.</i> , (2001) Dubbelman <i>et al.</i> , (2003)
Posterior lens surface (at the apex)	$1/[1/(5.9 - 0.0013A) + 0.0043D]$	Dubbelman <i>et al.</i> , (2005) Corrections in Bennett and Rabbetts (2007; Annex 12)

Table 2.1 The Dubbelman model eye as compiled by Norrby (2005). Shown are the component radii and thicknesses used, as well as the equations used to calculate them, as derived from the studies of Dubbelman and colleagues. The anterior chamber depth includes corneal thickness. 'A' is the age in years and 'D' is the accommodation in dioptres. Corrections to posterior lens surface are found in Bennett and Rabbetts (2007; Annex 12).

Medium	Refractive index	Reference
Cornea	1.376	Gullstrand (1909)
Aqueous and vitreous	1.336	Gullstrand (1909)
Lens (equivalent refractive index)	$1.441 - 0.00039A + 0.0013D$	Dubbelman <i>et al.</i> , (2001) Dubbelman <i>et al.</i> , (2005)

Table 2.2 Refractive indices of the Dubbelman eye model. 'A' is the age in years and 'D' the accommodation in dioptres. The lens assumes an equivalent refractive index that varies with age and accommodation. This is due to the lens paradox, whereby the refractive power of the lens compensates for the increase in lens convexity with age (Dubbelman and van der Heijde, 2001). After Norrby (2005).

2.1.2 Aims

The aim of this study is to explore the contribution each ocular component makes to the optical system in terms of vergence change with accommodation. This is to be done using a new schematic eye (Norrby, 2005) which accounts for age and accommodative stimulus. It is hoped that the work of Kirschcamp and colleagues can be expanded upon to investigate the apparent reduction in vergence contribution for some ocular components, which have hitherto been thought to promote the accommodative facility of the eye. It may therefore be possible to suggest improved methods of investigating optical changes associated with accommodation.

2.2 Methods

Utilising the Dubbelman eye model (Norrby, 2005), a reverse step-along ray trace was created using Microsoft *Excel* 2003 (Microsoft *Windows*[®] *XP*). The paraxial wavefronts were traced from the retina to the far point using the method advocated by Erickson (Erickson, 1984). In Erickson's original paper, he attributes symbols to various aspects of the ocular components which are contrary to a more standard practice of equation nomenclature advocated by Bennett and Rabbetts (2007), amongst others. This chapter and subsequent chapters will adopt this more conventional method.

The refractive status of the eye was calculated for the ages of 20, 30, 40 and 50 years, and at accommodation levels of 0.0 to 4.0 dioptres in steps of 1.0 D. These ages were chosen to correspond with the decades closest to the age ranges measured by Dubbelman and co-workers, who included subjects between the ages of 16 to 51 years (Dubbelman *et al.*, 2003), 16 to 62 years (Dubbelman *et al.*, 2002), and 16 to 65 years (Dubbelman and van der Heijde, 2001; Dubbelman *et al.*, 2001), respectively. Longitudinal studies also suggest that individual objective amplitudes of accommodation fall almost linearly with age to reach zero at approximately 50 years of age (Hofstetter, 1965; Ramsdale and Charman, 1989).

The step-along reverse ray-trace from the retinal plane to the anterior corneal plane is shown below.

2.2.1 Vergence from the vitreous chamber (L_8)

The vitreous chamber depth (d_4) is calculated from the sum of the other axial ocular distances (d_{1-3}) subtracted from axial length of the eye. The axial length of the model was set to 23.267 mm; to correspond with emmetropia at 20 years of age.

$$d_4 = 23.267 - (d_1 + d_2 + d_3). \quad (2.2)$$

Where d_1 is the corneal thickness, d_2 the anterior chamber depth, d_3 the thickness of the crystalline lens, and d_4 the length of the vitreous chamber.

A value for the vergence attributed to the vitreous chamber is adopted from Erickson (1984). Equation 2.1 has been modified to the standard nomenclature, and is thus labelled Equation 2.3.

$$L_8 = 1000n_4 / (-d_4 + 0.25). \quad (2.3)$$

Where L_8 is the vergence from the vitreous chamber and n_4 the refractive index of the vitreous (Table 2.2). The receptor layer is included in the Dubbelman model as derived by Norrby, and is given the value of 0.25 mm. The vitreous chamber depth is given a negative value due to the sign convention.

2.2.2 Vergence at the posterior crystalline lens surface (L_7)

The diverging wavefronts from the vitreous chamber are modified by the posterior crystalline lens surface.

$$F_4 = [1000(n_4 - n_3)] / r_4. \quad (2.4)$$

Where F_4 is the power of the posterior crystalline lens surface, n_3 the equivalent refractive index of the crystalline lens (Table 2.2) and r_4 the posterior crystalline lens surface radius (Table 2.1).

$$L_7 = L_8 + F_4, \quad (2.5)$$

where L_7 is the vergence at the posterior crystalline lens surface.

2.2.3 Vergence at the anterior crystalline lens surface (L_6)

Equation 2.6 is used to derive the vergence at the anterior crystalline lens surface once the wavefronts of light have been modified by crystalline lens matrix.

$$L_6 = 1000n_3 / (1000n_3 / L_7 - d_3). \quad (2.6)$$

Where L_7 is the vergence at the posterior crystalline lens surface, n_3 is the equivalent refractive index of the crystalline lens (Table 2.2) and d_3 the crystalline lens axial thickness (Table 2.1).

2.2.4 Vergence at the posterior aqueous chamber (L_5)

$$F_3 = [1000(n_3 - n_2)] / r_3. \quad (2.7)$$

Where F_3 is the power of the anterior crystalline lens, n_2 is the refractive index of the aqueous humour (Table 2.2) and r_3 is the radius of the anterior crystalline lens surface (Table 2.1). Equation 2.8 is used to calculate the vergence as it is modified by the anterior crystalline lens surface.

$$L_5 = L_6 + F_3. \quad (2.8)$$

2.2.5 Vergence at the anterior aqueous chamber (L_4)

The vergence of light passing through the aqueous chamber is modified as shown in Equation 2.9.

$$L_4 = 1000n_2 / (1000n_2 / L_5 - d_2). \quad (2.9)$$

Where L_5 is the vergence at the posterior aqueous chamber, n_2 is the refractive index of the aqueous humour (Table 2.2) and d_2 the anterior chamber depth (Table 2.1).

2.2.6 Vergence at the posterior corneal surface (L_3)

Equation 2.10 was used to calculate the power of the posterior corneal surface.

$$F_2 = [1000(n_2 - n_1)] / r_2. \quad (2.10)$$

Where F_2 is the power of the posterior corneal surface, n_1 is the refractive index of the cornea (Table 2.2) and r_2 is the radius of the posterior corneal surface. Equation 2.11 was used to calculate the vergence of light leaving the anterior chamber and entering the posterior corneal surface.

$$L_3 = L_4 + F_2. \quad (2.11)$$

2.2.7 Vergence at the anterior corneal surface (L_2)

The vergence of light passing through the cornea is modified as shown in Equation 2.12.

$$L_2 = 1000n_1 / (1000n_1 / L_3 - d_1). \quad (2.12)$$

Where L_3 is the vergence at the posterior corneal surface, n_1 is the refractive index of the cornea (Table 2.2) and d_1 the corneal thickness (Table 2.1).

2.2.8 Vergence of light leaving the eye: The back vertex power (L_1)

Equation 2.13 was used to calculate the power of the anterior corneal surface.

$$F_1 = [1000(n_1 - 1)] / r_1. \quad (2.13)$$

Where F_1 is the power of the anterior corneal surface, n_1 is the refractive index of the cornea (Table 2.2), 1 is the refractive index of air and r_1 is the radius of the anterior corneal surface. Equation 2.14 was used to calculate the vergence of light leaving the eye, hence the back vertex power.

$$L_1 = L_2 + F_1. \quad (2.14)$$

The vergence contribution of each refractive surface or axial distance was calculated by subtracting the entrance vergence from the exit vergence of the interface; this value was expressed in dioptres. Vergence contributions found under accommodative stimulus were subtracted from those found in under disaccommodation to provide a measure of the change in vergence contribution that took place with accommodation.

The magnitude of the effect each interface contributed to vergence change was calculated; this is expressed as the ratio of dioptric to axial position or radius change. The fraction is expressed in dioptres per millimetre (D/mm), and is termed the Vergence Contribution Factor (VCF).

2.3 Results

2.3.1 Paraxial versus off-axis modelling

Firstly, to qualify the method of using step-along vergence ray tracing, it must be noted that the Dubbelman eye model (Norrby, 2005) has a number of characteristics which must be made explicit. The schematic eye extracted from the papers of Dubbelman *et al.* (Table 2.1) is a wide angled model with aspheric surfaces and a finite pupil size. Vergence step-along ray tracing exploits paraxial rays, thus ignoring off axis surface contributions (Bennett and Rabbetts, 2007). It is necessary to compare both paraxial and aspheric models to explain any disparity or unexpected outcomes which may arise when considering the paraxial model alone. Accommodation and normalised refractive status were plotted for the paraxial and Dubbelman models; the latter with a 2.0, 4.0 and 6.0 mm pupil (Figures 2.1 to 2.4).

Figure 2.1A shows the data for the paraxial model. The normalised refractive status is approximately equivalent to the accommodation; the relationship is linear, with the younger eye producing a slightly greater output (4.5 D) than the older eye (4.1 D). Figures 2.1B to 2.1D show the data for the aspheric model using a 2.0, 4.0 and 6.0 mm pupil, respectively. The disparity between the accommodation and refractive status is greater between the ages of 20 and 50 years when compared to the paraxial model, however, the magnitude of the trend is inversely proportional to pupil size. There is also a negative relationship between refractive status output per unit accommodation and pupil size; a larger pupil producing a lower dioptric output.

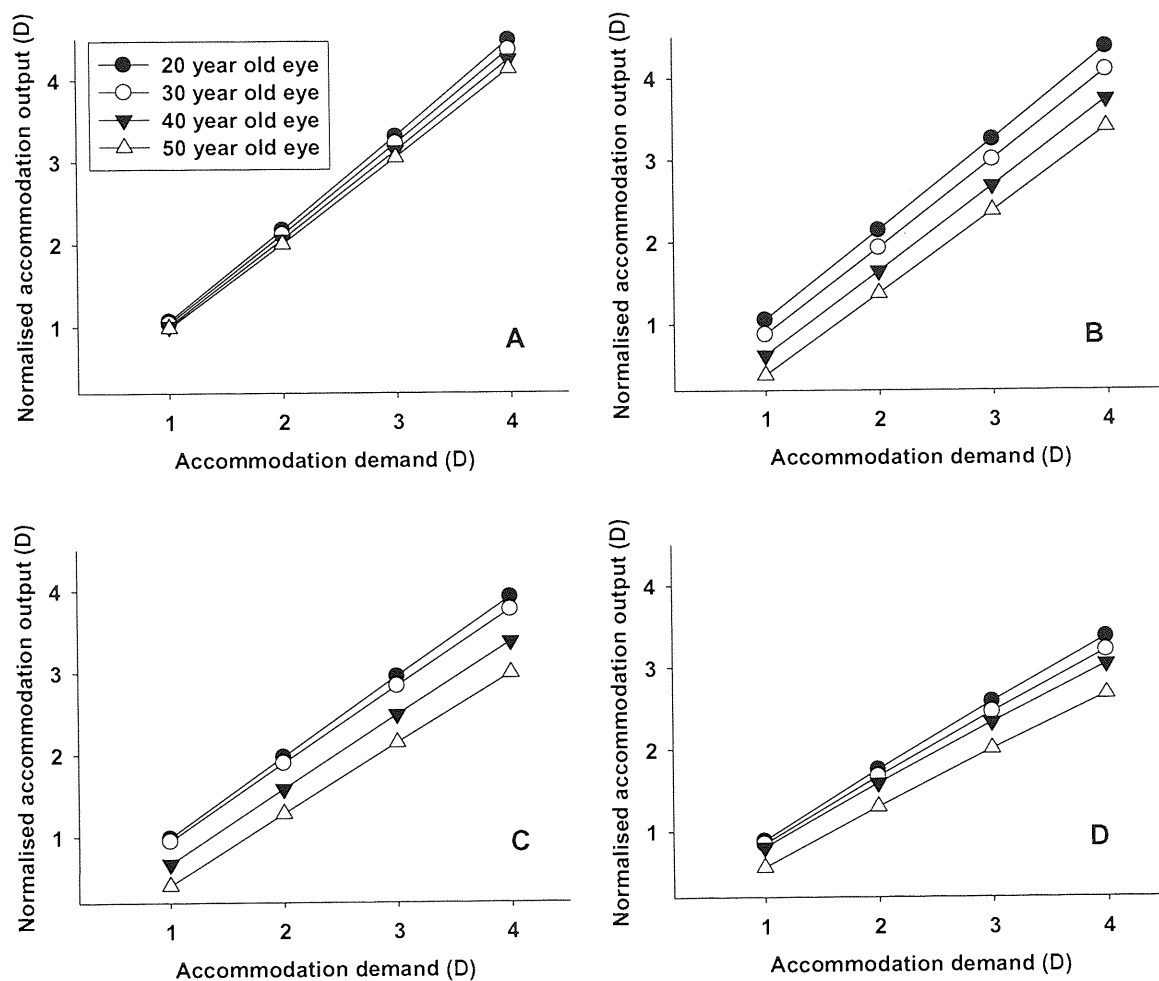


Figure 2.1 Normalised refractive status changes with accommodative demand for eyes of 20 to 50 years, in decade increments. Figure 2.1A represents the paraxial model, Figure 2.1B the aspheric model with a 2.0 mm pupil, Figure 2.1C the aspheric model with a 4.0 mm pupil and Figure 2.1D the aspheric model with a 6.0 mm pupil. The younger eye produces a greater refractive outcome than the older eye. The relationship between accommodation and normalised refractive status is linear for all models. There is a greater disparity between accommodation and normalised refractive status with age in the aspheric model compared to the paraxial model (A); the magnitude of the trend is inversely proportional to pupil size. The paraxial model elicits a greater refractive output per unit of accommodation than the aspheric models; this output diminishes with increasing pupil size.

2.3.2 Component changes with accommodation

Table 2.3 displays the component change in millimetres for each ocular component with accommodation from 0.0 to 4.0 D, in 1.0 D increments. The ocular components are the vitreous chamber depth, posterior crystalline lens radius, crystalline lens thickness, anterior

crystalline lens radius, anterior chamber depth, posterior corneal radius, corneal thickness and anterior corneal radius.

Vitreous chamber depth, posterior crystalline lens curvature, crystalline lens thickness and anterior crystalline lens curvature all increase with accommodation; becoming longer, increasing in diameter or assuming a more curved appearance. All corneal components show no alteration with accommodation; anterior chamber depth displays a negative relationship. The anterior crystalline lens radius shows the greatest change, decreasing by a factor of approximately three, over a four dioptre range of accommodation stimulus. Anterior chamber depth and lens centre thickness alter by a similar magnitude in contrary directions; anterior chamber depth decreases while crystalline lens thickness increases with accommodation.

Table 2.4 illustrates the component vergence change, in dioptres per unit accommodation. All ocular refractive elements exhibit a positive change to the initial diverging ray from the retina with the exception of the posterior corneal surface. However, when considering changes in vergence with accommodation, all axial distance changes decrease the convergent effect of the retinal ray; all surface radii changes causing the opposite and far greater convergent result. As in Table 2.3, the primary correlate is the anterior crystalline lens surface accounting for approximately 80% of the overall refractive outcome (Figure 2.2F). Anterior chamber depth decreases vergence with accommodation to a greater degree than crystalline lens thickness (Figure 2.2B and 2.2C). Corneal thickness also has a small negative effect on outcome refractive status despite remaining static (Figure 2.2D). Further, corneal radii have no effect on vergence changes. Older eyes display smaller contributions to vergence change by all ocular components with the exception of the crystalline lens (Figure 2.2C); overall refractive status is also reduced.

The unique property of expressing contributions to accommodation made by ocular surfaces and axial distances in terms of their vergence is that these powers are additive (Leary, 1981; Erickson, 1984). It is therefore possible to show the contribution made by each factor to the overall refractive status. Table 2.5 summarises these contributions, further highlighting the points discussed previously.

Age	A (D)	Component change (mm)				
		Vitreous depth	Posterior lens radius	Lens thickness	Anterior lens radius	Anterior chamber depth
20	1	0.008	-0.134	0.048	-0.942	-0.040
	2	0.016	-0.261	0.096	-1.741	-0.080
	3	0.024	-0.383	0.144	-2.429	-0.120
	4	0.032	-0.499	0.192	-3.026	-0.160
30	1	0.007	-0.128	0.043	-0.853	-0.036
	2	0.014	-0.249	0.086	-1.583	-0.072
	3	0.021	-0.366	0.129	-2.214	-0.108
	4	0.028	-0.477	0.172	-2.766	-0.144
40	1	0.006	-0.122	0.038	-0.768	-0.032
	2	0.012	-0.238	0.076	-1.431	-0.064
	3	0.018	-0.349	0.114	-2.008	-0.096
	4	0.024	-0.456	0.152	-2.515	-0.128
50	1	0.005	-0.116	0.033	-0.688	-0.028
	2	0.010	-0.227	0.066	-1.285	-0.056
	3	0.015	-0.333	0.099	-1.809	-0.084
	4	0.020	-0.435	0.132	-2.272	-0.112

Table 2.3 Ocular component changes for eyes aged 20 to 50 years (in decade increments) expressed in mm as a function of accommodation demand, A in dioptres (D). Both crystalline lens radii reduce with accommodation, indicating increasing curvature. Anterior and posterior corneal radii and corneal thickness show no change with accommodation demand, and are therefore not shown.

Age	A (D)	Component vergence change (D)						Total
		Vitreous depth	Posterior lens radius	Lens thickness	Anterior lens radius	Anterior chamber depth	Corneal thickness	
20	1	-0.040	0.654	-0.056	0.871	-0.315	-0.043	1.071
	2	-0.079	1.319	-0.117	1.762	-0.623	-0.087	2.175
	3	-0.119	1.996	-0.183	2.673	-0.922	-0.131	3.314
	4	-0.158	2.683	-0.255	3.605	-1.211	-0.175	4.487
30	1	-0.035	0.643	-0.075	0.847	-0.295	-0.043	1.042
	2	-0.070	1.297	-0.155	1.714	-0.584	-0.085	2.117
	3	-0.106	1.962	-0.239	2.601	-0.865	-0.129	3.225
	4	-0.141	2.638	-0.329	3.508	-1.138	-0.172	4.367
40	1	-0.031	0.632	-0.094	0.824	-0.275	-0.042	1.014
	2	-0.061	1.274	-0.192	1.667	-0.545	-0.084	2.060
	3	-0.092	1.928	-0.295	2.531	-0.808	-0.126	3.138
	4	-0.123	2.594	-0.403	3.415	-1.066	-0.168	4.249
50	1	-0.026	0.621	-0.113	0.801	-0.356	-0.041	0.986
	2	-0.052	1.253	-0.230	1.622	-0.507	-0.082	2.004
	3	-0.072	1.896	-0.352	2.463	-0.753	-0.123	3.053
	4	-0.104	2.551	-0.478	3.324	-0.994	-0.165	4.134

Table 2.4 Ocular component vergence changes for eyes aged 20 to 50 years (in decade increments) expressed in dioptres as a function of accommodation demand, A in dioptres (D). All axial distance changes result in a negative vergence change with accommodation. The crystalline lens radii are primarily responsive for positive vergence change with accommodation. Anterior and posterior corneal radii show no change with accommodation demand, and are therefore not shown.

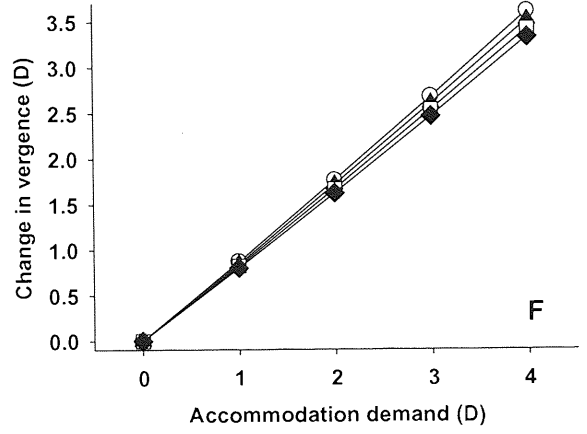
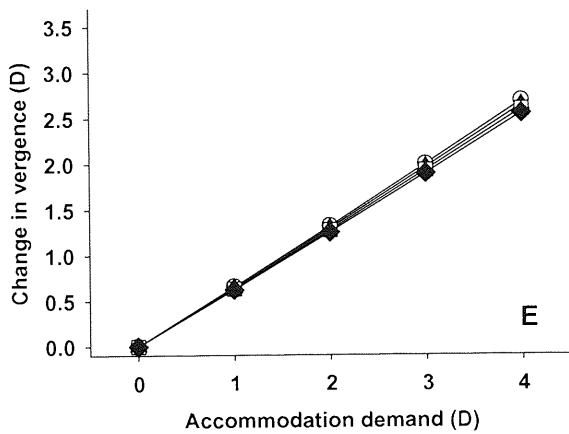
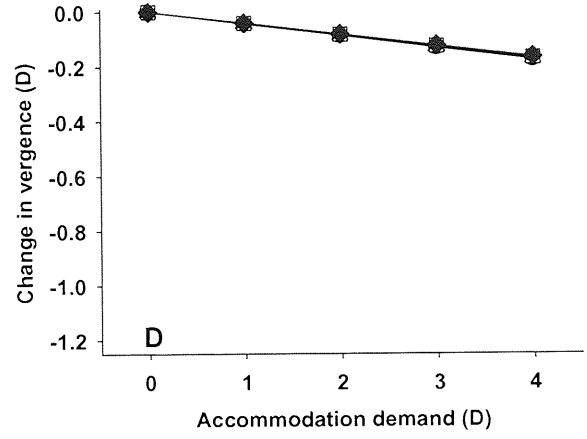
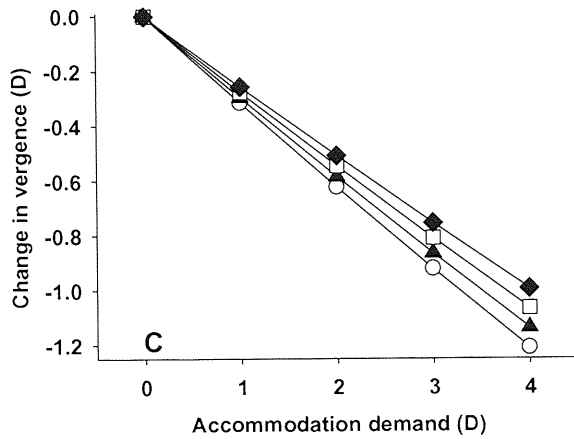
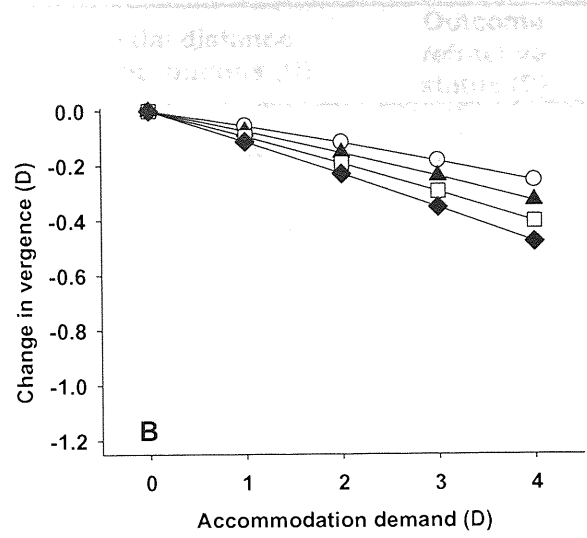
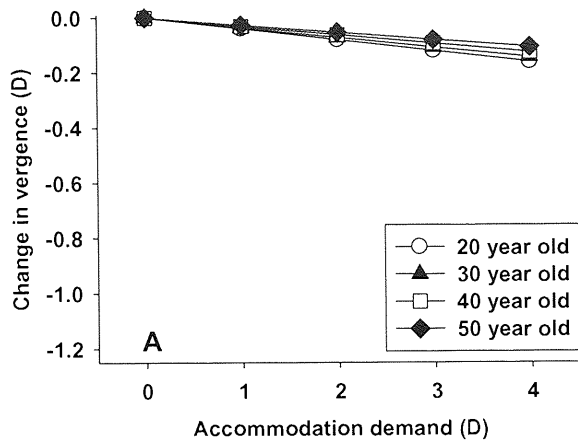


Figure 2.2 Ocular vergence changes as a function of accommodation demand for eyes aged 20 to 50, in decade increments. Figure 2.2A represents the vitreous chamber, Figure 2.2B the crystalline lens thickness, Figure 2.2C the anterior chamber depth, Figure 2.2D corneal thickness, Figure 2.2E the posterior crystalline lens radius and Figure 2.2F the anterior crystalline lens radius. The axial distances, Figures 2.2A to D, all have a negative effect on vergence change with accommodation. The primary correlate for this is anterior chamber depth (Figure 2.2C). Both crystalline lens surfaces produce positive vergence change with accommodation, the posterior surface being the most powerful (Figure 2.2F).

Age	A (D)	Surface radii contributions (D)	Axial distance contributions (D)	Outcome refractive status (D)
20	1	1.525	-0.454	1.071
	2	3.081	-0.906	2.175
	3	4.669	-1.355	3.314
	4	6.288	-1.800	4.487
30	1	1.490	-0.448	1.042
	2	3.011	-0.894	2.117
	3	4.563	-1.338	3.225
	4	6.146	-1.779	4.367
40	1	1.455	-0.441	1.014
	2	2.942	-0.882	2.060
	3	4.459	-1.322	3.138
	4	6.008	-1.759	4.249
50	1	1.422	-0.435	0.986
	2	2.875	-0.871	2.004
	3	4.359	-1.306	3.053
	4	5.875	-1.740	4.134

Table 2.5 Summary of surface radii and axial distance vergence contributions to outcome refractive status, as a function of age and accommodation. All surface radii have a positive influence on vergence change with accommodation. All axial separation changes dampen vergence change. The sum of vergence changes in the ocular system will produce total outcome refractive status.

Hitherto, the investigation into ocular changes with accommodation has been based on surface curvature and axial distance changes in millimetres, thereby showing real change. The same ocular accommodative changes have been displayed in terms of vergence change with accommodation, demonstrating how each interface modifies wavefronts of light passing through the ocular system. To illustrate this further, a ratio of the former two can be deduced, alluding to the ability each surface has to contribute to the overall refractive status. By dividing the vergence change in dioptres, by the radii/distance variation in millimetres, a useful ratio is produced and called the Vergence Contribution Factor (VCF) by the author. Table 2.6 displays this ratio and its modification with age and accommodation.

All changes in axial biometric changes with accommodation elicit negative effects on vergence change. Of these components, the anterior chamber depth has the greatest influence on vergence change with accommodation. Crystalline lens thickness changes alter the most physically yet produce less dioptric vergence change per dioptre of accommodation. The VCF of these components reflect this finding very well, with anterior chamber depth having a greater factor (7.5 to 9.1 D/mm) than the crystalline lens thickness (1.2 to 3.6 D/mm). The vitreous chamber depth alters little in terms of both biophysical and vergence change with accommodation. Corneal thickness fails to change physically with accommodation, yet it yields a small vergence change, giving it an infinitely large VCF (Figure 2.3).

The crystalline lens surface radii are solely responsible for positive vergence changes with accommodation. Of these, the anterior lens surface is the primary correlate, producing over 3.5 D of positive vergence change for a 4.0 D accommodation demand in the young eye. The posterior crystalline lens radius increases in curvature by approximately 1/6th that of the anterior radius, yet it contributes over 2.5 D of vergence change in the young eye (Figure 2.4). The VCF for these components is therefore quite in opposition to what would normally be expected. That is to say that the anterior crystalline lens radius has a smaller VCF (0.9 to 1.4 D/mm; Table 2.6) than the posterior lens radius (4.9 to 5.9 D/mm; Table 2.6).

Age	A (D)	Component change (D/mm)					
		Vitreous depth	Posterior lens radius	Lens thickness	Anterior lens radius	Anterior chamber depth	Corneal thickness
20	1	4.942	4.898	1.165	0.925	7.887	∞
	2	4.945	5.056	1.220	1.012	7.785	∞
	3	4.947	5.217	1.274	1.101	7.680	∞
	4	4.950	5.380	1.328	1.191	7.571	∞
30	1	5.025	5.040	1.741	0.925	8.200	∞
	2	5.027	5.201	1.798	1.012	8.105	∞
	3	5.029	5.365	1.855	1.101	8.006	∞
	4	5.031	5.530	1.911	1.191	7.903	∞
40	1	5.109	5.192	2.472	0.993	8.602	∞
	2	5.111	5.357	2.532	1.083	8.513	∞
	3	5.113	5.523	2.591	1.175	8.421	∞
	4	5.115	5.692	2.651	1.268	8.324	∞
50	1	5.196	5.357	3.427	1.072	9.132	∞
	2	5.198	5.524	3.492	1.165	9.050	∞
	3	5.199	5.694	3.557	1.261	8.965	∞
	4	5.201	5.866	3.626	1.358	8.874	∞

Table 2.6 Component change for eyes aged 20 to 50 years in decade increments. The component change is expressed in vergence (D) per mm increase, as a function of accommodation demand (A). The anterior chamber has the greatest VCF. Of the crystalline lens radii, the posterior surface has a larger factor, so has the greater ability to elicit accommodative change than the posterior chamber. Corneal thickness is static but alters vergence, so has an infinitely large VCF.

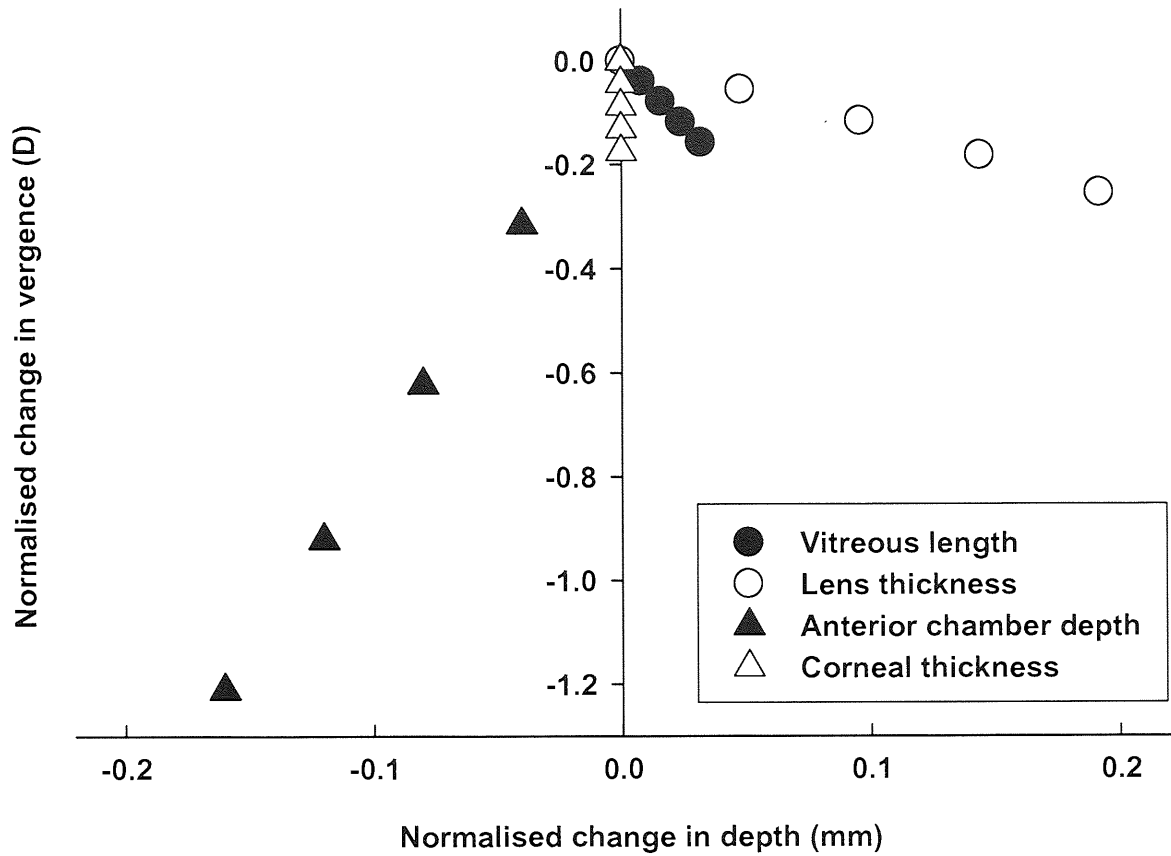


Figure 2.3 Axial distances: Normalised change in vergence for a 20 year old eye, for 4.0 D of accommodation demand. The anterior chamber produces the greatest (negative) change in vergence with accommodation. The crystalline lens thickness alters more physically yet elicits less vergence change. The corneal thickness is physically static but has a small affect on vergence change with accommodation. The vitreous chamber alters little physically and produces small dioptric changes within the optical system.

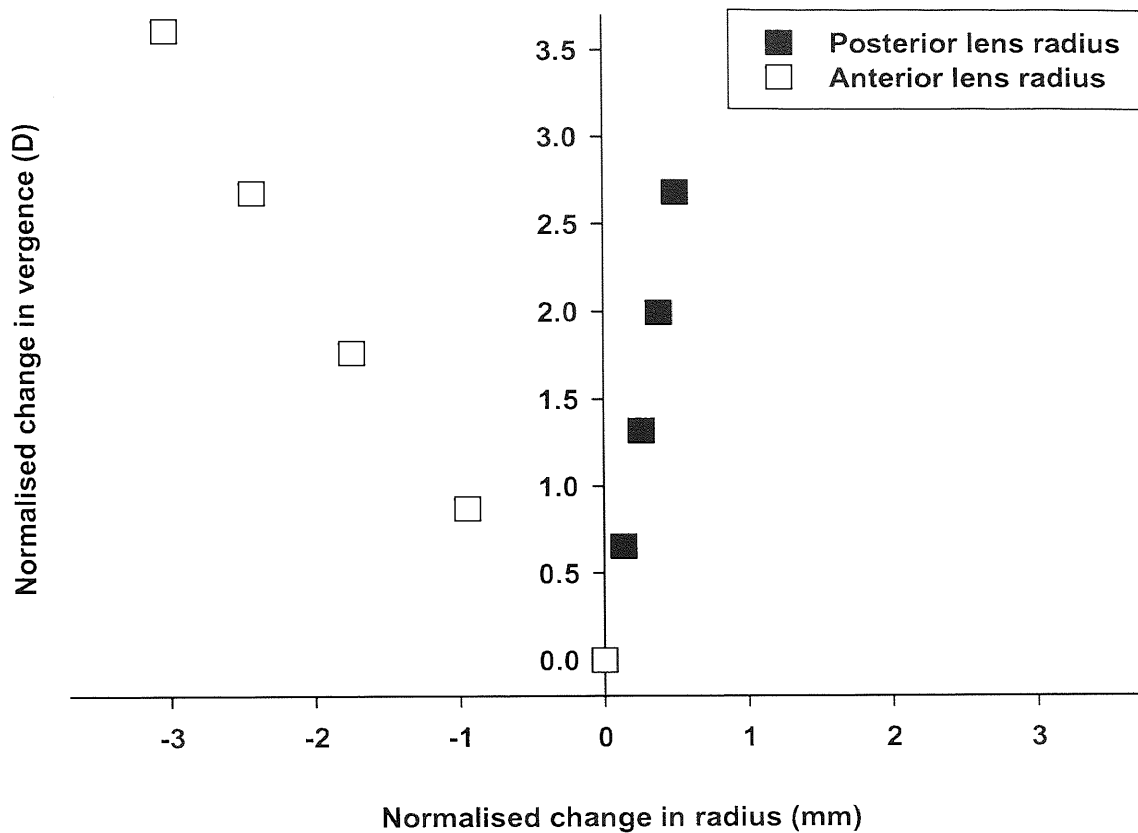


Figure 2.4 Crystalline lens surface radii: Normalised changes in vergence for a 20 year old eye, for 4.0 D of accommodation demand. The anterior crystalline lens radius is the primary correlate for vergence change with accommodation. However, the posterior crystalline lens surface produces a relatively large dioptric change with accommodation, yet its radius alters little.

2.4 Discussion

The aim of this study was to explore the contribution each ocular component makes to the optical system in terms of vergence change with accommodation. A new schematic eye derived from the papers of Dubbelman and colleagues was used (Dubbelman and van der Heijde, 2001; Dubbelman *et al.*, 2001; 2002; 2005), which contains formulae that allow the modification of the model for age and accommodation demand. Further, the study of ocular components and their contribution to vergence change with accommodation has been limited (Kirschcamp *et al.*, 2004). The value of studying vergence change is understated by many authors who work within the field of accommodation. One of the advantages of this method is that the role of each ocular component is made explicit and is not restricted to the biometric changes associated with accommodation.

The main biometric changes that occur in the eye with accommodation have been studied in-depth and are well known. However, there still remains debate as to the exact mechanism by which these changes occur. Many theories have been proposed and have evolved over a number of years; these have been reviewed by a number of authors (Cramer, 1853; Helmholtz, 1855, 1924; Fincham, 1937; Weale, 1992; Atchison, 1995; Schneider *et al.*, 2001; Strenk *et al.*, 2005; Charman, 2008, Glasser, 2008). In more recent times, some authors have challenged the classic Helmholtz theory of accommodation (Helmholtz, 1855; 1924; Glasser and Kaufman, 1999) by suggesting that ciliary contraction causes an increase in zonular tension (Schachar, 1994; Schachar *et al.*, 1994; 1996).

A number of studies have shown that with accommodation there is a decrease in the radius of curvature of the anterior surface of the crystalline lens (Koretz *et al.*, 1984; 1997b; 2002; Garner and Yap, 1997; Kirschcamp *et al.*, 2004; Rosales *et al.*, 2006), and a smaller decrease in the posterior lens radius (Fincham, 1924-5; Garner and Yap, 1997; Kirschcamp *et al.*, 2004). Along with the anterior movement of the anterior ciliary body (Glasser and Kaufman, 1999; Strenk *et al.*, 1999), these changes in radii collectively result in an increase in axial thickness and a small forward movement of the lens centre of mass, with a resultant decrease in anterior chamber depth (Drexler *et al.*, 1997; Garner and Yap, 1997; Kirschcamp *et al.*, 2004; Strenk *et al.*, 2004; 2005). Further, there is a subsequent decrease

in equatorial diameter (Brown 1973; Wilson, 1997; Glasser and Kaufman, 1999; Strenk *et al.*, 1999; Glasser *et al.*, 2006).

There appears to be little alteration in the radius of corneal curvature, although some authors advocate corneal change during accommodation (Pierscionek *et al.*, 2001; Yasuda *et al.*, 2003; He *et al.*, 2003; Buehren *et al.*, 2003). There is also little change in vitreous depth and axial length (Beauchamp and Mitchell, 1985; Koretz *et al.*, 1989; Garner and Yap, 1997; Kirschcamp *et al.*, 2004). However, this still appears to be equivocal due to variation in measurement methods. Some authors have reported accommodation-induced axial length growth by as much as 12.7 μm (Drexler *et al.*, 1998) with significant differences between emmetropic and myopic subjects (Mallen *et al.*, 2006).

Table 2.3 agrees with the ocular variations during accommodation stated previously. The model predicts no change in corneal status, and a small reduction in vitreous depth (less negative); which is also supported by the literature (Vilupuru and Glasser, 2005; Ostrin *et al.*, 2006)

The study of ocular component contributions is complicated by comparison of surface powers, measured in dioptres, to axial distances, measured in millimetres. Confusion such as this can be resolved by expressing both quantities in terms of their vergence powers (Leary 1981; Erickson, 1984). In recent times, few authors have studied accommodation-induced ocular surface and axial separation changes in terms of their vergence. Kirschcamp *et al.* (2004) conducted such an investigation using phakometric techniques. The study examined nine emmetropic subjects (age range 20 to 38 years) under cycloplegia and active accommodative (accommodation response of 3.7 ± 1.1 D; mean \pm 95% confidence interval).

The Dubbelman model relates closely to the results of Kirschcamp and co-authors. Further, in the study by Kirschcamp and colleagues, there was little change in vergence contribution noted from vitreous depth (0.2 ± 0.3 D) or the cornea (0.0 ± 0.2 D), although corneal thickness was not considered; these results are both comparable to Table 2.4 (ages 20 and 30 years).

In the same study, the anterior crystalline lens surface altered vergence to a greater extent (3.1 ± 0.8 D) compared to the posterior surface (2.1 ± 0.6 D), both corresponding well to the model eye data. Of note, the axial distances display a decreasing vergence contribution

with accommodation, with the anterior chamber being the primary root (-1.5 ± 0.3 D). The negative vergence change caused by the crystalline lens thickness is much smaller (-0.2 ± 0.2 D).

Anterior chamber depth and crystalline lens thickness alter in opposing directions but by similar amounts during accommodation, yet the vergence contribution by both is negative. Table 2.4 exhibits analogous figures, derived from the Dubbelman model.

All vergence contributions are reduced by age, including the outcome refractive status (actual accommodation). It must also be noted that the refractive status is higher than the accommodation input in the majority of cases. This may be in part due to the model being paraxial (Figure 2.1) and being based on accommodation stimulus and not response (Dubbelman and van der Heijde, 2001; Dubbleman *et al.*, 2001; 2002; 2005).

Considering each surface power in terms of its vergence contribution factor, is to the author's knowledge, a new and unique method of considering accommodation and ocular component analysis. The use of the VCF highlights the anterior chamber depth as having the highest factor (Table 2.6). It also shows that the posterior lens radius, although changing very little in comparison to the anterior surface, has the greatest ability to modify vergence (Figure 2.4); approximately five times higher VCF. This method stresses the fact that the posterior lens surface has a disproportionately large contribution to play in accommodation.

2.5 Conclusion

Ocular component change with accommodation can be analysed by studying axial length and surface radii variation in terms of real change (mm), vergence power (dioptries) and the ratio of the two (VCF; D/mm). Vergence contribution has the unique advantage of explicitly displaying the effect each surface has on outcome refraction, which may not be evident from studying component dimensions alone. The new method of using the VCF described in this chapter further stresses the ability each surface has to modify the vergence of light passing through the ocular system.

Although ocular component change in accommodation is well known and documented (Garner and Yap, 1997; Kirschcamp *et al.*, 2004; Strenk *et al.*, 1999; 2004; 2005; Glasser, 2006), vergence analysis shows that changes in axial distances have derogatory effects on accommodation, whereas the crystalline lens surface radii are solely responsible for the accommodative increase in refractive status (Kirschcamp *et al.*, 2004). The posterior crystalline lens radius is exposed as being more effective in altering vergence with accommodation (0.9 to 1.4 D/mm) than the associated anterior surface (4.9 to 5.9 D/mm), although the latter contributes more in total to the overall refractive alteration. Anterior chamber depth change, despite being opposite and approximately equal to lens thickness changes, has a far higher negative consequence for outcome refraction. Consequently, it has the greatest power to provoke change in the optical system with accommodation (7.5 to 9.1 D/mm).

The age of the model decreases all vergence components, as well as outcome accommodation produced. Corneal thickness, despite being static, has a small depressive effect on the overall vergence.

In conclusion, the key findings of this chapter are summarised below.

- Traditional methods of studying biometric change are by considering physical movements, changes in dimension, radius or axial separation of the ocular components. Considering accommodative changes in terms of the vergence contribution each interface has on outcome refractive status, provides more information on the role each component plays in the process of accommodation.

- This study improves on the work of Kirschcamp and colleagues (2004) by using a new schematic eye derived from the papers of Dubbelman and co-workers (Dubbelman and van der Heijde, 2001; Dubbelman *et al.*, 2001; 2002; 2005) by Norrby (2005). This model allows the modification of both age and accommodation to allow step-along ray tracing to be performed. From this, the biophysical and vergence changes which take place with accommodation have been studied.
- The model agrees well with published literature regarding the biometric ocular changes associated with accommodation.
- Considering component vergence changes with accommodation, all axial changes of components in the eye result in a dampening of the vergence. The crystalline lens radii are solely responsible for the positive vergence changes associated with accommodation.
- The anterior chamber and crystalline lens thickness alter in terms of physical size by similar amounts, yet the anterior chamber depth has a far larger negative effect on the vergence change with accommodation.
- The posterior crystalline lens radius alters less than the anterior surface per unit of accommodation demand, yet it exerts a significant positive vergence change. The VCF attributed to this surface is far larger than the anterior crystalline lens radius, despite this being the primary correlate for positive vergence change with accommodation.
- Corneal thickness dampens vergence change with accommodation, despite remaining physically static.
- Increasing age reduces both total outcome refractive status (accommodation) and the magnitude of all vergence changes.

Thus far, the Dubbelman eye model has been used to study accommodation in the phakic eye as discussed previously. However, the model has only been considered with a fixed axial length. Erickson (1984) discovered that using his technique of reverse ray-tracing, an

increase in vitreous chamber depth caused a decrease in its divergence contribution. This concurrently caused a decrease in the convergence contribution of the anterior segment. This was effectively a natural damping on refractive status due to changes in axial length caused by elongation of the posterior segment (Erickson, 1984).

Given this, a study is required to investigate the phenomenon of natural damping and to explore the effects it may have on accommodation and vergence contribution of the ocular components. This can be done using the same Dubbelman eye model, and by altering its axial length. It is hoped that this will enable suitable conclusions to be drawn about the role of axial length in accommodation.

CHAPTER 3

AMETROPIA: VERGENCE CHANGES WITH ACCOMMODATION

3.1 Introduction

Refractive error has been shown to have an effect on various accommodation measurements (Allen and O'Leary, 2006), including accuracy of the accommodative response (McBrien and Millodot, 1986; Gwiazda *et al.*, 1993; O'Leary and Allen, 2001), the accommodative convergence to accommodation ratio (AC/A; Rosenfield and Gilmartin, 1987; Jiang, 1995; Gwiazda *et al.*, 1999; Mutti *et al.*, 2000), tonic accommodation (Gwiazda *et al.*, 1995; Jiang, 1995; Zadnik *et al.*, 1999), and Nearwork-Induced Transient Myopia (NITM; Ciuffreda and Wallis, 1998; Ciuffreda and Lee, 2002; Vera-Díaz *et al.*, 2002; Wolffsohn *et al.*, 2003; Vasuvedan *et al.*, 2008).

It is well known that myopic subjects require aid for the symptoms of presbyopia later than both emmetropes and hyperopes. Corrected hypermetropes have a lower effective accommodation compared to emmetropes and will need near addition at a younger age; the converse applies to myopes (Bennett and Rabbetts, 2007). This is due to the lower effectiveness of convex lenses for near compared to concave lenses (Bennett and Rabbetts, 2007). Hypermetropes are therefore more symptomatic earlier than emmetropes or myopes. In a study of young students, amplitude of accommodation was found to be highest in late onset myopes (LOM) and lowest in hyperopes (McBrien and Millodot, 1986). Other studies have shown that refractive errors do not affect the dynamics of natural accommodation or amplitude of accommodation approaching presbyopia (Schaeffel *et al.*, 1993; Pointer, 1995).

Hitherto, the method of reverse ray tracing and component analysis by vergence contribution has been shown to be useful (see Chapter 2). However, Erickson's technique revealed an unexpected result. Erickson observed that increasing vitreous chamber depth caused a decrease in its divergence contribution, and a concurrent decrease in convergence contribution of the anterior segment. Essentially, he had discovered a natural damping

effect on refractive status variation due to changes in axial length (AL) caused by elongation of the posterior segment (Erickson, 1984). No study to date has considered natural damping with regard to accommodation and variation with age.

3.1.1 Aims

The aim of the study is to apply the Dubbelman model (Norrby, 2005) to the study of accommodation. By varying the axial length of the model, more information will be revealed with regard to accommodative vergence changes, output accommodation and the process of natural damping.

It is predicted that the damping effect of an elongated vitreous chamber will reduce the refractive error of the model. This effect should be greater in eyes with a longer rather than shorter AL. The result of which should be that an increase in AL will give rise to less myopia, whilst the same decrease in AL will result in relatively more hyperopia.

With regard to accommodation, it would seem sensible to suggest that the change in overall refractive status (accommodation output) will be damped by the same method, so that the hyperopic eye will produce a greater positive shift in refractive status compared to a myopic eye.

3.2 Methods

Using the Dubbelman eye model (Norrby, 2005), a reverse step-along ray trace was created using Microsoft *Excel* 2003 (Microsoft *Windows*®XP). The paraxial wavefronts were traced from the retina to the far point using the method advocated by Erickson (Erickson, 1984). The nomenclature has been altered from that of Erickson's original paper, to that more commonly adopted and advocated by Bennett and Rabbetts (2007).

The baseline axial length of the model was 23.267 mm, which corresponds with emmetropia at 20 years of age. From this baseline, axial length was adjusted by ± 2.0 mm to simulate myopia (+2.0 mm) and hyperopia (-2.0 mm); thus allowing investigation into the effects of axial length. The refractive status of the eye was calculated for the ages of 20, 30, 40 and 50 years, and at accommodation levels of 2.0 and 4.0 D.

The step-along reverse ray-trace from the retinal plane to the anterior corneal plane is shown below.

3.2.1 Vergence from the vitreous chamber (L_8)

The vitreous chamber depth (d_4) is calculated from the sum of the other axial ocular distances (d_{1-3}) subtracted from axial length of the eye. The axial length of the model (x) was varied from baseline at 23.267 mm by ± 2.0 mm.

$$d_4 = x - (d_1 + d_2 + d_3). \quad (3.1)$$

Where x is the axial length, d_1 is the corneal thickness, d_2 the anterior chamber depth, d_3 the thickness of the crystalline lens, and d_4 the length of the vitreous chamber.

A value for the vergence attributed to the vitreous chamber is adopted from Erickson (1984; Equation 3.2).

$$L_8 = 1000n_4 / (-d_4 + 0.25). \quad (3.2)$$

Where L_8 is the vergence from the vitreous chamber and n_4 the refractive index of the vitreous (Table 2.2; Chapter 2). The receptor layer is included in the Dubbelman model as

derived by Norrby, and is given the value of 0.25 mm. The vitreous chamber depth is given a negative value due to the sign convention.

3.2.2 Vergence at the posterior crystalline lens surface (L_7)

The diverging wavefronts from the vitreous chamber are modified by the posterior crystalline lens surface.

$$F_4 = [1000(n_4 - n_3)] / r_4. \quad (3.3)$$

Where F_4 is the power of the posterior crystalline lens surface, n_3 the equivalent refractive index of the crystalline lens (Table 2.2; Chapter 2) and r_4 the posterior crystalline lens surface radius (Table 2.1; Chapter 2).

$$L_7 = L_8 + F_4, \quad (3.4)$$

where L_7 is the vergence at the posterior crystalline lens surface.

3.2.3 Vergence at the anterior crystalline lens surface (L_6)

Equation 3.5 is used to derive the vergence at the anterior crystalline lens surface once the wavefronts of light have been modified by crystalline lens matrix.

$$L_6 = 1000n_3 / (1000n_3 / L_7 - d_3). \quad (3.5)$$

Where L_7 is the vergence at the posterior crystalline lens surface, n_3 is the equivalent refractive index of the crystalline lens (Table 2.2; Chapter 2) and d_3 the crystalline lens axial thickness (Table 2.1; Chapter 2).

3.2.4 Vergence at the posterior aqueous chamber (L_5)

$$F_3 = [1000(n_3 - n_2)] / r_3. \quad (3.6)$$

Where F_3 is the power of the anterior crystalline lens, n_2 is the refractive index of the aqueous humour (Table 2.2; Chapter 2) and r_3 is the radius of the anterior crystalline lens surface (Table 2.1; Chapter 2). Equation 3.7 is used to calculate the vergence as it is modified by the anterior crystalline lens surface.

$$L_5 = L_6 + F_3. \quad (3.7)$$

3.2.5 Vergence at the anterior aqueous chamber (L_4)

The vergence of light passing through the aqueous chamber is modified as shown in Equation 3.8.

$$L_4 = 1000n_2 / (1000n_2 / L_5 - d_2). \quad (3.8)$$

Where L_5 is the vergence at the posterior aqueous chamber, n_2 is the refractive index of the aqueous humour (Table 2.2; Chapter 2) and d_2 the anterior chamber depth (Table 2.1; Chapter 2).

3.2.6 Vergence at the posterior corneal surface (L_3)

Equation 3.9 was used to calculate the power of the posterior corneal surface.

$$F_2 = [1000(n_2 - n_1)] / r_2. \quad (3.9)$$

Where F_2 is the power of the posterior corneal surface, n_1 is the refractive index of the cornea (Table 2.2; Chapter 2) and r_2 is the radius of the posterior corneal surface. Equation 3.10 was used to calculate the vergence of light leaving the anterior chamber and entering the posterior corneal surface.

$$L_3 = L_4 + F_2. \quad (3.10)$$

3.2.7 Vergence at the anterior corneal surface (L_2)

The vergence of light passing through the cornea is modified as shown in Equation 3.11.

$$L_2 = 1000n_1 / (1000n_1 / L_3 - d_1). \quad (3.11)$$

Where L_3 is the vergence at the posterior corneal surface, n_1 is the refractive index of the cornea (Table 2.2; Chapter 2) and d_1 the corneal thickness (Table 2.1; Chapter 2).

3.2.8 Vergence of light leaving the eye: The back vertex power (L_1)

Equation 3.12 was used to calculate the power of the anterior corneal surface.

$$F_1 = [1000(n_1 - 1)] / r_1. \quad (3.12)$$

Where F_1 is the power of the anterior corneal surface, n_1 is the refractive index of the cornea (Table 2.2; Chapter 2), 1 is the refractive index of air and r_1 is the radius of the anterior corneal surface. Equation 3.13 was used to calculate the vergence of light leaving the eye, hence the back vertex power.

$$L_1 = L_2 + F_1. \quad (3.13)$$

The vergence contribution of each refractive surface or axial distance was calculated by subtracting the entrance vergence from the exit vergence of the interface; this value was expressed in dioptres. Vergence contributions found under accommodation stimulus were subtracted from those found in under relaxation to provide a measure of the change in vergence contribution that took place with accommodation.

The magnitude of the effect each interface contributed to vergence change was calculated; this is expressed as the ratio of dioptric to axial position or radius change. The fraction is expressed in dioptres per millimetre (D/mm), and is termed the Vergence Contribution Factor (VCF; see Chapter 2).

Results were displayed in terms of the ametropia of the model, the relative ametropia (from the model with an axial length of 23.267 mm) and refractive status or output accommodation. The ocular component contributions were again analysed in terms of vergence and VCF; physical biometric analysis proving to have limited use (see Chapter 2).

3.3 Results

Table 3.1 displays the level of ametropia, normalised ametropia and refractive status (accommodation output) for the different age groups with variation in axial length. The baseline axial length of the model is 23.267 mm. For the 20 year old eye, this equates to absolute emmetropia (0.0 D). In older eyes, this axial length gives rise to a small amount of hyperopia; approximately +0.2 D per decade. In order to analyse the model further, it is necessary to display the levels of normalised ametropia, which adjusts the ametropia to give 0.0 D for an axial length of 23.267 mm.

The table shows that the change in axial length equates to more hyperopia than myopia. Essentially, a 2.0 mm decrease in AL results in a greater change in ametropia than a 2.0 mm increase in AL (e.g. +6.34 D compared to -5.37 D; 20 year old eye). The ratio of this axial change is also greater in the hyperope (e.g. 3.17 D/mm; 20 year old) compared to the myope (e.g. 2.69 D/mm; 20 year old). There is also a shift towards hyperopia with age by approximately +0.2 D per decade.

The relative degree of ametropia (normalised) is nearly static with age, with a small reduction by approximately 0.02 D for the 50 year old compared to the 20 year old eye. Outcome accommodation is greatest for the myope in all ages, the hyperope producing the least dioptric output. The accommodation output decreases with age so that only the 50 year old hyperope underperforms to the 4.0 D accommodation stimulus (Figure 3.1).

As in Chapter 2, all ocular refractive elements exert a positive change in vergence to the initial diverging ray from the retina with the exception of the posterior corneal surface. Considering the model in terms of the component vergence change indicates the role of each surface during accommodation. As shown previously, all surface radii changes have a positive effect on accommodative vergence changes to the retinal ray. The opposite is true for axial depth changes and corneal thickness (Table 3.2). The crystalline lens surface radii reveal the greatest contributions to vergence change; however, the degree of this input remains static with axial length adjustment. Of the axial distances, the anterior chamber depth change depresses the overall vergence output the most, with vitreous chamber depth, lens thickness and corneal thickness playing a lesser role (Table 3.3). All component vergence contributions reduce with age with the exception of lens thickness (Figure 3.2).

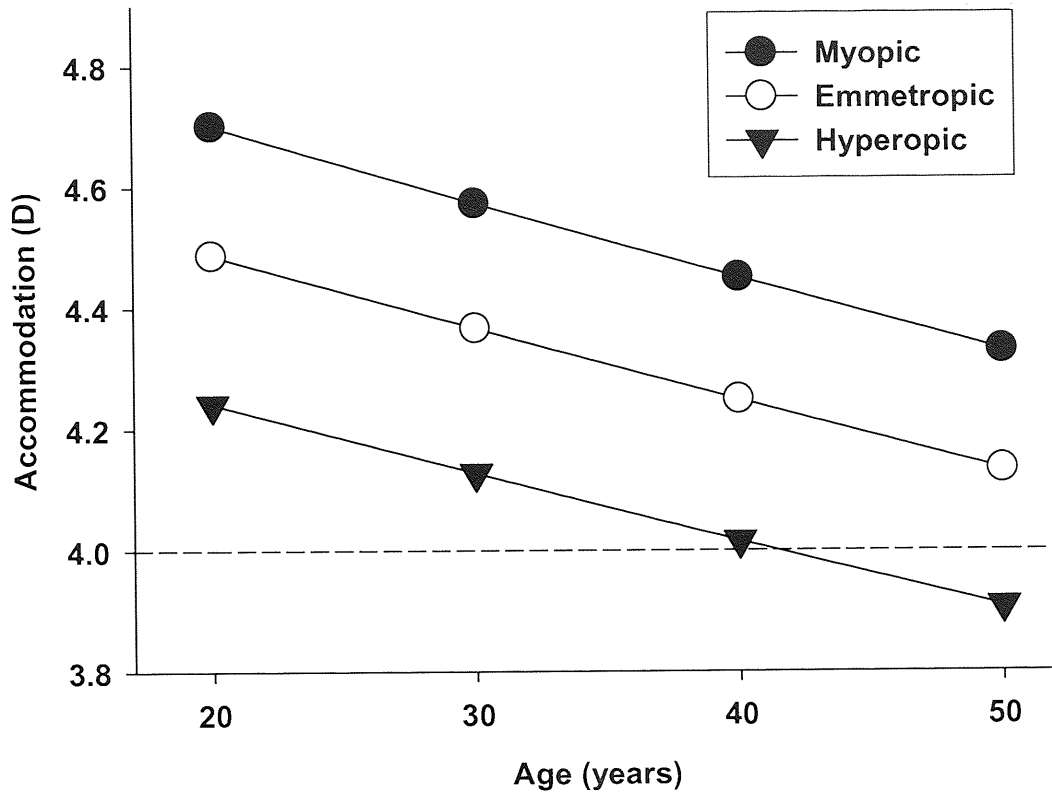


Figure 3.1 Outcome refractive status (accommodation) variations with age for an axial myope, hyperope and emmetrope with a 4.0 D accommodation stimulus (see Table 3.1). The myopic eyes produce a greater outcome refractive status (i.e. more accommodative output) compared to the hyperopic eyes. Age has a derogatory effect on refractive status. The 50 year old hyperope underperforms for the 4.0 D stimulus.

Age	Ametropia	Axial length (mm)	Ametropia (D)	Normalised Ametropia (D)	A (D)	Refractive status (D)
20	Myope	25.267	-5.37	-5.37	2	2.279
					4	4.701
	Emmetrope	23.267	0.00	0.00	2	2.175
					4	4.487
	Hyperope	21.267	+6.34	+6.34	2	2.055
					4	4.242
30	Myope	25.267	-5.15	-5.37	2	2.218
					4	4.574
	Emmetrope	23.267	+0.22	0.00	2	2.117
					4	4.367
	Hyperope	21.267	+6.55	+6.33	2	2.000
					4	4.128
40	Myope	25.267	-4.94	-5.36	2	2.158
					4	4.451
	Emmetrope	23.267	+0.42	0.00	2	2.060
					4	4.249
	Hyperope	21.267	+6.75	+6.33	2	1.946
					4	4.016
50	Myope	25.267	-4.73	-5.34	2	2.100
					4	4.331
	Emmetrope	23.267	+0.61	0.00	2	2.004
					4	4.134
	Hyperope	21.267	+6.93	+6.32	2	1.894
					4	3.908

Table 3.1 Level of ametropia, normalised ametropia and refractive status (accommodation output) as a function of age, ametropia, axial length and accommodation stimulus (A). Axial length is altered from baseline (emmetrope at 20 years old: 23.267 mm) by 2.0 mm to simulate myopia or hyperopia. Accommodation stimulus levels are set at 2.0 and 4.0 D.

Age	Ametropia	Ametropia (D)	A (D)	Total vergence changes (D)	
				Surfaces/Radii	Axial distances
20	Myope	-5.37	2	3.081	-0.802
			4	6.288	-1.587
	Emmetrope	0.00	2	3.081	-0.906
			4	6.288	-1.800
	Hyperope	+6.34	2	3.081	-1.026
			4	6.288	-2.046
30	Myope	-5.15	2	3.011	-0.793
			4	6.146	-1.572
	Emmetrope	+0.22	2	3.011	-0.894
			4	6.146	-1.779
	Hyperope	+6.55	2	3.011	-1.011
			4	6.146	-2.019
40	Myope	-4.94	2	2.942	-0.784
			4	6.008	-1.557
	Emmetrope	+0.42	2	2.942	-0.882
			4	6.008	-1.759
	Hyperope	+6.75	2	2.942	-0.996
			4	6.008	-1.992
50	Myope	-4.73	2	2.875	-0.775
			4	5.875	-1.543
	Emmetrope	+0.61	2	2.875	-0.871
			4	5.875	-1.740
	Hyperope	+6.93	2	2.875	-0.981
			4	5.875	-1.967

Table 3.2 Total vergence variations for both surface radii and axial distance changes for three levels of ametropia as a function of accommodation stimulus (A). All axial separation changes with accommodation have a negative effect on vergence. All surface radii changes have a positive effect on vergence. Accommodation stimulus levels are set at 2.0 and 4.0 D.

Age	Ametropia	Component vergence change (D)							Total
		A (D)	Vitreous depth	Posterior lens radius	Lens thickness	Anterior lens radius	Anterior chamber depth	Corneal thickness	
20	Myope	2	-0.063	1.319	-0.129	1.762	-0.530	-0.081	2.279
		4	-0.126	2.683	-0.276	3.605	-1.025	-0.161	4.701
	Emmetrope	2	-0.079	1.319	-0.117	1.762	-0.623	-0.087	2.175
		4	-0.158	2.683	-0.255	3.605	-1.211	-0.175	4.487
	Hyperope	2	-0.103	1.319	-0.092	1.762	-0.738	-0.094	2.055
		4	-0.205	2.683	-0.208	3.605	-1.443	-0.190	4.242
30	Myope	2	-0.056	1.297	-0.160	1.714	-0.498	-0.079	2.218
		4	-0.112	2.638	-0.336	3.508	-0.966	-0.158	4.574
	Emmetrope	2	-0.070	1.297	-0.155	1.714	-0.584	-0.085	2.117
		4	-0.141	2.638	-0.329	3.508	-1.138	-0.172	4.367
	Hyperope	2	-0.091	1.297	-0.138	1.714	-0.689	-0.092	2.000
		4	-0.183	2.638	-0.299	3.508	-1.350	-0.186	4.128
40	Myope	2	-0.049	1.274	-0.191	1.667	-0.467	-0.077	2.158
		4	-0.097	2.594	-0.397	3.415	-0.908	-0.155	4.451
	Emmetrope	2	-0.061	1.274	-0.192	1.667	-0.545	-0.084	2.060
		4	-0.123	2.594	-0.403	3.415	-1.066	-0.168	4.249
	Hyperope	2	-0.080	1.274	-0.185	1.667	-0.641	-0.090	1.946
		4	-0.160	2.594	-0.392	3.415	-1.259	-0.182	4.016
50	Myope	2	-0.041	1.253	-0.223	1.622	-0.436	-0.076	2.100
		4	-0.082	2.551	-0.459	3.324	-0.850	-0.152	4.331
	Emmetrope	2	-0.052	1.253	-0.230	1.622	-0.507	-0.082	2.004
		4	-0.104	2.551	-0.478	3.324	-0.994	-0.165	4.134
	Hyperope	2	-0.068	1.253	-0.232	1.622	-0.593	-0.088	1.894
		4	-0.136	2.551	-0.485	3.324	-1.169	-0.178	3.908

Table 3.3 Component vergence change at each level of ametropia, with a 2.0 and 4.0 D accommodation stimulus (A). The crystalline lens surface radii contribute the most to vergence change with accommodation; the axial length of the eye has no effect on this. Anterior chamber depth accommodative changes depress the overall vergence output the most, with vitreous chamber depth, lens thickness and corneal thickness playing a lesser role. All component vergence contributions reduce with age with the exception of lens thickness.

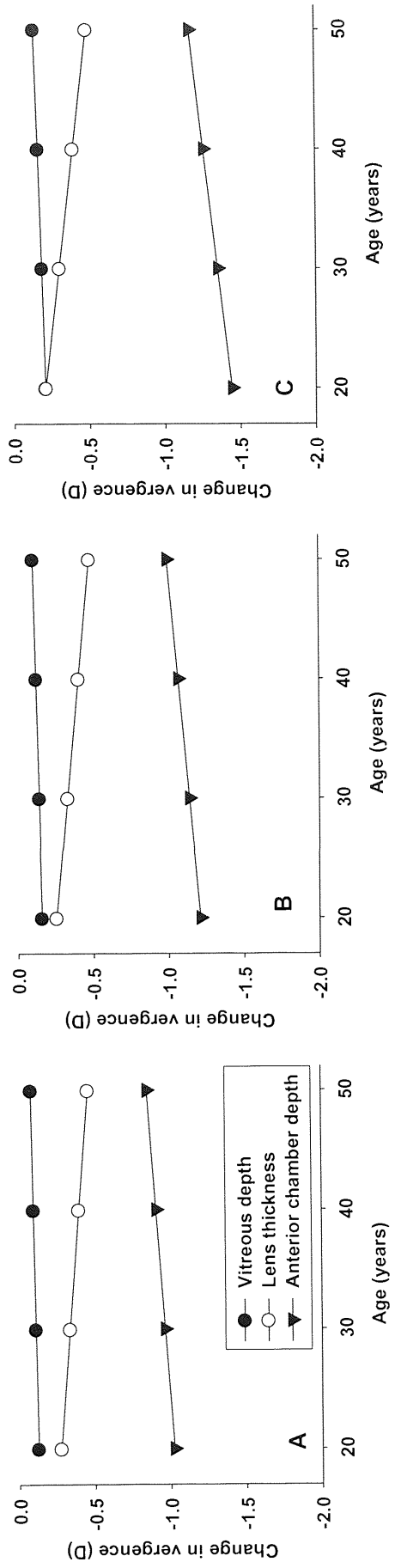


Figure 3.2 Variations in vergence change with age for a 4.0 D stimulus to accommodation. Figure 3.2A represents an axial myope, Figure 3.2B an emmetrope and Figure 3.2C an axial hyperope. The crystalline lens surface radii do not alter with ametropia and are therefore not included. Vergence changes with accommodation associated with the vitreous chamber reduce with increasing age by a small amount. Accommodative vergence changes attributed to the thickness of the crystalline lens reduces with age, where as those effects associated with the anterior chamber increase.

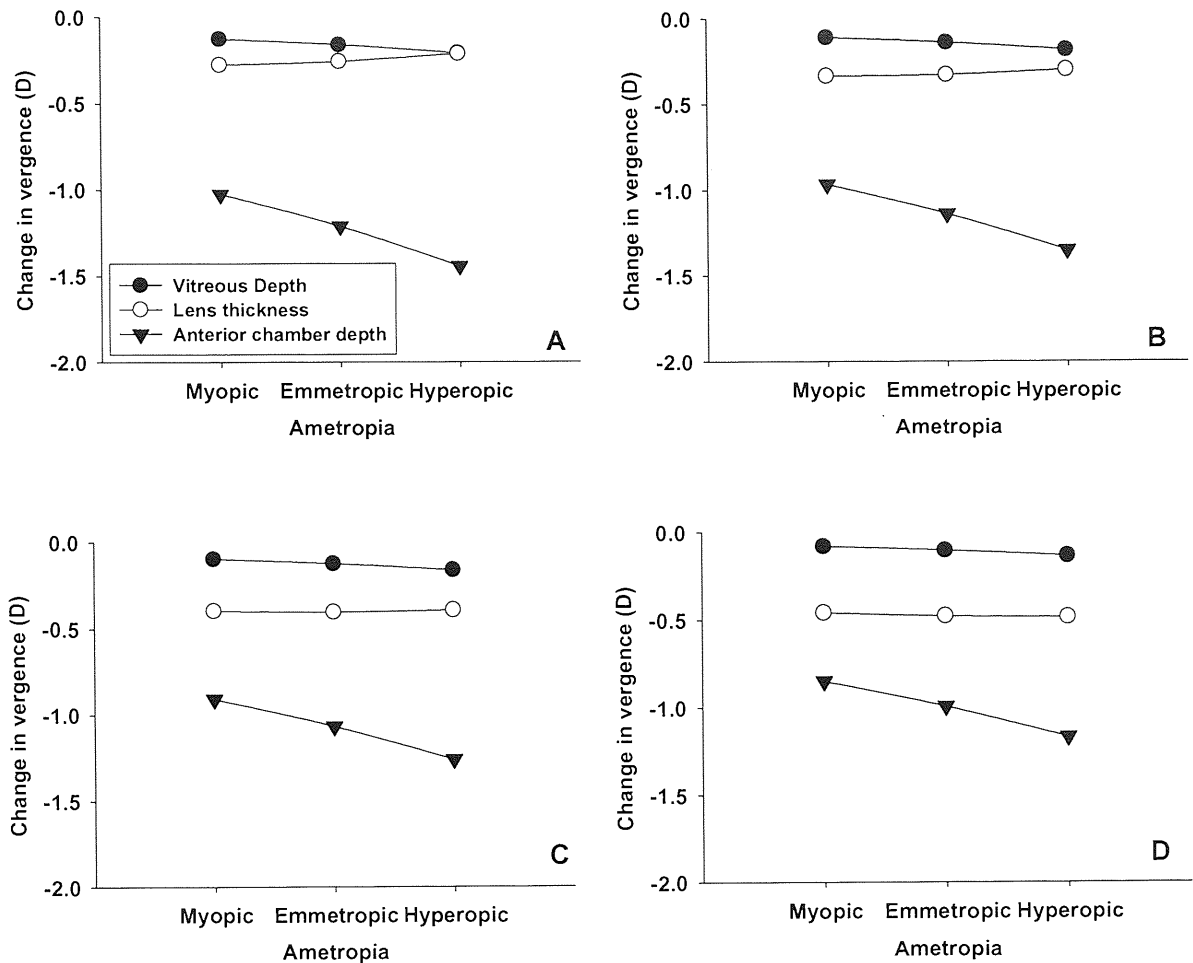


Figure 3.3 Variations in vergence change with ametropia for a 4.0 D stimulus to accommodation. Figure 3.3A represents a 20 year old eye, Figure 3.3B a 30 year old eye, Figure 3.3C a 40 year old eye and Figure 3.3D a 50 year old eye. All axial distance changes cause a negative change in vergence with accommodation. Vergence changes from the vitreous chamber remain similar across the age groups. The vergence contribution from the anterior chamber depth becomes more negative with age. It is this component which displays the largest disparity in vergence alteration with accommodation between the different ametropia classifications. Vergence changes caused by alteration in crystalline lens thickness with accommodation become gradually negative with age. However, the difference between the contribution of this component in myopic and hyperopic eyes becomes less; this is reflected in the change of the slope noted above. The crystalline lens surface radii do not alter with ametropia and are therefore not included.

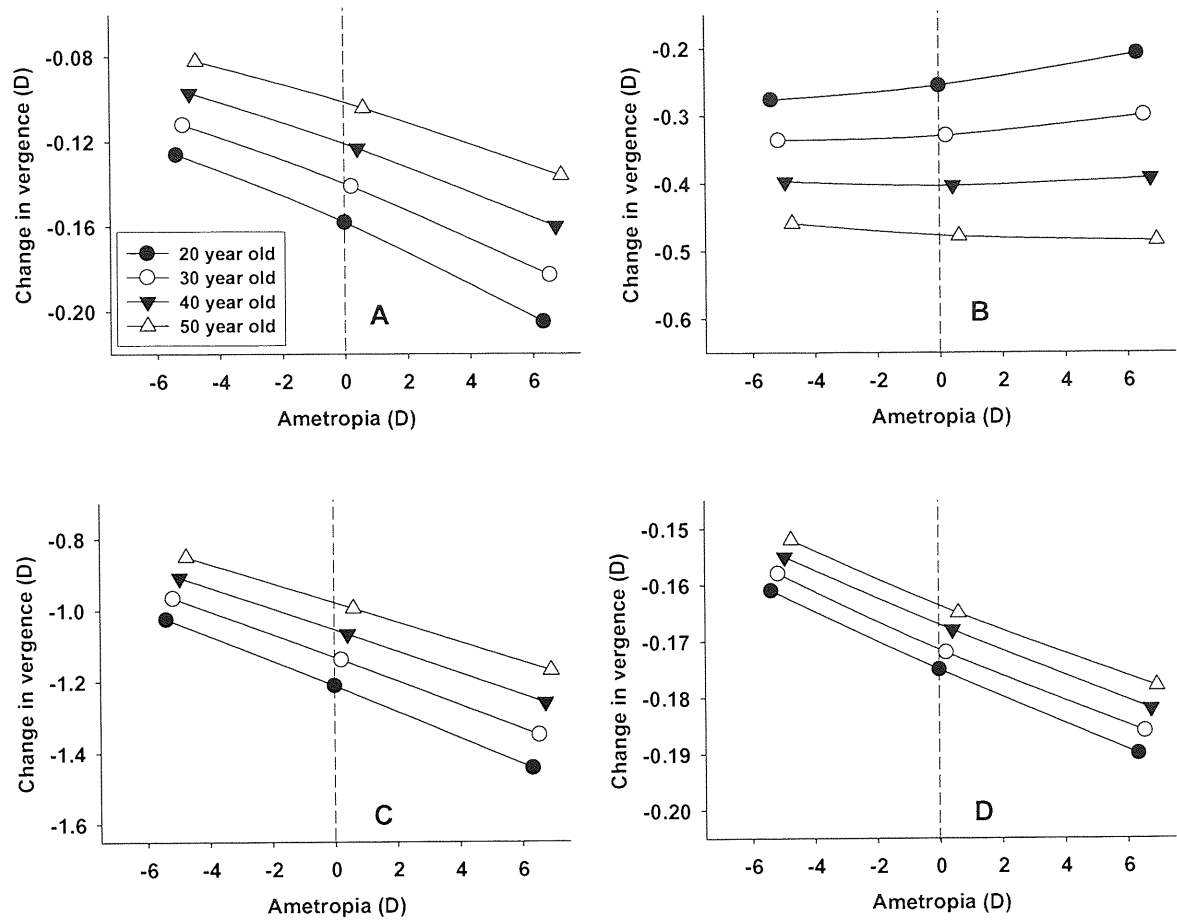


Figure 3.4 Variations in vergence change with ametropia at ages 20 to 50 years in decade increments. Figure 3.4A represents vitreous chamber depth, Figure 3.4B crystalline lens thickness, Figure 3.4C anterior chamber depth and Figure 3.4D corneal thickness. The scales have been individually enlarged in each plot to exploit the differences in the age groups. The vergence changes with accommodation for each of the axial distances produces a less negative change with age. The exception to this rule is the crystalline lens thickness (3.4B), where the change in vergence with accommodation becomes more negative with age. The shift towards hyperopia with age is also very evident in all of the above plots. The crystalline surface radii are not affected by axial length changes, so are therefore not included.

Figure 3.3 displays the accommodative vergence changes for the major axial components and their variation with ametropia in each age group. Figure 3.4 represent the same but on a much more detailed scale to highlight individual component variations.

With accommodation stimulus, the changes in vergence attributed to the vitreous chamber alter little. However, the vergence change is more negative in shorter eyes, but remains similar with age (Figure 3.4A). The crystalline lens thickness vergence changes are more negative in the young myopic eye (20 and 30 years old) when compared to the hyperope. There is a gradual alteration in this trend at the age of 40 years, where it is the emmetrope which displays the most vergence change; this trend is reversed in the older eye (50 years old; Figure 3.4B)

The Vergence Contribution Factor (VCF) gives useful information alluding to the ability each surface has to contribute to the power of the eye as a whole. Table 3.4 demonstrates that the anterior chamber is the component with the highest VCF. This factor is much higher in the hyperopic eye than in the longer myopic eye and increases with age. Vitreous chamber depth follows a similar trend to anterior chamber depth but has a smaller magnitude and shows less variation with age. Lens thickness has a relatively small VCF which increases markedly with age (1.083 D to 3.671 D, 20 to 50 year old hyperope; Figure 3.5).

Figure 3.6 shows the VCF changes with ametropia for each age level and for each biometric component. These figures further illustrate that the vitreous chamber changes little with age, but more significantly with ametropia. Crystalline lens thickness changes display the same trend in VCF as described for vergence change. There is a gradual decrease in VCF towards hyperopia in the younger eye. A gradual drift in this pattern is seen with advancing age, so that the trend is reversed at the age of 50 (Figure 3.6D).

Analysis of the component radii reveal the posterior crystalline lens surface as being the more powerful of the two surfaces, with a VCF approximately 5 times greater. These factors are static with variation in axial length, but increase to a small degree with age. Corneal thickness, although demonstrating vergence change, fails to change physically, and therefore has an infinite VCF.

Age	Ametropia	A (D)	Vitreous depth	Posterior lens radius	Lens thickness	Anterior lens radius	Anterior chamber depth	Corneal thickness
20	Myope	2	3.930	5.056	1.344	1.012	6.623	∞
		4	3.934	5.380	1.435	1.191	6.405	∞
	Emmetrope	2	4.945	5.056	1.220	1.012	7.785	∞
		4	4.950	5.380	1.328	1.191	7.571	∞
	Hyperope	2	6.410	5.056	0.954	1.012	9.226	∞
		4	6.417	5.380	1.083	1.191	9.017	∞
30	Myope	2	3.988	5.201	1.860	1.083	6.918	∞
		4	3.991	5.530	1.954	1.268	6.709	∞
	Emmetrope	2	5.027	5.201	1.798	1.083	8.105	∞
		4	5.031	5.530	1.911	1.268	7.903	∞
	Hyperope	2	6.531	5.201	1.607	1.083	9.570	∞
		4	6.538	5.530	1.741	1.268	9.376	∞
40	Myope	2	4.048	5.357	2.515	1.166	7.293	∞
		4	4.051	5.692	2.614	1.358	7.093	∞
	Emmetrope	2	5.111	5.357	2.532	1.166	8.513	∞
		4	5.112	5.692	2.651	1.358	8.324	∞
	Hyperope	2	6.656	5.357	2.435	1.166	10.013	∞
		4	6.662	5.692	2.576	1.358	9.835	∞
50	Myope	2	4.109	5.524	3.372	1.262	7.783	∞
		4	4.111	5.866	3.479	1.463	7.593	∞
	Emmetrope	2	5.198	5.524	3.492	1.262	9.050	∞
		4	5.201	5.866	3.620	1.463	8.874	∞
	Hyperope	2	6.785	5.524	3.519	1.262	10.598	∞
		4	6.790	5.866	3.671	1.463	10.437	∞

Table 3.4 Vergence contribution factors for all ocular components at each level of ametropia; at 2.0 and 4.0 D of accommodation stimulus (A).

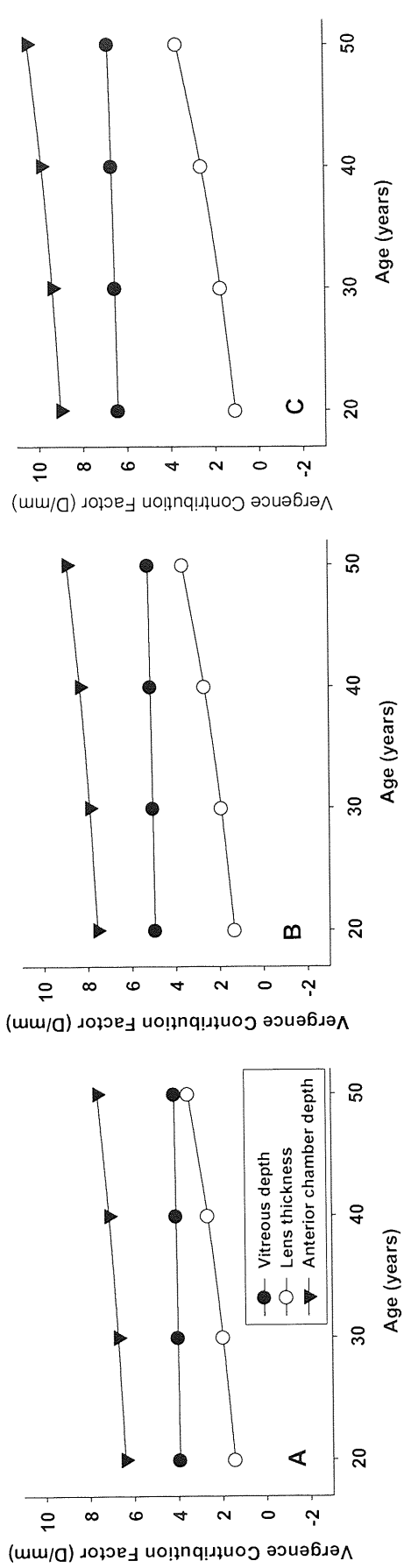


Figure 3.5 Variation in Vergence Contribution Factor (VCF) with age, for a 4.0 D accommodative stimulus. Figure 3.5A represents an axial myope, Figure 3.5B an emmetrope and Figure 3.5C an axial hyperope. The VCF for all components increases with age; this is more marked with regard to crystalline lens thickness. The hyperopic eye displays the greatest VCF values.

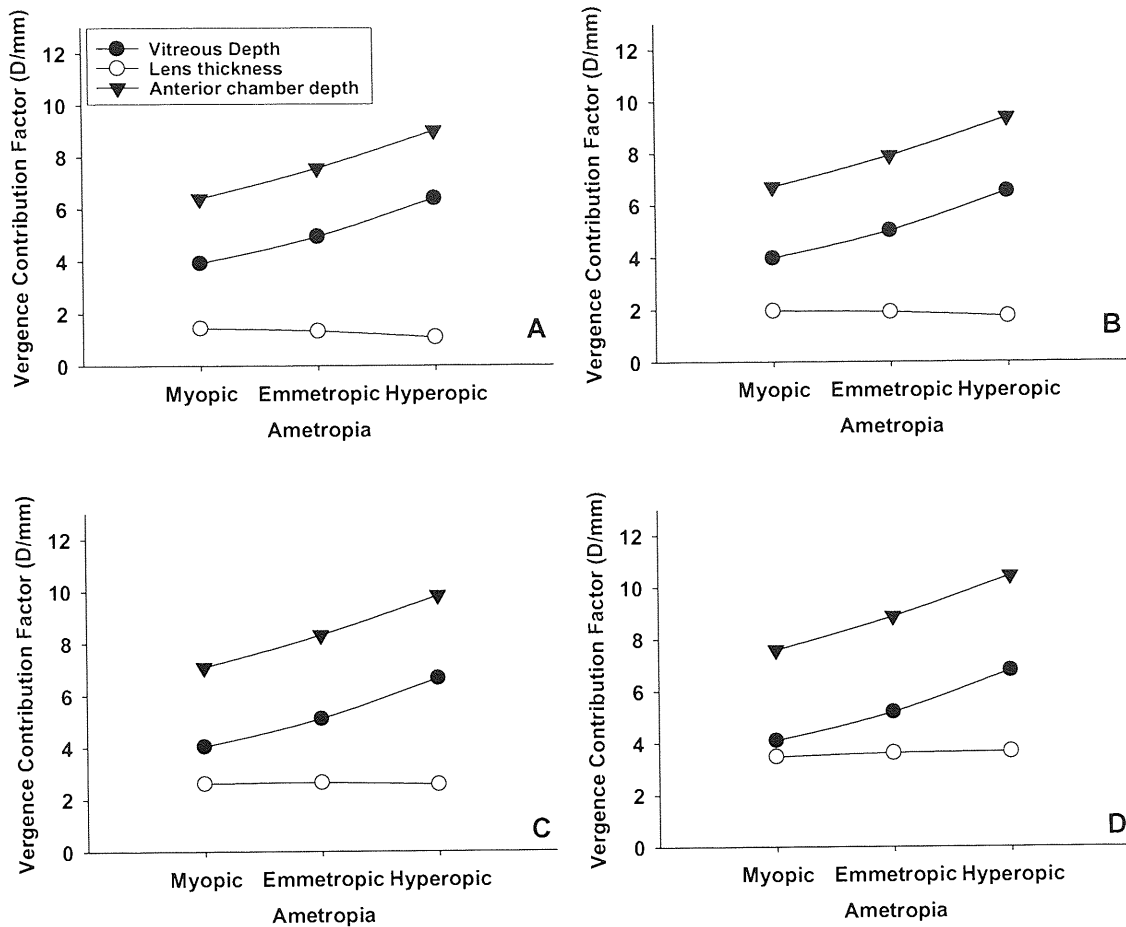


Figure 3.6 Variations in Vergence Contribution Factor (VCF) with ametropia, for a 4.0 D accommodative stimulus. Figure 3.6A represents a 20 year old eye, Figure 3.6B a 30 year old eye, Figure 3.6C a 40 year old eye and Figure 3.6D a 50 year old eye. The VCF for the anterior chamber depth is the greatest. Both the VCF for the vitreous depth and anterior chamber depth show large variations with axial length. The crystalline lens thickness VCF appears to be most independent of axial length changes.

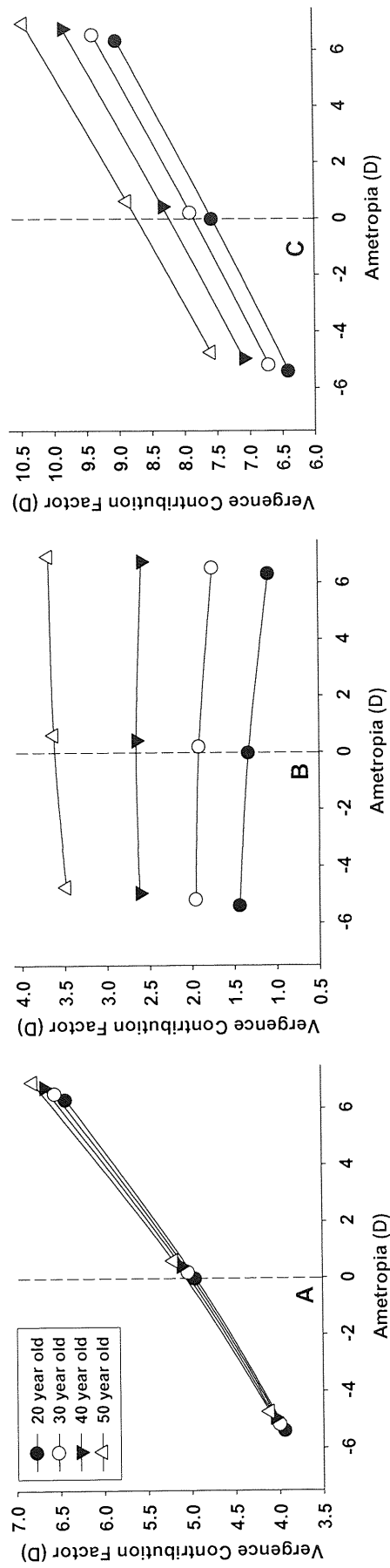


Figure 3.7 Variations in Vergence Contribution Factor (VCF) ametropia at ages 20 to 50 years in decade increments, for a 4.0 D accommodative stimulus. Figure 3.7A represents vitreous chamber depth, Figure 3.7B crystalline lens thickness and Figure 3.7C the anterior chamber depth. The scales have been individually enlarged in each plot to exploit the differences in the age groups. In all components, the VCF is highest in the older eye. The VCF for both vitreous chamber depth (A), and anterior depth (C) are negatively correlated with axial length. The VCF for crystalline lens thickness (B) follows the same trend in the older eye (50 years old), but this gradually reverses in the younger eye.

3.4 Discussion

This is the first study to compare the effect of natural damping with regard to accommodation in terms of vergence contribution. The relationship between refractive and biometric changes during accommodation with regard to ametropia has been investigated with regard to physical isometric alterations within the eye (Drexler *et al.*, 1998; Mallen *et al.*, 2006; Ostrin *et al.*, 2006; Bolz *et al.*, 2007). Erickson (1984) observed that a change in vitreous chamber depth from 18.0 to 19.0 mm reduced its divergence contribution by 3.9 D. Also noted was a concurrent reduction in convergence contribution of the anterior segment by 1.49 D; this was a natural damping effect on refractive status variation which accompanied axial length variations due to elongation of the posterior segment.

The model presents data describing the level of ametropia for changes in axial length and how this alters with age. There is a trend towards hyperopia with age (Hyams *et al.*, 1977; Saunders, 1986; Saunders, 1995), which has been corroborated in a number of large population based studies (Wang *et al.*, 1994; Attebo *et al.*, 1999).

For every millimetre change in axial length, there is a corresponding adjustment to the refractive error. The magnitude of this error is greater in the shorter hyperopic eye (3.17 D/mm; 20 year old), than in the longer myopic eye (2.69 D/mm; 20 year old); this is a good example of the natural damping effect described by Erickson. The refractive error is less with a longer vitreous length due to the reduction in divergence from this component. The damping is reduced slightly with age, but only by a minimal amount (0.02 D from 20 to 50 years old), due to a cumulative increase in anterior segment length (crystalline lens and anterior chamber depth).

As seen in Chapter 2, all surface radii changes increase vergence with accommodation. The converse is true for axial distance changes (Table 3.2). The initial hypothesis assumed that natural damping would affect accommodation, so that the myopic accommodative output is reduced. In fact, the opposite of this is true. Axial length induced vergence changes are damped; therefore, the overall negative contribution to accommodation is diminished. It is by this means that the myope produces a greater outcome refractive status for each unit of accommodation stimulus (Figure 3.1).

The anterior chamber is once again highlighted as the main component responsible for the reduction of outcome refractive status with accommodation, more so in the hyperopic eye due to reduced damping. The crystalline lens is also shown to be much less influential. The effect the lens has upon the accommodation output varies with age (Figure 3.4B). The younger crystalline lens reduces vergence change to a greater extent in the myopic eye, whereas in the older eye, it is the hyperopic lens which depresses this change the greatest. The relationship discovered can be attributed to the complex changes in lens equivalent refractive index, thickness and position which alter with age and ametropia.

The theories of presbyopia have been comprehensively reviewed in a number of publications (Gilmartin, 1995; Strenk *et al.*, 1999; 2004; 2005; Glasser, 2008; Charman, 2008). These theories vary between authors, with the exact cause remaining equivocal. The majority of studies place the cause of presbyopia on physical age-related changes to the ciliary body (Tamm *et al.*, 1992a; Strenk *et al.*, 1999; Strenk *et al.*, 2006), zonular lens insertions (Farnsworth and Shyne, 1979), capsular bag elasticity and thickness (Krag *et al.*, 1997; Krag and Andreassen, 2003), and crystalline lens size and mass changes (Glasser and Campbell, 1999). The most prevalent factor appears to be an increase in lens stiffness with age (Pau and Kranz, 1991; Weeber *et al.*, 2005; 2007). Vergence and refractive changes have played little part in the majority of these theories. The drift towards hyperopia and the small decrease in vergence contribution to accommodation with age, give further clues to the development of presbyopia.

The use of the VCF highlights the power of each component with respect to vergence changes, and gives greater information on the ocular vergence system. The anterior chamber has the highest overall VCF, highlighting the importance of this component in the ocular system. Of the crystalline lens, the posterior surface has a greater VCF than the anterior surface; this relationship remains the same with age and ametropia.

Damping of the VCF is very obvious in the myope, with the crystalline lens thickness displaying the greatest change with age (Figure 3.6). Vitreous depth VCF is the most dependent on ametropia as would be expected, but is relatively independent of ageing change.

3.5 Conclusion

The damping effect, as first described by Erickson (1984), has been analysed with regard to accommodation using the Dubbelman eye model (Norrby, 2005).

The key findings of this chapter are summarised below.

- The degree of ametropia as a result of equal axial length change is asymmetric, with a larger outcome refractive error in shorter eyes.
- The model confirms the hyperopic shift with age, as described by population based studies (Wang *et al.*, 1994; Attebo *et al.*, 1999).
- Accommodative output is larger in the myopic eye due to the damping of the negative vergence changes associated with axial distance alteration; surface radii remain static with ametropia.
- Reduced damping and the subsequent reduction in output accommodation with age is due to an overall increase in anterior segment length, and may add a new feature to the present biophysical theories of presbyopia.
- The crystalline lens thickness exhibits interesting trends in vergence change with ametropia and age. Relationships such as these can only be explained by the complex interactions of refractive index, thickness magnitude and position which alter with both parameters.

With age, the eye undergoes a number of physical and functional changes, many of which are responsible for the loss of accommodation, or presbyopia (Glasser, 2008). An additional major change includes modifications which take place within the crystalline lens; ultimately resulting in the formation of a cataract (Johns *et al.*, 2003). Johns and co-workers (2003) suggest that cataracts are the commonest cause of reversible loss of useful vision worldwide. Since the late 1940s, intraocular lenses (IOLs) have been used to correct the visual loss associated with this condition (Rosen, 1984). Today, most surgery consists of secure, in-the-bag (capsular) fixation of foldable silicone or acrylic IOLs (Linebarger *et al.*, 1999; Davies *et al.*, 2006).

More recently, 'accommodating' IOLs (AIOLs) have been introduced (Dick, 2005; Findl, 2005; Glasser, 2006; Wolffsohn *et al.*, 2006a; 2006b; Menapace *et al.*, 2007; Doane and Jackson, 2007; Glasser, 2008), many of which rely on the forward movement of the optic with accommodation to alter the refractive status (Langenbacher *et al.*, 2003; Nawa *et al.*, 2003; Rana *et al.*, 2003; Langenbacher *et al.*, 2004; Wolffsohn *et al.*, 2006a; 2006b).

It has been reported in the literature that the accommodative output associated with a 1.0 mm anterior shift in IOL position is dependant upon the axial length of the eye in which it has been implanted (Nawa *et al.*, 2003). Considering this, it may be possible to explain these findings by using the Dubbelman eye model with an IOL in place of the crystalline lens, and to consider the results in terms of natural damping. It may consequently be possible to provide more information to the surgical profession as to the viability of fitting accommodating IOLs in patients with specific AL parameters.

Considering the results of Chapters 2 and 3, the anterior movement of the natural crystalline lens equated to a reduction in vergence change with accommodation. If this is true, then further clarification is required to explain how the forward movement of an IOL can increase the accommodative output of the ocular system.

CHAPTER 4

MODELLING THE ACCOMMODATING INTRAOCULAR LENS

4.1 Introduction

One of the unresolved side-effects of cataract surgery is the loss of accommodation. Although less important for the presbyopic patient, it certainly provides obstacles for pre-presbyopic patients or those opting for clear lens extractions (Solomon *et al.*, 2002; Sandoval *et al.*, 2005). Accommodating intraocular lenses (AIOLs) have seen increased interest in recent years (Charman, 2008; Glasser, 2008). AIOLs work according to a number of different theories, mechanisms, and principles (Dick, 2005; Findl, 2005; Glasser, 2006; Menapace *et al.*, 2007; Doane and Jackson, 2007; Glasser, 2008). One such mechanism is the focus-shift principle, or the forward translation of a single optic intraocular lens (IOL; Langenbucher *et al.*, 2003; Nawa *et al.*, 2003; Rana *et al.*, 2003; Langenbucher *et al.*, 2004; Wolffsohn *et al.*, 2006a; 2006b). The mechanisms these AIOLs employ differ. Most are designed to be placed into the capsular bag in a posteriorly vaulted position with the optic against the posterior capsule and vitreous face (Cumming *et al.*, 2001).

One theory of how the IOL facilitates a dioptric increase in power, assumes that contraction of the ciliary muscle causes a pressure gradient between the aqueous and vitreous (Coleman, 1970; 1986). The increased pressure from the vitreous causes anterior displacement of the lens-zonule diaphragm (Coleman and Fish, 2001). Other theories rely on ciliary muscle contraction or capsular bag elasticity. The Kellen *Tetraflex KH-3500* (Lenstec, St. Petersburg, Florida), and the Eyeonics *Crystalens AT-45* and *AT-50* (Aliso Viejo, California, USA) are both based on these theories; the latter using hinged haptics, the former flexible plate haptics (Glasser, 2008).

Study	Method	Variables	Results
Nawa <i>et al.</i> (2003)	Ray tracing using Mathematica® (Wolfram). Ray-tracing from Horiuchi & Akagi, 2001.	Axial length, anterior corneal radius of curvature and IOL power. Outcome refraction plotted.	For 1.0 mm anterior shift of the IOL, accommodation varied from 0.8 D in the long eye to 2.3 D in the short eye.
Rana <i>et al.</i> , (2003)	Computer based ray-tracing using thin-lens formulae.	Single piece +20 D IOL and various combinations of doublet lenses (i.e. dual-optic IOLs).	For the single piece IOL: a 0.5 mm anterior shift provides 0.426 D, 1 mm shift gives 0.846 D, and 1.5 mm of movement provides 1.261 D of accommodation respectively.
Langenbucher <i>et al.</i> (2004)	Used the Gullstrand model eye. Simulated pseudo-accommodation by inducing a 1 mm forward shift of the single optic IOL.	Variation in axial length and equivalent single and dual-optic IOL to give emmetropia.	In shorter eyes, the single optic produces the greatest accommodative output. In longer eyes, it produces only 25% the amount of the dual-optic.
Missotten <i>et al.</i> (2004)	Used a thin lens approximation formula.	Axial length, anterior chamber depth and IOL power.	Short eyes with high IOL powers produce the greatest amplitudes of pseudo-accommodation.
Ho <i>et al.</i> (2006)	Used the Navarro (1985) model eye.	Tested single and dual element IOLs	In the single-optic IOL, 1.0 mm anterior shift gave rise to 1.25 D of accommodation.

Table 4.1 Studies which have evaluated single-piece intraocular lenses and their accommodative function using modelling techniques.

The other single optic IOLs (Bausch & Lomb *OPAL*, Rochester, New York, USA; HumanOptics *ICU*, Erlangen, Germany; Acuity *C-Well* [OrYehuda, Israel]; Morcher *BioComFold 43E* [Stuttgart, Germany]) rely on a decrease in capsular bag diameter in accordance to the natural accommodative mechanism. Such a decrease produces a lever action on the haptics, propelling the optic anteriorly (Glasser, 2008). The *Crystalens AT-45* and *AT-50* are approved for clinical use in the USA by the FDA. The Lenstec *Tetraflex* is undergoing US FDA clinical trials. The Morcher *BioComFold 43E*, Human Optics *ICU* and Lenstec *Tetraflex* have been or are being used clinically in Europe. The other AIOLs are in the research and development stage, or have had limited clinical use (Glasser, 2008).

Some authors have modelled refractive outcome using ray tracing to show total accommodation output with a variety of IOLs and schematic eyes (Nawa *et al.*, 2003; Rana *et al.*, 2003; Langenbucher *et al.*, 2004; Missotten *et al.*, 2004; Ho *et al.*, 2006; Table 4.1). However, they have not compared these results to a similar phakic model, or described changes in vergence during the process of pseudophakic accommodation.

4.1.1 Aims

The theory of damping and its analysis by vergence contribution has been shown in Chapter 2 and 3 to provide interesting and novel information using a current schematic eye (Norrby, 2005). What is still not clear is how a pseudophakic eye with a single optic will behave under the same conditions and constraints (i.e. changing age and accommodation) previously demonstrated in the phakic eye. Hitherto, vergence changes within the optical system have not been considered, neither has any comparison been made between the phakic and pseudophakic eye with regard to such changes. Consequently, it may be possible to provide more information to the surgical profession as to the viability of fitting AIOLs in patients with varying axial lengths.

4.2 Methods

The Dubbelman schematic eye (Norrby, 2005) was modified to represent a pseudophakic eye. The crystalline lens was replaced by a thin lens representing a single-optic AIOL. Three axial lengths were used, 21.267 mm (short eye), 23.267 mm (average eye; 20 year old emmetrope from eye model) and 25.267 mm (long eye). As in Chapter 3, the alteration of axial length from emmetropia (as represented by a 20 year old eye) was by ± 2.0 mm. The step-along reverse ray-trace from the retinal plane to the anterior corneal pole is shown below.

4.2.1 Vergence from the vitreous chamber (L_6)

The AIOL is placed in the centre of the crystalline lens capsular bag, so that the depth of the anterior chamber with the IOL *in-situ* ($d_{2(IOL)}$) is equivalent to the anterior chamber (d_2) plus half of the crystalline lens thickness (d_3 ; Chapter 3).

$$d_{2(IOL)} = d_2 + (d_3 / 2). \quad (4.1)$$

The IOL is moved anteriorly by 0.5, 1.0 and 1.5 mm to replicate the focus-shift principle of pseudophakic accommodation. To achieve this, the anterior chamber depth is modified accordingly. In Equation 4.2, x is the amount of IOL shift.

$$d_{2(IOL)} = [d_2 + (d_3 / 2)] - x. \quad (4.2)$$

It is important to note that the anterior chamber depth (d_3) is still subject to the formulae specified by Dubbelman *et al.* (2001), which alter with age and accommodation (Norrby, 2005; Table 2.1; Table 2.2; Chapter 2).

The vitreous chamber depth (d_4) is calculated from the sum of the other axial ocular distances (d_1 and $d_{2(IOL)}$) subtracted from axial length of the eye. The axial length of the model (y) was varied from baseline at 23.267 mm by ± 2.0 mm.

$$d_4 = y - (d_1 + d_{2(IOL)}). \quad (4.3)$$

Where y is the axial length, d_1 is the corneal thickness, $d_{2(IOL)}$ the anterior chamber depth with the IOL *in-situ*, and d_4 the length of the vitreous chamber.

A value for the vergence attributed to the vitreous chamber is adopted from Erickson (1984).

$$L_6 = 1000n_3 / (-d_4 + 0.25). \quad (4.4)$$

Where L_6 is the vergence from the vitreous chamber and n_3 the refractive index of the vitreous (Table 2.2; Chapter 2). The receptor layer is included in the Dubbelman model as derived by Norrby, and is given the value of 0.25 mm. The vitreous chamber depth is given a negative value due to the sign convention.

4.2.2 Vergence at the intraocular lens (L_5)

The power of the IOL (F_3) was adjusted to give functional emmetropia at the axial length specified. The diverging wavefronts from the vitreous chamber are modified by the IOL power.

$$L_5 = L_6 + F_3. \quad (4.5)$$

Here, L_5 is the vergence at the IOL, L_6 the vergence from the vitreous chamber and F_3 the power of the IOL.

4.2.3 Vergence at the anterior aqueous chamber (L_4)

The vergence of light passing through the aqueous chamber is modified as shown in Equation 4.6.

$$L_4 = 1000n_2 / (1000n_2 / L_5 - d_{2(IOL)}). \quad (4.6)$$

Where L_5 is the vergence at IOL, n_2 is the refractive index of the aqueous humour (Table 2.2; Chapter 2) and $d_{2(IOL)}$ the anterior chamber depth with the IOL *in situ* (Table 2.1; Chapter 2).

4.2.4 Vergence at the posterior corneal surface (L_3)

Equation 4.7 was used to calculate the power of the posterior corneal surface.

$$F_2 = [1000(n_2 - n_1)] / r_2. \quad (4.7)$$

Where F_2 is the power of the posterior corneal surface, n_1 is the refractive index of the cornea (Table 2.2; Chapter 2) and r_2 is the radius of the posterior corneal surface. Equation 4.8 was used to calculate the vergence of light leaving the anterior chamber and entering the posterior corneal surface.

$$L_3 = L_4 + F_2. \quad (4.8)$$

4.2.5 Vergence at the anterior corneal surface (L_2)

The vergence of light passing through the cornea is modified as shown in Equation 4.9.

$$L_2 = 1000n_1 / (1000n_1 / L_3 - d_1). \quad (4.9)$$

Where L_3 is the vergence at the posterior corneal surface, n_1 is the refractive index of the cornea (Table 2.2; Chapter 2) and d_1 the corneal thickness (Table 2.1; Chapter 2).

4.2.6 Vergence of light leaving the eye: The back vertex power (L_1)

Equation 4.10 was used to calculate the power of the anterior corneal surface.

$$F_1 = [1000(n_1 - 1)] / r_1. \quad (4.10)$$

Where F_1 is the power of the anterior corneal surface, n_1 is the refractive index of the cornea (Table 2.2; Chapter 2), 1 is the refractive index of air and r_1 is the radius of the anterior corneal surface. Equation 4.11 was used to calculate the vergence of light leaving the eye, hence the back vertex power.

$$L_1 = L_2 + F_1. \quad (4.11)$$

The vergence contribution of each refractive surface or axial distance was calculated by subtracting the entrance vergence from the exit vergence of the interface; this value was expressed in dioptres. Vergence contributions found with anterior IOL shift were subtracted from those found in under relaxation to provide a measure of the change in vergence contribution that took place with pseudophakic accommodation.

The magnitude of the effect each interface contributed to vergence change was calculated; this is expressed as the ratio of dioptric to axial position or radius change. The fraction is expressed in dioptres per millimetre (D/mm), and is termed the Vergence Contribution Factor (VCF; Chapter 2).

Results were displayed in terms of the AIOL position under relaxed conditions (no IOL shift), the AIOL power to maintain emmetropia, and refractive status or output accommodation. The ocular component contributions were again analysed in terms of vergence and VCF.

4.3 Results

For all anterior forward movements in AIOL position and subsequent reduction in anterior chamber depth, there is a net increase in refractive status (i.e. pseudophakic accommodation; Table 4.2 and 4.3; Figure 4.1).

The accommodation output is inversely proportional to axial length (Figure 4.1). AIOL position (anterior chamber depth; ACD) and its power required for emmetropia, both increase with age; thus there is an increase in ACD. Accommodation output is also positively correlated to the age of the eye (Table 4.2). In the shorter eye, change in refractive status per millimetre axial shift in AIOL position, is over twice the magnitude when compared to the longer eye. Differences in AIOL position, AIOL power and refractive status alter by very small increments with age.

Due to the crystalline lens being replaced with a thin-lens AIOL, the vergence contribution from the lens is now simply its power. This power does not change with anterior movement and, therefore, does not influence vergence change with accommodation, directly. This leaves only three components responsible for vergence change: the vitreous chamber; anterior chamber; and corneal thickness. The component primarily responsible for vergence change is the vitreous chamber (Table 4.3). The vergence change increases in the positive direction with anterior shift of the AIOL, in opposition to negative axial vergence changes seen in previous models (Chapter 2 and 3). The magnitude of vergence change is damped in the longer eye compared to the shorter eye, with the longer vitreous chamber providing less dioptric input to vergence change (Figure 4.2).

Age	Axial length (mm)	IOL position/ACD at O D stimulus (mm)	IOL power (D)	IOL shift (mm)	Refractive status (D)
20	25.267	4.797	16.165	-0.5	0.490
				-1.0	0.985
				-1.5	1.487
	23.267		23.474	-0.5	0.755
				-1.0	1.517
				-1.5	2.286
	21.267		32.593	-0.5	1.123
				-1.0	2.255
				-1.5	3.393
30	25.267	4.815	16.190	-0.5	0.490
				-1.0	0.986
				-1.5	1.488
	23.267		23.512	-0.5	0.755
				-1.0	1.518
				-1.5	2.288
	21.267		32.652	-0.5	1.125
				-1.0	2.259
				-1.5	3.399
40	25.267	4.833	16.215	-0.5	0.490
				-1.0	0.987
				-1.5	1.489
	23.267		23.552	-0.5	0.756
				-1.0	1.520
				-1.5	2.292
	21.267		32.710	-0.5	1.126
				-1.0	2.261
				-1.5	3.403
50	25.267	4.851	16.242	-0.5	0.491
				-1.0	0.988
				-1.5	1.491
	23.267		23.592	-0.5	0.757
				-1.0	1.522
				-1.5	2.294
	21.267		32.769	-0.5	1.128
				-1.0	2.265
				-1.5	3.408

Table 4.2 Refractive status (pseudophakic accommodation) with anterior IOL shift of 0.5, 1.0 and 1.5 mm. Axial length is shown for a long (25.267 mm), short (21.267 mm) and average eye (23.267 mm; emmetropia at 20 years of age; Dubbelman model eye). Intraocular lens power is calculated to give emmetropia at each axial length stated. IOL position is stated when the eye is relaxed and is equal to the anterior chamber depth plus half the crystalline lens thickness, as stated in the original schematic eye. The age of the model is adjusted from 20 to 50 years of age in decade increments.

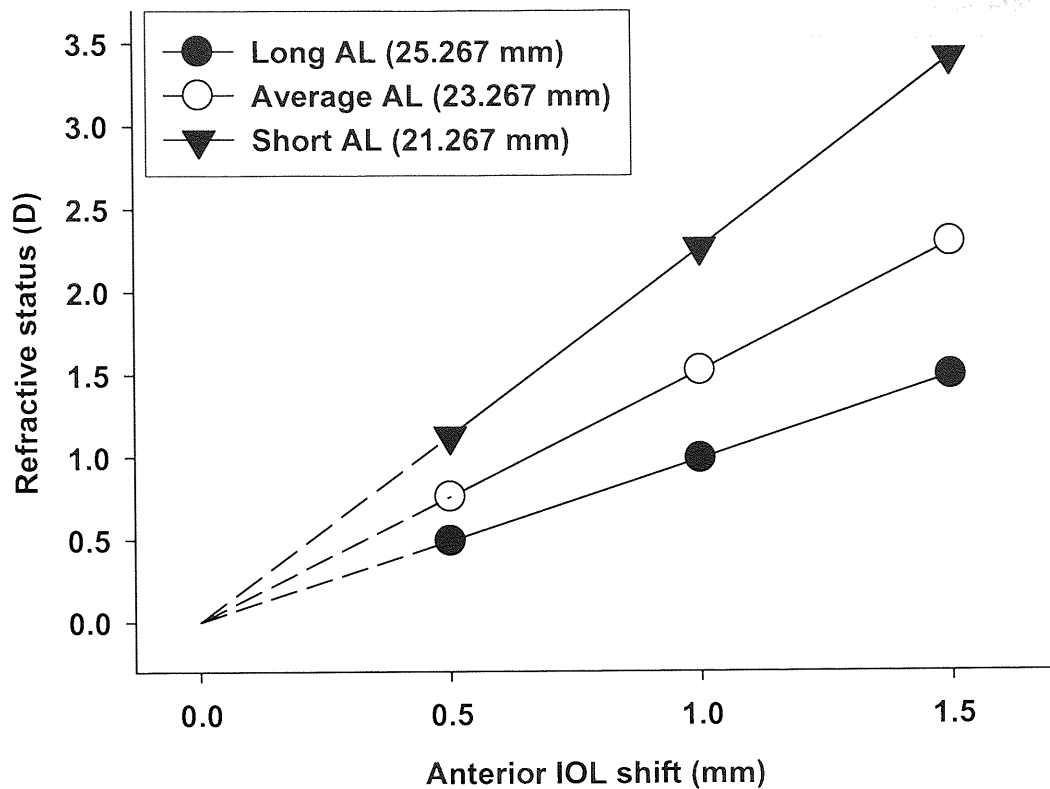


Figure 4.1 Refractive status (pseudophakic accommodation) as a function of anterior shift in IOL position. The results for three axial lengths (AL) are displayed, a long, average and short eye, with a 2.0 mm difference in AL between each. Refractive changes shown are for a 50 year old eye.

As ACD reduces with anterior IOL shift, there is a relatively negative change in vergence change. Further, the amount of negative vergence contribution increases with this anterior lens movement, but alters little with axial length in comparison to vitreous chamber depth (Figure 4.2). Vergence in this component (ACD) is therefore damped only slightly. Corneal thickness displays a small negative contribution to vergence change as seen in previous chapters; this effect is damped in the longer eye.

The VCF (Table 4.4; Figure 4.3) shows very well the damping taking place in the longer eye, and that the vitreous chamber is the most effective ocular component, with the greatest ability to elicit vergence change with accommodation. The VCF for the anterior chamber is lower, and alters little with axial length. Corneal thickness has an infinitely large VCF as its thickness fails to alter, but is still responsible for a degree of vergence modification. The VCF for both axial components reduces with anterior placement of the IOL, contrary to actual vergence change, suggesting that the effectivity of these elements is reduced with an anteriorly located IOL.

Axial length (mm)	IOL shift (mm)	Vergence change (D)		
		Vitreous depth	Anterior chamber depth	Corneal thickness
25.267	-0.5	1.615	-1.104	-0.020
	-1.0	3.152	-2.124	-0.040
	-1.5	4.619	-3.068	-0.060
23.267	-0.5	1.986	-1.198	-0.031
	-1.0	3.868	-2.284	-0.062
	-1.5	5.654	-3.267	-0.092
21.267	-0.5	2.502	-1.328	-0.046
	-1.0	4.857	-2.502	-0.091
	-1.5	7.079	-3.536	-0.135

Table 4.3 Vergence changes for each ocular component with anterior IOL shift of 0.5, 1.0 and 1.5 mm. Vergence change is shown for a long (25.267 mm), short (21.267 mm) and average eye (23.267 mm; emmetropia at 20 years of age; Dubbelman model eye); for a 50 year old eye.

Axial length (mm)	IOL shift (mm)	Vergence Contribution Factor (D/mm)		
		Vitreous depth	Anterior chamber depth	Corneal thickness
25.267	-0.5	3.229	2.207	∞
	-1.0	3.152	2.124	∞
	-1.5	3.079	2.045	∞
23.267	-0.5	3.972	2.396	∞
	-1.0	3.868	2.284	∞
	-1.5	3.769	2.178	∞
21.267	-0.5	5.004	2.656	∞
	-1.0	4.857	2.502	∞
	-1.5	4.719	2.357	∞

Table 4.4 Vergence contribution factor (VCF) for each ocular component with anterior IOL shift of 0.5, 1.0 and 1.5 mm. VCF is shown for a long (25.267 mm), short (21.267 mm) and average eye (23.267 mm; emmetropia at 20 years of age; Dubbelman model eye). Corneal thickness fails to move physically, thereby producing an infinitely large VCF. Vergence Contribution Factors shown are for a 50 year old eye.

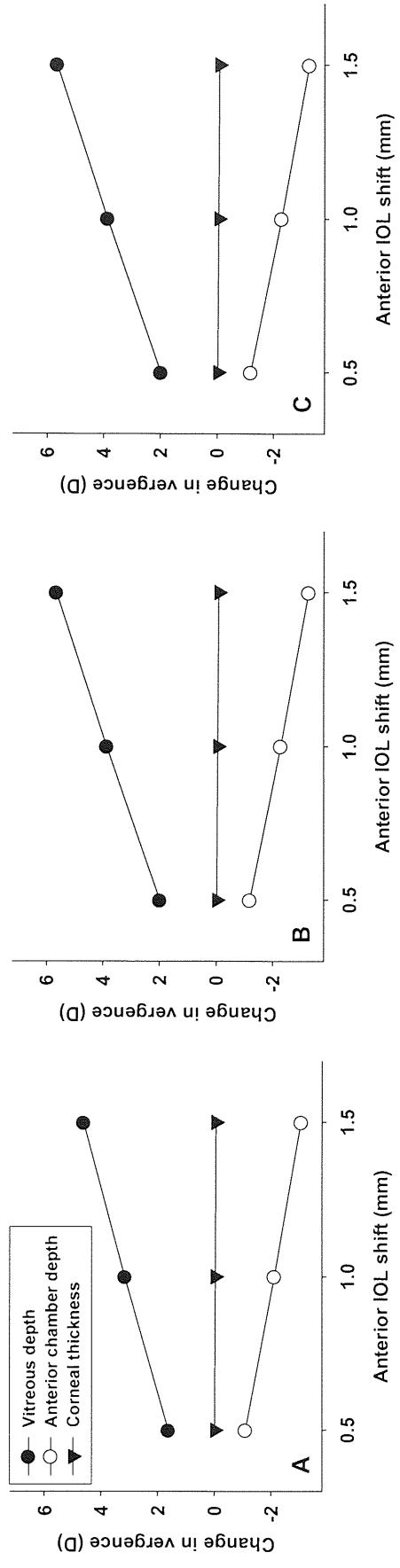


Figure 4.2 Vergence changes for each ocular component with anterior IOL shift of 0.5, 1.0 and 1.5 mm. Figure 4.2A represents long eye (25.267 mm AL), Figure 4.2B an average eye (23.267 mm AL; emmetropia at 20 years of age; Dubbelman model eye), and Figure 4.2C a short eye (21.267 mm). Vergence changes shown are for a 50 year old eye.

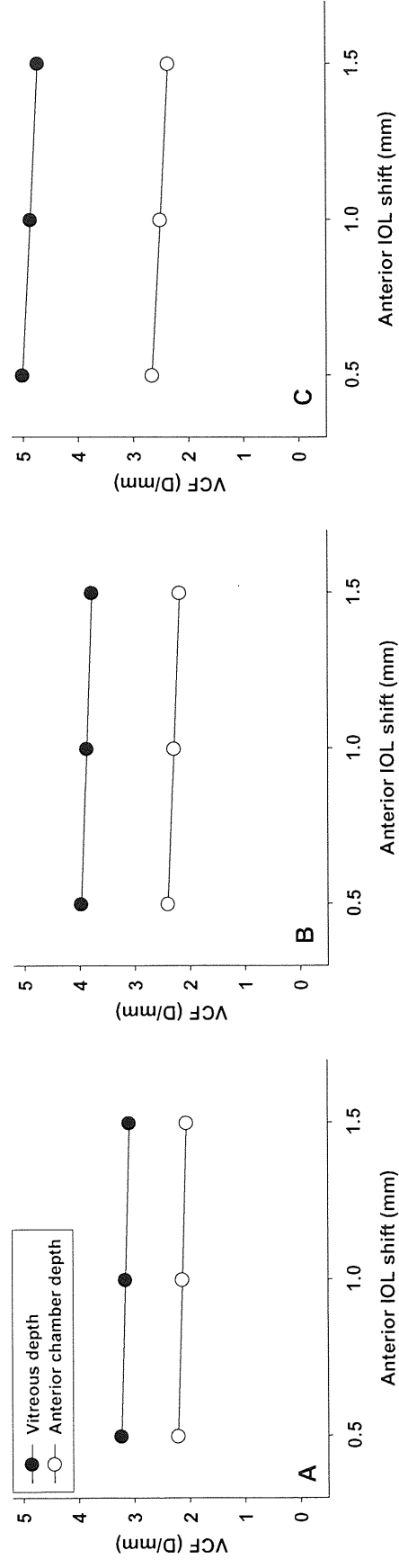


Figure 4.3 Vergence Contribution Factor (VCF) for each ocular component with anterior IOL shift of 0.5, 1.0 and 1.5 mm. Figure A represents a long eye (25.267 mm AL), Figure B an average eye (23.267 mm AL); emmetropia at 20 years of age; Dubbelman model eye), and Figure C a short eye (21.267 mm AL). Corneal thickness fails to move physically, thereby producing an infinitely large VCF, and so is not included. Vergence contribution factors shown are for a 50 year old eye.

4.4 Discussion

The aim of this study was to investigate optically the behaviour of a single-piece AIOL using a recent published schematic eye (Norrby, 2005). Further, comparison of phakic and pseudophakic accommodation in the same model, using the same optical parameters, is a novel method of examining human accommodation. The theory of damping, initially produced by Erickson (1984), has been shown to reduce refractive output (accommodation) in eyes with a long AL.

One option in modern cataract surgery involves the implantation of AIOLs. These lenses are designed to utilise some part of the accommodative physiology to induce a movement or change in shape of the IOL and elicit optical changes within the eye (Glasser, 2008). It is important to ensure that the biophysical properties of the patient's eye do not become confounding factors in the success of that surgery. It is for this reason that investigation into the effect of natural damping on accommodating IOLs is so important.

A number of studies have found variations in accommodative output with anterior shift IOLs (Cumming *et al.*, 2001; K uchle *et al.*, 2002; Ali o *et al.*, 2004; Claou e *et al.*, 2004; Marchini *et al.*, 2004). Glasser (2008) used the Bennett and Rabbetts (1998) schematic eye to investigate accommodative output from a one millimetre forward shift of a one millimetre thick optic. The long eye (26.04 mm AL) produced 0.8 D, the average eye (24.09 mm AL) 1.3 D, and the short eye (22.04 mm AL) 1.85 D. These results show a very similar trend to the Dubbelman model.

Nawa *et al.* (2003) modelled the 0.5 mm thick Alcon *AcrySof*[®] IOL (Alcon Laboratories Inc., USA) with 1.0 mm anterior movement. Axial length was varied from 21.0 to 27.0 mm with IOL powers varying from 11.0 to 30.0 D. Using a fixed anterior corneal radius of curvature (7.7 mm), 1.0 mm of forward IOL movement elicited 0.8 D (27.0 mm AL; 11.0 D IOL), 1.3 D (24.0 mm AL; 20.0 D IOL) and 2.3 D (21.0 mm AL; 30.0 D IOL) of pseudophakic accommodation (Nawa *et al.*, 2003). Calculations were also made by varying anterior corneal curvature whilst keeping IOL power and axial length constant. Results were consistent with the Bennett and Rabbetts eye and similar to the Dubbelman model.

Rana and co-workers (2003) studied the effects of IOL movement and pseudophakic accommodation using singlet lenses (+20.0 D) and a combination of doublet lenses (total power +20.0 D). For the single piece IOL, 1.261 mm of forward movement produced 1.5 D of pseudophakic accommodation, whilst a 0.846 mm shift gave 1.0 D. When calculated, this lens should give approximately 1.2 D of accommodation for a shift of 1.0 mm; however, little reference is made to axial length changes or vitreous effects. Nawa and co-authors (2003) state that a 20.0 D IOL moving forward by 1.0 mm should give rise to 1.3 D of accommodation.

Langenbucher *et al.* (2004) used the Gullstrand model eye to plot pseudoaccommodation with anterior movement of a mono- and dual-optic IOL. The single IOL produced smaller levels of accommodation per unit shift, and it was noted that shorter eyes with higher powered lenses produced greater optical changes per millimetre. Variations in AL from 18.0 to 28.0 mm were plotted against pseudoaccommodation with 1.0 mm of shift. Accommodation output varied from approximately 3.7 D with the extremely short eye (18.0 mm AL) to approximately 0.5 D with the extremely long eye (28.0 mm AL).

When comparing the Dubbelman model to the Gullstrand/Langenbucher schematic, a similar magnitude of pseudoaccommodation is noted. For AL of 21.0, 23.0 and 25.0 mm, Langenbucher's model produced approximately 2.2, 1.5 and 1.0 D of accommodation, respectively, which matches very well the data presented here (Table 4.2).

Missotten *et al.* (2004) used thin lens approximation equations to obtain a formula containing axial length, mean keratometry, anterior chamber depth, and anterior chamber shift due to the IOL, as variables. Considering a forward IOL movement of 1.0 mm, the formula generated for a long AL (28.0 mm; mean keratometry, 38.0 to 48.0 D) yielded an accommodative amplitude (AA) ranging from -0.83 to 0.03 D. For a short AL (20.0 mm; mean keratometry, 38.0 to 48.0 D), the calculated AA ranged from -3.62 to -1.97 D. The study presents model data confirming that shorter axial lengths have the potential for greater pseudoaccommodation than longer axial lengths.

Ho and colleagues (2006) utilised the Navarro model eye (Navarro *et al.*, 1985) with its aspheric surfaces. With the single piece IOL with a power for effective emmetropia, a 1.5 mm forward IOL shift produced 1.9 D of accommodation. The rate of accommodation is therefore 1.2 D/mm, similar to the Bennett and Rabbetts (1.3 D/mm; average AL; Bennett

and Rabbetts, 2007) and the Dubbelman (1.5 D/mm; emmetropia; 20 years old; Norrby, 2005) models.

Comparing the phakic model eye to the pseudophakic model eye is a novel technique. The Dubbelman pseudophakic eye changes with age by showing an increase in ACD, contrary to a phakic eye with the crystalline lens *in situ*. The crystalline lens, however, also increases in axial thickness with a concurrent reduction in anterior and posterior radii of curvature (Dubbelman and van der Heijde, 2001; Strenk *et al.*, 2004). The forward shift in the AIOL is the only cause of dioptric change with accommodative stimulus within the pseudophakic model. In the phakic eye, the root of this is the curvature changes associated with the crystalline lens (see Chapter 2).

Vergence changes in the pseudophakic eye are similar with regard to corneal thickness contributions. In both phakic, and pseudophakic situations, the corneal thickness provides little alteration to the path of light exiting the eye. For example, in the phakic 50 year old average eye (23.267 mm AL) with a 4.0 D stimulus to accommodation, the corneal thickness alters in vergence by -0.165 D. In the same pseudophakic eye with an axial lens shift of 1.5 mm, this figure is -0.092 D (Table 4.3).

The ACD still provides a negative vergence contribution with accommodation, with both the crystalline and replacement intraocular lens; however, with the IOL in place its magnitude is increased. In a 50 year old average eye (23.267 mm AL) with a 4.0 D stimulus to accommodation, the contribution change from the anterior chamber is -1.066 D. In the same pseudophakic eye with 1.5 mm of axial lens shift it is -3.267 D (Table 4.3).

The contribution from the vitreous undergoes the greatest change, not only in terms of magnitude but also in sign. Vitreous change with accommodation is negative in a phakic model eye (-0.123 D; 50 year old eye with 4.0 D accommodation stimulus; 23.267 mm AL). This becomes positive and is vastly increased in the pseudophakic model (5.654 D; 50 year old eye with 1.5 mm axial shift; 23.267 mm AL).

VCFs of the vitreous and anterior chambers are both reduced in the IOL model compared to the natural phakic model. In the 50 year old eye with a 4 D accommodation stimulus (average 23.267 mm AL) the VCF is 5.115 D/mm and 8.874 D/mm, respectively. This is compared to the same model with a 1.5 mm axial shift in IOL position, where the VCF is

now 3.769 D/mm and 2.178 D/mm, respectively. The anterior chamber VCF is reduced dramatically, and is no longer the primary root of vergence change in the pseudophakic model.

4.5 Conclusion

The major findings of this chapter are summarised below.

- Anterior translocation of a spherical intraocular lens along the visual axis of the eye gives rise to a dioptric increase in eye power, also known as pseudophakic accommodation.
- The magnitude of pseudophakic accommodation is dependant on the axial length of the eye and the subsequent power of the AIOL to give emmetropia.
- Eyes with shorter AL and greater AIOL powers produce a greater outcome refractive status (i.e. pseudo-accommodation) compared to eyes with longer AL.
- In the pseudophakic model, ACD, and therefore AIOL position, increase/move posteriorly with age. This has little effect on the vergence changes with accommodation, but does give rise to the need for a slightly more positive IOL and subsequently, a slightly larger refractive status (pseudo-accommodation output).
- The vitreous chamber is the primary component responsible for positive vergence change with accommodation in the pseudophakic model in contradiction to the role it plays in the phakic eye.
- The anterior chamber still produces a negative vergence change with accommodation; this is largely increased compared to the natural eye model, although is less responsive with change (lower VCF).
- A posterior placed IOL in a shorter eye will give rise to the greatest dioptric output per unit of anterior axial displacement. Further, the amount of pseudophakic accommodation should be more than enough to read comfortably at 40.0 cm (> 2.5 D), but only in the shortest AL tested, and in the older eye, where the anterior chamber depth is the greatest (i.e. most posteriorly placed IOL).

Thus far, phakic and pseudophakic accommodation has been investigated using a schematic eye. This method has produced some new and interesting results regarding human accommodation. Biometric changes associated with accommodation have been studied by a number of authors and with a variety of techniques (Koretz *et al.*, 1987; 1997b; Drexler *et al.*, 1997; Strenk *et al.*, 1999; Dubbelman and van der Heijde, 2001; Dubbleman *et al.*, 2001; 2002; 2005; Vilupuru and Glasser, 2005; Strenk *et al.*, 2005; Ostrin *et al.*, 2006; Jones *et al.*, 2007).

The introduction of a new imaging technique allows the study of human accommodation to be advanced. Anterior Segment Optical Coherence Tomography (AS-OCT) provides the advantage of producing direct, non-contact images of the anterior segment in static conditions. An optometer-based system with negative or positive lenses can be used to reproduce the conditions of natural accommodation. Hitherto, the use of this instrument in the study of accommodation has been limited (Baikoff *et al.*, 2004; 2005a; 2005b; Richdale *et al.*, 2008).

A study into phakic accommodation using this relatively new optical method of examining anterior segment changes with accommodation is required. The comparison of subsequent data with the Scheimpflug photography based Dubbelman model eye, as well as other published techniques, will allow verification of this instrument in a research and clinical setting.

CHAPTER 5

ANALYSIS OF PHAKIC ACCOMMODATION WITH ANTERIOR SEGMENT OPTICAL COHERENCE TOMOGRAPHY

5.1 Introduction

The biometric changes associated with accommodation in primates have been the subject of interest of a number of authors over the years. The exact process of accommodation remains equivocal, with authors such as Schachar (Schachar, 1994; Schachar *et al.*, 1996) disputing the long held theory proposed by Helmholtz (Helmholtz, 1855; 1924).

The accommodative refractive change is primarily brought about by alterations in the surface curvatures of the crystalline lens (Young, 1801; Cramer, 1853; Helmholtz, 1924). During accommodation, the anterior radius of curvature decreases (Koretz *et al.*, 1984; 1997; 2002; Garner and Yap, 1997; Kirschcamp *et al.*, 2004; Rosales *et al.*, 2006), with a smaller simultaneous steepening of the posterior surface (Fincham, 1924-5; Ciuffreda, 1991; Garner and Yap, 1997; Kirschcamp *et al.*, 2004). The lens equatorial diameter decreases (Brown 1973; Wilson, 1997; Glasser and Kaufman, 1999; Strenk *et al.*, 1999), with the curvature changes resulting in a reduction of the anterior chamber depth and an increase in lens axial thickness (Drexler *et al.*, 1997; Garner and Yap, 1997; Kirschcamp *et al.*, 2004; Strenk *et al.*, 2004; 2005). It is widely accepted that the change in shape of the crystalline lens, in youth at least, is dictated by the elasticity of the lens capsule (Fincham, 1924-5, 1937; Glasser and Campbell, 1998, 1999; Glasser *et al.*, 2001) although some studies still dispute this (Ziebarth *et al.*, 2008).

Although the crystalline lens surface changes are the primary cause of dioptric change with accommodation (Dubbelman *et al.*, 2005; Rosales *et al.*, 2006), it is still believed that a smaller contribution is also made by changes in axial lens position (Dubbelman *et al.*, 2003). Previous chapters in this thesis have shown that this is in fact untrue. The decrease in anterior chamber depth and increase in crystalline lens thickness actually reduce vergence with accommodation (see Chapter 2).

A number of different methods have been employed to quantify changes in biometric distance. A-scan ultrasonography has been used to measure static changes in ocular biometry in humans and monkeys, the latter using Edinger-Westphal (EW) and pharmacological stimulation (Storey and Rabie, 1983; Beauchamp and Mitchell, 1985; Koretz *et al.*, 1987; Vilupuru and Glasser, 2005). Dynamic changes in biometry have been studied in human subjects and monkeys using continuous high-resolution ultrasonography (de Vries *et al.*, 1987; Van der Heijde and Weber, 1989; Beers and Van der Heijde, 1994a, 1994b, 1996; Van der Heijde *et al.*, 1996; Vilupuru and Glasser, 2005; Ostrin *et al.*, 2006).

Other imaging techniques are also capable of quantifying the optical biometric changes associated with accommodation. These include Scheimpflug photography (Brown, 1973; Koretz *et al.*, 1997; 2002; Dubbelman and van der Heijde, 2001; Dubbelman *et al.*, 2001; 2002; 2005), Magnetic Resonance Imaging (MRI; Strenk *et al.*, 1999; 2005; Jones *et al.*, 2007), Optical Coherence Tomography (OCT; Baikoff *et al.*, 2004; 2005a; 2005b; Richdale *et al.*, 2008), and Partial Coherence Interferometry (PCI; Drexler *et al.*, 1997; Tsorbatzoglou *et al.*, 2007).

Modifications of the anterior segment during accommodation of the eye under examination cannot be studied in a simple and direct way with anterior segment imaging techniques such as Scheimpflug photography and Ultrasound Biomicroscopy (UBM). With such techniques, it is often necessary to stimulate the fellow eye in order to observe the variations of the eye being measured (Dubbelman and van der Heijde, 2001; Dubbelman *et al.*, 2001; 2002; 2005). This method assumes that the eye under investigation will perform in the same manner, and reveal the same results, as the stimulated eye. The techniques using ultrasound equipment can only be used with contact systems or with water baths that may modify the anatomical dimensions or the pressure of the anterior segment (Fledelius, 1997). With the Scheimpflug photographic technique, geometrical reconstructions are necessary and cannot be used in certain axes (Dubbelman and van der Heijde, 2001; Dubbelman *et al.*, 2001; 2002; 2005).

OCT is a non-invasive optical method which allows cross-sectional anterior chamber imaging at a resolution of 6–25 μm . An infra-red light source is divided into a measurement beam, reflected from the ocular structures, and a reference light which are recombined causing interference. Coherent (positive) interference is measured by an

interferometer, to allow an image of the reflected light from the ocular structures to be built up (Hirano *et al.*, 2001). OCT can penetrate the clear or opaque cornea and human sclera *in vivo*, allowing high-resolution, cross-sectional imaging of the anterior chamber angle and the ciliary body (Goldsmith *et al.*, 2005).

OCT has the advantage of producing images of the anterior segment via a non-contact method under static conditions. The internal pinwheel target of the optical system can be focused using an optometer-based system with negative or positive lenses, thus providing different accommodative stimulus levels. With a normal subject, the morphological modifications of the crystalline lens behind the iris screen cannot be studied because the infrared light source used is blocked by the pigment epithelium.

Baikoff and colleagues (Baikoff *et al.*, 2004; 2005a; 2005b) have used this technique to explore anterior segment variations under a number of different conditions. In one such study (Baikoff *et al.*, 2004), 104 eyes of 56 subjects were examined using the anterior segment OCT (AS-OCT) with a 1310 nm wavelength of light. The subjects were aged 7 to 82 years, with refractions ranging from -5.0 D to +5.0 D. Accommodation was stimulated using the instrument's internal target and the application of negative lenses. At rest, the mean anterior chamber depth was 3.606 ± 0.377 mm, the average pupil diameter 4.258 ± 0.872 mm; both of which decreased with age. For 1.0 D of accommodation stimulated, the anterior pole moved forward by 30 microns, the radius of the anterior lens decreased by 0.3 mm and pupil diameter reduced by 0.15 mm; the method of calculating the anterior crystalline lens radius is not made explicit in the study.

Hitherto, AS-OCT has been used for anterior chamber depth, width and angle measurement (Baikoff *et al.*, 2004; Goldsmith *et al.*, 2005; Dawczynski *et al.*, 2007; Lavanya *et al.*, 2007; Nemeth *et al.*, 2007; Dang Burgener *et al.*, 2008; Leung *et al.*, 2008), the evaluation of phakic intraocular lens implants (Baikoff, 2006; Güell *et al.*, 2007; Koivula and Kugelberg, 2007) and the determination of corneal integrity (Konstantopoulos *et al.*, 2007; Cheng *et al.*, 2008; Kaiserman *et al.*, 2008). The accuracy of this ocular biometric data is important in determining the risk of angle closure glaucoma, and for pre- and post-operative assessment in cataract and kerato-refractive surgery (Lavanya *et al.*, 2007). *Visante*TM (Carl Zeiss Meditec, Dublin, California) AS-OCT has built-in software to allow acquisition of corneal thickness and anterior chamber depth (Baikoff, 2006).

A recent study by Richdale and colleagues (2008) utilised the *Visante* to measure changes in the crystalline lens with age and accommodation. Twenty-two subjects aged 36 to 50 years were assessed with mean amplitudes of accommodation ranging from 2.17 to 6.38 D subjectively (push-up test) and 0.22 to 4.56 D objectively (Grand Seiko *WR 5100K* auto-refractor and Badal lens system). For a 5.0 D accommodative stimulus, the authors found a mean lens thickness increase from 0.01 to 0.26 mm. For those subjects who showed at least 1.0 D of objective accommodation, this equated to an increase of $51 \pm 19 \mu\text{m}$ per dioptre. The group also found an increase in lens thickness of $21 \mu\text{m}$ per year of age (Richdale *et al.*, 2008).

Dunne and colleagues (2007) tested the AS-OCT using a model eye described by Kirschkamp and co-authors (Kirschkamp *et al.*, 1998), which has been used experimentally for the evaluation of phakometry (Barry *et al.*, 2001) and aberrometry (Cervino *et al.*, 2007). Five variations of the model eye were tested, including a range of corneal radii (anterior: 6.8 to 8.7 mm; posterior: 6.3 to 8.1 mm), lens radii (anterior: 7.6 to 13.6 mm; posterior: -8.3 to -4.5 mm), anterior chamber depths (1.9 to 4.1 mm), and lens thicknesses (3.5 to 4.5 mm). Corneal thickness was kept constant at 0.8 mm. The model corneas and lenses were manufactured from PMMA (refractive index 1.493) and were separated by water (refractive index 1.333; Dunne *et al.*, 2007). The authors derived a new scheme for the reduction of measurement errors, and revealed that the accuracy of the AS-OCT with the model eye was comparable to another non-contact technique, that of corrected Scheimpflug photography (Dubbelman *et al.*, 2001). The improved computing scheme appears to reduce the errors of the built-in OCT software and enables measurement of surface curvature in the form of vertex radii and conic constants.

5.1.1 Aims

The *Visante* (Carl Zeiss Meditec, Dublin, California) AS-OCT is a new instrument, which allows measurement of ocular biometric changes associated with the accommodative response (Richdale *et al.*, 2008). These have been shown to be comparable to previous findings using Scheimpflug photography (Dubbelman *et al.*, 2003), ultrasound (Garner and Yap, 1997), MRI (Jones *et al.*, 2007) and PCI (Bolz *et al.*, 2007; Tsorbatzoglou *et al.*, 2007) in relation to changes in crystalline lens thickness with age and accommodation.

However, Richdale and colleagues plotted biometric changes against accommodative stimulus and not response, which may have lead to erroneous conclusions. The use of the computing scheme enunciated by Dunne *et al.* (2007) to improve the accuracy the OCT has not been validated on a human cohort. Further, the measurement of ocular surface radii (cornea and crystalline lens) and their variability with accommodation has been approached to a limited degree using the *Visante* (Baikoff *et al.*, 2004). The schematic produced by Dunne and colleagues allows the examination of these components with correction for optical and instrument distortion.

The aim of this study is to apply this new method to the assessment of accommodative biometric changes in human subjects, to see if the same computing scheme is applicable to phakic eyes, and to qualify the use of the *Visante* AS-OCT in a clinical setting. Further, by comparing these changes with accommodative response, as opposed to accommodative stimulus, the work of Richdale *et al.* (2008) will be improved upon.

5.2 Methods

5.2.1 Subjects

Forty subjects from Aston University were recruited for the study, aged between 18 to 36 years (mean \pm SD, 20.0 \pm 3.4 years). After analysis, taking into account image quality and ability to image and measure ocular components on different individuals, the cohort was reduced to 30 subjects aged 18 to 25 years (mean \pm SD, 19.4 \pm 2.0 years) of whom 40 % were male. The mean spherical equivalent (MSE; sphere + [cylinder / 2]) of the reduced cohort was -1.85 \pm 2.68 D (range: +1.94 to -6.87 D). Subjects with astigmatism \geq 1.0 D were excluded from the study.

Subjects were furnished with a full explanation of the procedures involved in the investigation and gave informed consent to their participation in the study under the terms of the Declaration of Helsinki (copy of consent form is provided in Appendix 2). Ethical approval was granted by the human ethics committee of Aston University (Appendix 1).

5.2.2 Autorefractometry and stimulus response function

Uncorrected distance autorefractometry was performed on each subject using the previously validated Shin-Nippon *NVision-K 5001* (Shin-Nippon Commerce Inc., Tokyo, Japan) open view autorefractor (Davies *et al.*, 2003). A comprehensive examination of the anterior eye was performed on each subject using a slit-lamp bio-microscope (Haag-Streit, UK). Subjects were rendered functionally emmetropic with conventional daily disposable spherical soft contact lenses (etafilcon A, 58% water content; 1-Day Acuvue, Johnson & Johnson Vision Care, Jacksonville, Florida, USA) to ensure that the accommodative demand was virtually identical for each subject. Sufficient time was given for adaptation to the soft contact lenses (approximately 15 minutes); all subjects had previously worn soft contact lenses and no subject experienced difficulties. Using a Bailey-Lovie (90 % contrast) logMAR progression chart (Haag-Streit, UK), all subjects achieved 0.0 logMAR visual acuity or better in the eye tested. Subjective amplitude of accommodation was \geq 8.0 D in all subjects (RAF gauge, Clement Clarke/Haag-Streit, Harlow, UK). No subject had any form of visual or pathological anomaly other than an ametropic refractive error. All

subjects were experienced with visual experiments and were able to maintain steady fixation in order to limit artefacts in the data.

Initially, the residual refractive error of each subject with contact lens correction was measured through the Badal system with the target placed at 0.0 D. Subjects were excluded if their mean residual refractive error was greater than ± 0.25 D or if the cylindrical component was > 0.50 DC. On commencement, the right eye of each subject viewed a stationary high contrast (90 %), 37.0 cdm^{-2} Maltese cross through a +5.0 D Badal optical system, fitted to the modified autorefractor; the left eye was occluded with a patch. Five stimulus conditions were employed in a random order within the Badal system (0.0 D to 4.0 D in 1.0 D steps). Subjects were encouraged to concentrate on the target at all times, as attentional factors can affect accommodation measurement (Francis *et al.*, 2003). Five measures were recorded at each stimulus level and the mean spherical equivalent refraction calculated.

5.2.3 Optical Coherence Tomography

Before measurement began, the contact lens was removed from the right eye of the subject and disposed of. Sufficient time was given for the subject to recover from the lens wear (approximately 15 minutes). The anterior eye and adnexa was examined with a slit-lamp bio-microscope (Haag-Streit type) for any anomaly following contact lens wear.

The habitual refractive error of each subject was entered into the *Visante* to allow appropriate correction and focus of the internal pinwheel target. The subject was aligned using the automated chin and headrest so the image of the eye was central in the OCT integral computer monitor window. Subjects were encouraged to concentrate on the target at all times.

Two images were captured along the 180° meridian in the anterior segment single-image capture mode. The first image included corneal thickness, anterior chamber depth and corneal surface curvature. The second image involved changing the focal plane of the *Visante*, enabling measurement of crystalline lens thickness and surface curvature. Five accommodative stimulus conditions were employed in a random order using the internal pinwheel target and the addition of negative lenses (0.0 D to 4.0 D in 1.0 D steps).

The *Visante* AS-OCT has built-in edge detection software (version 1.0.12.1896). This attempts to detect the corneal surfaces, but as they are not present, the image is often distorted in a random manner. The curves which the software plots to detect the surfaces were therefore removed prior to analysis.

Intraocular distances

From the uncorrected (U) AS-OCT images, measures were taken of corneal thickness (d_1U), anterior chamber depth (posterior cornea to anterior lens; d_2U) and crystalline lens thickness (d_3U). All distances were measured using the built-in *Visante* measuring callipers (Figure 5.1). Each intraocular distance was measured three separate times. Means and standard deviations were calculated using a Microsoft *Excel* spreadsheet. A Shapiro-Wilk analysis of variance (ANOVA; Shapiro and Wilk, 1965) was conducted with SPSS 12.0.1 for Microsoft *Windows*.

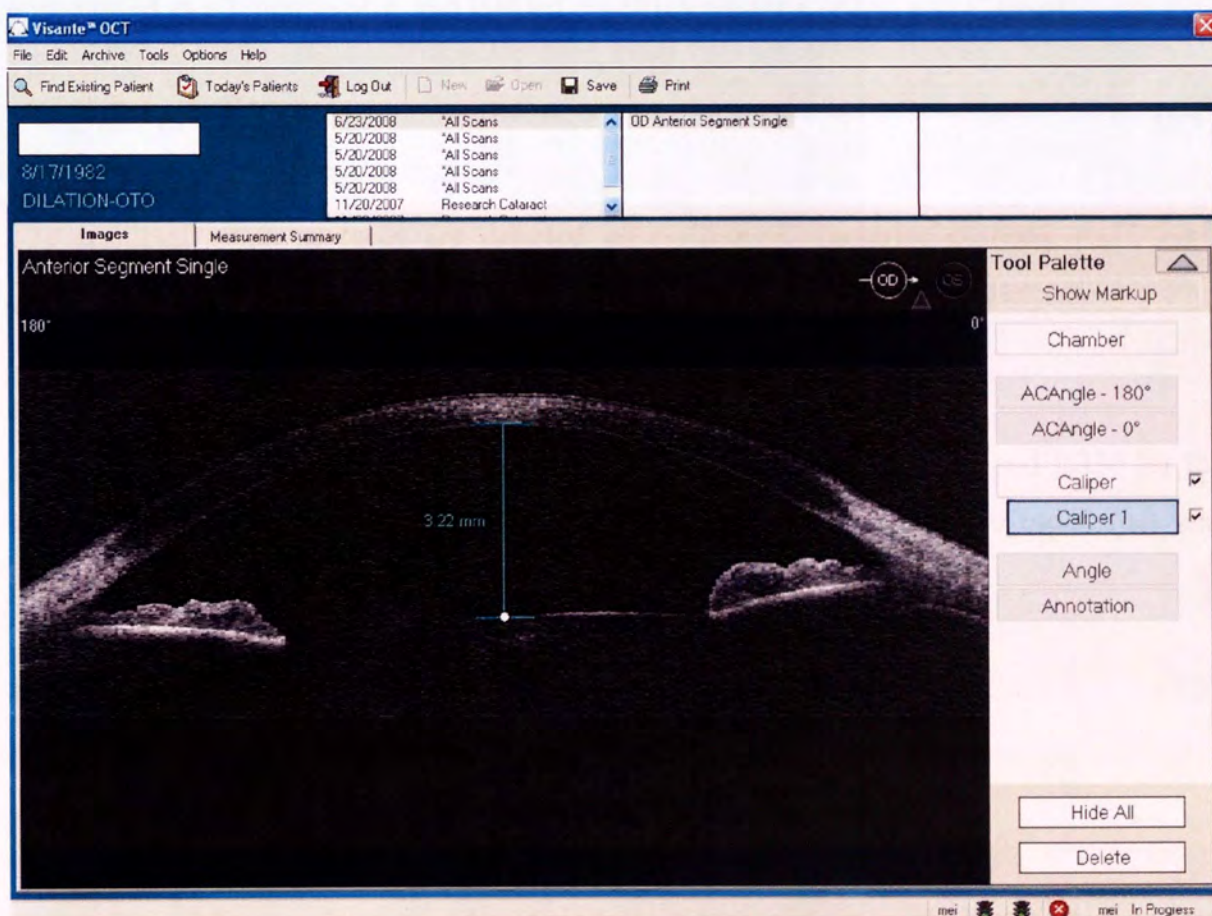


Figure 5.1 The *Visante* AS-OCT screen displaying the anterior segment image with the measuring callipers *in situ*. Shown is the measurement of the anterior chamber depth.

Surface curvatures

The *Visante* does not currently measure surface curvatures. The Liberty BASIC 4.0 (Shoptalk Systems, Framingham, Massachusetts) program described by Dunne and co-authors (2007) was used to measure coordinates of corneal and lens surfaces. Twenty x and y coordinates were determined for each surface using a cursor. It must be noted that the sub-pixel analysis described by Dunne *et al.* (2007) can not be applied to human corneas, as this system relies on the edges of model corneas and lenses which appear as a narrow band.

Equation 5.1 was used to derive conic sections from the surface coordinates. In this equation r_0 is the vertex radius, and p the conic constant which determines if a surface is becoming steeper ($p > 1$) or flatter ($p < 1$) in the periphery (Dunne, 1995). A spreadsheet was created (Microsoft *Excel*) in which a second-order polynomial was fitted to y^2 . This was plotted as a function of x , and yielded co-efficients for x ($=2r_0$) and x^2 ($=-p$):

$$y^2 = 2r_0x - px^2. \quad (5.1)$$

The resultant conic surfaces are denoted as $r_{10}U$, $r_{1p}U$ (anterior cornea), $r_{20}U$, $r_{2p}U$ (posterior cornea), $r_{30}U$, $r_{3p}U$ (anterior lens) and $r_{40}U$, $r_{4p}U$ (posterior lens).

Refractive indices

Assumed refractive indices were 1 for air (n_1), 1.376 for the cornea (n_2) and 1.336 for the aqueous (n_3) humour (Gullstrand, 1909). The lens equivalent refractive index (n_4) was found from Equation 5.2 below (Dubbelman *et al.*, 2001; 2005).

$$1.441 - 0.0003A + 0.0013D, \quad (5.2)$$

where A is the age in years and D the accommodation in dioptres.

Correction of the anterior corneal surface (r_1)

Fixed values for y were attributed to the corneal (from 0.5 to 5.0 mm in 0.5 mm steps) and lenticular surfaces (0.5 to 3.0 mm in 0.5 mm steps) due to the physical limitations of the

measurable image dimensions. The rearranged conic surface formula was used to determine uncorrected surface xU coordinates for specific y values:

$$xU = r_0 - (r_0^2 - py^2)^{0.5} / p. \quad (5.3)$$

Equation 5.4 was used to derive surfaces coordinates corrected (I) for the distortion through the *Visante* (Dunne *et al.*, 2007). No correction for optical distortion was required as the cornea is viewed in air.

$$r_1xI = r_1xU(1.5582 - 0.0037y + 0.0025y^2). \quad (5.4)$$

These corrected coordinates (xI and y) were converted into apical radii (r_{10}) and conic constants (r_{1p}) using the same second-order polynomial as described above.

Correction of corneal thickness (d_1)

The apparent corneal thickness was calculated using Equation 5.5, which makes adjustment for *Visante* instrument distortion (Dunne *et al.*, 2007):

$$d_1I = d_1U(0.6350). \quad (5.5)$$

As the anterior corneal surface exerts optical distortion on subsequent interfaces, it is necessary to correct for this using well established paraxial ray-tracing formulae:

$$F_{10}I = [1000(n_2 - n_1)] / r_{10}I. \quad (5.6)$$

$$L_1 = (1000n_2) / d_1I. \quad (5.7)$$

$$L_1' = F_{10}I + L_1. \quad (5.8)$$

$$d_1 = (1000n_2) / L_1'. \quad (5.9)$$

Where F_1 is the anterior corneal vertex power, L_1 is the entrance vergence, L_1' is the exit vergence and d_1 is the optically corrected corneal thickness.

Correction of the posterior corneal surface (r_2)

The rearranged conic surface formula Equation 5.3 was used to determine uncorrected surface xU coordinates for specific y values. Equation 5.10 was used to derive apparent surface coordinates corrected for *Visante* instrument distortion (Dunne *et al.*, 2007).

$$r_2xI = r_2xU(1.5454 - 0.0012y + 0.002y^2). \quad (5.10)$$

The new coordinates r_2xI and y were converted into apical radii (r_{20}) and conic constants (r_2p) using the second-order polynomial previously described. Apparent sagittal radii were calculated for each y value using equation below (Bennett, 1988).

$$r_s = [r_0^2 + (1 - p)y^2]^{0.5}, \quad (5.11)$$

where r_s is the sagittal radius. Apparent sagittal radii were converted into real sagittal radii using the following paraxial formulae:

$$L_1 = 1000n_1 / (d_1I + r_{2s}I), \quad (5.12)$$

where $r_{2s}I$ is the uncorrected sagittal radius of the posterior cornea.

$$L_1' = F_{10}I + L_1. \quad (5.13)$$

$$r_{2s} = [(1000n_2) / L_1'] - d_1. \quad (5.14)$$

Douthwaite's scheme was used to derive optically corrected sagittal radii for each fixed y coordinate. On the y axis, r_s^2 was plotted against y^2 on the x axis. This produced a straight line, for which the intercept is r_0^2 and the slope is $(1 - p)$; Douthwaite, 1995; Equation 5.15).

$$r_s^2 = r_0^2 + (1 - p)y^2. \quad (5.15)$$

Correction of the anterior chamber (d_2)

The apparent anterior chamber depth was calculated using the equation below, which makes adjustment for *Visante* instrument distortion (Dunne *et al.*, 2007):

$$d_2I = d_2U(0.9002 - 0.0848d_2U + 0.0314d_2U^2). \quad (5.16)$$

Correction for optical distortion (through both corneal surfaces) was carried out using the following paraxial formulae:

$$F_{20}I = [1000(n_3 - n_2)] / r_{20}I, \quad (5.17)$$

where $F_{20}I$ is the posterior corneal vertex power.

$$L_1 = 1000n_1 / (d_1I + d_2I). \quad (5.18)$$

$$L_1' = F_{10}I + L_1. \quad (5.19)$$

$$L_2 = L_1' / \{1 - [d_1 / (1000n_2)]L_1'\}. \quad (5.20)$$

$$L_2' = L_2 + F_{20}I. \quad (5.21)$$

$$d_2 = (1000n_3) / L_2'. \quad (5.22)$$

Correction of the anterior crystalline lens surface (r_3)

The rearranged conic surface formula (Equation 5.3) was used to determine uncorrected surface xU co-ordinates for specific y values. Equation 5.23 was used to derive apparent surface coordinates corrected for OCT distortion (Dunne *et al.*, 2007):

$$r_3xI = r_3xU(1.8412 + 0.0501y - 0.0519y^2) \quad (5.23)$$

These corrected coordinates (r_3xI and y) were converted into apparent apical radii (r_{30}) and conic constants (r_3p) using the second-order polynomial described previously (Equation 5.1). Equation 5.11 was used to calculate apparent sagittal radii for each y value. Apparent sagittal radii were converted to real sagittal radii using the following paraxial formulae:

$$L_1 = 1000n_1 / (d_1I + d_2I + r_{3s}I). \quad (5.24)$$

$$L_1' = L_1 + F_{10}I. \quad (5.25)$$

$$L_2 = L_1' / \{1 - [d_1 / (1000n_2)] L_1'\}. \quad (5.26)$$

$$L_2' = L_2 + F_{20}I. \quad (5.27)$$

$$r_{3s} = [(1000n_3) / L_2'] - d_2. \quad (5.28)$$

Douthwaite's formula (Equation 5.15) was used to derive the real surface apical radii (r_{30}) and conic constant (r_{3p} ; Douthwaite, 1995).

Correction of crystalline lens thickness (d_3)

Apparent lens thickness was calculated using the formula below which makes adjustment for *Visante* instrument distortion (Dunne *et al.*, 2007).

$$d_3I = d_3U(28.184 - 13.634d_3U + 1.7017d_3U^2). \quad (5.29)$$

Correction for optical distortion (through both corneal surfaces and the anterior lens surface) was carried out using the following paraxial formula:

$$F_{30}I = [1000(n_4 - n_3) / r_{30}I], \quad (5.30)$$

where $F_{30}I$ is the anterior lens vertex power.

$$L_1 = 1000 / (d_1I + d_2I + d_3I). \quad (5.31)$$

$$L_1' = L_1 + F_{10}I. \quad (5.32)$$

$$L_2 = L_1' / \{1 - [d_1 / (1000n_2)] L_1'\}. \quad (5.33)$$

$$L_2' = L_2 + F_{20}I. \quad (5.34)$$

$$L_3 = L_2' / \{1 - [d_2 / (1000n_3)] L_2'\}. \quad (5.35)$$

$$L_3' = L_3 + F_{30}I. \quad (5.36)$$

$$d_3 = (1000n_4) / L_3'. \quad (5.37)$$

Correction of the posterior crystalline lens surface (r_4)

The rearranged conic surface formula (Equation 5.3) was used to determine uncorrected surface xU coordinates for specific y values. Equation 5.38 was used to derive apparent surface coordinates corrected for *Visante* instrument distortion (Dunne *et al.*, 2007).

$$r_4xI = r_4xU(1.5373 + 0.0036y - 0.0035y^2). \quad (5.38)$$

These new r_4xI and y coordinates were converted into apparent apical radii (r_{40}) and conic constants (r_{4p}) using the second-order polynomial described in Equation 5.1. The formula described in Equation 5.11 was used to calculate apparent sagittal radii for each y value. Apparent sagittal radii were converted to real sagittal radii using the following paraxial formulae:

$$L_1 = 1000n_1 / (d_1I + d_2I + d_3I + r_{3s}I). \quad (5.39)$$

$$L_1' = L_1 + F_{10}I. \quad (5.40)$$

$$L_2 = L_1' / \{1 - [d_1 / (1000n_2)] L_1'\}. \quad (5.41)$$

$$L_2' = L_2 + F_{20}I. \quad (5.42)$$

$$L_3 = L_2' / \{1 - [d_2 / (1000n_3)] L_2'\}. \quad (5.43)$$

$$L_3' = L_3 + F_{30}I. \quad (5.44)$$

$$r_{4s} = [(1000n_4) / L_3'] - d_3. \quad (5.45)$$

Douthwaite's plot of r_{4s} as a function of y^2 gave r_{40} (square-root of the intercept) and r_{4p} (1 – slope) for the fitted real surface (Douthwaite, 1995; Equation 5.15).

5.3 Results

5.3.1 *Visante* instrument and optical correction

When attempting to plot surface curvatures, the quality of the images was such that placing the cursor at the relevant surface interface was extremely difficult. There was also a degree of noise in the image. Often, the humours appeared grey or flecked instead of black, creating difficulty delineating the ocular interfaces. Close inspection of the data revealed discrepancies which are contrary to commonly reported values for ocular surface curvatures. Although the results for the whole cohort ($n = 30$) were analysed, the results were deemed unacceptable. For the purposes of demonstration, typical data for one subject are presented (Table 5.1 and 5.2).

Possible sources of error include difficulties placing the cursor to select the surfaces. Small misalignments in identifying the surface position appear to result in disproportionate changes in conic constants and apical radii. Further, this version of the *Visante* does not include the complex curvature and edge detection software as is used in other such techniques (i.e. Scheimpflug photography). One such method could be the use of a Canny filter (Canny, 1986). This filter smoothes the image by Gaussian convolution then applies a 2-D first derivative operator to highlight regions with high first spatial derivatives, as used in other studies (Hermans *et al.*, 2008). Edges are shown as ridges in the gradient magnitude image, intraocular surfaces are therefore found by determining the maximum gradient values.

The results shown in Tables 5.1 and 5.2 highlight the data derived from the cohort using the techniques and formulae previously described (Dunne *et al.*, 2007). Without greater resolution and the introduction of edge detection techniques, the data remains erratic. However, analysis of the crystalline lens reveals that its axial thickness appears to be shrinking with accommodation stimulus (Table 5.1); contrary to what is commonly believed and is well known (Drexler *et al.*, 1997; Garner and Yap, 1997; Kirschcamp *et al.*, 2004; Strenk *et al.*, 2004; 2005).

Accommodative stimulus (D)	Corneal thickness (mm)	Anterior chamber depth (mm)	Lens thickness (mm)
0	0.51	3.87	3.44
1	0.50	3.75	3.43
2	0.50	3.81	3.43
3	0.51	3.73	3.28
4	0.50	3.64	3.04

Table 5.1 Corneal thickness, anterior chamber depth and lens thickness measures for each level of accommodation stimulus corrected for instrument and optical distortion. Of note, the lens thickness is decreasing with increased accommodation stimulus. The data presented are for one subject only, and are shown as a typical representation of the data analysed over the whole cohort (n = 30). Anatomical anterior chamber depth is taken from the posterior corneal apex to the anterior lens apex.

A (D)	Anterior cornea (mm)		Posterior cornea (mm)		Anterior crystalline lens (mm)		Posterior crystalline lens (mm)	
	r_0	p	r_0	p	r_0	p	r_0	p
0	7.02	0.57	6.08	0.66	6.56	-12.25	6.52	3.78
1	6.70	0.43	5.86	0.59	9.03	1.70	5.67	3.88
2	7.27	0.68	6.24	0.68	6.57	-14.92	n/a	n/a
3	7.35	0.75	5.98	0.55	8.82	-25.60	7.85	8.25
4	7.55	0.81	6.61	0.80	2.23	-0.82	n/a	n/a

Table 5.2 Corrected ocular surface apical radii (r_0) and conic constants (p) for each level of accommodation stimulus (A) corrected for OCT and optical distortion. The data presented are for one subject only (AF), and are shown as a typical representation of the data analysed over the whole cohort (n = 30).

Examination of the original formulae revealed the source of this discrepancy, which lies in the equation used to correct lens thickness for instrument error. The formula in question is Equation 5.29:

$$d_3I = d_3U(28.184 - 13.634d_3U + 1.7017d_3U^2). \quad (5.29)$$

Quantities d_3U and d_3I represent, respectively, the crystalline lens thickness before and after correction for *Visante* instrument distortion. An explanation of the theory behind this equation follows.

Uncorrected *Visante* lens thickness measurements observed in Dunne *et al.* (2007) of the five physical model eyes, exceeded the physically measured values by $218 \pm 90 \mu\text{m}$ (mean \pm SD). A correction factor could have been generated by dividing the known lens thickness by its corresponding uncorrected measurement in each model eye. However, this would not have been transferable to humans as the model eye components did not have refractive indices typically found in human eyes. Instead, it was considered that uncorrected measurements required correction for instrument and optical distortion. It then followed that if paraxial ray-tracing was performed to add optical distortion to the known lens thickness of each eye model, any discrepancy between the optically distorted and uncorrected lens thickness was then attributed to instrument distortion. A correction factor could then be derived from measurements on each model eye by dividing the known optically distorted lens thickness by the corresponding uncorrected *Visante* measurement and this would be transferable to human eyes (Figure 5.2).

Logically, a correction factor equal to 1 would indicate that no instrument distortion was present. Conversely, a correction factor of less than or greater than 1 would indicate, respectively, that instrument distortion either overestimated or underestimated lens thickness. The measurements from the original study (Dunne *et al.*, 2007) showed that this correction factor varied from 0.879 to 1.337, with an average of 1.035.

The average correction factor was used to correct uncorrected model eye lens thickness measurements for instrument distortion (i.e. $d_3I = d_3U \times 1.035$) followed by correction for optical distortion, again using paraxial ray tracing calculations. This approach yielded corrected lens thickness errors of $52 \pm 569 \mu\text{m}$ (mean \pm SD); although the mean error was only one quarter of that found for the uncorrected lens thickness measurements, the range of errors were six times larger. Clearly, refinement of the correction factor was needed.

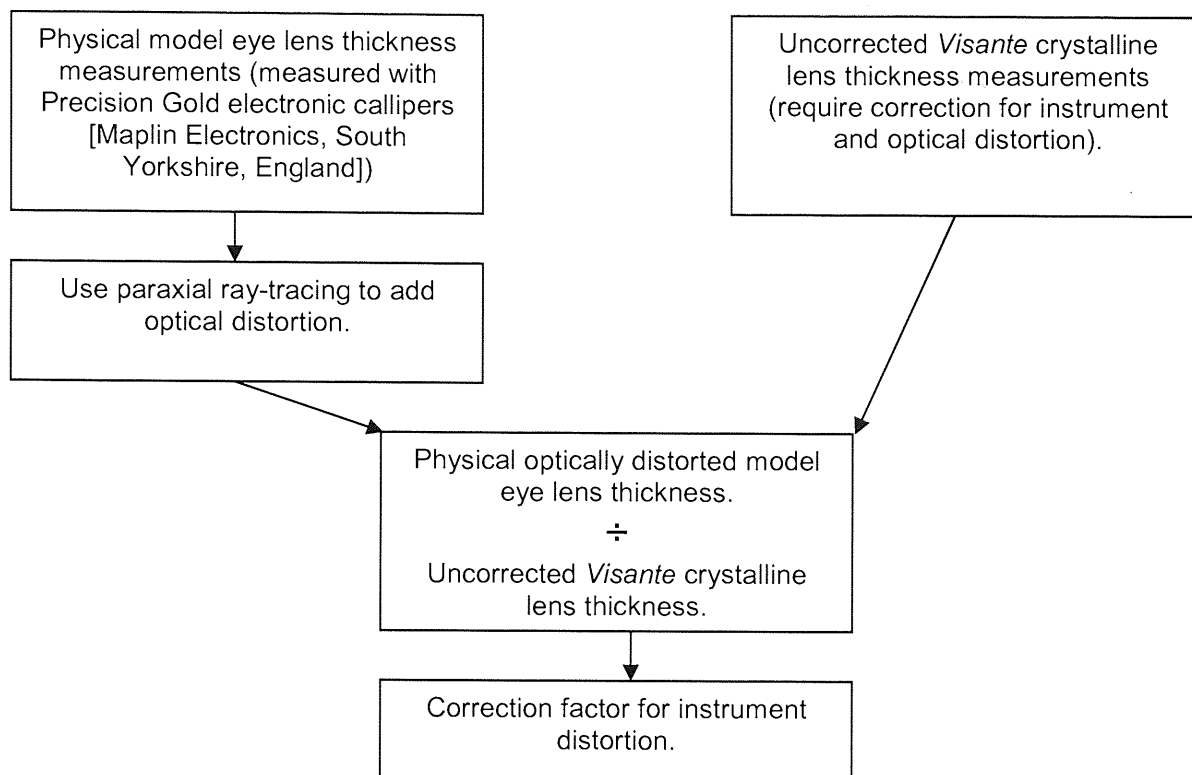


Figure 5.2 Flow chart showing the theory and methods in deducing a correction factor for *Visante* instrument distortion. Uncorrected *Visante* crystalline lens thickness measurements require correction for both optical and instrument distortion. By adding optical distortion to the physical measurements of the physical model eyes, and dividing this by the uncorrected *Visante* measurements, any discrepancy will be due to instrument distortion (after Dunne *et al.* 2007).

If the correction factor varied in a systematic way as a function of the uncorrected lens thickness measurements, then this might offer a solution. This approach involved the derivation of either (i) a linear equation or (ii) a second order polynomial equation for the dependence of the correction factor on the uncorrected lens thickness measurement. These calculations were performed using the average, scatter plot and trend line functions included with Microsoft *Excel 2003*. The results are expressed in Figure 5.3 in which the filled circles represent the datum points derived from the five physical model eyes (Dunne *et al.*, 2007). The dashed line represents the straight line (correction factor = $0.478d_3U - 0.865$) fitted to the datum points.

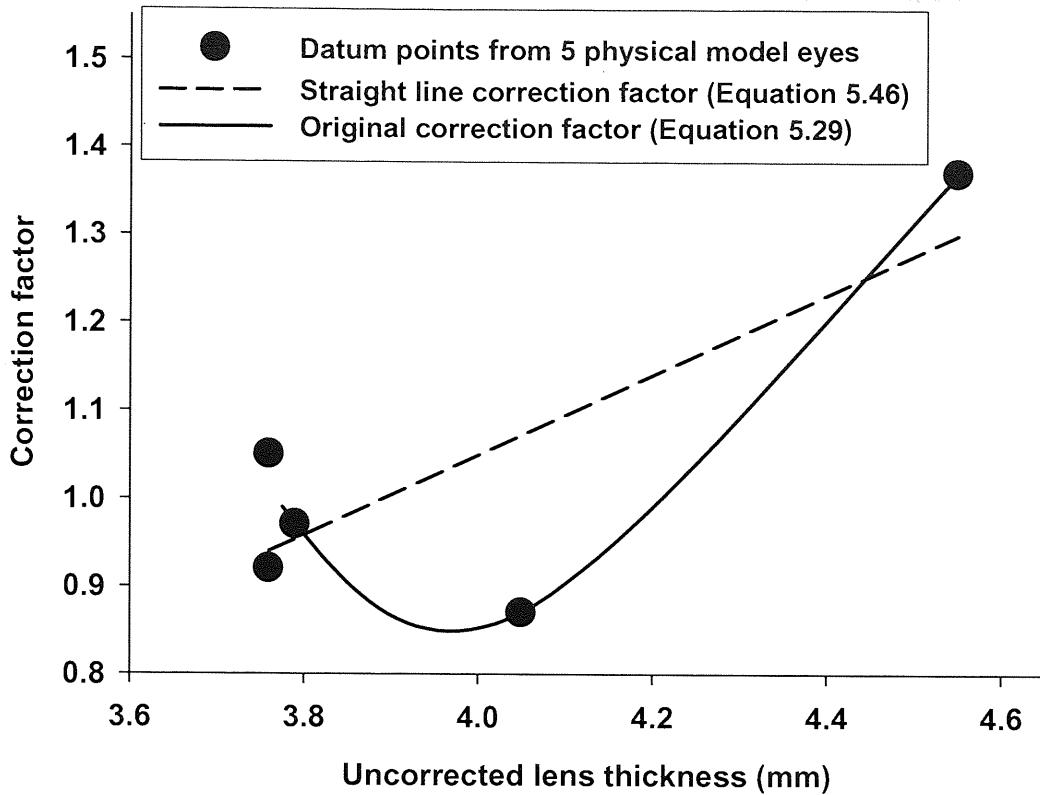


Figure 5.3 The dependence of correction factor on uncorrected lens thickness measurements made using the *Visante*. The filled circles represent the datum points derived from the five physical model eyes. The polynomial represents the original correction factor which best represented these points (Equation 5.29). The new correction factor (Equation 5.46) is represented by the dashed line.

Use of this equation (Equation 5.46) to correct for instrument distortion lead to corrected lens thickness errors of $33 \pm 383 \mu\text{m}$ (mean \pm SD) and improved a little on using an average correction factor:

$$d_3I = d_3U(0.478d_3U - 0.865) \quad (5.46)$$

The solid line represents the second order polynomial; (correction factor = $28.184 - 13.634d_3U + 1.7017 d_3U^2$) fitted to the datum points. Use of this equation to correct for instrument distortion lead to corrected lens thickness errors of $14 \pm 123 \mu\text{m}$ (mean \pm SD), which represented a significant improvement; this equation was, therefore, adopted in the original paper.

Note, however, that this equation is based on a curve that reaches a minimum at approximately 4.0 mm. So, for instance, after correction for instrument distortion, an uncorrected lens thickness of 4.0 mm resulted in an uncorrected lens thickness of 3.8 mm. This could lead to the observed errors when measuring crystalline lens thickness changes that accompany accommodation (Jones *et al.*, 2007).

This effect can be modelled theoretically using a schematic eye such as the latest version of the Dubbelman model eye (Norrby, 2005). The parameters of this model eye alter according to age and accommodation and are based on extensive biometric measurements made using Scheimpflug photography (Dubbelman and van der Heijde, 2001; Dubbleman *et al.*, 2001; 2002; 2005). For example, accommodation of 0.0 to 4.0 D involves an increase in crystalline lens thickens from 3.4 to 3.6 mm at 20 years of age; a difference of +0.2 mm. When converting these values to uncorrected lens thicknesses (i.e. subjecting them to instrument and optical distortion) as would be measured using the *Visante*, the lens thickness changes become 3.82 to 3.90 mm; a difference of just +0.08 mm. So the measured lens thickness increase is not only smaller than will actually have occurred but, in addition to this, both measurements lie on the descending limb of the curve shown in Figure 5.2. Using Equation 5.29 to correct instrument distortion followed by correction of optical distortion, the final recorded lens thicknesses for 0.0 and 4.0 D of accommodation become 3.44 and 3.40 mm respectively; a difference of -0.04 mm. Thus, lens thickness decreases with accommodation, in opposition to intuitive trends previously reported.

Neither of the two alternative methods of deriving an instrument distortion correction factor for lens thickness suffers from this problem. As the second of these (Equation 5.46) yields the least error, then it is suggested that this equation should be used instead. Table 5.3 summarises the errors arising from use of the original (Equation 5.29) and alternative (Equation 5.46) formulae. The errors shown represent those that remain after correction for optical distortion using the paraxial formulae listed previously. Also shown are the x -coordinate errors that emerged at a y -coordinate value of 3.0 mm for the posterior crystalline lens surface. These are shown because the errors involved in correcting this surface for instrument and optical distortion are dependent on lens thickness errors. Table 5.3 shows that although the recommended alternative equation increases the errors involved with determining lens thickness, it reduces those relating to posterior lens curvature.

It is therefore recommend that Equation 5.46 rather than Equation 5.29 be used, particularly if *in vivo* lens thickness changes accompanying accommodation are being measured.

Component	Uncorrected (μm)	Correction (μm)	
		Equation 5.29	Equation 5.46
Lens thickness error	+218 \pm 90	+14 \pm 123	+33 \pm 383
Posterior lens surface x-coordinate error	-246 \pm 213	+11 \pm 71	+10 \pm 32

Table 5.3 Errors (mean \pm SD) remaining after correction for optical distortion for crystalline lens thickness and the posterior lens surface x-coordinate error for a specific y-coordinate value; using the original (Equation 5.29) and modified (Equation 5.46) equations.

Raw OCT axial changes with accommodation

After detailed exploration of the data, it was discovered that the mean uncorrected *Visante* measures were remarkably similar in magnitude of change with accommodation, to the published data (i.e. that of Scheimpflug photography [Norrby, 2005]). When compared to the Dubbelman model previously described, the measures for corneal thickness, anterior chamber depth (ACD), lens thickness (LT) and lens centre of mass (lens centroid = ACD + LT/2) and the anterior segment length (ASL = ACD + LT; the position of the posterior crystalline lens surface) were remarkably similar (Table 5.4a and Figure 5.4). The largest discrepancy appears to be lens thickness and subsequently, the ASL, where the *Visante* data appears to overestimate these elements in comparison to the Scheimpflug cohort used by Dubbelman (Dubbelman and van der Heijde, 2001; Dubbelman *et al.*, 2001; 2002; 2005).

Many studies, which have studied anterior segment biometric changes, consider the ACD to be the distance between the anterior vertex of the cornea and the anterior vertex of the crystalline lens, thus including the thickness of the cornea. The absolute values displayed in Table 5.4a therefore require the addition of the corneal thickness to allow comparisons to be made across studies. For example, the mean ACD of the Dubbelman model at rest (0.0 D stimulus) is 3.67 mm. A similar calculation must be made when considering lens centroid and ASL. These corrected data are shown in Table 5.4b.

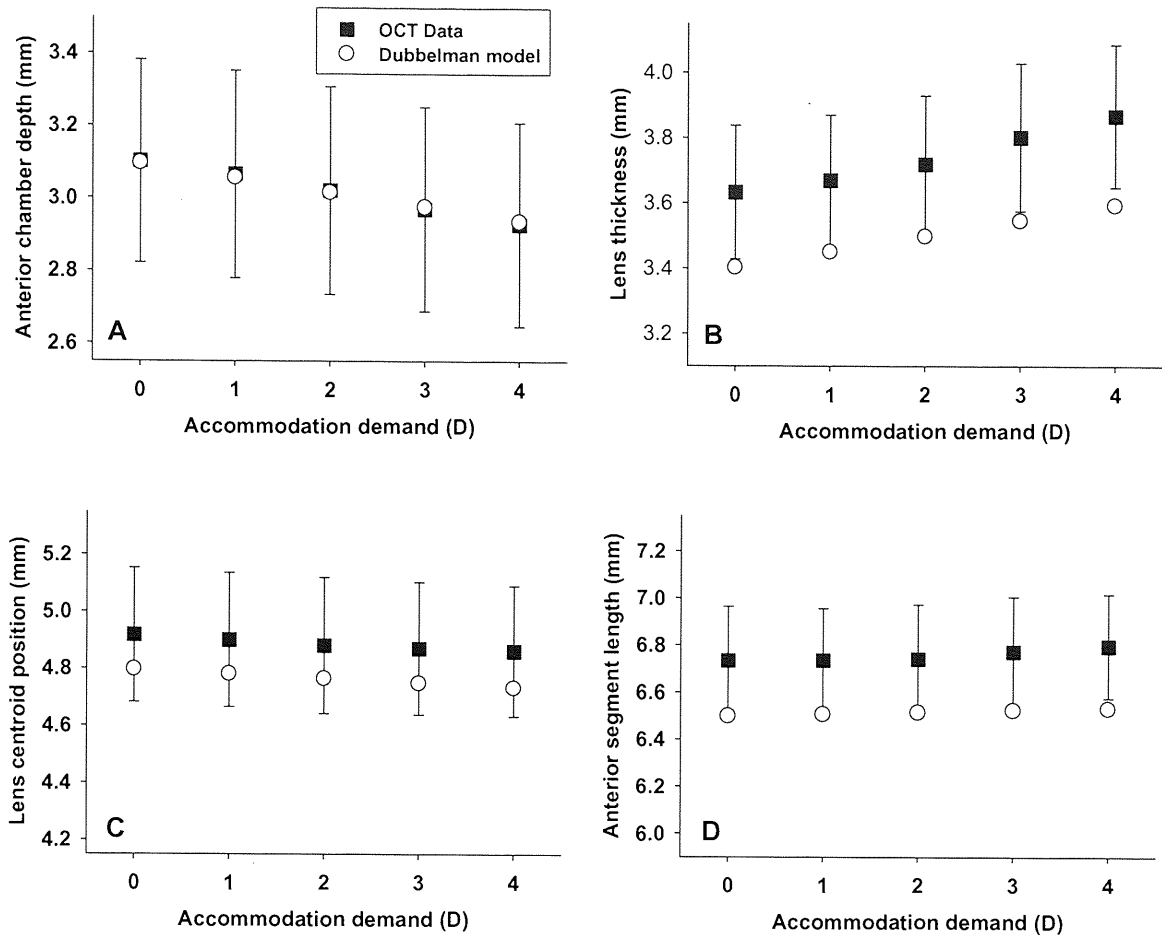


Figure 5.4 Anterior eye axial distances and their variation with accommodation demand measured with the *Visante*, compared to the Dubbelman model eye data (Norrby, 2005). Figure 5.4A represents the ACD, Figure 5.4B LT, Figure 5.4C lens centroid and Figure 5.4D ASL. Data points represent the mean, error bars the standard deviation. The average age of the cohort has been matched to that of the model (19.4 years old; $n = 30$). The ACD is the distance between the posterior corneal surface and the anterior lenticular surface. The *Visante* data and the model data show a close correlation, with the exception of lens thickness and anterior segment length.

Accommodation demand (D)	Dubbelman model (mm)	Visante (mm \pm SD)
<i>Corneal thickness</i>		
0	0.574	0.551 \pm 0.030
1	0.574	0.552 \pm 0.033
2	0.574	0.553 \pm 0.029
3	0.574	0.554 \pm 0.029
4	0.574	0.552 \pm 0.033
<i>Anterior chamber depth (ACD)</i>		
0	3.096	3.102 \pm 0.280
1	3.056	3.066 \pm 0.287
2	3.016	3.021 \pm 0.287
3	2.976	2.970 \pm 0.283
4	2.936	2.928 \pm 0.282
<i>Lens thickness (LT)</i>		
0	3.402	3.632 \pm 0.205
1	3.450	3.669 \pm 0.200
2	3.498	3.719 \pm 0.210
3	3.546	3.802 \pm 0.226
4	3.594	3.867 \pm 0.219
<i>Lens centroid (ACD + LT/2)</i>		
0	4.797	4.918 \pm 0.235
1	4.781	4.900 \pm 0.235
2	4.765	4.881 \pm 0.239
3	4.749	4.871 \pm 0.232
4	4.733	4.861 \pm 0.228
<i>Anterior segment length (ACD + LT)</i>		
0	6.498	6.734 \pm 0.230
1	6.506	6.735 \pm 0.220
2	6.514	6.740 \pm 0.231
3	6.522	6.772 \pm 0.232
4	6.530	6.795 \pm 0.221

Table 5.4a Anterior eye axial distances and their variation with accommodation demand measured with the *Visante*, compared to the Dubbelman model eye data (Norrby, 2005). The average age of the cohort has been matched to that of the model (19.4 years old; n = 30). The ACD is the distance between the posterior corneal surface and the anterior crystalline lens surface.

Accommodation demand (D)	Dubbelman model (mm)	Visante (mm \pm SD)
<i>Anterior chamber depth (ACD)</i>		
0	3.670	3.653 \pm 0.277
1	3.630	3.618 \pm 0.285
2	3.590	3.574 \pm 0.286
3	3.550	3.524 \pm 0.278
4	3.510	3.480 \pm 0.280
<i>Lens thickness (LT)</i>		
0	3.402	3.632 \pm 0.205
1	3.450	3.669 \pm 0.200
2	3.498	3.719 \pm 0.210
3	3.546	3.802 \pm 0.226
4	3.594	3.867 \pm 0.219
<i>Lens centroid (ACD + LT/2)</i>		
0	5.371	5.469 \pm 0.232
1	5.355	5.452 \pm 0.233
2	5.339	5.434 \pm 0.237
3	5.323	5.425 \pm 0.229
4	5.307	5.413 \pm 0.226
<i>Anterior segment length (ACD + LT)</i>		
0	7.072	7.285 \pm 0.229
1	7.080	7.287 \pm 0.218
2	7.088	7.294 \pm 0.230
3	7.096	7.326 \pm 0.231
4	7.104	7.347 \pm 0.218

Table 5.4b Anterior eye axial distances and their variation with accommodation demand measured with the *Visante*, compared to the Dubbelman model eye data (Norrby, 2005). The average age of the cohort has been matched to that of the model (19.4 years old; n = 30). The ACD and subsequent measures have been altered to include the corneal thickness; ACD displayed is the distance between the anterior corneal apex and the anterior lenticular apex.

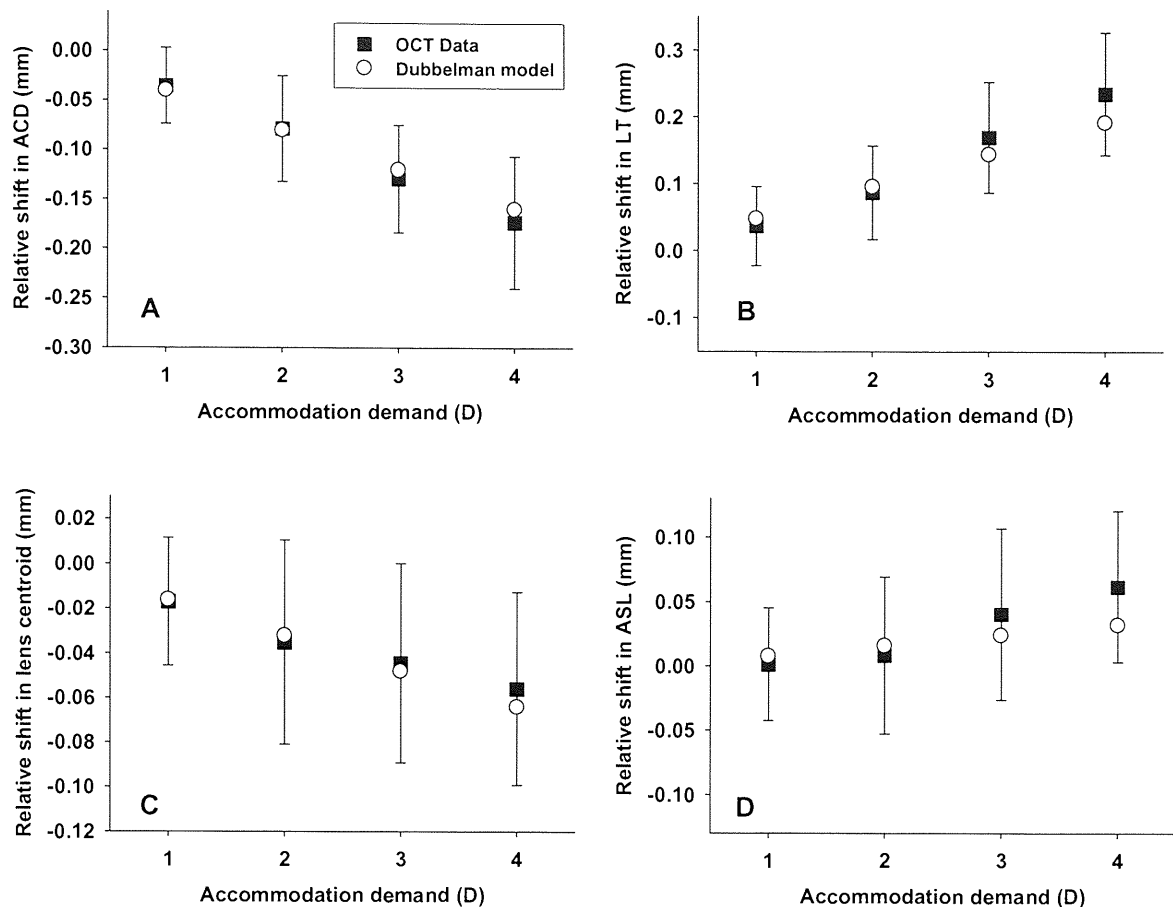


Figure 5.5 Anterior eye relative changes in axial distance with accommodation demand measured with the *Visante*, compared to the Dubbelman model eye data (Norrby, 2005). Figure 5.5A represents the anterior chamber depth (ACD), Figure 5.5B lens thickness (LT), Figure 5.5C lens centroid and Figure 5.5D anterior segment length (ASL). The average age of the cohort has been matched to that of the model (19.4 years old; $n = 30$). The ACD is the distance between the posterior corneal surface and the anterior crystalline lens surface. The *Visante* data and the model data show a close correlation for all measures.

When comparing the relative changes in axial distances, the two methods (Scheimpflug and *Visante* AS-OCT) appear to be more closely correlated (Table 5.5; Figure 5.5). These axial measures are very similar, with the AS-OCT data falling very close to the model distances. Corneal thickness changes with accommodation were not found to be statistically significant ($F_{(4,29)} = 0.40$; $p = 0.81$). All other measures, however, reached statistical significance (ACD: $F_{(4,29)} = 116.96$; $p < 0.01$, LT: $F_{(4,29)} = 128.97$; $p < 0.01$, Lens centroid: $F_{(4,29)} = 17.30$; $p < 0.01$, ASL: $F_{(4,29)} = 13.67$; $p < 0.01$). When the *Visante* distances were corrected to include corneal thickness, the accommodative changes

remained statistically significant (ACD: $F_{(4,29)} = 117.56$; $p < 0.01$, Lens centroid: $F_{(4,29)} = 17.45$; $p < 0.01$, ASL: $F_{(4,29)} = 14.72$; $p < 0.01$).

The studies by Dubbelman and colleagues, from which the model is based, rely on measures attributed to accommodative demand (Dubbelman and van der Heijde, 2001; Dubbelman *et al.*, 2001; 2002; 2005). A degree of error may be inherent in the model, as the axial distances and relative changes given may be related to a different accommodative response. Figure 5.6 demonstrates the differences seen when considering ocular biometric changes using accommodative response and accommodative demand. It is very clear that the accommodative response is less than that of demand; there is a lag of accommodation. What is also of interest is that the lens changes appear to be biphasic. Up until approximately 1.5 D of response (approximately 2.0 D demand), the anterior crystalline lens surface appears to be the primary correlate. After this point, the posterior surface begins to alter position. The model data (Figure 5.6C), however, shows a more linear trend.

Accommodation demand (D)	Dubbelman model (mm)	Visante (mm \pm SD)
<i>Anterior chamber depth (ACD)</i>		
1	-0.040	-0.035 \pm 0.038
2	-0.080	-0.079 \pm 0.054
3	-0.120	-0.129 \pm 0.055
4	-0.160	-0.173 \pm 0.067
<i>Lens thickness (LT)</i>		
1	0.048	0.037 \pm 0.059
2	0.096	0.087 \pm 0.070
3	0.144	0.170 \pm 0.083
4	0.192	0.235 \pm 0.091
<i>Lens centroid (ACD + LT/2)</i>		
1	-0.016	-0.017 \pm 0.029
2	-0.032	-0.035 \pm 0.046
3	-0.048	-0.045 \pm 0.045
4	-0.064	-0.056 \pm 0.043
<i>Anterior segment length (ACD + LT)</i>		
1	0.008	0.001 \pm 0.044
2	0.016	0.008 \pm 0.061
3	0.024	0.040 \pm 0.067
4	0.032	0.062 \pm 0.059

Table 5.5 Anterior eye relative axial distance changes with accommodation demand measured with the *Visante*, compared to the Dubbelman model eye data (Norrby, 2005). The average age of the cohort has been matched to that of the model (19.4 years old; n = 30).

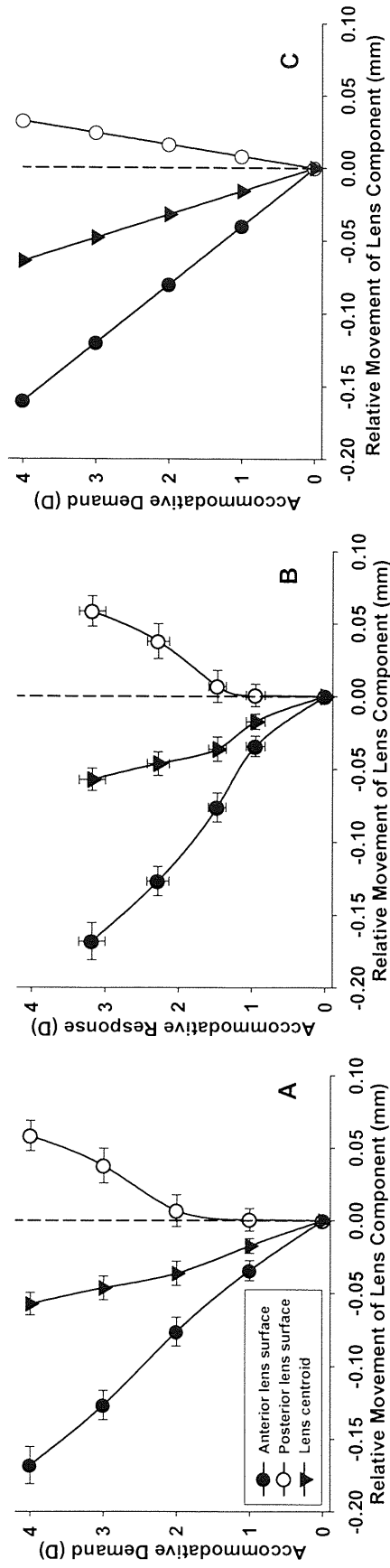


Figure 5.6 Relative movements of the various lens parameters as a function of accommodative demand or response. Figure 5.6A shows the relative movement of the lens components for the *Visante* data with accommodative demand (error bars represent \pm SEM). Figure 5.6B shows the relative movement of the lens components for the *Visante* data with accommodative response (\pm SEM). Figure 5.6C shows the relative movement of the lens components for the Dubbelman model eye (Norrby, 2005) with accommodative demand. Negative numbers indicate forward (anterior) movement.

5.4 Discussion

Measurement of the anterior segment parameters such as ACD, LT, and ASL is useful in understanding the mechanism of accommodation and subsequently, the development of presbyopia. These parameters can be measured with different techniques such as ultrasound biometry (Ostrin *et al.*, 2006), high-resolution MRI (Strenk *et al.*, 1999; 2005), ultrasound biomicroscopy (Glasser and Kaufman, 1999), Scheimpflug imaging (Dubbelman and van der Heijde, 2001; Dubbelman *et al.*, 2001; 2002; 2005), AS-OCT (Baikoff *et al.*, 2004; 2005a; 2005b; Richdale *et al.*, 2008), and PCI (Drexler *et al.*, 1997; Tsorbatzoglou *et al.*, 2007). The current study has utilised the relatively new technique of AS-OCT, and has compared the results to a new model eye based on Scheimpflug photography. The same model has been used in previous chapters to demonstrate biometric and vergence changes with accommodation.

At the present time, the current version of the *Visante* AS-OCT does not have the ability to analyse surface curvatures. Baikoff and colleagues (2004) present data on crystalline lens horizontal radius of curvature. However, the author does not make explicit the methods used. Attempts by other authors to overcome this problem appeared to have been successful when using model eyes (Dunne *et al.*, 2007). However, the application of the correction factors derived in this study, with the inherent difficulty in assessing variable images of human anterior segments, did not allow the successful application of this method to a human cohort. Further refinement of the correction factors for use in human subjects appears to provide an improved method of defining surface curvatures using the *Visante*. Unfortunately, poor image quality and the lack of more complex edge detection software have precluded the use of this technique at the current time.

Following detailed exploration of the data, the axial separations measured on uncorrected *Visante* images has been found to be very close to the data from an accommodating model eye compiled by Norrby; produced from the work of Dubbelman and co-authors (Norrby, 2005). The similarities between the absolute axial distance changes are close, with only the lens thickness, and subsequently, ASL data appearing to be overestimated by the *Visante*; this finding being confirmed by Dunne and colleagues (2007).

It is difficult to compare both *Visante* and model data accurately, as the number of subjects in the studies of Dubbelman which are similar to the cohort used in the current study is

unknown, and may account for any discrepancies found. The Dubbelman model is based on a cohort of over 100 subjects whose age ranges from 16 to 65 years (mean, 39.2 years old; Dubbelman and van der Heijde, 2001; Dubbelman *et al.*, 2001; 2002); of which an unspecified number lie close to the age of the model used in this study (age 19.4 years old, to match the mean age of the cohort recruited).

Lack of image correction for optical and instrument distortion may also be partially responsible. Relative changes in axial separation of the ocular components were compared on the assumption that any distortion or manipulation of the image by the *Visante* is constant throughout the image taken, thereby allowing comparison with other techniques. In this instance, the data points from the OCT and from the model eye are very close, with all model data falling well within the compass of any errors (SD) from the *Visante* cohort.

The AS-OCT imaging technique does have some limitations. Firstly, it is very difficult to ensure that the image slice taken through the anterior segment is equal for images and accommodation levels. To image the lens, the subject is moved forward towards the instrument using an automatic chin-rest controlled by a mouse attached to the instrument. Although best efforts were made to ensure that the patient's forehead was in contact with the forehead rest at all times, small movements, or the fact that the subject was now tilted slightly towards the machine, may induce some errors in slice placement and subsequent measures.

Small cyclotorsion effects with accommodation are well documented (Buehren *et al.*, 2003; Read *et al.*, 2007), and these may also induce uncorrected errors into the study. The *Visante* allows variation in the position of the image slice taken, however, this is accurate to one degree, which may not be enough to compensate for the small amounts associated with this phenomenon. In a recent study, mean cyclotorsion was 0.62 ± 2.18 degrees excyclorotated and ranged from 4.54 degrees excyclorotated to 3.47 degrees incyclorotated for the anterior cornea. For the posterior cornea, the mean change in corneal cylinder axis was 1.17 ± 3.29 degrees excyclorotated for a 5.0 D stimulus (range 6.80 degrees excyclorotated to 4.42 degrees incyclorotated; Read *et al.*, 2007). The effect of this factor on the accuracy of the study is unknown, and therefore requires further investigation.

Richdale and co-workers (2008) highlighted that the *Visante* AS-OCT, like other optical imaging techniques, assumes a single refractive index of the lens (e.g. 1.42; Garner and

Smith, 1997; Glasser and Campbell, 1999; Jones *et al.*, 2007) and does not take into account the gradient refractive index of the crystalline lens as reported by other authors (Garner and Smith, 1997; Dubbelman and van der Heijde, 2001; Jones *et al.*, 2007).

Considering the limitations of the study, the advantages must also be highlighted. Firstly, *ex vivo* studies of the eye suffer from post-mortem changes in dimensions and water content (Weale, 1983; Weeber and van der Heijde, 2008). Scheimpflug photography, ultrasound and PCI are *in vivo* techniques which make assumptions of refractive indices or the speed of sound. Ultrasound techniques can only be used with contact or with water based systems (Fledelius, 1997), often in the supine position, which have the potential to alter anatomical physiology. Scheimpflug techniques require geometrical reconstructions which are not possible in certain axes and have the added disadvantage of requiring artificial dilation of the pupil (Atchison, 1995). Sympathomimetic mydriatics may decrease natural accommodation leading to a lessened accommodative response (Atchison, 1995; Dubbelman *et al.*, 2005; Koepl *et al.*, 2005). OCT has the advantage of being able to image the eye under investigation, unlike other techniques such as Scheimpflug photography, A Scan, B Scan and UBM, where it is necessary to stimulate the fellow eye in order to observe accommodative variations of the eye being measured. With AS-OCT, the in-built target allows modification of accommodation and observation of the same eye simultaneously.

MRI has overcome many of these problems. It allows the visualisation of the eye without physical distortion or pharmacological intervention. However, the patient must be supine, which may affect the natural movement and amplitude of accommodation of the crystalline lens (Atchison *et al.*, 1994). At this time, clinical MRI has limited resolution of 100 to 300 μm , depending on the coil or sequence used (Strenk *et al.*, 2004; Jones *et al.*, 2007). The problems of resolution are overcome by using PCI, which is less than 10 μm (Drexler *et al.*, 1997; Bolz *et al.*, 2007) and is commonly used to assess axial length (e.g. *IOLMaster*; Carl Zeiss Meditec, Jena, Germany), but can measure ACD and LT (e.g. *ACMaster*; Carl Zeiss Meditec, Jena, Germany; Tsorbatzoglou *et al.*, 2007). The AS-OCT allows imaging of the corneal and crystalline lens to a spatial resolution of less than 20 μm (Baikoff *et al.*, 2004; Güell *et al.*, 2007).

Many studies have investigated biometric changes with accommodation. Vilupuru and Glasser (2005) used continuous ultrasound biomicroscopy on Edinger-Wesphal stimulated

rhesus monkeys to find a linear relationship between accommodation and the changes in ACD, LT and ASL. An OCT study by Baikoff (2004) found that for 1.0 D of accommodation, the ACD decreased by 30 μm , which is very similar to the results of the current study and the Dubbelman model (34 μm ; 40 μm respectively; Table 5.5). Ostrin *et al.* (2006) found this decrease to be in the region of 51 μmD^{-1} using A Scan while using a young cohort of between 21 and 30 years, while Bolz *et al.* (2007) found a decrease by 47 μmD^{-1} and 57 μmD^{-1} in emmetropes and myopes respectively using PCI.

Richdale and colleagues (2008) found a 51 μmD^{-1} increase in lens thickness using AS-OCT. Similarly, measures taken using ultrasound were 42 μmD^{-1} (Garner and Yap, 1997), 36 μmD^{-1} for one PCI study (Tsorbatzoglou *et al.*, 2007) and 63 to 72 μmD^{-1} in another (emmetropes-myopes; Bolz *et al.*, 2007). The Dubbelman model predicts a lens thickness increase of 45 μmD^{-1} , all compared to the current study which states a 58 μmD^{-1} thickness change. It must be stressed that these values are based on accommodative demands and not response, but assumes that the subject was accommodating accurately to the target. The stimuli used these studies inevitably vary with instrumentation and study group.

It is well known that the changes in lenticular radius during accommodation are greater for the anterior surface of the lens (Kirschcamp *et al.*, 2004; Koretz *et al.*, 1997b; 2002; Rosales *et al.*, 2006). There is only a small posterior movement of the posterior lens surface, perhaps as a result of the resistance provided by the vitreous body, and a larger forward movement of the anterior surface. In combination, these result in an increase in axial thickness and a small forward movement of the centre of mass of the lens (Drexler *et al.*, 1997; Strenk *et al.*, 2004; 2005). Fincham (1937) suggested that the posterior lens surface moves backward with accommodation, as the increase in LT was greater than the decrease in ACD; this has been corroborated by studies in more recent times (Drexler *et al.*, 1997; Dubbelman *et al.*, 2005; Tsorbatzoglou *et al.*, 2007).

This study has produced an interesting finding in the behaviour of the posterior lenticular surface to an accommodative stimulus. The surface in question appears to be relatively static until approximately 1.5 D of response (approximately 2.0 D demand), after which it partakes in a posterior motion. It is possible that this finding is affected in some way by the method of analysis. Many biometric studies fail to consider accommodative response (Dubbelman *et al.*, 2002; 2004; Richdale *et al.*, 2008); this may attenuate any accommodative trends seen (Figure 5.4). Some human and animal studies have found an

equal and linear change in anterior and posterior portions of the lens with accommodation (Koretz *et al.*, 1997b; Vilupuru and Glasser, 2005). Drexler and colleagues (1997) plotted the position of the anterior and posterior poles of the crystalline lens with change in fixation from distance to targets at various closer distances. The results show a static posterior lens surface from distance observation until viewing a target at 40.0 cm (2.5 D stimulus). From this point, closer targets elicit a posterior movement of the surface of just over 0.5 mm for a target at 10.0 cm (10.0 D stimulus); this phenomenon is, however, not alluded to in the text; it appears to be relatively new in the study of accommodative lenticular changes.

5.5 Conclusion

The *Visante* AS-OCT allows direct, non-invasive measurement of the anterior ocular structures (CT, ACD and LT) under the influence of the accommodative mechanism driven by the ciliary body. At this time, the instrument does not allow for the calculation and comparison of corneal surface parameters. Attempts to remedy this situation had limited success due to the lack of edge detection techniques, poor image contrast and lack of very high resolution to retain accuracy. The correction of instrument and optical distortion proposed by a previous study to changes in accommodation demand (Dunne *et al.*, 2007) prove to be inapplicable to human subjects with current techniques.

The use of uncorrected axial distance measures taken directly from the *Visante* using the built-in callipers (Figure 5.1) has been found to compare well with a recent schematic eye (Norrby, 2005). The *Visante* appears to overestimate lens thickness and consequentially, anterior segment length in this comparison, which is corroborated by Dunne *et al.* (2007). However, parameter changes in relation to accommodative stimuli are very close, and can be found within the spectrum of values previously published using a variety of imaging techniques.

The majority of studies of this type employ the use of accommodation stimulus as opposed to accommodation response. Although it is very difficult to inextricably link one to the other, the latter would suggest a better evaluation of actual accommodative performance. The *Visante* data produced gives rise to a biphasic response to accommodation with regard to the posterior lenticular surface; a phenomenon which has little been discussed in previous studies.

The key findings of this chapter are summarised below.

- Uncorrected *Visante* measurements in ACD and lens centroid, are comparable to a schematic eye based on Scheimpflug photography (Norrby, 2005); measurements of LT and ASL are less well correlated.
- Relative accommodative changes in all components, using both the *Visante* and the Dubbelman model are comparable.

- Ocular component changes with accommodation, measured with the *Visante*, were statistically significant with the exception of CT.
- The posterior crystalline lens surface displays a unique biphasic trend which, thus far, has not been alluded to in the literature.

The *Visante* AS-OCT is a useful tool in examining the ocular components *in vivo*. Although it does have limitations, it is comparable to other imaging techniques in many respects, and may allow a better understanding of accommodative biometric changes.

Thus far, phakic biometric changes with accommodation have been modelled using a recent schematic eye, and have been measured experimentally using a new imaging technique. Further, the pseudophakic eye has been modelled using a theoretical accommodating intraocular lens (AIOL), with the same schematic eye and rationale.

A number of studies have imaged the pseudophakic eye using a variety of methods (Tsorbatzoglou *et al.*, 2006; Vámosi *et al.*, 2006; Marchini *et al.*, 2008). However, few have investigated AIOLs using the same techniques (Langenbacher *et al.*, 2003; Findl *et al.*, 2004; Kriechbaum *et al.*, 2005; Koeppel *et al.*, 2005); no evidence of AIOL research using the *Visante* AS-OCT could be found. A study assessing accommodation-induced AIOL movements using the *Visante*, therefore, may reveal more information regarding the method of action of these lenses.

CHAPTER 6

ACCOMMODATING INTRAOCULAR LENSES: A 2 YEAR FOLLOW-UP

6.1 Introduction

The restoration of accommodative ability in pseudophakic patients is one of the most challenging tasks of modern cataract surgery. Attempts to solve the problem of presbyopia correction without spectacles or contact lenses, has been approached in many ways with varying degrees of success. These methods include the use of multifocal intraocular lenses (IOLs; Lane *et al.*, 2006), refilling the capsular bag with an inflatable endocapsular balloon (Nishi *et al.*, 1991) or biocompatible silicone gel (Parel *et al.*, 1986), scleral expansion surgery (Schachar, 1992; Mathews, 1999), zonal photorefractive keratectomy (Vinciguerra *et al.*, 1998) and decentred laser *in situ* keratomileusis (LASIK; Bauerberg, 1999). These methods have had varying degrees of success, and many are still under investigation.

A further alternative for the correction of presbyopia is the use of ‘accommodating IOLs’ (AIOLs). AIOLs are designed to use some part of the accommodative physiology: This may be in the form of ciliary muscle contraction (Glasser and Kaufman, 1999; Bacskulin *et al.*, 1995; 1996; Strenk *et al.*, 1999), utilising the elasticity of the capsular bag (Fisher, 1988; Ziebarth *et al.*, 2008), or possibly changes in vitreous pressure with accommodative effort (Coleman, 1970; 1986; Coleman and Fish, 2001). These physiological changes must elicit a change in shape or position of the AIOL in order to alter the optical properties of the system. There have been a number of designs which have sought to use these accommodative changes by a variety of mechanisms (Dick, 2005; Findl, 2005; Glasser, 2006; Menapace *et al.*, 2007; Doane and Jackson, 2007). Of these many designs, the single-optic IOL is currently the most widely used.

Single-optic AIOLs are designed to rely on a forward translation of the optic with accommodative effort (Glasser, 2008). As the optic moves forward along the optical axis, it increases the optical power of the eye; modelling of a pseudophakic schematic eye has shown this to be true (see Chapter 4). Moreover, the amount of pseudophakic accommodation has been shown by the same method to be reliant on optical factors such

as the power of the AIOL, its position within the eye, and axial length (Chapter 4; Nawa *et al.*, 2003).

The subject of AIOLs, from theory to practical application, has been extensively reviewed by a number of authors (Dick, 2005; Findl, 2005; Tonekaboni and Whitsett, 2005; Beiko, 2007; Doane and Jackson, 2007; Menapace *et al.*, 2007; Findl and Leydolt, 2007). A number of studies have investigated the refractive outcomes of AIOLs (Claoué, 2004; Langenbacher *et al.*, 2004; Marchini *et al.*, 2004; Kriechbaum *et al.*, 2005; Stachs *et al.*, 2005; Dick and Dell, 2006; Glasser, 2006; Hancox *et al.*, 2006; Wolffsohn *et al.*, 2006a; 2006b; Hancox *et al.*, 2007; Mastropasqu *et al.*, 2007; Harman *et al.*, 2008). Further, studies have used a variety of imaging techniques to quantify axial movements of AIOLs associated with the accommodative mechanism; these are summarised in Table 6.1. Accommodative movements have also been reported in conventional IOLs (Table 6.1).

The Kellen *Tetraflex KH3500* (Lenstec, St. Petersburg, Florida, USA) IOL is one such AIOL currently undergoing US FDA trials and is being used clinically in Europe (CE marked). It is a single-piece, spherical optic with flexible anteriorly angled (by 10°) closed-loop haptics. It is manufactured from medical grade hydroxyethyl methacrylate (26 % water content) with a short-wavelength blocker. It has a refractive index of 1.46, a central optic portion of 5.75 mm and an overall diameter of 12.0 mm.

The proposed mode of action involves the anterior shift of the lens optic on contraction of the ciliary muscle. The lens is designed to be implanted within the capsular bag in a posteriorly vaulted position, with the optic against the posterior capsule and anterior vitreous face. During the process of accommodation, the anterior ciliary body moves forward towards the axis of the eye, (Glasser and Kaufman, 1999; Bacskulin *et al.*, 1995; 1996; Strenk *et al.*, 1999) causing an increase in vitreous pressure (Coleman, 1970; 1986), and a subsequent transient forward movement of the optic. The *Tetraflex* has flexible plate haptics to allow this accommodative shift within the capsule. Arching or bending of the optic due to increasing vitreous pressure, or by pressure from the haptics on the softer optic, have been suggested to aid further these dioptric accommodative changes (Dick and Dell, 2006).

Study (Year)	IOL Type	Mean ACD Shift ± SD (mm)	Post-op time (Months)	Accommodation stimulation method	Imaging method
Legeais <i>et al.</i> (1999)	BioComFold (Morcher) PhacoFlex II SI-40NB (Allergan)	-0.72 ± 0.58 -0.28 ± 0.38	1	Pilocarpine 2% Cyclopentolate 1%	A-Scan
Auffarth <i>et al.</i> (2002)	1CU (HumanOptics)	-0.83 ± 0.25 [1.04 ± 0.39*] {0.28 ± 0.14}	3	Pilocarpine 2%	Zeiss IOLMaster [Orbscan II] {UBM}
Küchle <i>et al.</i> (2002)	1CU (HumanOptics)	-0.63 ± 0.16	3	Pilocarpine 2%	Zeiss IOLMaster
Findl <i>et al.</i> (2003)	BioComFold 43A (Morcher) BioComFold 43E (Morcher) AA4203VF (Staar) MC 220 (Dr. Schmidt) AR40e (Allergan) AcrySof MA60BM (Alcon)	-0.12 ± 0.11 -0.22 ± 0.24 -0.16 ± 0.17 0.00 0.00 0.16 ± 0.11*	3	Pilocarpine 2% Cyclopentolate 1%	PCI
Langenbucher <i>et al.</i> (2003)	1CU (HumanOptics)	-0.78 ± 0.12 [-0.63 ± 0.15]	6	Pilocarpine 2%	Zeiss IOLMaster [Immersion UBM]
Findl <i>et al.</i> , (2004)	1CU (HumanOptics) AR40e (Allergan)	-0.37 ± 0.29 0.06 ± 0.13*	3	Pilocarpine 2%	PCI
Marchini <i>et al.</i> (2004)	AT-45 (Crystalens)	-0.32 ± 0.16 [-0.33 ± 0.25]	1 [6]	Fixation at 30 cm Fixation at 2.8 m	UBM
Koeppel <i>et al.</i> (2005)	AT-45 (Crystalens)	0.15 ± 0.08*	3	Pilocarpine 2%	PCI

Muftuoglu <i>et al.</i> (2005)	AcrySof MA30MB (Alcon) AcrySof MA60MB (Alcon)	0.11 ± 0.13* 0.05 ± 0.14*	14	Pilocarpine 2% Cyclopentolate 1%	UBM
Sauder <i>et al.</i> (2005)	1CU (HumanOptics) AR40e (Allergan)	-0.82 ± 0.30 -0.40 ± 0.32	8	Pilocarpine 2% Tropicamide 0.5%	Zeiss IOLMaster
Hancox <i>et al.</i> (2006)	1CU (HumanOptics) AcrySof MA30 (Alcon)	-0.01 ± 0.03 [-0.22 ± 0.17] 0.03 ± 0.10*	18-24	Fixation at 40 cm [Pilocarpine 4%] Pilocarpine 4%	Zeiss ACMaster
Schneider <i>et al.</i> (2006)	1CU (HumanOptics)	-0.30 ± 0.32	3	Pilocarpine 2%	Jäeger's Haag-Streit slit-lamp attachment
Stachs <i>et al.</i> (2006)	AT-45 (Crystalens)	-0.13 ± 0.08	1	Pilocarpine 2%	3D Ultrasound
Tsorbatzoglou <i>et al.</i> (2006)	AcrySof MA60AC (Alcon) AcrySof SA60AT (Alcon) AcrySof SA60D3 ReSTOR (Alcon)	-0.02 ± 0.06 -0.05 ± 0.05 -0.02 ± 0.02	10	Near fixation Distance fixation Cyclopentolate 1%	Zeiss ACMaster
Vámosi <i>et al.</i> (2006)	AcrySof MA60BM (Alcon) Akreos Disc (Chauvin Optia)	-0.57 ± 0.23 -0.42 ± 0.24	12	Fixation at 30 cm Cyclopentolate 1%	A-Scan
Marchini <i>et al.</i> (2008)	Tecnis Z9000 (AMO) AcrySof SA60AT (Alcon) Akreos Fit (B&L) Concept 360 (Corneal)	-0.04 ± 0.09 [-0.03 ± 0.30]	7	Fixation at 30 cm Fixation at 2.8 m	UBM (HiScan) UBM 840

Table 6.1 Studies that have measured IOL shift with either physiological blur or pharmacological stimulation of accommodation. Negative shifts in ACD indicate anterior movements of the IOL, positive shifts posterior movements (*indicates a posterior shift of the IOL). IOLs listed in *italics* are conventional monofocal IOLs (i.e. not AIOLs). PCI = Partial Coherence Interferometry, UBM = Ultrasound Biomicroscopy.

To assess the performance of AIOLs, the key outcome measures are the near vision achieved with the best distance correction (DCNVA) at 40 cm, the range of accommodation assessed by both subjective and objective techniques (which isolate the optical effect of changes in the lens) and posterior capsular opacification (PCO) rate.

Wolffsohn and colleagues (2006b) studied 28 patients implanted monocularly with a *Tetraflex KH3500* AIOL, and 20 controls with a monofocal IOL (*Softecl*, Lenstec, St. Petersburg, Florida, USA). Outcome measures of refractive error, visual acuity (logMAR progression chart), subjective amplitude of accommodation (Royal Air Force accommodation and vergence measurement rule [RAF rule]), objective accommodative stimulus response curve (*SRW-5000*; Shin-Nippon Commerce Inc., Tokyo, Japan), aberrometry (optical path difference [OPD] skiascopy wavefront sensing device, Nidek, Gamagori, Japan), and Scheimpflug imaging to assess PCO rate (Pentacam, Oculus, Wetzlar, Germany) were taken at approximately 3 weeks and 6 months (± 1.5 weeks) after surgery.

Approximately one month post-operatively, Mean Spherical Equivalent (MSE) refraction was -0.23 ± 0.69 D (mean \pm SD) for the *Tetraflex*, compared to -0.06 ± 0.69 D for the *Softecl* ($p = 0.57$). best-corrected distance visual acuity (BCDVA) was $+0.06 \pm 0.13$ logMAR with the *Tetraflex* lens compared to $+0.08 \pm 0.15$ with the *Softecl*, the difference was not significant ($p = 0.52$). Mean DCNVA was 0.58 ± 0.20 logMAR and 0.62 ± 0.25 logMAR with the *Tetraflex* and *Softecl*, respectively ($p = 0.68$). Contrast sensitivity was similar in both lenses (*Tetraflex*: $+1.57 \pm 0.27$ log units; *Softecl*: $+1.58 \pm 0.15$ log units; $p = 0.91$; Wolffsohn *et al.*, 2006b)

Objective amplitude of accommodation was found to be significantly greater for the *Tetraflex KH3500* compared to the *Softecl* (*Tetraflex*: 0.39 ± 0.53 D; *Softecl*: 0.17 ± 0.13 D; $p = 0.03$), with some variation in individual stimulus response curves. The same was true with regard to subjective amplitude of accommodation (*Tetraflex*: 3.1 ± 1.6 D; *Softecl*: 2.0 ± 0.9 D). The subjects were re-examined 6 months post-operatively. Results at this stage showed no significant change in the data except for a decrease in the smallest print size seen at near ($p < 0.05$) accompanied by a decrease in the subjective amplitude of accommodation; this was not significant ($p = 0.06$). There was a significant increase in

Posterior Capsule Opacification (PCO) light scatter ($p < 0.01$) in the *Tetraflex* lens but not in the monofocal IOL (Wolffsohn *et al.*, 2006b).

Sanders and Sanders (2007) implanted the *Tetraflex* AIOL in 95 eyes of 59 patients (36 bilaterally). Post-operative assessments were performed at 1 day, 1 week, 1 month, 3 months and 6 months after surgery. They assessed manifest refraction, BCDVA, uncorrected distance visual acuity (UCDVA), DCNVA and subjective amplitude of accommodation (RAF rule).

At 6 months post-surgery, the manifest refraction was within ± 1.0 D of emmetropia (MSE) in 92.2 % of cases. BCDVA was 0.3 logMAR or better in 98.7 % of cases and 0.4 logMAR or better in all eyes. UCDVA was 0.3 logMAR or better in 92.2 %, 0.1 logMAR or better in 72.7 % and 0.0 logMAR or better in 50.6 % of eyes at 6 months. DCNVA was 0.3 logMAR or better in 63.2 % of eyes after 6 months. All eyes had a subjective amplitude of accommodation of more than 1.0 D after 6 months. Over three quarters (75.7 %) could accommodate more than 2.0 D, 71.6 % more than 2.5 D and 18.9 % over 3.0 D, at 6 months after surgery (Sanders and Sanders, 2007).

Few studies have reported on the long-term outcome of AIOLs at 2 years post-implantation (Kriechbaum *et al.*, 2005; Hancox *et al.*, 2006; Wolffsohn *et al.*, 2006a; Hancox *et al.*, 2007; Mastropasqu *et al.*, 2007). These longer-term studies of AIOLs have suggested that the initial benefits of AIOLs over conventional monofocal IOLs decrease over time, while significant PCO rates are high (50 % for of a 1CU AIOL [HumanOptics]; Hancox *et al.*, 2007). All of these longer-term studies have examined the 1CU AIOL (HumanOptics, Erlangen, Germany), which has a hinged haptic arrangement, compared to the *Tetraflex* AIOL, where the lens is designed to move forward as a whole with ciliary muscle contraction.

6.1.1 Aims

The aim of this study was to assess the long-term subjective and objective performance of the *Tetraflex KH3500* AIOL in patients implanted for 2 years or longer. Hitherto, the imaging of AIOLs has produced equivocal results (Table 6.1). As in Chapter 5 of this thesis, the use of Anterior Segment Optical Coherence Tomography (AS-OCT) has been shown to be comparable to Scheimpflug photography in assessing phakic accommodative changes in ocular components. The use of AS-OCT in quantifying AIOL movement has thus far been limited. The application of this new technique to the study of objective AIOL movement with accommodative stimulus is novel. It is predicted that small anterior shifts will be detected in line with recent studies who have examined other AIOLs with various imaging techniques (Table 6.1).

6.2 Methods

6.2.1 Subjects

A single-centre prospective data collection study was performed in Birmingham, United Kingdom. A cohort was recruited from a local National Health Service trust hospital (Birmingham Heartlands & Solihull NHS Trust); this was the same cohort used in a previous study (Wolffsohn *et al.*, 2006b). Informed consent was obtained from the subjects prior to inclusion in the study after explanation of the nature and possible consequences of the study. The inclusion criteria were patients undergoing routine cataract surgery to remove a lenticular opacity affecting the visual demand of the patient and had been implanted with the *Tetraflex KH3500* AIOL for two years or more. Patients were excluded from the study if they had associated co-morbidity. The research followed the tenets of the Declaration of Helsinki and was approved by the Solihull Local Research Ethics Committee (Appendix 4).

Of the thirty-seven possible patients who fulfilled these criteria, one had passed away, four were unable to be contacted and three declined to take part in the study (due to current ill health). The remaining twenty-nine patients aged 31-92 years (average 69.4 ± 14.5 years) were assessed, corresponding to a 78% response rate.

All subjects underwent standard phacoemulsification cataract surgery with clear corneal incision, performed by the same surgeon. All assessments of visual and accommodative function were performed under the same conditions and using the same methodology as that of the previous study by Wolffsohn and co-workers (2006b).

6.2.2 Assessment of visual function

Distance inter-pupillary distance was measured using a ruler prior to the fitting of a standard trial frame (Oculus, Washington, USA). Static retinoscopy was performed followed by cross-cylinder to determine both the axis (in 2.5° increments) and power (in 0.25 D increments) of the cylindrical component. Best sphere and binocular balancing was used to refine the spherical component of the prescription (in 0.25 D increments). The endpoint was achieved with the maximum positive spectacle prescription consistent with optimum visual acuity (Bennett and Rabbetts, 2007).

Optimally distance-corrected letter acuity at distance (6.0 m) and near (40.0 cm) was measured with Bailey-Lovie (90 % contrast) logMAR progression charts (Haag-Streit, UK) as well as near acuity with a +2.50 D addition lens. Bailey-Lovie logMAR charts have five letters on each row. This ensures that the task is equivalent for each row and helps to ensure equal contour interaction. It also provides more letters for patients with poorer visual acuity. The letter spacing on each row is equal to one letter width. Likewise, the row spacing is equal to the height of the letters below. In this way, contour interaction is scaled in relation to letter size. The letter size follows a logarithmic progression, increasing in 0.1 logMAR steps. LogMAR is an acronym for Log_{10} of the Minimum Angle of Resolution (MAR). The MAR is taken as the stroke width of the letters, which is one fifth of their vertical angular subtense. Thus a 6/6 Snellen letter which subtends 5 minutes of arc, equates to a MAR of one minute of arc and a logMAR of 0.0 ($\text{Log}_{10}(1) = 0.0$; Thomson, 2005).

Contrast sensitivity was measured with a Pelli-Robson chart (Clement Clarke, UK). The Pelli-Robson chart allows presentation of letters of a constant spatial frequency (1 cycle per degree at 1.0 m) in groups of 16 triplets; each triplet decreasing in contrast by 0.15 log units. The manufacturer's recommended testing procedures were followed with a testing distance of 1.0 m and room illumination of 85.0 cdm^{-2} .

6.2.3 Assessment of accommodative function

Mean subjective amplitude-of-accommodation was measured with the push-up RAF gauge (Clement Clarke/Haag-Streit, UK; Goss, 1992). The accommodative amplitude was measured with the patient trying to read the smallest letter (N5) on the RAF rule target. With the RAF rule in place the target was moved from 50.0 cm to the point where the last line became slightly blurred. Then the target was slowly pushed back until the last line was just clearly read. This point was taken as the near point of accommodation. Three measures on each subject were averaged; the process was repeated with a +2.50 D spherical lens *in situ*.

The subjective range of clear focus for maintaining best visual acuity was measured with spherical lenses from +2.00 D to -2.00 D in 0.50 D steps. Letters were presented using a

computerised test chart (Test Chart 2000; Thomson Software Solutions, I.O.O. Sales Ltd., UK) on a Microsoft *Windows* based portable laptop computer. Lines of letters in logMAR format were randomised between presentations of defocus lenses, also presented in a random order (Gupta *et al.*, 2007; 2008).

Monocular objective accommodative responses were measured using the *SRW-5000* (Shin-Nippon Commerce Inc., Tokyo, Japan) through un-dilated pupils (Mallen *et al.*, 2001). Subjects were rendered functionally emmetropic using full aperture trial lenses set into a standard trial frame (Oculus, Washington, USA). On commencement, the eye under investigation viewed a stationary high contrast (90%) 37.0 cdm⁻² Maltese cross, through a +5.0 D Badal optical system fitted to the modified autorefractor; the other eye was occluded with a patch. Nine stimulus conditions were employed in a random order within the Badal system (0.0 D to 4.0 D in 0.5 D steps). Subjects were encouraged to concentrate on the target at all times, as attentional factors can affect accommodation measurement (Francis *et al.*, 2003). Five measures were recorded at each stimulus level and the MSEs averaged.

6.2.4 Imaging the AIOL: Optical Coherence Tomography

The distance refractive error of each subject, as found by subjective refraction, was entered into the *Visante*TM (Carl Zeiss Meditec, Dublin, California) AS-OCT to allow appropriate correction and focus of the internal pinwheel target. The subject was aligned using the automatic chin and headrest so the image of the eye was central in the OCT integral computer monitor window. Subjects were encouraged to concentrate on the target at all times. A single image was captured along the 180° meridian in the anterior segment single-image capture mode. The image included corneal thickness, anterior chamber depth, corneal surface curvature, and the AIOL *in situ*. Six accommodative stimulus conditions were employed in a random order using the internal pinwheel target (0.0, 0.5, 1.0, 2.0, 3.0 and 4.0 D). The *Visante* AS-COT has built-in edge detection software (version 1.0.12.1896). This attempts to detect the corneal surfaces, but as they are not always present, the image is often distorted in a random manner. The correction was therefore removed prior to analysis.

From the uncorrected *Visante* images, measures were taken of anterior chamber depth (corneal apex to anterior AIOL surface). All distances were measured using the built-in *Visante* measuring callipers. Each measurement was repeated three separate times. Means and standard deviations were calculated using a Microsoft *Excel* spreadsheet. A Shapiro-Wilk analysis of variance (ANOVA; Shapiro and Wilk, 1965) was conducted with SPSS 12.0.1 for Microsoft *Windows*.

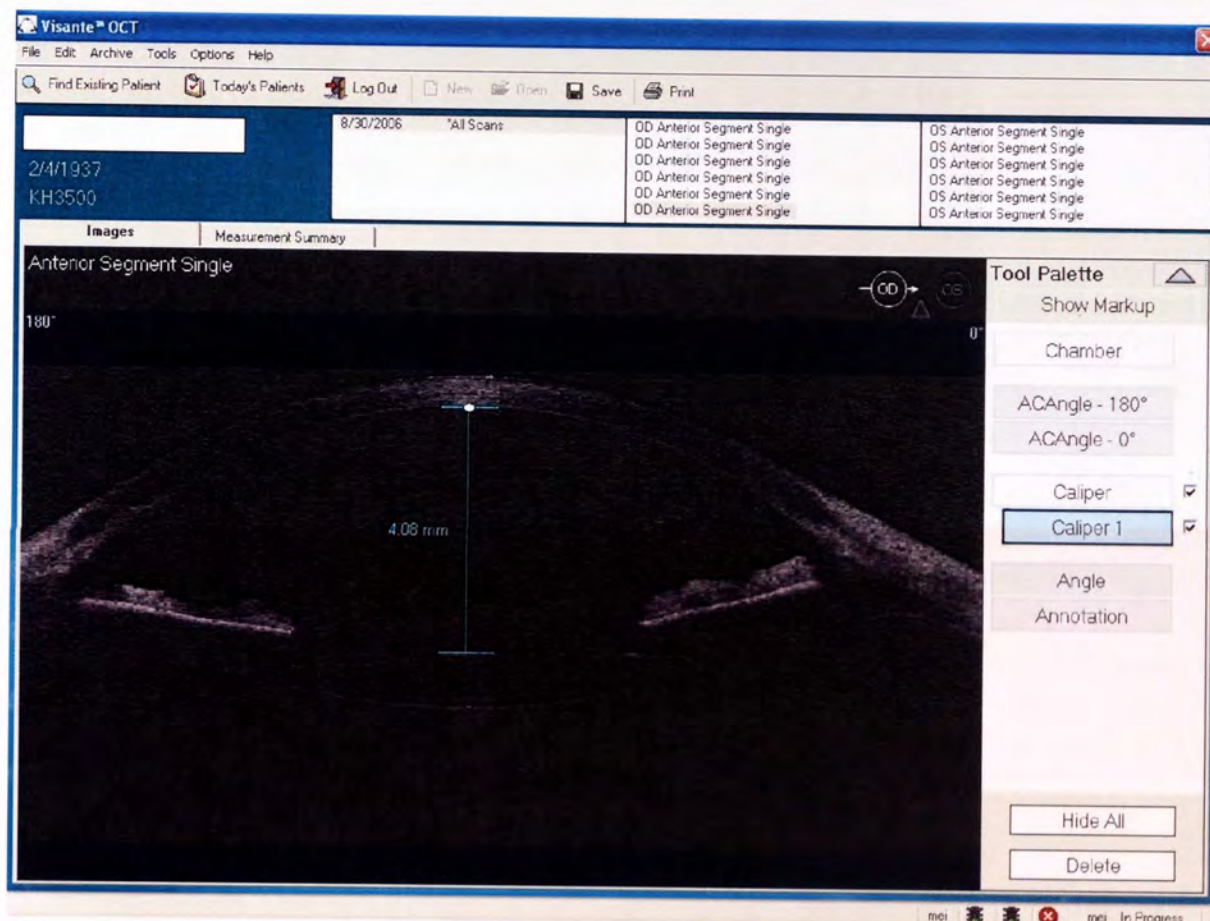


Figure 6.1 The *Visante* AS-OCT screen displaying the measuring callipers *in situ*. The *Tetraflex* AIOL can clearly be seen.

6.2.5 Aberrometry

Hartmann–Shack ocular aberrometry was attempted on all subjects using a commercially available aberrometer (Topcon *KR-9000PW*; Topcon, Tokyo, Japan). Unfortunately, due to pupil miosis and the large number of eyes with PCO, collection and analysis of these data was not possible. These data have therefore been omitted.

6.2.6 Nd:YAG capsulotomy rates

The occurrence of a Nd:YAG capsulotomy was extracted from the patient's medical notes and reported history. The anterior chamber was examined for the presence of fibrosis and PCO using a slit-lamp biomicroscope.

6.2.7 Binocular data

Nineteen patients had been implanted binocularly with the *Tetraflex* AIOL. Right eye data are presented for these patients for monocular measures. Additional binocular measures of optimally distance-corrected visual acuity at distance and near, contrast sensitivity and push-up subjective amplitude of accommodation were conducted on these patients.

6.3 Results

6.3.1 Monocular measures

The average time since implantation of the *Tetraflex* lens was 2.64 ± 0.32 years (mean \pm standard deviation), range 2.05 to 3.16 years. For all eyes, monocular uncorrected distance visual acuity was $+0.19 \pm 0.26$ logMAR. The MSE refractive error was $+0.23 \pm 1.01$ D which produced a BCDVA of $+0.04 \pm 0.24$ logMAR and contrast sensitivity score of $+1.35 \pm 0.21$ log units. DCNVA was $+0.61 \pm 0.17$ logMAR improving to $+0.23 \pm 0.22$ logMAR with a +2.5 DS near addition (t-test, $p < 0.001$).

The monocular subjective amplitude of accommodation was 1.53 ± 0.64 D (range, 0.8 to 3.0 D) and range of clear focus (calculated from defocus curves) 0.77 ± 0.29 D (range, 0.2 to 1.4 D; Figure 6.2). The monocular objective amplitude of accommodation was 0.21 ± 0.19 D (range 0.0 to 0.7 D).

Individual stimulus-response curves showed a linear increase in accommodative response with increasing stimulus demand in 5 eyes. An increase in response followed by a flattening or decrease was noted in 11 eyes. Eight eyes displayed an increase in stimulus response only at higher levels of stimulus-demand, and no apparent increase in accommodative response in was seen in 5 eyes (Appendix 5). Twenty-three of 48 eyes (48%) had already received or were waiting for a Nd:YAG capsulotomy.

6.3.2 Binocular measures

In the 19 patients binocularly implanted with the *Tetraflex* lens, the results measured binocularly were better for contrast sensitivity and DCNVA than the better eye, and all binocular measures were better than the average of the two eyes measured monocularly (Table 6.2). Sixteen patients (20 eyes) had data at 1 and 6 months following Tetraflex IOL implantation from a previous study using the same methodology (Wolffsohn *et al.*, 2006b). Contrast sensitivity had decreased by 6 months post implantation and subsequently stabilised at this level. The MSE refraction and subjective amplitude of accommodation changed significantly from the first month post implantation to 6 months, but had largely recovered by 2 years (Table 6.3).

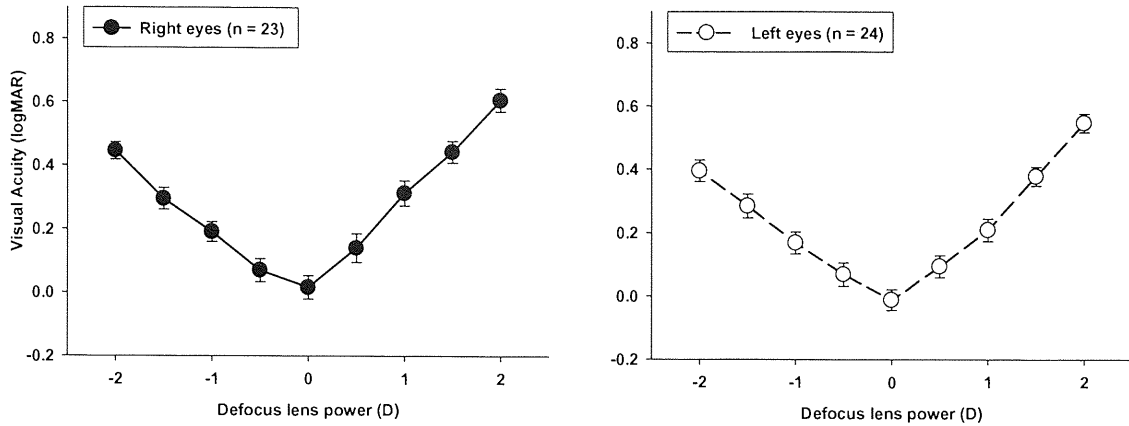


Figure 6.2 Defocus curves for monocular right and left eyes. Shown is the mean visual acuity for each defocus lens used. Error bars represent the standard error of the mean (SEM).

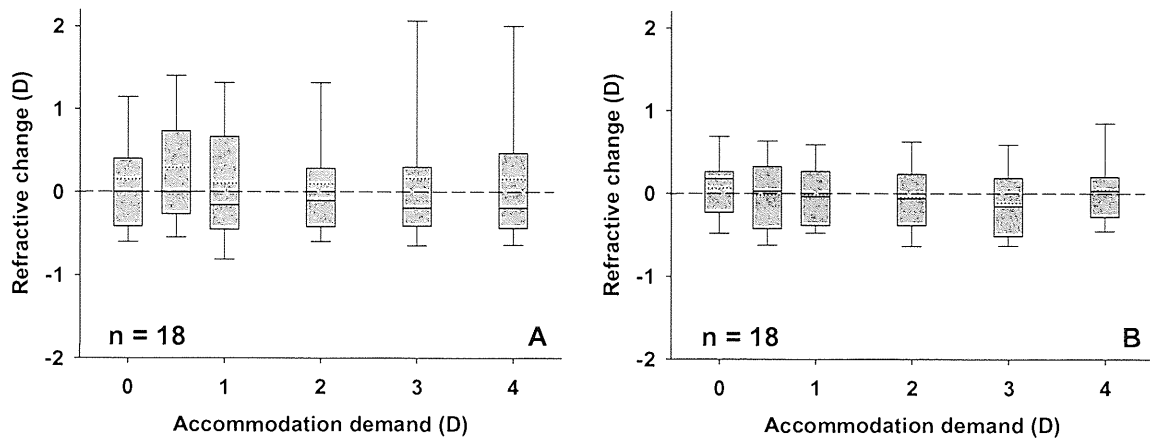


Figure 6.3 Objective accommodation, as measured using the Shin-Nippon *SRW-5000* and a +5.0 D Badal optical system, for monocular right eyes (6.3A) and monocular left eyes (6.3B). The bottom boundary of the box indicates the 25th percentile, the solid line within the box marks the median, and the top boundary of the box indicates the 75th percentile. Error bars above and below the box indicate the 90th and 10th percentiles. The dotted black line within the box indicates the mean value. Data points indicate outliers outside the 95 % confidence interval.

	BCDVA (logMAR)	Distance CS (log units)	DCNVA (logMAR)	Subjective AA (D)
Best Monocular	-0.06 ± 0.11	1.47 ± 0.15	0.51 ± 0.16	1.82 ± 0.63
Average Monocular	0.01 ± 0.15	1.41 ± 0.13	0.56 ± 0.14	1.53 ± 0.64
Average Binocular	-0.04 ± 0.13	1.58 ± 0.11	0.44 ± 0.12	1.88 ± 0.90

Table 6.2 Comparison of binocular and monocular measures of visual function of the Tetraflex KH3500 AIOL (mean ± standard deviation). BCDVA = best corrected distance visual acuity, CS = contrast sensitivity, DCNVA = distance corrected near visual acuity, AA = amplitude of accommodation.

	MSE (D)	BCDVA (logMAR)	Distance CS (log)	DCNVA (logMAR)	Subjective AA (D)	Objective AA (D)
Comparison: 1 month (Wolffsohn et al., 2006b).	0.69 ± 0.72 <i>p</i> < 0.001	-0.05 ± 0.25 <i>p</i> = 0.428	-0.26 ± 0.25 <i>p</i> < 0.001	0.04 ± 0.20 <i>p</i> = 0.408	-1.86 ± 1.72 <i>p</i> < 0.001	-0.19 ± 0.75 <i>p</i> = 0.371
Comparison: 6 months (Wolffsohn et al., 2006b)	-0.30 ± 1.18 <i>p</i> = 0.442	-0.10 ± 0.22 <i>p</i> = 0.801	-0.27 ± 0.15 <i>p</i> < 0.001	-0.05 ± 0.11 <i>p</i> = 0.194	-0.47 ± 1.26 <i>p</i> = 0.270	-0.11 ± 0.24 <i>p</i> = 0.239

Table 6.3 Change in ocular measures from 1 and 6 months (from Wolffsohn et al., 2006b) to 2 years (mean ± standard deviation). MSE = mean spherical equivalent refraction. BCDVA = best corrected distance visual acuity, CS = contrast sensitivity, DCNVA = distance corrected near visual acuity, AA = amplitude of accommodation. Statistical significance is shown as *p* value (ANOVA); *p* < 0.05 is considered statistically significant.

6.3.3 AIOL movement: Optical Coherence Tomography

Of the 29 subjects included in the 2 year follow-up study, only 23 were imaged using the *Visante* AS-OCT due to postural instability. Measurements of IOL position were possible on 14 eyes of 13 subjects. It was not possible to measure the remaining subjects due to difficulty in detecting the AIOL surfaces. Mean movement of the AIOL on accommodation was posteriorly, away from the corneal apex, by 0.01 ± 0.04 mm (mean \pm SD) for a 0.5 D stimulus, 0.02 ± 0.03 mm for a 1.0 D stimulus, 0.01 ± 0.03 mm for a 2.0 D stimulus, 0.02 ± 0.03 mm for a 3.0 D stimulus and 0.02 ± 0.03 mm for a 4.0 D stimulus (Figure 6.4). These changes, however, were not found to be statistically significant ($F_{(4,13)} = 1.19$; $p = 0.33$).

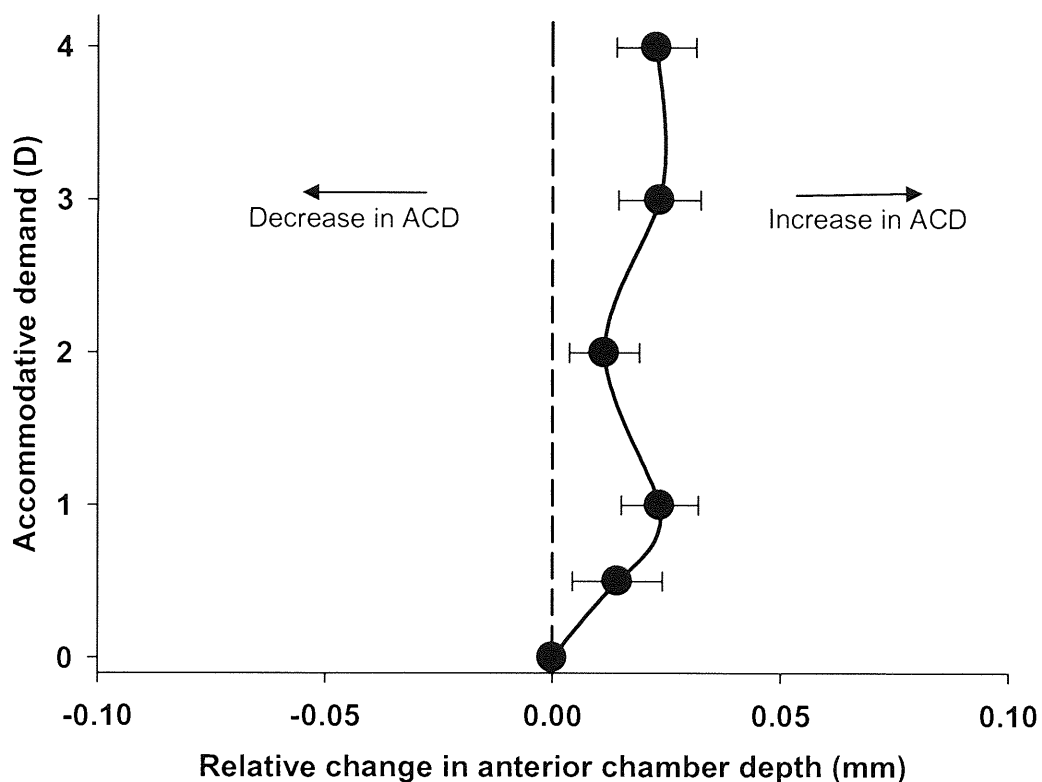


Figure 6.4 Mean shift in IOL position with accommodative demand ($n = 14$ eyes). Error bars represent the standard error of the mean (SEM). Distances are measured from the corneal apex to the IOL anterior surface. Positive shifts represent a deeper anterior chamber and therefore a posterior movement of the IOL.

6.4 Discussion

The Lenstec Kellen *Tetraflex KH3500* AIOL performed generally well at 2 to 3 years post-implantation. The residual subjective refraction was small and best-corrected acuity and contrast sensitivity was good. Newspaper print (~ 0.6 logMAR) could be read by 59% of patients with their best distance correction, improving to 97% with a standard near addition. Binocular visual performance was generally better than monocular results, particularly for contrast sensitivity and BCNVA.

Although the subjective and objective amplitude of accommodation had decreased compared to that measured previously at 1 month post-implantation, some recovery was evident with respect to the decrease seen at 6 months (Wolffsohn *et al.*, 2006b). The 1CU AIOL subjective amplitude of accommodation at 2 years or greater after implantation, has been reported to be both higher (Hancox *et al.*, 2006; Wolffsohn *et al.*, 2006a), but also much lower (Mastropasqua *et al.*, 2007) than this study. Defocus curve translation into the range of clear focus shows that the *Tetraflex* AIOL performs better than the 1CU AIOL if compared on the same criteria (the mean negative sphere that could be overcome to maintain a best corrected distance vision of 0.3 logMAR or greater; 1.53 ± 0.56 D compared to the previously reported 1.09 D; Hancox *et al.*, 2006).

As found previously, subjective defocus curve measures of amplitude of accommodation were lower than those of the push-up assessment (Gupta *et al.*, 2008). Objective amplitude of accommodation, measured at a similar post-operative interval in the 1CU AIOL, was higher than the *Tetraflex* AIOL by approximately 0.3 D (Wolffsohn *et al.*, 2006a); this was still greater than a conventional monofocal IOL (Wolffsohn *et al.*, 2006a). Individual stimulus response curves indicate active eye focus in some individuals and again confirm that previous methods of measuring the difference in refractive power of the eye at only two viewing distances is likely to lead to erroneous objective results (Wolffsohn *et al.*, 2006a; 2006b).

The large disparity between subjective (push-up) and objective (autorefractor) accommodation responses may be explained to some degree by pseudoaccommodation (Langenbucher *et al.*, 2003). Pseudophakic pseudoaccommodation occurs independently of ciliary muscle function-lead accommodative effects. It is caused by static optical features

of the pseudophakic eye such as corneal multifocality and against-the-rule myopic astigmatism. It is also caused by increased depth of field induced by a small pupil; which is augmented by the near vision triad (Nakazawa and Ohtsuki, 1983; Ravalico and Baccara, 1990; Yamamoto and Adachi-Usami, 1992; Fukuyama *et al.*, 1999; Oshika *et al.*, 2002).

Subjective assessments of accommodative amplitude incorporate a patient's blur tolerance (depth of focus; Goss, 1992; Wang and Ciuffreda, 2006). This tolerance is dependent on pupil size as depth of focus is known to be inversely proportional to pupil size (Charman *et al.*, 1978; Sergienko and Tutchenko, 2007). Spherical aberrations are positively correlated to pupil size, which can counteract this effect. Measurement of these features may, retrospectively, have been beneficial in assessing these effects in this study.

The Neodymium-doped Yttrium Aluminium Garnet (Nd:YAG; $Nd:Y_3Al_5O_{12}$) laser capsulotomy rate was similar to, or lower than that reported at 2 or more years after implantation of the 1CU AIOL (Hancox *et al.*, 2006), which has been as high as 100% (Wolffsohn *et al.*, 2006a; Mastropasqua *et al.*, 2007). Hancox and colleagues showed that posterior capsular opacification in eyes implanted with the 1CU AIOL tended to be as a result of lens epithelial cell migration through the optic-haptic junction, which differs in design from the *Tetraflex* IOL (Hancox *et al.*, 2007). The proposed differences in mechanism of action between the *Tetraflex* and 1CU AIOLs may also account for this lower rate. It has been suggested that capsular fibrosis may reduce the movement of a single optic AIOL, reducing the amplitude of accommodation (Hancox *et al.*, 2006) and this has been shown to be improved by Nd:YAG capsulotomy in eyes implanted with the 1CU AIOL (Nguyen *et al.*, 2005). There was no strong support for this hypothesis with the *Tetraflex* AIOL, as although the three eyes of two patients listed for YAG capsulotomy following the study showed an increased in subjective (by $+0.42 \pm 0.46$ D) and objective (by $+0.15 \pm 0.25$ D) amplitude of accommodation, 4 weeks later the range of clear focus decreased (by -0.19 ± 0.13 D).

Although the AS-OCT has been used in evaluating phakic IOLs (Baikoff, 2006; Donoson and Castillo, 2006; Maldonado *et al.*, 2006; Güell, *et al.*, 2007) and post-operative posterior capsular opacification (Moreno-Montañés *et al.*, 2005; Elgohary *et al.*, 2006; Kaluzny, *et al.*, 2006; Moreno-Montañés *et al.*, 2008), its use in quantifying posterior chamber AIOL movement with accommodation has hitherto been limited.

The direction of AIOL shift induced by contraction of the ciliary muscle is still equivocal (Table 6.1). Some authors have observed forward (Legeais *et al.*, 1999; Auffarth *et al.*, 2002; Kchle *et al.*, 2002; Findl *et al.*, 2003; Langenbacher *et al.*, 2003; Findl *et al.*, 2004; Marchini *et al.*, 2004; Sauder *et al.*, 2005; Hancox *et al.*, 2006; Schneider *et al.*, 2006; Stachs *et al.*, 2006) and others backward movements of AIOLs (Auffarth *et al.*, 2002; Koepl *et al.*, 2005). In addition, accommodative movements of conventional IOLs have been observed in both directions (Legeais *et al.*, 1999; Findl *et al.*, 2003; 2004; Muftuoglu *et al.*, 2005; Hancox *et al.*, 2006; Tsorbatzoglou *et al.*, 2006; Marchini *et al.*, 2008)

Findl and colleagues (2003) have suggested that the reason behind the posterior IOL shift in their study was due to the overall size of the AcrySof MA60 (13.0 mm in diameter) being too large for the average capsular bag, which has a mean diameter of 10.4 mm. The Tetraflex AIOL has a central optic portion of 5.75 mm and an overall size of 12.0 mm. Clearly, placement in the capsular bag plays a key role in accommodation-induced AIOL movements. It may be the case that the placement and size of the Tetraflex lens is such that accommodative effort causes a vaulting of the lens, but in the posterior direction, away from the corneal apex.

In the current study, the amount of AIOL shift was small, in the posterior direction (towards the retina) and was not statistically significant. The complete cohort could not be imaged, possibly due to difficulties with *Visante* AS-OCT resolution or patients' media, which caused degradation of image quality; this resulted in an inability to detect one or both AIOL surfaces in a number of the patients. Posterior movement of the AIOL does not correlate with the better visual acuity noted at near (Table 6.2); this phenomenon must therefore be explained by pseudoaccommodation rather than pseudophakic accommodation.

The measurement of IOL curvature and tilt has been shown to be possible using Scheimpflug photographic methods (de Castro *et al.*, 2007). Evaluation of these characteristics is worth considering, as they may also influence accommodative changes; however, this was beyond the scope of the study. Further investigation is required to assess and clarify the relationship between AIOL movements, change in AIOL curvature and accommodation response. However, this cohort does show that the method of action advocated by the lens manufacturers is not occurring in this case.

6.5 Conclusion

The key findings of this chapter are summarised below.

- The *Tetraflex* AIOL allows relatively good simultaneous distance and near visual acuity 2 to 3 years post-implantation, which improves with binocular implantation.
- Higher subjective amplitudes of accommodation (RAF rule and defocus curves) were observed compared to objective accommodation measures; this is likely to be due to pseudoaccommodation.
- Individual stimulus response curves show some active accommodation.
- Subjective amplitudes of accommodation with the *Tetraflex* AIOL, derived from defocus curves, are greater than other reported studies using the *1CU* AIOL (Hancox *et al.*, 2006).
- This is the first known study in which *Visante* AS-OCT has been used to quantify the *Tetraflex* AIOL movements with accommodation.
- A small mean posterior movement of the AIOL was observed with accommodation; this was not statistically significant.
- PCO occurrence was moderate, and less than reported by authors assessing other AIOLs. Nd:YAG capsulotomy rates were similar to or lower than similar studies which have used the *1CU* AIOL (Hancox *et al.*, 2006; Wolffsohn *et al.*, 2006a; Mastropasqua *et al.*, 2007).

The study of AIOLs after 2 or more years implantation is a vital part of medical research. It allows quantification of visual stability and accommodative facility in the long term. The *Tetraflex* lens has been shown to be both visually stable and at least subjectively effective at near. Objective measures and imaging does not corroborate the accommodative mechanism in this lens at the present time. Further work is required to account for the

disparity between subjective and objective amplitudes of accommodation. The assessment of pupil size, aberrometry, corneal multifocality and corneal curvature may clarify the reasons behind the subjective increase in near visual ability. The former measures were attempted in this study, but complete data was not achieved from the whole cohort; this was due to both pupil miosis in an aging cohort and moderate PCO rates.

The *Visante* AS-OCT has been shown to be effective in quantifying AIOL movement with accommodation. Further work with this instrument in large scale studies would advance our understanding of the mechanism of action of these lenses. The measurement of AIOL curvature and tilt is also an important factor which must be considered in future work. Information on PCO rates and AIOL movements with accommodation can be translated to improvements in AIOL design, which will aid manufacturers to attain the ultimate goal of providing effective pseudophakic accommodation.

CHAPTER 7

GENERAL CONCLUSIONS

7.1 General conclusions

The principal theme of this thesis has been the examination of phakic and pseudophakic accommodation. Studies have been conducted into the component contributions to vergence change with accommodation using a method of reverse ray-tracing described by Leary (1981) and Erickson (1984). These methods were applied to a new schematic eye derived from studies using corrected Scheimpflug photographic techniques on a large cohort (Dubbelman and van der Heijde, 2001; Dubbelman *et al.*, 2001; 2002; 2005). Importantly, the model allows alteration of both accommodative stimulus and age.

Currently, ocular component changes with accommodation have been analysed by studying axial distance separation and surface radii variation in terms of real change (mm; Garner and Yap, 1997; Kirschcamp *et al.*, 2004; Strenk *et al.*, 1999; 2004; 2005; Glasser, 2006; Mallen *et al.*, 2006). Little is currently known about vergence changes within the whole ocular system with accommodation. Chapter 2 develops the hypothesis outlined by Kirschcamp and colleagues (2004). Data were presented, which agree with this study, and showed categorically, that alteration in component axial distances have derogatory effects on vergence and output accommodation. The model illustrates that crystalline lens surface radii are solely responsible for the accommodative increase in refractive status. The posterior crystalline lens radius was shown as being far more effective in altering vergence with accommodation (0.9 to 1.4 D/mm) than the associated anterior surface (4.9 to 5.9 D/mm), although the latter contributes more in total to the overall refractive alteration; this is not widely reported in the literature (Kirschcamp *et al.*, 2004). Anterior chamber depth change, despite being opposite and approximately equal to lens thickness changes, had a far higher negative consequence for outcome refraction.

Chapter 2 also highlights the use of the Vergence Contribution Factor; a ratio of vergence change per unit of physical change with accommodation (VCF; D/mm). Consideration of ocular components in this way is new, and emphasises the role of each component in the accommodative response.

Examination of Erickson's work (1984) revealed an interesting phenomenon; that of natural damping. Erickson showed that alteration of axial length (AL) resulted in a disproportionate amount of myopic compared to hyperopic ametropia. The vergence from an elongated vitreous chamber was damped compared to a shorter vitreous. The application of the methods used in Chapter 2 allowed further investigation of this phenomenon, and explored the implications on accommodation. It was initially hypothesised that the myopic damping would effectively reduce the myopic accommodative output.

Chapter 3 confirmed that alterations in AL of the same magnitude of elongation or shortening resulted in asymmetric refractive errors, with a larger outcome refractive error in shorter eyes. The model also confirmed the hyperopic shift in refractive error described in large population based studies (Wang *et al.*, 1994; Attebo *et al.*, 1999). The hypothesis, however, was proven incorrect. Accommodative output in myopic eyes was greater than in hyperopic eyes; this was due to damping of the negative vergence effects associated with accommodative axial component changes. This discovery, along with the confirmation of the hyperopic deviation in refractive error with age, adds a new feature to the theories of accommodation and presbyopia. Further, the study found that the crystalline lens displayed some interesting trends with ametropia and age. These trends altered in magnitude and direction, and can only be explained by the complex interactions of refractive index, thickness magnitude and position; all of which alter with age and accommodation.

Chapter 5 extends the area of research associated with physical biometric changes associated with accommodation. The use of a new technique (*Visante* Anterior Segment Optical Coherence Tomography [AS-OCT]) allows direct observation of the anterior ocular structures under accommodative effort, by employing an internal target which can be defocused. This technique has significant advantages over similar methods (Wolffsohn and Davies, 2007). These include direct (eye under observation) *in vivo* measurement, use of a natural pupil (un-dilated), upright position and high resolution (Richdale *et al.*, 2008). Initial attempts to quantify surface curvatures, using a method enunciated by Dunne *et al.* (2007), proved to have limited success. Use of raw axial distances extracted directly from the *Visante*, proved to be comparable with the Dubbelman model described previously. The only exception was measurement of crystalline lens thickness, which was marginally overestimated; a finding previously discovered by Dunne and colleagues (2007). The

disparity between the Scheimpflug-based model and the *Visante* can be explained to some degree by the examination of the cohort used by Dubbelman and colleagues. The Dubbelman model is based on a cohort of over 100 subjects whose age ranges from 16 to 65 years (mean, 39.2 years old; Dubbelman and van der Heijde, 2001; Dubbelman *et al.*, 2001; 2002); of which an unspecified number lie close to the age of the model used in Chapter 5 (age 19.4 years old, to match the mean age of the cohort recruited). If relative changes in the eye with accommodation were considered, both the *Visante* and Dubbelman data were comparable.

Biometric changes with accommodation were found to be similar to studies which have employed various different methods (Garner and Yap, 1997; Baikoff *et al.*, 2004; Ostrin *et al.*, 2006; Bolz *et al.*, 2007; Tsorbatzoglou *et al.*, 2007; Richdale *et al.*, 2008). The majority of these studies have compared biophysical morphology with changes in accommodative stimulus or following pharmacological stimulation. The study presented in this thesis (Chapter 5) employed accommodative response; arguably a more appropriate correlate than accommodative stimulus.

An interesting discovery was made pertaining to the posterior crystalline lens surface. The surface in question appears to be relatively static in its axial position until approximately 1.5 D of accommodative response (approximately 2.0 D demand), after which it shifts in a posterior direction. Human (Koretz *et al.*, 1997b) and animal (Vilupuru and Glasser, 2005) studies have found an equal and linear change in anterior and posterior portions of the lens with accommodation. Drexler and colleagues (1997) correlated the position of the anterior and posterior poles of the crystalline lens with change in fixation from distance to targets at various closer distances. The results show a static posterior lens surface from distance observation until viewing a target at 40.0 cm (2.5 D stimulus). From this point, closer targets elicit a posterior movement of the surface of just over 0.5 mm for a target at 10.0 cm (10.0 D stimulus); this phenomenon is, however, not alluded to in the text and appears to be relatively new in the study of accommodative lenticular changes.

The use of accommodating intraocular lenses (AIOLs) has seen an increase in scientific interest over recent years (for reviews see Dick, 2005, and Glasser, 2008). The amount of accommodation reported has been shown to vary with AIOL type and measurement technique (Table 1.1; Chapter 1). The most common variety of AIOL in use at the current

time is the single-optic AIOL, which relies on the focus shift principle. Hitherto, axial changes in the ocular components has resulted in negative vergence change with accommodation. The anterior movement of an AIOL has been shown to produce variable refractive outputs (Nawa *et al.*, 2003). To examine this theoretically, Chapter 3 employed the Dubbelman model by effectively implanting the eyes with a single-optic AIOL. The study confirmed that anterior translocation of a spherical intraocular lens along the visual axis of the eye gave rise to a dioptric increase, also known as pseudophakic accommodation. The magnitude of which was dependant on the axial length of the eye and the subsequent power of the IOL to give emmetropia. Eyes with shorter ALs, and subsequently, higher powered IOLs, gave rise to greater pseudophakic accommodation per unit of anterior axial shift.

In Chapter 4, the AIOL was placed in the geometric centre of the capsular bag. As this lens centroid moves posteriorly with age, so did the position of the AIOL. In this posterior location, the AIOL produced larger dioptric changes than in the younger eye with the relatively anteriorly located lens. This was due to the vitreous chamber, which is the primary correlate to vergence change in the absence of the crystalline lens, in opposition to its role in the phakic eye. Chapter 6 discusses the empirical evaluation of implanted AIOLs, and more specifically, the magnitude of their movement with accommodation or pharmacological stimulation. In those studies (Table 6.1), it is seldom that an AIOL exceeds 1.0 mm of anterior shift with accommodation (Auffarth *et al.*, 2002). Considering this, none of the model data exceeds 2.5 D of accommodation, with only the shorter, older eye approaching this figure (age 50 years; 21.267 mm AL; 2.27 D of accommodation for an AIOL shift of 1.0 mm). Chapter 4 does not suggest that shorter eyes would not be able to reach greater amplitudes of pseudophakic accommodation. It is clear, however, that a very long AL would be a contraindication to the successful accommodative outcome in this type of lens.

Chapter 6 also employs the use of the previously described *Visante* AS-OCT. The use of this instrument in quantifying AIOL movement is novel. Mean AIOL movements were found to be small and in the direction of the posterior pole; however, this was not statistically significant ($p = 0.33$). It has been suggested that the reason behind this movement lies in the AIOL being too big for the capsular bag, and that reduction in

capsular bag diameter in conjunction with the natural mechanism of accommodation, causes a vaulting of the lens (Findl *et al.*, 2003); in this case posteriorly.

Chapter 6 is a follow-up study of a previously implanted AIOL (Lenstec *Tetraflex*). It showed that patients had relatively good simultaneous distance and near visual acuity 2 to 3 years post-implantation (best-corrected distance visual acuity [BCDVA]: $+0.04 \pm 0.24$ logMAR; distance-corrected near visual acuity [DCNVA]: $+0.61 \pm 0.17$ logMAR), which improved with binocular implantation (BCDVA: -0.04 ± 0.13 logMAR; DCNVA: 0.44 ± 0.12 logMAR). As shown in other studies, higher subjective amplitudes of accommodation were observed compared to objective accommodation measures. Principally, this can be explained by pseudoaccommodation (Langenbacher *et al.*, 2003). It consists of static optical features of the pseudophakic eye such as corneal multifocality, against-the-rule myopic astigmatism, and increased depth of field induced by a small pupil (Nakazawa and Ohtsuki, 1983; Ravalico and Baccara, 1990; Yamamoto and Adachi-Usami, 1992; Fukuyama *et al.*, 1999; Oshika *et al.*, 2002). Some individuals displayed some active objective accommodation; however, mean objective response was low. The occurrence of posterior capsular opacification was moderate, and less than, or similar to, those reported by authors assessing other AIOLS (Hancox *et al.*, 2006; Wolffsohn *et al.*, 2006b; Mastropasqua *et al.*, 2007).

7.2 Analysis of experimental work: suggestions for improvement

The main instrument used in the latter part of this thesis was the *Visante* AS-OCT. The current version of this instrument (version 1.0.12.1896) does not provide a measure of surface curvature. Baikoff *et al.* (2004) provides some measure of horizontal anterior crystalline lens radius, but the methodology used is not clear. Chapter 5 utilised a system described by Dunne and co-authors (2007) to measure coordinates of corneal and lens surfaces, and to convert these mathematically using ray-tracing, into measures of surface radii. After the employment of much time, it was discovered that this system was not applicable to the phakic cohort, and correctional formulae were subsequently suggested (see Chapter 5). Further problems were discovered due to the resolution of the AS-OCT image. Distinct difficulties were found in Chapters 5 and 6 in the detection of some ocular surfaces; more often the posterior crystalline or intraocular lens surface. Intuitively, the clarity of the patients' media may have had some influence on this factor to some degree. The use of ultrahigh resolution OCT, or the use of more complex surface and edge detection software, may help to resolve this issue in future studies.

A large disparity was discovered between subjective and objective measures of pseudophakic amplitude of accommodation (Chapter 6); this has been attributed to pseudoaccommodation (Langenbacher *et al.*, 2003). Many authors have credited a number of different properties of the eye to this phenomenon. To explain some or all of the pseudoaccommodative discrepancy, the study in Chapter 6 employed the measurement of aberrations using a commercially available aberrometer. Acquisition of these data was not possible on a large number of the cohort. Essentially, this was due to problems with measuring aberrations through miotic pupils, with the added disadvantage of posterior capsule opacification (PCO). The use of bespoke instrumentation and software that enables calculation of aberrations over a small pupil area would be advantageous in future studies. Further, the examination of IOL curvature and tilt has been shown to be possible using Scheimpflug photographic methods (de Castro *et al.*, 2007). Evaluation of these characteristics is worth considering, as they may also influence accommodative changes. Further investigation is required to assess and clarify the relationship between AIOL movements, change in AIOL curvature and accommodation response.

7.3 Concluding statement

Collectively, the investigations discussed in this thesis explore the characteristics of human phakic and pseudophakic accommodation, providing novel information about vergence and biometric changes associated with the accommodative reflex. The findings of this work support and develop the findings of previous studies (Nawa *et al.*, 2003; Kirschcamp *et al.*, 2004; Baikoff *et al.*, 2004; Richdale *et al.*, 2008). These conclusions are important in continuing the advancement of our knowledge of the accommodative mechanism, and in providing the ultimate goal of restoring functional near vision in the ageing eye. Evidence is provided that supports current work in this field, and continues to highlight the research areas required to improve our current technologies for the correction of pseudophakic presbyopia.

This thesis, with the preceding and concurrent literature in this area, has merely begun to explore this complex field of research. Much work in this discipline remains to be done. With new methods of understanding accommodation, and new ways to mimic its function in the pseudophakic eye under constant development, research into phakic and pseudophakic accommodation continues to be both exciting and perplexing.

REFERENCES

- Agarwal, L.P., Narsimhan, E.C., & Mohan, M. (1967). Experimental lens refilling. *Orient Arch Ophthalmol*, 76, 596-598.
- Al-Ahdali, L.H., & El-Messiery, M.A. (1995). Examination of the effect of the fibrous structure of the lens on the optical characteristics of the human eye: A computer-simulated model. *Applied Optics*, 32 (25), 5738.
- Alió, J., Rodriguez-Prats, J. L., Galal, A. (2006). Advances in microincision cataract surgery intraocular lenses *Curr Opin Ophthalmol*, 17, 80-93.
- Alió, J.L., Tavolato, M., De la Hoz, F., Claramonte, P., Rodríguez-Prats, J.L., & Galal, A. (2004). Near vision restoration with refractive lens exchange and pseudoaccommodating and multifocal refractive and diffractive intraocular lenses: comparative clinical study. *J Cataract Refract Surg*, 30 (12), 2494-2503.
- Allen, D., Vasavada, A. (2006). Cataract and surgery for cataract. *British Medical Journal*, 333, 128-132.
- Allen, P.M., & O'Leary, D.J. (2006). Accommodation functions: co-dependency and relationship to refractive error. *Vision Res*, 46 (4), 491-505.
- Alpar, J.J. (1986). On-the-table posterior capsulotomy and 1% sodium hyaluronate. *J Cataract Refract Surg*, 12, 391-393.
- Alpern, M., & David, H. (1958). Effects of illuminance quantity on accommodation of the eyes. *Indust Med Surg*, 27, 551-555.
- Apple, D.J., Mamalis, N., Lofffield, K., Googe, J.M., Novak, L.C., Kavka-Van Norman, D., Brady, S.E., & Olson, R.J. (1984). Complications of intraocular lenses. A historical and histopathological review. *Surv Ophthalmol*, 29, 1-54.

- Armaly, M., & Rubin, M. (1961). Accommodation and applanation tonometry. *Arch Ophthalmol*, 65, 415-423.
- Atchison, D.A., Claydon, C.A., & Irwin, S.E. (1994). Amplitude of accommodation for different head positions and different directions of eye gaze. *Optom Vis Sci*, 71 (5), 339-345.
- Atchison, D.A. (1995). Accommodation and presbyopia. *Ophthalmic and Physiological Optics*, 15, 255-272.
- Atchison, D.A. (2006). Optical models for human myopic eyes. *Vision Res*, 46 (14), 2236-2250.
- Attebo, K., Ivers, R.Q., & Mitchell, P. (1999). Refractive errors in an older population: the Blue Mountains Eye Study. *Ophthalmology*, 106 (6), 1066-1072.
- Auffarth, G.U., Martin, M., Fuchs, H.A., Rabsilber, T.M., Becker, K.A., & Schmack, I. (2002). Validity of anterior chamber depth measurements for the evaluation of accommodation after implantation of an accommodative Humanoptics 1CU intraocular lens. *Ophthalmologe*, 99 (11), 815-819.
- Bacskulin, A., Bergmann, U., Horóczy, Z., & Guthoff, R. (1995). Continuous ultrasound biomicroscopic imaging of accommodative changes in the human ciliary body. *Klin Monatsbl Augenheilkd.*, 207 (4), 247-252.
- Bacskulin, A., Gast, R., Bergmann, U., & Guthoff, R. (1996). Ultrasound biomicroscopy imaging of accommodative configuration changes in the presbyopic ciliary body. *Ophthalmologe*. 1996 Apr;93(2):199-203, 93 (2), 199-203.
- Baikoff, G., Lutun, E., Ferraz, C., & Wei, J. (2004). Static and dynamic analysis of the anterior segment with optical coherence tomography. *J Cataract Refract Surg*, 30 (9), 1843-1850.

- Baikoff, G., Lutun, E., Ferraz, C., & Wei, J. (2005a). Analysis of the eye's anterior segment with optical coherence tomography. Static and dynamic study. *J Fr Ophthalmol*, 28 (4), 343-352.
- Baikoff, G., Lutun, E., Wei, J., & Ferraz, C. (2005b). An in vivo OCT study of human natural accommodation in a 19-year-old albino. *J Fr Ophthalmol*, 28 (5), 514-519.
- Baikoff, G. (2006). Anterior segment OCT and phakic intraocular lenses: a perspective. *J Cataract Refract Surg*, 32 (11), 1827-1835.
- Bakaraju, R.C., Ehrmann, K., Papas, E., & Ho, A. (2008). Finite schematic eye models and their accuracy to in-vivo data. *Vision Res*, 48 (16), 1681-1694.
- Barry, J.C., Dunne, M.C.M., & Kirschkamp, T. (2001). Phakometric measurement of ocular surface radius of curvature and alignment: evaluation of method with model eyes. *Ophthalmic and Physiol Opt*, 21 (6), 450-460.
- Bauerberg, J.M. (1999). Centred vs inferior off-center ablation to correct hyperopia and presbyopia. *J Refract Surg*, 15, 66-69.
- Beauchamp, R., & Mitchell, B. (1985). Ultrasound measures of vitreous chamber depth during ocular accommodation. *Am J Optom Physiol Opt*, 62 (8), 523-532.
- Beers, P., Van der Heijde, G.L. (1994a). Presbyopia and velocity of sound in the lens. *Optom Vis Sci*, 71, 250-253.
- Beers, A.P.A., & Van der Heijde, G.L. (1994b). In vivo determination of the biomechanical properties of the component elements of the accommodation mechanism. *Vision Res*, 34, 2897-2905.
- Beers, P., Van der Heijde, G.L. (1996). Age-related changes in the accommodation mechanism. *Optom Vis Sci*, 73, 235-242

- Beiko, G. (2007). Status of accommodative intraocular lenses. *Curr Opin Ophthalmol*, 18 (1), 74-79.
- Ben-Nun, J., & Alió, J.L. (2005). Feasibility and development of a high-power real accommodating intraocular lens. *J Cataract Refract Surg*, 31 (9), 1802-1808.
- Ben-Nun, J. (2006). The NuLens accommodating intraocular lens. *Ophthalmol Clin North Am*, 19 (1), 129-134.
- Bennett, A.G. (1988). A method of determining the equivalent powers of the eye and its crystalline lens without resort to phakometry. *Ophthalmic Physiol Opt*, 8 (1), 53-59.
- Bennett, A.G., Rabbetts, R. B. (2007). *Clinical Visual Optics*, 4th edn. (Philadelphia, USA): Butterworth Heinemann.
- Binkhorst, C.D. (1962). Use of the papillary lens (iris clip lens) in aphakia. Our experiences based on the first fifty implantations. *Br J Ophthalmol*, 46, 343.
- Bito, L.Z., & Miranda, O.C. (1989). Accommodation and presbyopia. *Ophthalmology Annual* (pp. 103-128). New York, USA: Raven.
- Blaker, J.W. (1980). Toward an adaptive model of the human eye. *J Opt Soc Am*, 70 (2), 220-223.
- Blumenthal, M., Ashkenazi, I., Assia, E., Cahane, M. (1992). Small-incision manual extracapsular cataract extraction using selective hydrodissection. *Ophthalmic Surgery* 23, 699-701.
- Bolz, M., Prinz, A., Drexler, W., & Findl, O. (2007). Linear relationship of refractive and biometric lenticular changes during accommodation in emmetropic and myopic eyes. *Br J Ophthalmol*, 91, 360-365.
- Breinin, G.M., & Chin, N.B. (1973). Accommodation, convergence and aging. *Doc Ophthalmol*, 34, 109-121.

- Brown, N.P. (1973). The change in shape and internal form of the lens of the eye on accommodation. *Exp Eye Research*, 15, 441-459.
- Brown, N.P. (1974). The shape of the lens equator. *Exp Eye Research*, 19, 571-576.
- Bruce, A.S., Atchison, D.A., & Bhoola, H. (1995). Accommodation-convergence relationships and age. *Invest Ophthalmol Vis Sci*, 36, 406-413.
- Buehren, T., Collins, M., Loughridge, J., Carney, L., & Iskander, D. (2003). Corneal topography and accommodation. *Cornea*, 22, 311-316.
- Bullimore, M., & Gilmartin, B. (1987). Tonic accommodation, cognitive demand, and ciliary muscle innervation. *Am J Optom Physiol Opt.*, 64 (1), 45-50.
- Bullimore, M., & Gilmartin, B. (1988). The accommodative response, refractive error and mental effort: 1. The sympathetic nervous system. *Doc Ophthalmol.*, 69 (4), 385-397.
- Campbell, F.W. (1954). The minimum quantity of light required to elicit the accommodation reflex in man. *J Physiol*, 123 (2), 357-366.
- Campbell, F.W., & Westheimer, G. (1960). Dynamics of the focussing response of the human eye. *J Physiol*, 151, 285-295.
- Canny, J.F. (1986). A computational approach to edge detection. . *IEEE Trans. Pattern Analysis and Machine Intelligence*, 8 (6), 679-698.
- Cervino, A., Hosking, S.L., & Dunne, M.C.M. (2007). Operator induced errors in Hartmann-Shack wavefront sensing: model eye study. *J Cataract Refract Surg*, 33 (1), 115-121.
- Charman, W.N., Jennings, J.A., & Whitefoot, H. (1978). The refraction of the eye in the relation to spherical aberration and pupil size. *Br J Physiol Opt*, 32, 78-93.

- Charman, W.N. (1986). Static accommodation and the minimum angle of resolution. *Am J Optom Physiol Opt*, 63 (11), 915-921.
- Charman, W.N., & Heron, G. (1988). Fluctuations in accommodation: a review. *Ophthalmic and Physiol Opt*, 8 (2), 153-164.
- Charman, W.N. (2000). Accommodation and the through-focus changes of the retinal image. In: O. Franzén, H. Richter, & L. Stark (Eds.), *Accommodation and Vergence Mechanisms in the Visual System* (pp. 115-127). Basel: Birkhäuser Verlag.
- Charman, W.N. (2008). The eye in focus: accommodation and presbyopia. *Clin Exp Optom*, 91 (3), 207-225.
- Chen, L., Kruger, P.B., Hofer, H., Singer, B., & Williams, D.R. (2006). Accommodation with higher-order monochromatic aberrations corrected with adaptive optics. *J Opt Soc Am A*, 23, 1-8.
- Cheng, A.C., Rao, S.K., Lau, S., Leung, C.K., & Lam, D.S. (2008). Central corneal thickness measurements by ultrasound, Orbscan II, and Visante OCT after LASIK for myopia. *J Refract Surg*, 24 (4), 361-365.
- Cheng, C.L., & Tan, D.T.H. (1999). Lamellar corneal autograft for corneal perforation. *Australian and New Zealand J Ophthalmol*, 27 (437-439)
- Ciuffreda, K.J., Hokoda, S.C., Hung, G.K., & Semmlow, J.L. (1984). Accommodative stimulus/response function in human amblyopia. *Doc Ophthalmol*, 56 (4), 303-326.
- Ciuffreda, K. (1991). Accommodation and its anomalies. *Vision and Visual Dysfunction*, Vol 1 (p. 231). London, UK: Macmillan Press.
- Ciuffreda, K.J., & Wallis, D.M. (1998). Myopes show increased susceptibility to nearwork aftereffects. *Invest Ophthalmol Vis Sci*, 39 (10), 1797-1803.

Ciuffreda, K.J., & Lee, M. (2002). Differential refractive susceptibility to sustained nearwork. *Ophthalmic Physiol Opt*, 22 (5), 372-379.

Claoué, C. (2004). Functional vision after cataract removal with multifocal and accommodating intraocular lens implantation: prospective comparative evaluation of Array multifocal and 1CU accommodating lenses. *J Cataract Refract Surg*, 30 (10), 2088-2091.

Cogan, D.G. (1937). Accommodation and the autonomic nervous system. *Arch Ophthalmol*, 18, 739-766.

Coleman, D. (1970). Unified model for accommodative mechanism. *Am J Ophthalmol*, 69 (6), 1063-1079.

Coleman, D.J. (1986). On the hydrolic suspension theory of accommodation. *Trans Am Ophthalmol Soc*, 84, 846-868.

Coleman, D.J., & Fish, S.K. (2001). Presbyopia, accommodation, and the mature catenary. *Ophthalmology*, 108 (9), 1544-1551.

Cook, C.A., Koretz, J.F., & Kaufman, P.L. (1991). Age-dependent and accommodation dependent increases in sharpness of human crystalline lens curvatures. *Invest Ophthalmol Vis Sci*, 32, 358.

Cook, C.A., Koretz, J.F., Pfahnl, A., Hyun, J., & Kaufman, P.L. (1994). Aging of the human crystalline lens and anterior segment *Vision Res*, 34, 2945-2954.

Cramer, A. (1853). The accommodative ability of the eyes. (Haarlem, The Netherlands): De Erven Loosjes.

Cumming, J.S., Slade, S.G., Chayet, A., & AT-45 Study Group (2001). Clinical evaluation of the model AT-45 silicone accommodating intraocular lens: results of feasibility and the initial phase of a Food and Drug Administration clinical trial. *Ophthalmology*, 108 (11), 2005-2009.

Dang Burgener, N.P., Cottet, L., & Dosso, A.A. (2008). Evaluation of the anterior chamber depth after cataract surgery with OCT Visante. *Klin Monatsbl Augenheilkd*, 225 (5), 438-440.

Davies, L.N., Mallen, E.A., Wolffsohn, J.S., & Gilmartin, B. (2003). Clinical evaluation of the Shin-Nippon NVision-K 5001/Grand Seiko WR-5100K autorefractor. *Optom Vis Sci*, 80 (4), 320-324.

Davies, L.N., Wolffsohn, J.S., & Gilmartin, B. (2005). Cognition, ocular accommodation, and cardiovascular function in emmetropes and late-onset myopes. *Invest Ophthalmol Vis Sci*, 46 (5), 1791-1796.

Davies, L.N., Wolffsohn, J.S., & Naroo, S. (2006). The intraocular lens (IOL): A brief history of surgical procedures and IOL technology. *Optician*, 232, 26-28.

Dawczynski, J., Koenigsdoerffer, E., Augsten, R., & Strobel, J. (2007). Anterior optical coherence tomography: a non-contact technique for anterior chamber evaluation. *Graefes Arch Clin Exp Ophthalmol*, 245 (3), 423-425.

de Castro, A., Rosales, P., & Marcos, S. (2007). Tilt and decentration of intraocular lenses in vivo from Purkinje and Scheimpflug imaging. Validation study. *J Cataract Refract Surg*, 33 (3), 418-429.

de Vries, F.R., Van der Heijde, G.L., & Goovaerts, H.G. (1987). System for continuous high-resolution measurement of distances in the eye. *J Biomed Eng*, 9, 32-37.

Descartes, R. (1677). *Traite' de l'homme*.

Dick, H.B. (2005). Accommodative intraocular lenses: current status. *Curr Opin Ophthalmol*, 16, 8-26.

Dick, H.B., & Dell, S. (2006). Single optic accommodative intraocular lenses. *Ophthalmol Clin North Am*, 19 (1), 107-124.

- Doane, J.F., & Jackson, R.T. (2007). Accommodative intraocular lenses: considerations on use, function and design. *Curr Opin Ophthalmol*, 18, 318-324.
- Dogru, M., Honda, R., Omoto, M., Toda, I., Fujishima, H., Arai, H., Matsuyama, M., Nishijima, S., Hida, Y., Yagi, Y., & Tsubota, K. (2005). Early visual results with the 1CU accommodating intraocular lens. *J Cataract Refract Surg*, 31 (5), 895-902.
- Donders, F.C. (1864). On the anomalies of accommodation and refraction of the eye: with a preliminary essay on physiological dioptrics. (London: The New Sydenham Society).
- Donoso, R., & Castillo, P. (2006). Correction of high myopia with the PRL phakic intraocular lens. *J Cataract Refract Surg*, 32 (8), 1296-1300.
- Douthwaite, W.A. (1995). EyeSys corneal topography measurement applied to calibrated ellipsoidal convex surfaces. *Br J Ophthalmol*, 79 (9), 797-801.
- Drasdo, N., & Fowler, C.W. (1974). Non-linear projection of the retinal image in a wide-angle schematic eye. *Br J Ophthalmol*, 58 (8), 709-714.
- Drexler, W., Baumgartner, A., Findl, O., Hitzenberger, C., & Fercher, A. (1997). Biometric investigation of changes in the anterior eye segment during accommodation. *Vision Res*, 37, 2789-2800.
- Drexler, W., Findl, O., Schmetterer, L., Hitzenberger, C.K., & Fercher, A.F. (1998). Eye elongation during accommodation in humans: differences between emmetropes and myopes. *Invest Ophthalmol Vis Sci*, 39 (11), 2140-2147.
- Duane, A. (1922). Studies in monocular and binocular accommodation with their clinical applications. *Am J Ophthalmol*, 5, 865-877.
- Duane, A. (1925). Are the current theories of accommodation correct? *Am J Ophthalmol*, 8, 196-202.

Dubbelman, M., & Van der Heijde, G.L. (2001). The shape of the aging human lens: curvature, equivalent refractive index and the lens paradox. *Vision Res*, 41 (14), 1867-1877.

Dubbelman, M., Van der Heijde, G.L., & Weeber, H.A. (2001). The thickness of the aging human lens obtained from corrected Scheimpflug images. *Optom Vis Sci*, 78 (6), 411-416.

Dubbelman, M., Weeber, H.A., van der Heijde, R.G., & Völker-Dieben, H.J. (2002). Radius and asphericity of the posterior corneal surface determined by corrected Scheimpflug photography. *Acta Ophthalmologica Scand.*, 80 (4), 379-383.

Dubbelman, M., Van der Heijde, G.L., Weeber, H.A., & Vrensen, G.F. (2003). Changes in the internal structure of the human crystalline lens with age and accommodation. *Vision Res*, 43 (22), 2363-2375.

Dubbelman, M., Van der Heijde, G.L., & Weeber, H.A. (2005). Change in shape of the aging human crystalline lens with accommodation. *Vision Res*, 45 (1), 117-132.

Dunne, M.C.M. (1995). A computing scheme for determination of retinal contour from peripheral refraction, keratometry and A-scan ultrasonography. *Ophthalmic and Physiol Opt*, 15 (2), 133-143.

Dunne, M.C.M., Davies, L.N., & Wolffsohn, J.S. (2007). Accuracy of cornea and lens biometry using anterior segment optical coherence tomography. *J Biomed Opt*, 12 (6)

Elgohary, M.A., Chauhan, D.S., & Dowler, J.G. (2006). Optical coherence tomography of intraocular lens implants and their relationship to the posterior capsule: a pilot study comparing a hydrophobic acrylic to a plate-haptic silicone type. *Ophthalmic Res*, 38 (3), 116-124.

Emsley, H.H. (1952). Visual optics, 5th edn. Vol 1 (Butterworths).

Erickson, P. (1984). Complete ocular component analysis by vergence contribution. *Am J Optom Physiol Opt*, 61 (7), 469-472.

Erie, J.C., Raecker, M. A., Baratz, K. H., Schleck, C. D., Burke, J. P., Robertson, D. M. (2006). Risk of retinal detachment after cataract extraction, 1980-2004: a population-based study. *Ophthalmology*, 113 (11), 2026-2032.

Escudero-Sanz, I., & Navarro, R. (1999). Off-axis aberrations of a wide-angle schematic eye model. *J Opt Soc Am A Opt Image Sci Vis*, 16 (8), 1881-1891.

Eskridge, J.B. (1983). The AC/A ratio and age - a longitudinal study. *Am J Optom Physiol*, 60, 911-913.

Farnsworth, P.N., & Shyne, S.E. (1979). Anterior zonular shifts with age. *Exp Eye Research*, 28 (291-7)

Fincham, E.F. (1924-5). The changes in the form of the crystalline lens in accommodation. *Trans Opt Soc Great Britain*, 24, 239-269.

Fincham, E.F. (1937). The mechanism of accommodation. *Br J Ophthalmol*, 8, 5-80.

Fincham, E.F., & Walton, J. (1957). The reciprocal actions of accommodation and convergence. *J Physiol (Lond.)*, 137, 488-508.

Findl, O., Kiss, B., Petternel, V., Menapace, R., Georgopoulos, M., Rainer, G., & Drexler, W. (2003). Intraocular lens movement caused by ciliary muscle contraction. *J Cataract Refract Surg*, 29 (4), 669-676.

Findl, O., Kriechbaum, K., Menapace, R., Koepl, C., Sacu, S., Wirtitsch, M., Buehl, W., & Drexler, W. (2004). Laserinterferometric assessment of pilocarpine-induced movement of an accommodating intraocular lens: a randomized trial. *Ophthalmology*, 111 (8), 1515-1521.

Findl, O. (2005). Intraocular lenses for restoring accommodation: hope and reality. *J Refract Surg*, 21, 321-323.

- Findl, O., & Leydolt, C. (2007). Meta-analysis of accommodating intraocular lenses. *J Cataract Refract Surg*, 33 (3), 522-527.
- Fine, I.H. (1992). Cortical cleaving hydrodissection. *J Cataract Refract Surg.*, 18, 508-512.
- Fisher, R.F. (1977). The force of contraction of the human ciliary muscle during accommodation. *J Physiol (Lond.)*, 270, 51-74.
- Fisher, R.F. (1977). The force of contraction of the human ciliary muscle during accommodation. *J Physiol*, 270 (1), 51-74.
- Fisher, R.F. (1988). The mechanics of accommodation in relation to presbyopia. *Eye*, 2 (Pt 6), 646-649.
- Fledelius, H.C. (1997). Ultrasound in ophthalmology. *Ultrasound Med Biol*, 23 (3), 365-375.
- Francis, E.L., Jiang, B.C., Owens, D.A., & Tyrrell, R.A. (2003). Accommodation and vergence require effort-to-see. *Optom Vis Sci*, 80 (6), 467-473.
- Fry, G.A. (1959). The effect of age on the ACA ratio. *Am J Optom Arch Am Acad Optom*, 36, 299-303.
- Fukuyama, M., Oshika, T., Amano, S., & Yoshitomi, F. (1999). Relationship between apparent accommodation and corneal multifocality in pseudophakic eyes. *Ophthalmology*, 106 (6), 1178-1181.
- Garner, L.F., & Smith, G. (1997). Changes in equivalent and gradient refractive index of the crystalline lens with accommodation. *Optom Vis Sci*, 74 (2), 114-119.
- Garner, L.F., & Yap, M.K. (1997). Changes in ocular dimensions and refraction with accommodation. *Ophthalmic and Physiol Opt*, 17 (1), 12-17.
- Gilmartin, B. (1986). A review of the role of sympathetic innervation of the ciliary muscle in ocular accommodation. *Ophthalmic and Physiol Opt*, 6 (1), 23-37.

- Gilmartin, B., Bullimore, M.A., Rosenfield, M., Winn, B., & Owens, H. (1992). Pharmacological effects on accommodative adaptation. *Optom Vis Sci*, 69 (4), 276-282.
- Gilmartin, B. (1995). The aetiology of presbyopia: a summary of the role of lenticular and extralenticular structures. *Ophthalmic Physiol Opt*, 15, 431-437.
- Gilmartin, B. (1998). Autonomic correlates of near-vision in emmetropia and myopia. In: B. Gilmartin, & M. Rosenfield (Eds.), *Myopia and Nearwork* (pp. 117-146). Oxford, UK: Butterworth-Heinemann.
- Gimbel, H., & Neuhann, T. (1990). Development, advantages and methods of continuous circular capsulorrhexis techniques. *J Cataract Refract Surg*, 16, 31-37.
- Gindi, J.J., Wan, W.L., & Schanzlin, D.J. (1985). Endocapsular cataract. surgery. I. Surgical technique. *Cataract*, 2, 6-10.
- Glasser, A., Campbell, MC. (1998). Presbyopia and the optical changes in the human crystalline lens with age. *Vision Res*, 38, 209-229.
- Glasser, A., & Campbell, M.C.W. (1999). Biometric, optical and physical changes in the isolated human crystalline lens with age in relation to presbyopia. *Vision Res*, 39, 1991-2015.
- Glasser, A., & Kaufman, P. (1999). The mechanism of accommodation in primates. *Ophthalmology*, 106, 863-872.
- Glasser, A., Croft, M.A., & Kaufman, P.L. (2001). Aging of the human crystalline lens and presbyopia. *Int Ophthalmol Clin*, 41, 1-15.
- Glasser, A. (2006). Restoration of accommodation. *Curr Opin Ophthalmol.*, 17, 12-18.
- Glasser, A., Wendt, M., & Ostrin, L. (2006). Accommodative changes in lens diameter in rhesus monkeys. *Invest Ophthalmol Vis Sci*, 47, 278.

Glasser, A. (2008). Restoration of accommodation: surgical options for correction of presbyopia. *Clin Exp Optom.*, 91 (3), 279-295.

Goldsmith, J.A., Li, Y., Chalita, M.R., Westphal, V., Patil, C.A., Rollins, A.M., Izatt, J.A., & Huang, D. (2005). Anterior chamber width measurement by high-speed optical coherence tomography. *Ophthalmology*, 112 (2), 238-244.

Goncharov, A.V., & Dainty, C. (2007). Wide-field schematic eye models with gradient-index lens. *J Opt Soc Am A Opt Image Sci Vis*, 24 (8), 2157-2174.

Goss, D.A. (1992). Clinical accommodation testing. *Curr Opin Ophthalmol*, 3 (1), 78-82.

Gray, P.J., & Lyall, M.G. (1992). Diffractive multifocal intraocular lens implants for unilateral cataracts in prepresbyopic patients. *Br J Ophthalmol*, 76 (7), 336-337.

Güell, J.L., Morral, M., Gris, O., Gaytan, J., Sisquella, M., & Manero, F. (2007). Evaluation of Verisyse and Artiflex phakic intraocular lenses during accommodation using Visante optical coherence tomography. *J Cataract Refract Surg*, 33 (8), 1398-1404.

Gullstrand von, A. (1909). Appendix II and IV. Mechanism of accommodation. [Translated from the third German edition]. In: H. Helmholtz von (Ed.) *Handbuck der Physiologischen Optik*, Vol 1 (pp. 301-358, 382-415): Optical Society of America.

Gullstrand von, A. (1924). Appendix IV. Mechanism of accommodation. [Translated from the third German edition]. In: H. Helmholtz von (Ed.) *Handbuck der Physiologischen Optik*, 1 (pp. 382-415): Optical Society of America.

Gupta, N., Naroo, S.A., & Wolffsohn, J.S. (2007). Is randomisation necessary for measuring defocus curves in pre-presbyopes? *Cont Lens Anterior Eye*, 30 (2), 119-124.

Gupta, N., Wolffsohn, J.S., & Naroo, S.A. (2008). Optimizing measurement of subjective amplitude of accommodation with defocus curves. *J Cataract Refract Surg*, 34 (8), 1329-1338.

Gwiazda, J., Thorn, F., Bauer, J., & Held, R. (1983). Myopic children show insufficient accommodative response to blur. *Invest Ophthalmol Vis Sci*, 34, 690-694.

Gwiazda, J., Thorn, F., Bauer, J., & Held, R. (1993). Myopic children show insufficient accommodative response to blur. *Invest Ophthalmol Vis Sci*, 34, 690-694.

Gwiazda, J., Bauer, J., Thorn, F., & Held, R. (1995). Shifts in tonic accommodation after near work are related to refractive errors in children. *Ophthalmic Physiol Opt*, 15 (2), 93-97.

Gwiazda, J., Grice, K., & Thorn, F. (1999). Response AC/A ratios are elevated in myopic children. *Ophthalmic and Physiol Opt*, 19 (2), 173-179.

Haefliger, E., Parel, J.M., Fantes, F., Norton, E.W., Anderson, D.R., Forster, R.K., Hernandez, E., & Feuer, W.J. (1987). Accommodation of an endocapsular silicone lens (Phaco-Ersatz) in the nonhuman primate. *Ophthalmology*, 94 (5), 471-477.

Haeliger, E., & Parel, J.M. (1994). Accommodation of an endocapsular silicone lens (Phaco-Ersatz) in the aging rhesus monkey. *J Refract Corneal Surg*, 10 (5), 550-555.

Hancox, J., Spalton, D., Heatley, C., Jayaram, H., & Marshall, J. (2006). Objective measurement of intraocular lens movement and dioptric change with a focus shift accommodating intraocular lens. *J Cataract Refract Surg*, (32), 7.

Hancox, J., Spalton, D., Heatley, C., Jayaram, H., Yip, J., Boyce, J., & Marshall, J. (2007). Fellow-eye comparison of posterior capsule opacification rates after implantation of ICU accommodating and AcrySof MA30 monofocal intraocular lenses. *J Cataract Refract Surg*, 33 (3), 413-417.

Hara, T., Hara, T., Yasuda, A., & Yamada, Y. (1990). Accommodative intraocular lens with spring action. Part 1. Design and placement in an excised animal eye. *Ophthalmic Surg*, 21 (2), 128-133.

- Harman, F.E., Maling, S., Kampougeris, G., Langan, L., Khan, I., Lee, N., & Bloom, P.A. (2008). Comparing the 1CU accommodative, multifocal, and monofocal intraocular lenses: a randomized trial. *Ophthalmology*, *115* (6), 993-1001.
- He, J., Gwiazda, J., Thorn, F., Held, R., & Huang, W. (2003). Change in corneal shape and corneal wavefront aberrations with accommodation. *J Vision*, *3*, 456-463.
- Heath, G.G. (1956). Components of accommodation. *Am J Optom Arch Am Acad Optom*, *33* (11), 569-579.
- Hecht, E. (1987). *Optics* 2nd Ed. (Addison Wesley).
- Helmholtz von, H.H. (1855). Uber die akkommodation des auges. *Graefes Arch Clin Exp Ophthalmol.*, *1*, 1-74.
- Helmholtz von, H.H. (1909). *Handbuch der Physiologischen Optik*. Vol 1, 3rd edn. (English Translation edited by J.P. Southall, Optical Society of America, 1924).
- Hemenger, R.P., Garner, L.F., & Ooi, C.S. (1995). Change with age of the refractive index gradient of the human ocular lens. *Invest Ophthalmol Vis Sci*, *36* (703-707)
- Hermans, E., Pouwels, P., Dubbelman, M., Kuijjer, J., van der Heijde, R., & Heethaar, R. (2008). Constant volume of the human lens and decrease in surface area of the capsular bag during accommodation: an MRI and Scheimpflug study. *Invest Ophthalmol Vis Sci*, [Epub ahead of print]
- Heron, G., Charman, W.N., & Gray, L.S. (1999). Accommodation responses and ageing. *Invest Ophthalmol Vis Sci*, *40* (12), 2872-2883.
- Hess, C. (1901). Arbeiten aus dem Gebiete der Accommodationslehre. *Graefes Arch Clin Exp Ophthalmol*, *52*, 143-174.

- Hirano, K., Ito, Y., Suzuki, T., Kojima, T., Kachi, S., & Miyake, Y. (2001). Optical coherence tomography for the noninvasive evaluation of the cornea. *Cornea*, 20 (3), 281–289.
- Ho, A., Manns, F., Therese, & Parel, J.M. (2006). Predicting the performance of accommodating intraocular lenses using ray tracing. *J Cataract Refract Surg*, 32 (1), 129-136.
- Hofstetter, H. (1965). A longitudinal study of the amplitude changes in presbyopia. *Am J Optom Arch Am Acad Optom*, 42, 3-8.
- Hollins, M. (1974). Does central human retina stretch during accommodation? *Nature*, 251, 729-730.
- Hung, G.K., Ciuffreda, K.J., & Rosenfield, M. (1996). Proximal contribution to a linear static model of accommodation and vergence. *Ophthalmic Physiol Opt*, 16 (1), 31-41.
- Hyams, S.W., Pokotilo, E., & Shkurko, G. (1977). Prevalence of refractive errors in adults over 40: a survey of 8102 eyes. *Br J Ophthalmol*, 61 (428-432)
- Jaschinski-Kruza, W., & Toenies, U. (1988). Effect of a mental arithmetic task on dark focus of accommodation. *Ophthalmic and Physiol Opt*, 8 (4), 432-437.
- Javitt, J.C., & Steinert, R.F. (2000). Cataract extraction with multifocal intraocular lens implantation: a multinational clinical trial evaluating clinical, functional, and quality-of-life outcomes. *Ophthalmology*, 107 (11), 2040-2048.
- Jiang, B.C. (1995). Parameters of accommodative and vergence systems and the development of late-onset myopia. *Invest Ophthalmol Vis Sci*, 36 (8), 1737-1742.
- Johns, K.J., Feder, R. S., Hammill, B. M., Miller-Meeks, M. J., Rosenfeld, S. I., Perry, P. E. (2003). Lens and cataract: section 11, basic and clinical science course. *Lens and cataract* (San Francisco: American Academy of Ophthalmology).

Jones, C.E., Atchison, D.A., & Pope, J.M. (2007). Changes in lens dimensions and refractive index with age and accommodation. *Optom Vis Sci*, 84 (10), 990-995.

Jumblatt, J.E. (1999). Innervation and pharmacology of the iris and ciliary body. In: G. Burnstock, & A.M. Sillito (Eds.), *Nervous Control of the Eye* (pp. 1-40). Amsterdam: Harwood Academic.

Kaiserman, I., Bahar, I., & Rootman, D.S. (2008). Corneal wound malapposition after penetrating keratoplasty: an optical coherence tomography study. *Br J Ophthalmol*, 92 (8), 1103-1107.

Kaluzny, B.J., Szkulmowska, A., Kaluzny, J.J., Bajraszewski, T., Szkulmowski, M., Kowalczyk, A., & Wojtkowski, M. (2006). In vivo imaging of posterior capsule opacification using Spectral Optical Coherence Tomography. *J Cataract Refract Surg*, 32 (11), 1892-1895.

Kamalarajah, S., Ling, R., Silvestri, G., Sharma, N. K., Cole, M. D., Cran, G., Best, R. M. (2006). Presumed infectious endophthalmitis following cataract surgery in the UK: a case-control study of risk factors. *Eye*, 21 (5), 580-586.

Kamlesh., Dadeya, S., & Kaushik, S. (2001). Contrast sensitivity and depth of focus with aspheric multifocal versus conventional monofocal intraocular lens. *Can J Ophthalmol*, 36 (4), 197-201.

Kasprzak, H.T. (2000). New approximation for the whole profile of the human crystalline lens. *Ophthalmic and Physiol Opt*, 20 (1), 31-43.

Kasthurirangan, S., Vilupuru, A.S., & Glasser, A. (2003). Amplitude dependent accommodative dynamics in humans. *Vision Res*, 43 (2945-2956)

Kasthurirangan, S., & Glasser, A. (2005). Influence of amplitude and starting point on accommodative dynamics in humans. *Invest Ophthalmol Vis Sci*, 46, 3463-3472.

- Kaufman, P. (1992). Accommodation and presbyopia: neuromuscular and biophysical aspects. *Adler's Physiology of the Eye* (pp. 391-411). Mosby, St. Louis, USA.
- Kelman, C. (1967). Phaco-emulsification and aspiration: a new technique of cataract removal. *Am J Ophthalmol.*, 64, 23-35.
- Kessler, J. (1964). Experiment in refilling the lens. *Arch Ophthalmol*, 71, 412-417.
- Kessler, J. (1966). Refilling the rabbit lens. Further experiments. *Arch Ophthalmol*, 76 (4), 596-598.
- Kirschkamp, T., Jöckel, M., Wählich, G., & Barry, J.C. (1998). Construction of a model eye for simulation of Purkinje reflections for determining the radii of curvature and the position of the crystalline lens. *Biomed Tech (Berl)*, 43 (11), 318-325.
- Kirschkamp, T., Dunne, M., & Barry, J.C. (2004). Phakometric measurement of ocular surface radii of curvature, axial separations and alignment in relaxed and accommodated human eyes. *Ophthalmic and Physiol Opt*, 24, 65-73.
- Koepl, C., Findl, O., Kriechbaum, K., & Drexler, W. (2005). Comparison of pilocarpine-induced and stimulus-driven accommodation in phakic eyes. *Exp Eye Res*, 80 (6), 795-800.
- Koivula, A., & Kugelberg, M. (2007). Optical coherence tomography of the anterior segment in eyes with phakic refractive lenses. *Ophthalmology*, 114 (11), 2031-2037.
- Konstantopoulos, A., Hossain, P., & Anderson, D.F. (2007). Recent advances in ophthalmic anterior segment imaging: a new era for ophthalmic diagnosis? *Br J Ophthalmol*, 91 (4), 551-557.
- Kooijman, A.C. (1983). Light distribution on the retina of a wide-angle theoretical eye. *J Opt Soc Am.*, 73 (11), 1544-1550.
- Koopmans, S.A., Terwee, T., Glasser, A., Wendt, M., Vilupuru, A.S., van Kooten, T.G., Norrby, S., Haitjema, H.J., & Kooijman, A.C. (2006). Accommodative lens refilling in rhesus monkeys. *Invest Ophthalmol Vis Sci*, 47 (7), 2976-2984.

- Koretz, J.F., Handelman, G.H., & Phelps Brown, N. (1984). Analysis of human crystalline lens curvature as a function of accommodative state and age. *Vision Res*, 24, 1141-1151.
- Koretz, J.F., Bertasso, A.M., Neider, M.W., True-Gabelt, B., & Kaufman, P.L. (1987). Slit-lamp studies of the rhesus monkey eye. II. Changes in crystalline lens shape, thickness and position during accommodation and aging. *Exp Eye Res*, 45, 317-326.
- Koretz, J., & Handelman, G. (1988). How the human eye focuses. *Sci Am.*, 259 (1), 92-99.
- Koretz, J.F., Kaufman, P.L., Neider, M.W., & Goeckner, P.A. (1989). Accommodation and presbyopia in the human eye - aging of the anterior segment. *Vision Res.*, 29, 1685-1692.
- Koretz, J., Cook, C., & Kaufman, P. (1997a). Accommodation and presbyopia in the human eye. *Invest Ophthalmol Vis Sci*, 38, 569-578.
- Koretz, J.F., Cook, C.A., & Kaufman, P.L. (1997b). Accommodation and presbyopia in the human eye. Changes in the anterior segment and crystalline lens with focus. *Invest Ophthalmol Vis Sci*, 38 (3), 569-578.
- Koretz, J.F., Cook, C.A., & Kaufman, P.L. (2001). Aging of the human lens: changes in lens shape at zero-diopter accommodation. *J Opt Soc Am A Opt Image Sci Vis*, 18 (2), 265-272.
- Koretz, J., Cook, C., & Kaufman, P. (2002). Aging of the human lens: changes in lens shape with accommodation and with accommodative loss. *J Opt Soc Am A*, 19, 144-151.
- Koretz, J.F., Strenk, S.A., Strenk, L.M., & Semmlow, J. (2004). Scheimpflug and high-resolution magnetic resonance imaging of anterior segment: a comparative study. *J Opt Soc Am A Opt Image Sci Vis*, 21 (3), 346-354.
- Kotulak, J.C., & Schor, C.M. (1987). The effects of optical vergence, contrast, and luminance on the accommodative response to spatially bandpass filtered targets. *Vision Res*, 27 (10), 1797-1806.

Krag, S., Olsen, T., & Andreassen, T.T. (1997). Biomechanical characteristics of the human anterior lens capsule in relation to age. *Invest Ophthalmol Vis Sci*, 38, 357-363.

Krag, S., & Andreassen, T.T. (2003). Mechanical properties of the human posterior lens capsule. *Invest Ophthalmol Vis Sci*, 44, 691-696.

Kriechbaum, K., Findl, O., Koepl, C., Menapace, R., & Drexler, W. (2005). Stimulus-driven versus pilocarpine-induced biometric changes in pseudophakic eyes. *Ophthalmology*, 112 (3), 453-459.

Küchle, M., Nguyen, N.X., Langenbucher, A., Gusek-Schneider, G.C., Seitz, B., & Hanna, K.D. (2002). Implantation of a new accommodative posterior chamber intraocular lens. *J Refract Surg*, 18 (3), 208-216.

Lane, S.S., Morris, M., Nordan, L., Packer, M., Tarantino, N., & Wallace, R.B. (2006). Multifocal intraocular lenses. *Ophthalmol Clin North Am*, 19 (1), 89-105.

Langenbucher, A., Seitz, B., Huber, S., Nguyen, N.X., & Kuchle, M. (2003). Theoretical and measured pseudophakic accommodation after implantation of a new accommodative posterior chamber intraocular lens. *Arch Ophthalmol*, 121 (12), 1722-1727.

Langenbucher, A., Reese, S., Jakob, C., & Seitz, B. (2004). Pseudophakic accommodation with translation lenses--dual optic vs mono optic. *Ophthalmic Physiol Opt*, 24 (5), 450-457.

Lavanya, R., Teo, L., Friedman, D.S., Aung, H.T., Baskaran, M., Gao, H., Alfred, T., Seah, S.K., Kashiwagi, K., Foster, P.J., & Aung, T. (2007). Comparison of anterior chamber depth measurements using the IOLMaster, scanning peripheral anterior chamber depth analyser, and anterior segment optical coherence tomography. *Br J Ophthalmol*, 91 (8), 1023-1026.

Le Grand, Y., & El Hage, S.G. (1980). *Physiological optics*. (Springer-Verlag).

- Leary, G.A. (1981). Ocular component analysis by vergence contribution to the back vertex power of the anterior segment. *Am J Optom Physiol Opt*, 58 (11), 899-909.
- Ledley, R.S., Cheng, G.C., & Ludlam, W.M. (1966). Computer ray tracing of the optical system of the schematic eye. *Nature*, 211 (5052), 930-932.
- Legeais, J.M., Werner, L., Werner, L., Abenhaim, A., & Renard, G. (1999). Pseudoaccommodation: BioComFold versus a foldable silicone intraocular lens. *J Cataract Refract Surg*, 25 (2), 262-267.
- Leibowitz, H.W., & Owens, D.A. (1975). Night myopia and the intermediate dark focus of accommodation. *J Opt Soc Am*, 65 (10), 1121-1128.
- Leung, C.K., Li, H., Weinreb, R.N., Liu, J., Cheung, C.Y., Lai, R.Y., Pang, C.P., & Lam, D.S. (2008). Anterior chamber angle measurement with anterior segment optical coherence tomography: a comparison between slit lamp OCT and Visante OCT. *Invest Ophthalmol Vis Sci*, 49 (8), 3469-3474.
- Levy, B., & Sivak, J.G. (1980). Mechanisms of accommodation in the bird eye. *J Comp Physiol A*, 137, 267-272.
- Linebarger, E., Hardten, D., Shah, G., & RL, L. (1999). Phacoemulsification and modern cataract surgery. *Surv Ophthalmol*, 44, 123-147.
- Liou, H.L., & Brennan, N.A. (1997). Anatomically accurate, finite model eye for optical modeling. *J Opt Soc Am A Opt Image Sci Vis*, 14 (8), 1684-1695.
- Liu, Y.-J., Zhao-Qi, W., Li-Pei, S., & Guo-Guang, M. (2005). An anatomically accurate eye model with a shell-structure lens. *Optik*, 116, 241-246.
- Lotmar, W. (1971). Theoretical eye model with aspherics. *J Opt Soc Am*, 61, 1522-1529.
- Luckiesh, M. & Moss, F.K. (1937). *The Science of Seeing* (D. Van Nostrand Company, Inc., New York)

- Lutjen-Drecoll, E., Tamm, E., & Kaufman, P.L. (1988a). Age changes in the rhesus monkey ciliary muscle: light and electron microscopy. *Exp Eye Res*, 47 (885-99)
- Lutjen-Drecoll, E., Tamm, E., & Kaufman, P.L. (1988b). Age related loss of morphologic responses to pilocarpine in rhesus monkey ciliary muscle. *Arch Ophthalmol*, 106 (1591-8)
- Macasai, M.S., Padnick-Silver, L., & Fontes, B.M. (2006). Visual outcomes after accommodating intraocular lens implantation. *J Cataract Refract Surg*, 32 (4), 628-633.
- Maldonado, M.J., García-Feijóo, J., Benítez Del Castillo, J.M., & Teutsch, P. (2006). Cataractous changes due to posterior chamber flattening with a posterior chamber phakic intraocular lens secondary to the administration of pilocarpine. *Ophthalmology*, 113 (8), 1283-1288.
- Mallen, E.A., Wolffsohn, J., Gilmartin, B., & Tsujimura, S. (2001). Clinical evaluation of the Shin-Nippon SRW-5000 autorefractor in adults. *Ophthalmic and Physiol Opt*, 21 (2), 101-107.
- Mallen, E.A., Gilmartin, B., & Wolffsohn, J.S. (2005). Sympathetic innervation of ciliary muscle and oculomotor function in emmetropic and myopic young adults. *Vision Res*, 45 (13), 1641-1651.
- Mallen, E.A., Kashyap, P., & Hampson, K.M. (2006). Transient Axial Length Change during the Accommodation Response in Young Adults. *Invest Ophthalmol Vis Sci*, 47 (3), 1251-1254.
- Malmstrom, F., Randle, R., Bendix, J., & Weber, R. (1980). The visual accommodation response during concurrent mental activity. *Perscept Psychophys.*, 28 (5), 440-448.
- Marchini, G., Pedrotti, E., Sartori, P., & Tosi, R. (2004). Ultrasound biomicroscopic changes during accommodation in eyes with accommodating intraocular lenses: pilot study and hypothesis for the mechanism of accommodation. *J Cataract Refract Surg*, 30 (12), 2476-2482.

- Marchini, G., Pedrotti, E., Modesti, M., Visentin, S., & Tosi, R. (2008). Anterior segment changes during accommodation in eyes with a monofocal intraocular lens: high-frequency ultrasound study. *J Cataract Refract Surg*, 34 (6), 949-956.
- Martin, H., Guthoff, R., Terwee, T., & Schmitz, K.-P. (2005). Comparison of the accommodation theories of Coleman and of Helmholtz by finite element simulations. *Vis Res*, 45, 2910-2915.
- Mastropasqua, L., Toto, L., Falconio, G., Nubile, M., Carpineto, P., Ciancaglini, M., Di Nicola, M., & Ballone, E. (2007). Longterm results of 1 CU accommodative intraocular lens implantation: 2-year follow-up study. *Acta Ophthalmol Scand.*, 85 (4), 409-414.
- Mathews, S. (1999). Scleral expansion surgery does not restore accommodation in human presbyopia. *Ophthalmology*, 106, 873-877.
- McBrien, N.A., & Millodot, M. (1986). The effect of refractive error on the accommodative response gradient. *Ophthalmic and Physiol Opt*, 6 (2), 145-149.
- McLeod, S.D. (2006). Optical principles, biomechanics, and initial clinical performance of a dual-optic accommodating intraocular lens (an American Ophthalmological Society thesis). *Trans Am Ophthalmol Soc*, 104, 437-452.
- McLeod, S.D., Portney, V., & Ting, A. (2003). A dual optic accommodating foldable intraocular lens. *Br J Ophthalmol*, 87 (9), 1083-1085.
- McLeod, S.D., Vargas, L.G., Portney, V., & Ting, A. (2007). Synchrony dual-optic accommodating intraocular lens. Part 1: optical and biomechanical principles and design considerations. *J Cataract Refract Surg*, 33 (1), 37-46.
- McLin, L.N., & Schor, C.M. (1988). Voluntary effort as a stimulus to accommodation and vergence. *Invest Ophthalmol Vis Sci*, 29 (11), 1739-1746.

Menapace, R., Findl, O., Kriechbaum, K., & Leydolt-Koepl, C. (2007). Accommodating intraocular lenses: a critical review of present and future concepts. *Graefes Arch Clin Exp Ophthalmol*, 245, 473-489.

Mentes, J., Erakgun, T., Afrashi, F., Kerici, G. (2003). Incidence of cystoid macular edema after uncomplicated phacoemulsification. *Ophthalmologica*, 217 (6), 408-412.

Millodot, M. (1997). Dictionary of Optometry and Vision Science, 4th edn. (Oxford, UK): Butterworth-Heinemann.

Minassian, D.C., Rosen, P., Dart, J.K., Reidy, A., Desai, P., Sidhu, M., Kaushal, S., & Wingate, N. (2001). Extracapsular cataract extraction compared with small incision surgery by phacoemulsification: a randomised trial. *Br J Ophthalmol*, 85, 822-829.

Missotten, T., Verhamme, T., Blanckaert, J., & Missotten, G. (2004). Optical formula to predict outcomes after implantation of accommodating intraocular lenses. *J Cataract Refract Surg*, 30 (10), 2084-2087.

Mordi, J.A., & Ciuffreda, K.J. (1998). Static aspects of accommodation: age and presbyopia. *Vision Res*, 38 (11), 1643-1653.

Moreno-Montañés, J., Alvarez, A., & Maldonado, M.J. (2005). Objective quantification of posterior capsule opacification after cataract surgery, with optical coherence tomography. *Invest Ophthalmol Vis Sci*, 46 (11), 3999-4006.

Moreno-Montañés, J., Alvarez, A., Bes-Rastrollo, M., & García-Layana, A. (2008). Optical coherence tomography evaluation of posterior capsule opacification related to intraocular lens design. *J Cataract Refract Surg*, 34 (4), 643-650.

Morgan, M.W. (1944). The nervous control of accommodation. *Am J Optom Arch Am Acad Optom*, 21, 87-93.

- Muftuoglu, O., Hosal, B.M., Karel, F., & Zilelioglu, G. (2005). Drug-induced intraocular lens movement and near visual acuity after AcrySof intraocular lens implantation. *J Cataract Refract Surg*, 31 (7), 1298-1305.
- Mutti, D.O., Jones, L.A., Moeschberger, M.L., & Zadnik, K. (2000). AC/A ratio, age, and refractive error in children. *Invest Ophthalmol Vis Sci*, 41 (9), 2469-2478.
- Myers, G.A., & Stark, L. (1990). Topology of the near response triad. *Ophthalmic and Physiol Opt*, 10 (2), 175-181.
- Nakao, S., Fujimoto, S., Nagata, R., Iwata, K. (1968). Model of refractive index distribution in the rabbit crystalline lens. *J Opt Soc Am A*, 58, 1125-1130.
- Nakao, S., Ono, T., Nagata, R., Iwata, K. (1969). Model of refractive indices in the human crystalline lens. *Jap J Clin Ophthalmol.*, 23, 903-906.
- Nakazawa, M., & Ohtsuki, K. (1983). Apparent accommodation in pseudophakic eyes after implantation of posterior chamber intraocular lenses. *Am J Ophthalmol*, 96 (4), 435-438.
- Navarro, R., Santamaría, J., & Bescós, J. (1985). Accommodation-dependent model of the human eye with aspherics. *J Opt Soc Am*, 2 (8), 1273-1281.
- Navarro, R., González, L., & Hernández-Matamoros, J.L. (2006). On the prediction of optical aberrations by personalized eye models. *Optom Vis Sci*, 83 (6), 371-381.
- Nawa, Y., Ueda, T., Nakatsuka, M., Tsuji, H., Marutani, H., Hara, Y., & Uozata, H. (2003). Accommodation obtained per 1.0 mm forward movement of a posterior chamber intraocular lens. *J Cataract Refract Surg.*, 29, 2069-2072.
- Neider, M.W., Crawford, K., Kaufman, P.L., & Bitto, L.Z. (1990). In vivo videography of the rhesus monkey accommodative apparatus. Age-related loss of ciliary muscle response to central stimulation. *Arch Ophthalmol.*, 108 (1), 69-74.

- Nemeth, G., Vajas, A., Tsorbatzoglou, A., Kolozsvari, B., Modis, L.J., & Berta, A. (2007). Assessment and reproducibility of anterior chamber depth measurement with anterior segment optical coherence tomography compared with immersion ultrasonography. *J Cataract Refract Surg.*, 33 (3), 443-447.
- Nguyen, N.X., Seitz, B., Reese, S., Langenbacher, A., Kuchle, M. (2005). Accommodation after Nd: YAG capsulotomy in patients with accommodative posterior chamber lens ICU.
- Nikica, G., Ljerka, H.P., Jelena, P., Metez-Soldo, K., & Mladen, B. (1992). Cystoid macular edema in anterior chamber lens implantation following posterior capsule rupture. *Doc Ophthalmol*, 81 (3), 309-315.
- Nishi, O., Hara, T., Sakka, Y., Hayashi, H., Nakamae, K., & Yamada, Y. (1991). Refilling the lens with inflatable endocapsular balloon. *Dev Ophthalmol*, 22, 122-125.
- Nishi, O., T., H., Hara, T., Sakka, Y., Hayashi, F., Nakamae, K., & Yamada, Y. (1992). Refilling the lens with a inflatable endocapsular balloon: surgical procedure in animal eyes. *Graefes Arch Clin Exp Ophthalmol*, 230 (1), 47-55.
- Nishi, O., Nakai, Y., Yamada, Y., & Mizumoto, Y. (1993). Amplitudes of accommodation of primate lenses refilled with two types of inflatable endocapsular balloons. *Arch Ophthalmol*, 111 (12), 1677-1684.
- Nishi, O., Nakai, Y., Mizumoto, Y., & Yamada, Y. (1997). Capsule opacification after refilling the capsule with an inflatable endocapsular balloon. *J Cataract Refract Surg*, 23 (10), 1548-1555.
- Nishi, O., & Nishi, K. (1998). Accommodation amplitude after lens refilling with injectable silicone by sealing the capsule with a plug in primates. *Arch Ophthalmol*, 116 (10), 1358-1361.
- Nishi, O., Nishi, K., Mano, C., Ichihara, M., & Honda, T. (1998). Lens refilling with injectable silicone in rabbit eyes. *J Cataract Refract Surg*, 24 (7), 975-982.

- Nishi, O. (2003). Restoration of accommodation by refilling the lens capsule after endocapsular phacoemulsification. In: R. Guthoff, & K. Ludwig (Eds.), *Current Aspects of Human Accommodation II* (Heidelberg: Kaden Verlag).
- Norrby, S. (2005). The Dubbelman eye model analysed by ray tracing through aspheric surfaces. *Ophthalmic and Physiol Opt*, 25 (2), 153-161.
- Norrby, S., Koopmans, S., & Terwee, T. (2006). Artificial crystalline lens. *Ophthalmol Clin North Am*, 19 (1), 143-146.
- O'Leary, D.J., & Allen, P.M. (2001). Facility of accommodation in myopia. *Ophthalmic and Physiol Opt*, 21 (5), 352-355.
- Ohtsuka, K., Maekawa, H., Takeda, M., Uede, N., & Chiba, S. (1988). Accommodation and convergence insufficiency with left middle cerebral artery occlusion. *Am J Ophthalmol*, 106 (1), 60-64.
- Ong, E., Ciuffreda, K.J., & Tannen, B. (1993). Static accommodation in congenital nystagmus. *Invest Ophthalmol Vis Sci*, 34 (1), 194-204.
- Ong, E., & Ciuffreda, K.J. (1997). Accommodation, nearwork and myopia. *Optometric Extension Program Foundation* (Santa Ana, USA).
- Oshika, T., Mimura, T., Tanaka, S., Amano, S., Fukuyama, M., Yoshitomi, F., Maeda, N., Fujikado, T., Hirohara, Y., & Mihashi, T. (2002). Apparent accommodation and corneal wavefront aberration in pseudophakic eyes. *Invest Ophthalmol Vis Sci*, 43 (9), 2882-2886.
- Ossma, I.L., Galvis, A., Vargas, L.G., Trager, M.J., Vagefi, M.R., & McLeod, S.D. (2007). Synchrony dual-optic accommodating intraocular lens. Part 2: pilot clinical evaluation. *J Cataract Refract Surg*, 33 (1), 47-52.
- Ostrin, L., Kasthurirangan, S., Win-Hall, D., & Glasser, A. (2006). Simultaneous measurements of refraction and A-scan biometry during accommodation in humans. *Optom Vis Sci*, 83, 657-665.

- Pardue, M.T., & Sivak, J.G. (2000). Age-related changes in human ciliary muscle. *Optom Vis Sci*, 77 (4), 204-210.
- Parel, J.M., Gelender, H., Trefers, W.F., & Norton, E.W.D. (1986). Phaco-ersatz: cataract surgery designed to preserve accommodation. *Graefes Arch Clin Exp Ophthalmol.*, 224, 165-173.
- Pau, H., & Kranz, J. (1991). The increasing sclerosis of the human lens with age and its relevance to accommodation and presbyopia. *Graefes Arch Clin Exp Ophthalmol*, 229, 294-296.
- Pearce, J.L. (1977). Sixteen months experience with 140 posterior chamber intraocular lens implants. *Br J Ophthalmol*, 61, 310.
- Pflugk von, A. (1932). Neue wege zur erforschung der lehre von der akkommodation. *Graefes Arch Ophthalmol.*, 133, 545-558.
- Phillips, S.D., Shirachi, D., & Stark, L. (1972). Analysis of accommodation times using histogram information. *Am J Optom Arch Am Acad Optom*, 49 (389-401)
- Pieh, S., Lackner, B., Hanselmayer, G., Zöhrer, R., Sticker, M., Weghaupt, H., Fercher, A., & Skorpik, C. (2001). Halo size under distance and near conditions in refractive multifocal intraocular lenses. *Br J Ophthalmol*, 85 (7), 816-821.
- Pierscionek, B.K. (1989). Growth and ageing effects on the refractive index gradient in the equatorial plane of the bovine lens. *Vision Res.*, 29, 1759-1766.
- Pierscionek, B.K. (1990). Presbyopia-effect of refractive index. *Clin Exp Optom.*, 73 (23-30)
- Pierscionek, B., Popiolek-Masajada, A., & Kasprzak, H. (2001). Corneal shape change during accommodation. *Eye*, 15 (766-769)

- Pointer, J.S. (1995). The presbyopic add. II. Age-related trend and a gender difference. *Ophthalmic and Physiol Opt*, 15 (4), 241-248.
- Pomerantzeff, O., Fish, H., Govignon, J., & Schepens, C.L. (1971). Wide angle optical model of the human eye. *Ann Ophthalmol*, 3 (8), 815-819.
- Popiolek-Masajada, A. (1999). Numerical study of the influence of the shell structure of the crystalline lens on the refractive properties of the human eye. *Ophthalmic and Physiol Opt*, 19 (1), 41-49.
- Popiolek-Masajada, A., & Kasprzak, H. (2002). Model of the optical system of the human eye during accommodation. *Ophthalmic and Physiol Opt*, 22 (3), 201-208.
- Poyer, J.F., Kaufman, P.L., & Flugel, C. (1993). Age does not effect contractile responses of the isolated rhesus monkey ciliary muscle to muscarinic agonists. *Curr Eye Res*, 12, 413-422.
- Purkinje, J.E. (1823). De examine physiologico organi visus et systematis cutanei. *Wratislaviae*,
- Rai, G., Gilmartin, B., Wolffsohn, J., & Cervino, A. (2006). The Effect of Accommodation on IOP: Evidence for Dose Dependency. *Invest Ophthalmol Vis Sci*, 47: E-Abstract 5859
- Ramsdale, C., & Charman, W. (1989). A longitudinal study of the changes in the static accommodation response. *Ophthalmic and Physiol Opt*, 9, 255-263.
- Rana, A., Miller, D., & Magnante, P. (2003). Understanding the accommodating intraocular lens. *J Cataract Refract Surg*, 29 (12), 2284-2287.
- Ravalico, G., & Baccara, F. (1990). Apparent accommodation in pseudophakic eyes. *Acta Ophthalmol (Copenh)*, 68 (5), 604-606.
- Read, S.A., Buehren, T., & Collins, M.J. (2007). Influence of accommodation on the anterior and posterior cornea. *J Cataract Refract Surg*, 33 (11), 1877-1885.

- Richdale, K., Bullimore, M.A., & Zadnik, K. (2008). Lens thickness with age and accommodation by optical coherence tomography. *Ophthalmic and Physiol Opt*, 28 (5), 441-447.
- Ridley, N.H.L. (1951). Intraocular acrylic lenses. *Trans Ophthalmol Soc UK & Oxford Ophthalmol Congress LXXI*, 617-621.
- Ridley, N.H.L. (1952). Intraocular acrylic lenses after cataract extraction. *Lancet*, 1, 118-119.
- Ridley, N.H.L. (1953). Further observations on intraocular acrylic lenses in cataract surgery. *Trans Am Acad Ophthalmol Otolaryngol.*, 57, 98-106.
- Rohen, J. (1979). Scanning electron microscopic studies of the zonular apparatus in human and monkey eyes. *Invest Ophthalmol Vis Sci*, 18, 133-144.
- Rosales, P., Dubbelman, M., Marcos, S., & van der Heijde, R. (2006). Crystalline lens radii of curvature from Purkinje and Scheimpflug imaging. *J Vision*, 6 (1057-1067)
- Rosales, P., & Marcos, S. (2007). Customized computer models of eyes with intraocular lenses. *Optics Express*, 15 (5), 2204-2218.
- Rosen, E.S. (1984). The development and characterisation of the intraocular lens. In: E.S. Rosen, W.M. Haining, & E.J. Arnott (Eds.), *Intraocular lens implantation* (pp. 50-58). St. Louis, Missouri, USA: Mosby.
- Rosenfield, M., & Gilmartin, B. (1987). Effect of a near-vision task on the response AC/A of a myopic population. *Ophthalmic and Physiol Opt*, 7 (3), 225-233.
- Rosenfield, M., & Gilmartin, B. (1989). Temporal aspects of accommodative adaptation. *Optom Vis Sci*, 66 (4), 229-234.
- Rosenfield, M., & Gilmartin, B. (1990). Effect of target proximity on the open-loop accommodative response. *Optom Vis Sci*, 67 (2), 74-79.

- Rosenfield, M., & Ciuffreda, K.J. (1991). Effect of surround propinquity on the open-loop accommodative response. *Invest Ophthalmol Vis Sci*, 32 (1), 142-147.
- Rosenfield, M., Ciuffreda, K.J., Hung, G.K., & Gilmartin, B. (1993). Tonic accommodation: a review. I. Basic aspects. *Ophthalmic and Physiol Opt*, 13 (3), 266-284.
- Rosenfield, M., Ciuffreda, K.J., Hung, G.K., & Gilmartin, B. (1994). Tonic accommodation: a review. II. Accommodative adaptation and clinical aspects. *Ophthalmic and Physiol Opt*, 14 (3), 265-277.
- Saladin, J.J., Usui, S., & Stark, L. (1974). Impedance cyclography as an indicator of ciliary muscle contraction. *Am J Optom Physiol Opt.*, 51 (9), 613-625.
- Saladin, J.J., & Stark, L. (1975). Presbyopia: new evidence from impedance cyclography supporting the Hess-Gullstrand theory *Vision Res*, 15 (4), 537-541.
- Sanders, D.R., & Sanders, M.L. (2007). Visual performance results after Tetraflex accommodating intraocular lens implantation. *Ophthalmology*, 114 (9), 1679-1684.
- Sandoval, H.P., de Castro, L.E.F., Vroman, D.T., & Solomon, K.D. (2005). Refractive Surgery Survey 2004. *J cataract Refract Surg*, 31 (1), 221-233.
- Sarfarazi, F.M. (2006). Sarfarazi dual optic accommodative intraocular lens. *Ophthalmol Clin North Am*, 19 (1), 125-128.
- Sauder, G., Degenring, R.F., Kampeter, B., & Hugger, P. (2005). Potential of the 1 CU accommodative intraocular lens. *Br J Ophthalmol*, 89 (10), 1289-1292.
- Saunders, H. (1986). A longitudinal study of the age-dependence of human ocular refraction—I. Age-dependent changes in the equivalent sphere. *Ophthalmic and Physiol Opt*, 6, 39-46.
- Saunders, K.J. (1995). Early refractive development in humans. *Surv Ophthalmol*, 401, 207-216.

Saxena, R.C. (1965). Couching and its hazards (a review of 62 cases). *J All India Ophthalmol Soc*, 13 (3), 100-104.

Schachar, R. (1992). Cause and treatment of presbyopia with a method for increasing the amplitude of accommodation. *Ann Ophthalmol*, 24, 445-452.

Schachar, R.A. (1994). Zonular function: a new hypothesis with clinical implications. *Ann Ophthalmol*, 26 (2), 36-38.

Schachar, R.A., Cudmore, D.P., Torti, R., Black, T.D., & Huang, T. (1994). A physical model demonstrating Schachar's hypothesis of accommodation. *Ann Ophthalmol*, 26 (1), 4-9.

Schachar, R.A., & Anderson, D.A. (1995). The mechanism of ciliary muscle function. *Ann Ophthalmol*, 27, 126-132.

Schachar, R.A., Tello, C., Cudmore, D.P., Liebmann, J.M., Black, T.D., & Ritch, R. (1996). In vivo increase of the human lens equatorial diameter during accommodation. *Am J Physiol*, 271 (3 Pt 2), R670-676.

Schaeffel, F., Wilhelm, H., & Zrenner, E. (1993). Inter-individual variability in the dynamics of natural accommodation in humans: relation to age and refractive errors. *J Physiol*, 461, 301-320.

Schmitz, S., Dick, H.B., Krummenauer, F., Schwenn, O., & Krist, R. (2000). Contrast sensitivity and glare disability by halogen light after monofocal and multifocal lens implantation. *Br J Ophthalmol*, 84 (10), 1109-1112.

Schneider, H., Baeskuin, A., & Guthoff, R. (2001). History of Accommodation Research. In: *Current Aspects of Human Accommodation* (pp. 11-23). Hidelberg: Kaden Verlag.

Schneider, H., Stachs, O., Göbel, K., & Guthoff, R. (2006). Changes of the accommodative amplitude and the anterior chamber depth after implantation of an accommodative intraocular lens. *Graefes Arch Clin Exp Ophthalmol*, 244 (3), 322-329.

Schor, C.M., Johnson, C.A., & Post, R.B. (1984). Adaptation of tonic accommodation. *Ophthalmic and Physiol Opt*, 4 (2), 133-137.

Sergienko, N.M., & Tutchenko, N.N. (2007). Depth of focus: clinical manifestation. *Eur J Ophthalmol*, 17 (5), 836-840.

Shapiro, S.S., Wilk, M. B. (1965). Analysis of variance test for normality (complete samples). *Biometrika*, 52, 591-611.

Smith, G., Atchison, D.A., & Pierscionek, B.K. (1992). Modeling the power of the aging human eye. *J Opt Soc Am*, 9, 2111-2117.

Snell, R.S., & Lemp, M.A. (1998). *Clinical Anatomy of the Eye*, 2nd edn. (Blackwell Science, Inc.).

Solomon, K., Holzer, M., Sandoval, H., Vargas, L., Werner, L., Vroman, D., Kasper, T., & Apple, D. (2002). Refractive Surgery Survey 2001. *J Cataract Refract Surg*, 28 (2), 346-355.

Spalton, D.J. (1999). Harold Ridley's first patient. *J Cataract Refract Surg*, 25, 156.

Stachs, O., Schneider, H., Stave, J., & Guthoff, R. (2005). Potentially accommodating intraocular lenses--an in vitro and in vivo study using three-dimensional high-frequency ultrasound. *J Refract Surg*, 21 (1), 37-45.

Stachs, O., Schneider, H., Beck, R., & Guthoff, R. (2006). Pharmacological-induced haptic changes and the accommodative performance in patients with the AT-45 accommodative IOL. *J Refract Surg*, 22 (2), 145-150.

Stark, L. (1988). Presbyopia in light of accommodation. *Am J Optom Physiol Opt*, 65 (5), 407-416.

- Steinert, R.F., Aker, B.L., Trentacost, D.J., Smith, P.J., & Tarantino, N. (1999). A prospective comparative study of the AMO ARRAY zonal-progressive multifocal silicone intraocular lens and a monofocal intraocular lens. *Ophthalmology*, *106* (7), 1243-1255.
- Storey, J.K., & Rabie, E.P. (1983). Ultrasound—a research tool in the study of accommodation. *Ophthalmic and Physiol Opt*, *3*, 315-320.
- Streeten, B.W. (1982). Ciliary body. In: *Biomedical Foundations of Ophthalmology*. 1 (pp. 1-28). Philadelphia, USA: Harper and Row.
- Streeten, B.W. (2000). Pathology of the lens. *Principles and practice of ophthalmology, 2nd edn* (pp. 3685-3749). Philadelphia, USA.
- Strenk, S., Semmlow, J., Strenk, L., Munoz, P., Gronlund-Jacob, J., & DeMarco, J. (1999). Age-related changes in human ciliary muscle and lens: a magnetic resonance imaging study. *Invest Ophthalmol Vis Sci*, *40* (6), 1162-1169.
- Strenk, S., Strenk, L., Semmlow, J., & DeMarco, J. (2004). Magnetic resonance imaging study of the effects of age and accommodation on the human lens cross-sectional area. *Invest Ophthalmol Vis Sci*, *45* (2), 539-545.
- Strenk, S., Strenk, L., & Koretz, J. (2005). The mechanism of presbyopia. *Prog Retin Eye Res*, *24* (3), 379-393.
- Strenk, S.A., Strenk, L.M., & Guo, S. (2006). Magnetic resonance imaging of aging, accommodating, phakic, and pseudophakic ciliary muscle diameters. *J Cataract Refract Surg*, *32* (11), 1792-1798.
- Swaine, W. (1921). Geometrical and ophthalmic optics - VII: paraxial schematic and reduced eyes. *The Optician and Scientific Instrument Maker*, *62*, 133-136.
- Swegmark, G., & Olsson, T. (1968). Impedance cyclography. A new method for accommodation recording. *Acta Ophthalmol (Copenh)*, *46* (5), 946-968.

Tamm, E., Lutjen-Drecoll, E., Jungkunz, W., & Rohen, J.W. (1991). Posterior attachment of ciliary muscle in young, accommodating old, presbyopic monkeys. *Invest Ophthalmol Vis Sci*, 32 (5), 1678-1692.

Tamm, S., Tamm, E., & Rohen, J. (1992a). Age-related changes of the human ciliary muscle. A quantitative morphometric study. *Mech Ageing Dev*, 62 (2), 209-221.

Tamm, E., Croft, M.A., Jungkunz, W., Lutjen-Drecoll, E., & Kaufman, P.L. (1992b). Age-related loss of ciliary muscle mobility in the rhesus monkey. Role of the choroid. *Arch Ophthalmol*, 110 (6), 871-876.

Tappin, M.J., Larkin, D. F. (2000). Factors leading to lens implant decentration and exchange. *Eye*, 14, 773-776.

Thibos, L.N., Ye, M., Zhang, X., & Bradley, A. (1992). The chromatic eye: A new reduced-eye model of ocular chromatic aberration in humans. *Applied Optics*, 31, 3594-3600.

Thomson, D. (2005). VA testing in optometric practice part 2: Newer chart designs. *Optometry Today*, 6th May, 22-24.

Tonekaboni, K., & Whitsett, A.J. (2005). The IOL horizon: accommodative intraocular lenses. *Optometry*, 76 (3), 185-190.

Trivedi, R.H., Apple, D. J., Pandey, S. K., Werner, L., Izak, A. M., Vasavada, A. R., Ram, J. (2003). Sir Nicholas Harold Ridley. He changed the world, so that we might better see it. *Indian J Ophthalmol*, 51 (3), 211-216.

Tscherning, M. (1909). H. v. Helmholtz et la theorie de l'accommodation. Paris.

Tsorbatzoglou, A., Németh, G., Máth, J., & Berta, A. (2006). Pseudophakic accommodation and pseudoaccommodation under physiological conditions measured with partial coherence interferometry. *J Cataract Refract Surg*, 32 (8), 1345-1350.

Tsorbatzoglou, A., Németh, G., Széll, N., Biró, Z., & Berta, A. (2007). Anterior segment changes with age and during accommodation measured with partial coherence interferometry. *J Cataract Refract Surg.*, 33 (9), 1597-1601.

Tucker, J., & Charman, W.N. (1979). Reaction and response times for accommodation. *Optom Physiol Opt*, 56, 490-503.

Vámosi, P., Nemeth, G., & Berta, A. (2006). Pseudophakic accommodation with 2 models of foldable intraocular lenses. *J Cataract Refract Surg*, 32 (2), 221-226.

van Alphen, G.W. (1976). The adrenergic receptors of the intraocular muscles of the human eye. *Invest Ophthalmol*, 15 (6), 502-505.

Van der Heijde, G.L., Weber, J. (1989). Accommodation used to determine ultrasound velocity in the human lens. *Optom Vis Sci*, 66, 830-833.

Van der Heijde, G.L., Beers, A.P.A., & Dubbelman, M. (1996). Microfluctuations of steady-state accommodation measured with ultrasonography. *Ophthalmic and Physiol Opt*, 16, 216-221.

Vargas, L.G., Peng, Q., Escobar-Gomez, M., Schmidbauer, J.M., & Apple, D.J. (2001). Overview of modern foldable intraocular lenses and clinically relevant anatomy and histology of the crystalline lens. In: L. Werner, & D.J. Apple (Eds.), *Complications of aphakic and refractive intraocular lenses* (pp. 1-15). Philadelphia, Pennsylvania, USA.: Lippincott, Williams & Wilkins).

Vera-Díaz, F.A., Strang, N.C., & Winn, B. (2002). Nearwork induced transient myopia during myopia progression. *Curr Eye Res*, 24 (4), 289-295.

Vilupuru, A., & Glasser, A. (2005). The relationship between refractive and biometric changes during Edinger-Westphal stimulated accommodation in rhesus monkeys. *Exp Eye Res*, 80, 349-360.

- Vinciguerra, P., Nizzola, G.M., Bailo, G., Nizzola, F., Ascari, A., & Epstein, D. (1998). Excimer laser photorefractive keratectomy for presbyopia: 24-month follow-up in three eyes. *J Refract Surg*, *14*, 31-37.
- Wang, B., & Ciuffreda, K.J. (2006). Depth-of-focus of the human eye: theory and clinical implications. *Surv Ophthalmol*, *51* (1), 75-85.
- Wang, J., Fu, J., Wang, N.L., Kang, H.J., & Yang, W.L. (2005). Accommodation in pseudophakic eyes with the 1CU accommodative intraocular lens. *Zhonghua Yan Ke Za Zhi*, *41* (9), 807-811.
- Wang, Q., Klein, B.E.K., Klein, R., & Moss, S.E. (1994). Refractive status in the Beaver Dam Eye Study. *Invest Ophthalmol Vis Sci*, *35*, 4344-4347.
- Wax, M., & Molinoff, P. (1987). Distribution and properties of beta-adrenergic receptors in human iris-ciliary body. *Invest Ophthalmol Vis Sci*, *28* (3), 420-430.
- Weale, R.A. (1982). The age variation of 'senile' cataract in various parts of the world. *Br J Ophthalmol*, *66* (1), 31-34.
- Weale, R.A. (1983). Transparency and power of post-mortem human lenses: variation with age and sex. *Exp Eye Res*, *36* (5), 731-741.
- Weale, R.A. (1992). *The Senescence of Human Vision*. (Oxford: Oxford University Press).
- Weale, R. (2000). Why we need reading-glasses before a zimmer-frame. *Vision Res*, *40* (17), 2233-2240.
- Weeber, H.A., Eckert, G., Soergel, F., Meyer, C.H., Pechhold, W., & van der Heijde, R.G.L. (2005). Dynamic mechanical properties of human lenses. *Exp Eye Res*, *80*, 425-434.

Weeber, H.A., Eckert, G., Pechhold, W., & van der Heijde, R.G.L. (2007). Stiffness gradient in the crystalline lens. *Graefes Arch Clin Exp Ophthalmol*, 245, 1357-1366.

Weeber, H.A., & van der Heijde, R.G. (2008). Internal deformation of the human crystalline lens during accommodation. *Acta Ophthalmol*, 86 (6), 642-647.

Whitacre, M., & Stein, R. (1993). Sources of error with use of Goldmann-type tonometers. *Surv Ophthalmol*, 38 (1), 1-30.

Whitefoot, H., & Charman, W.N. (1992). Dynamic retinoscopy and accommodation. *Ophthalmic and Physiol Opt*, 12 (1), 8-17.

Wilson, R. (1997). Does the lens diameter increase or decrease during accommodation? Human accommodation studies: a new technique using infrared retro-illumination video photography and pixel unit measurements. *Trans Am Ophthalmol Soc*, 95, 261-267 discussion 267-270.

Winn, B., Gilmartin, B., Mortimer, L.C., & Edwards, N.R. (1991). The effect of mental effort on open- and closed-loop accommodation. *Ophthalmic and Physiol Opt*, 11 (4), 335-339.

Wobig, J.L., Wirtschafer, J. D., Jones, L. T. (1981). *Ophthalmic Anatomy: A Manual with some Clinical Applications*. (San Francisco: American Academy of Ophthalmology).

Woldemussie, E., Feldmann, B. J., & Chen, J. (1993). Characterization of muscarinic receptors in cultured human iris and ciliary smooth muscle cells. *Experimental Eye Research*, 56, 385-392.

Wolffsohn, J.S., Gilmartin, B., Thomas, R., & Mallen, E.A. (2003). Refractive error, cognitive demand and nearwork-induced transient myopia. *Curr Eye Res*, 27 (6), 363-370.

Wolffsohn, J.S., Hunt, O.A., Naroo, S., Gilmartin, B., Shah, S., Cunliffe, I.A., Benson, M.T., & Mantry, S. (2006a). Objective accommodative amplitude and dynamics with the 1CU accommodative intraocular lens. *Invest Ophthalmol Vis Sci*, 47 (3), 1230-1235.

Wolffsohn, J.S., Naroo, S.A., Motwani, N.K., Shah, S., Hunt, O.A., Mantry, S., Sira, M., Cunliffe, I.A., & Benson, M.T. (2006b). Subjective and objective performance of the Lenstec KH-3500 "accommodative" intraocular lens. *Br J Ophthalmol*, 90 (6), 693-696.

Wolffsohn, J.S., & Davies, L.N. (2007). Advances in anterior segment imaging. *Curr Opin Ophthalmol*, 18 (1), 32-38.

World Health Organization and International Agency for the Prevention of Blindness (2000). Global initiative for the elimination of avoidable blindness. Fact sheet number 213. Geneva: WHO,

World Health Organization and International Agency for the Prevention of Blindness (2004). Developing an Action Plan to prevent blindness at national, provincial and district levels. (World Health Organization).

Yamamoto, S., & Adachi-Usami, E. (1992). Apparent accommodation in pseudophakic eyes as measured with visually evoked potentials. *Invest Ophthalmol Vis Sci*, 33 (2), 443-446.

Yasuda, A., Yamaguchi, T., Ohkoshi, K. (2003). Changes in corneal curvature with accommodation. *J Cataract Refract Surg*, 30 (3), 531-533.

Young, T. (1801). The Bakerian Lecture. On the mechanism of the eye. *Philos Trans R Soc Lond.*, 23-88.

Zadnik, K., Mutti, D.O., Kim, H.S., Jones, L.A., Qiu, P.H., & Moeschberger, M.L. (1999). Tonic accommodation, age, and refractive error in children. *Invest Ophthalmol Vis Sci*, 40 (6), 1050-1060.

Zadnik, K., Manny, R.E., Yu, J.A., Mitchell, G.L., Cotter, S.A., Quiralte, J.C., Shipp, M., Friedman, N.E., Kleinstein, R.N., Walker, T.W., Jones, L.A., Moeschberger, M.L., Mutti, D.O., & Collaborative Longitudinal Evaluation of Ethnicity and Refractive Error

(CLEERE) Study Group (2003). Ocular component data in schoolchildren as a function of age and gender. *Optom Vis Sci*, 80 (3), 226-236.

Zetterstrom, C., & Hahnenberger, R. (1988). Pharmacological characterization of human ciliary muscle adrenoceptors in vitro. *Exp Eye Research*, 46 (3), 421-430.

Ziebarth, N.M., Borja, D., Arrieta, E., Aly, M., Manns, F., Dortonne, I., Nankivil, D., Jain, R., & Parel, J.M. (2008). Role of the lens capsule on the mechanical accommodative response in a lens stretcher. *Invest Ophthalmol Vis Sci*, 49 (10), 4490-4496.

Zodpey, S., Ughade, S., Khanolkar, V., & Shrikhande, S. (1999). Dehydrational crisis from severe diarrhoea and risk of age-related cataract. *J Indian Med Assoc*, 97 (1), 13-15, 24.

APPENDIX 1

HUMAN SCIENCES ETHICAL COMMITTEE SUBMISSION

The following document details the application to the Human Sciences Ethical Committee, School of Life and Health Sciences, Aston University, for the approval of the investigation of anterior eye biometry on human subjects. The memorandum received which confirms the approval of the study is also included.

ASTON UNIVERSITY

PROJECT NO...06 / 12.....

THE SENATE

REG/00/174

HUMAN SCIENCE ETHICAL COMMITTEE

Application for approval of a research project involving human volunteers

Please read the enclosed guidelines before completing this form - in typescript or black ink - and return the form to: The Secretary of the Human Science Ethical Committee, Registry. If you intend to administer any substance or expose the volunteers to a physical procedure other than simple venepuncture **you must also submit an experimental protocol.**

Project title: Investigation of anterior eye biometry in patients undergoing cataract surgery or wearing a near vision correction

Outline Scientific Purpose/Objectives for Project and Potential Benefits:

To achieve a better understanding of the progression of cataract, the performance of implanted intraocular lenses and the effects of presbyopic correction.

Investigator(s):

Department/address:

Telephone:

(First name should be a member of Aston's Academic staff who will act as main contact)

...Dr J S Wolffsohn.....	...Vision Sciences Building.....4140.....
...Dr S A Naroo.....	...Vision Sciences Building.....4132.....
...Dr L N Davies.....	...Vision Sciences Building.....4152.....
...Mr N Gupta.....	...Vision Sciences Building.....4135.....
...Mr G A Gibson.....	...Vision Sciences Building.....3900.....
...Dr O A Hunt.....	...Vision Sciences Building.....4143.....
...Dr J Craig.....	...Vision Sciences Building.....3900.....
...Mr S Shah.....	...Midland Eye Institute, Solihull.....0121 712020...

A

Details of sponsoring/collaborating organisation (if any) NONE

1. Name:
2. Does the sponsoring/collaborating organisation provide insurance?
YES/NO*
3. If drugs are used, do any require a clinical trials certificate or clinical trials exemption certificate? YES/NO*

*If yes, please provide a copy of the certificate

B**Summary of Project**

- 1 Starting date: 1st June 2006
- 2 Duration: Three years
- 3 Location: Heart of England NHS Trust and Birmingham & Midland Eye Centre
Midland Eye Institute, Lode Lane, Solihull
Visions Sciences Building, Aston University, Birmingham
- 4 Physical procedures:

Assessment with recognised ophthalmic equipment -

Clinical tests to measure Visual Acuity, Reading Speed, Contrast Sensitivity and Amplitude of Accommodation (non-contact) following a refraction

Keeler Tearscope to assess tear quality (non-contact device)

Allows observation of a light source reflected from the tears – available commercially

Slit lamp (non-contact devices)

Allows viewing and digital imaging of the front of the eye using magnification and various illumination techniques. Commonly used in optometric and ophthalmic practice – available commercially

Oculus Pentacam Scheimplug camera (non-contact device)

Takes an image of a light section through the front of the eye – available commercially

Shin-Nippon, Bausch and Lomb, Topcon & Nidek Arc autorefractor/corneal topographers (non-contact devices)

Measures refractive error and corneal curvature by reflecting IR light off the retina and cornea, and measuring the resultant size and shape. Commonly used in optometric and ophthalmic practice – available commercially

Nidek OPD, Topcon & Tracey aberrometers (non-contact devices)

Measures the deviation of light passed through the optics of the eye – available commercially

Metrum ocular thermography (non-contact device)

Measures infra-red radiation reflected from the eye.

Zeiss IOLMaster (non-contact device)

Measures the partial coherence of a laser light reflected from the retina (software limited to 10 measures per eye per day) as well as anterior chamber depth, corneal curvature and iris diameter by visible light imaging – available commercially

Ultrasonography (contact device)

Measures the thickness of the cornea, the anterior chamber depth, lens thickness and axial length of the eye using high frequency reflected waves – used extensively in hospital eye departments and within the scope of optometric procedures – available commercially

100-Hue Colour Vision (non-contact technique)

Assesses colour discrimination by the arrangement of a series of coloured caps – available commercially

Humphreys Visual Field analysis (non-contact device)

Assesses light sensitivity in the central and peripheral field – available commercially

Zeiss Optical Coherence Tomographer (non contact device)

Images the anterior eye using assessment of reflected light – available commercially

All these techniques are commonly used in optometric and ophthalmic practice (except thermography which is used in general medical practice and is a non-contact sensing technique) and all are available commercially

5. Substances to be administered (a substance is anything other than normal food - chemical constituents of food stuffs, ethanol and variation of the diet should be included here) and method of delivery should be specified:

Tropicamide HCL 0.5%/1.0% - a topically applied synthetic antimuscarinic that has been used routinely in general optometric practice for many years and produces mydriasis and cycloplegia. Two drops of 0.5%/1% tropicamide will be administered with a five minute period between the drops. Cycloplegia occurs after approximately 15 minutes and the full amplitude of accommodation returns after 6 hours, although, mydriasis may remain for another hour or two. Patients will be warned not to drive, cycle or use heavy machinery for about 6 hours following the instillation if their vision has been adversely affected. Alternatively phenylephrine HCL 2.5% may be used as a dilating agent.

Proxymetacaine HCL 0.5% - a topical local anaesthetic used routinely in optometric practice for many years. One drop induces anaesthesia in approximately 20s, typically lasting 20 minutes. Patients will be warned not to rub their eyes for 30 minutes following instillation.

Pilocarpine HCL 1% - a topical miotic which stimulated the ciliary muscle to contract mimicking the bodies response to induce near eye focus.

Contact lenses – commercially available, worn for up to 2 weeks. Although complications can occur from contact lens wear, they are rare and do not occur in periods less than 1 month. The contact lenses will be fitted by a qualified Optometrist highly experienced in fitting and evaluating contact lenses. Spectacle lenses will be fitted as an alternative.

- 6 Psychological assessment:

NONE

- 7 Questionnaires: (only to be completed when project contains questionnaire(s) which fall within the types of questionnaire requiring HSEC approval [Guidelines D (3)])

NONE

C
Volunteers

- 1 Number of volunteers to be used: 1,000
- 2 Over what time span? Three years
- 3 Age of volunteers: 18 to 90 years old
- 4 Sex of volunteers: Mixed
- 5 Source: Volunteers from Solihull hospital, Midland Eye Institute and Vision Sciences at Aston University
- 6 Will payments be made to the volunteers and if so, how much will each be paid? Up to £70 will be paid to cover travel expenses / time of volunteers.
- 7 Are the volunteers patients or healthy volunteers? (If patients, give diagnosis, clinic/responsible practitioner).

There will be a mix of healthy volunteers and patients with cataract. The patients will be under the care of Solihull based Consultant Ophthalmologist, Mr Sunil Shah.

- 8 Will any volunteers be excluded and if so, on what grounds?
NO
- 9 Is the activity of the volunteer to be restricted in any way either before or after the procedure? (eg diet, driving)

Patients will be advised not to drive, cycle or use heavy machinery for 6 hours after the testing procedure if dilation is used to increase the size of small pupils. These are used routinely during ophthalmological assessment, so the patients will not be additionally inconvenienced

Also, patients will be advised not to rub their eyes for 30 minutes since the ultrasonography measurement requires instillation of short duration acting topical anaesthetic drop (these are used during routine ophthalmic assessment).

- 10 Consent: Please attach a copy of the consent form you intend to use, detailing how procedures and hazards will be explained.

D

Risk Assessment: *a thorough Risk Assessment of the project must be undertaken (including for example welfare issues arising from the procedure, and the possible risk of residual effects in volunteers and the consequences thereof).*

1. Please give full details of any hazards which could affect the health, safety or welfare of any volunteer, or any other person who might be harmed as a result of the experiment.

The induced mydriasis and cycloplegia may produce blurred vision and photophobia (glare). There is also a minimal risk of causing acute closed angle glaucoma. However, this condition has an incidence of 1 in 10,000 people over the age of 40. Driving is prohibited for about 6 hours after the session has concluded if dilation is required. Phenylephrine can cause dizziness, fast, irregular, or pounding heartbeat, increased sweating, increase in blood pressure, paleness and trembling although side effects are very rare with 2.5% topical instillation. However, it will not be instilled in patients with high blood pressure or children.

Ocular adverse reactions to proxymetacaine HCl are also rare. Sensitivity reactions have only been reported in repeated instillation of the drug. The allergic reaction manifests as marked epithelial stippling and slight stromal oedema. Conjunctival hyperaemia, slight puffiness of the eyelids, pain and lacrimation have also been reported in allergic reaction to proxymetacaine. Systemic effects of proxymetacaine are minimal if small volumes of the drug are used.

Pilocarpine HCL 1% side effects include an allergic reaction (difficulty breathing; closing of the throat; swelling of the lips, tongue, or face; or hives), difficulty breathing, irregular heartbeats, eye pain; or confusion or changes in mental status or behaviour Other, less serious side effects include: changes in vision, increased sweating, dizziness, headache, runny nose, nausea, redness of the face and neck, chills or an increased urge to urinate. Side effects are rare and minimal if small topical volumes of the drug are used.

2. What levels of risk are associated with these hazards ?

Low – see above. A consultant ophthalmologist will be available at all times and Optometrists are trained to use each of these drugs.

3. How do you propose to control the risks associated with these hazards?

All instruments will be used by qualified Optometric personnel or medically trained personnel To overcome the blurred vision and glare, the subjects will be advised to rest for a 1/2 to 1 hour after the drops are instilled. To minimise the very small risk of acute closed angle glaucoma, the subject's intraocular pressure and anterior chamber angles will be assessed before the tropicamide drops are instilled. The intraocular pressure will be recorded again after the drops have been instilled. An increase in the intraocular pressure of more than 5 mmHg indicates a possibility of acute angle glaucoma. In this case the subject would be closely monitored and referred immediately to Mr Sunil Shah or the eye department located at the nearest hospital, if required.

Any risks can be minimised by avoiding over dosage of the drug. The puncta can be occluded as a preventative measure against systemic absorption.

4. What criteria have you used to determine whether the risks are acceptable ?

All the instruments used are commercially available CE marked diagnostic equipment used routinely. Risks ascertained by reviewing ophthalmic literature.

5. Is there any precedent for these experiments? If so, please give details with references if possible.

Instillation of tropicamide a standard procedure in the optometric teaching programme and general open clinic for many years. Please see previous Ethical Committee records for acceptance of 97(K) May 1998; 87(vii) June 1987; 86B/87(x) February 1986 and 87(xi) June 1987, 00/N etc Autorefractor: e.g Screening of refractive error and axial length. Ref 01/D

Contact Lens Fitting:e.g. Quantifying Nearwork-Induced Transient Pseudo-Myopia in Human Eyes, Autonomic correlates of myopia onset and development in young adults and Investigation of tear film composition changes with age and the use of contact lenses
Thermography:Investigation of tear film composition changes with age and the use of contact lenses

6. Has this project been considered/is it being considered by any other Ethical Committee? If so, please give details and decision made.

Yes, NHS local ethics is currently being sought for any patients selected because of their link with the NHS or any part of the study to be conducted within the NHS

E
STATEMENT BY NAMED INVESTIGATORS, HEAD OF SCHOOL AND (if necessary) RESEARCH SUPERVISOR

I consider that the details given constitute a true summary of the project and that the hazards and potential risks to any volunteer are accurately described. The Principal Investigator is the main point of contact for the Human Sciences Ethical Committee, and accordingly should be a member of academic staff of the University (this implies that supervisors of research students will be the main point of contact)

Principal Investigator or.....date.....
Supervisor of Student

Investigator.....date.....

Investigator.....date.....

Investigator.....date.....

Investigator.....date.....

Head of School.....date.....
(or nominee)

The following should be attached:

- * volunteer consent form
- * insurance certificate (if available)
- * clinical trials certificate or clinical trials exemption certificate (if appropriate)
- * experimental protocol

APPENDIX 2
INFORMATION AND CONSENT FORMS FOR
EXPERIMENTAL PARTICIPANTS

The following documents are copies of the information and consent forms given to subjects participating in the study taking place in Chapter 5 of this thesis.

**Investigation of anterior eye shape in patients undergoing
cataract surgery or wearing a near vision correction**

Investigators involved

Dr J S W Wolffsohn *BSc(Hons), PhD, PGDipAdvClinOptom, PgC, MCOptom, FAAO, FIACLE, FBCLA*

Dr S A Naroo *BSc(Hons), MSc, PhD, MCOptom, FIACLE, FBCLA*

Dr L N Davies *BSc(Hons), PhD, MCOptom, FAAO*

Mr N Gupta *BSc(Hons), MCOptom*

Mr G A Gibson *BSc(Hons), MCOptom*

Dr O A Hunt *BSc(Hons), PhD, MCOptom, FBCLA*

Dr J Craig *BSc(Hons), PhD, MCOptom, FBCLA*

Mr S Shah *MB ChB, FRCS(Ed), FRCOphth, MD, FBCLA*

Dr Wolffsohn is a senior lecturer, Dr Naroo and Dr Davies are lecturers, Mr Gibson and Mr Gupta are postgraduate students, and Dr Hunt and Dr Craig are Research Fellows in Optometry at Aston University. Mr Shah is a consultant ophthalmologist (eye surgeon) at Heart of England NHS Trust and Birmingham & Midland Eye Centre and the Midland Eye Institute.

Description of project

To investigate the changes in the eye that occur prior to and with cataract surgery, including examining the effect of the implanted intraocular lens, contact lenses and spectacle lenses.

Explanation of procedures

Pictures and measurements will be taken of your eyes by qualified eye care practitioners using different commercially available instruments, as detailed below:

1. Reading and vision charts following optimisation of your best vision using lenses
2. Anterior eye imaging to assess the quality of the surgery and the health of the eye and tears (Tearscope, Thermography, Slit lamp and Scheimplug)
3. Measurement of the light passing through the optics of your eye to assess the quality of the refracting surfaces (autorefractometry, corneal topography and aberrometry)
4. Imaging of the position of the intraocular lens and refracting surfaces of the eye to assess their position before and after surgery (IOLMaster, Optical Coherence Tomography and Ultrasonography)
5. Colour vision assessment involving you arranging the order of coloured tiles
6. Light sensitivity involving you pressing a button every time you detect a series of lights.
7. A questionnaire examining how you find your vision before and after surgery.

We may use eye drops that make the pupil of the eye bigger or smaller. The action of the drops will last for around 6 hours and you should not drive, cycle or use heavy machinery in that time if your eyes become sensitive to bright lights or have difficulty focusing.

EXPLANATION AND CONSENT FORM FOR VOLUNTEER SUBJECTS

We may also use eye drops that numb the front of the eye. The action of the drops will last for 30 minutes and you should not rub your eyes in this time.

Contact lenses or spectacle lenses may be fitted (with your permission) to optimise your refractive correction for the measures we will be taking.

Statement of volunteer

I have read and understood the above explanation. I have had the opportunity to discuss it with at least one of the investigators and to ask any questions. I understand that I am free to withdraw from the study at any time. I understand that partaking in this experiment is not a requirement of my course of study or my treatment plan and that no sanctions will be taken against me if I refuse to participate or withdraw from the project. I understand that participation in this study does not replace the need for my regular eye examinations or eye appointments

I agree to take part in the above project.

Name of volunteer:.....

Signed:.....

Date:.....

APPENDIX 3
SOLIHULL NHS RESEARCH ETHICAL COMMITTEE
SUBMISSION

The following document details the application to the Solihull NHS Research Ethics Committee for the approval of the investigation of the KH3500 intraocular lens (2 year follow-up).

APPLICANT'S CHECKLIST

All studies except clinical trials of investigational medicinal products


REC Ref:	
Short Title of Study:	Two Year Follow-up of KH3500 Intraocular Lens
CI Name:	Mr Sunil Shah
Sponsor:	Aston University

Please complete this checklist and send it with your application

- ◆ Send ONE copy of each document (except where stated)
- ◆ ALL accompanying documents must bear version numbers and dates (except where stated)
- ◆ When collating please do NOT staple documents as they will need to be photocopied.

Document	Enclosed?	Date	Version	Office use
Covering letter on headed paper	<input type="radio"/> Yes <input type="radio"/> No			
NHS REC Application Form, Parts A&B	Mandatory			
NHS REC Application Form, Part C (SSA)	<input type="radio"/> Yes <input type="radio"/> No			
Research protocol or project proposal (6 copies)	Mandatory			
Summary C.V. for Chief Investigator (CI)	Mandatory			
Summary C.V. for supervisor (student research)	<input type="radio"/> Yes <input type="radio"/> No			
Research participant information sheet (PIS)	<input type="radio"/> Yes <input type="radio"/> No			
Research participant consent form	<input type="radio"/> Yes <input type="radio"/> No			
Letters of invitation to participants	<input type="radio"/> Yes <input type="radio"/> No			
GP/Consultant information sheets or letters	<input type="radio"/> Yes <input type="radio"/> No			
Statement of indemnity arrangements	<input type="radio"/> Yes <input type="radio"/> No			
Letter from sponsor	<input type="radio"/> Yes <input type="radio"/> No			
Letter from statistician	<input type="radio"/> Yes <input type="radio"/> No			
Letter from funder	<input type="radio"/> Yes <input type="radio"/> No			
Referees' or other scientific critique report	<input type="radio"/> Yes <input type="radio"/> No			
Summary, synopsis or diagram (flowchart) of protocol in non-technical language	<input type="radio"/> Yes <input type="radio"/> No			
Interview schedules or topic guides for participants	<input type="radio"/> Yes <input type="radio"/> No			
Validated questionnaire	<input type="radio"/> Yes <input type="radio"/> No			
Non-validated questionnaire	<input type="radio"/> Yes <input type="radio"/> No			
Copies of advertisement material for research participants, e.g. posters, newspaper adverts, website. For video or audio cassettes, please also provide the printed script.	<input type="radio"/> Yes <input type="radio"/> No			

WELCOME TO THE NHS RESEARCH ETHICS COMMITTEE APPLICATION FORM

An application form specific to your project will be created from the answers you give to the following questions.  Please read this guidance carefully before selecting your answers.

1. Is your project an audit or service evaluation?

Yes No

2. Select one research category from the list below:

- Clinical trials of investigational medicinal products (including phase 1 drug development)
- Clinical investigations or other studies of medical devices
- Other clinical trial or clinical investigation
- Research administering questionnaires/interviews for quantitative analysis, or using mixed quantitative/qualitative methodology
- Research involving qualitative methods only
- Research limited to working with human tissue samples and/or data

If your work does not fit any of these categories, select the option below:

Other research

2a. Select one category from the list below:

- Is this a clinical investigation of a medical device?
- Is this a performance evaluation of an in vitro diagnostic device?
- Is this a drug/device combination of both an investigational medical device and an investigational medicinal product?
- Is this a post-market surveillance study of a CE Marked product?

2b . Please answer the following questions:

- | | | |
|--|---------------------------|-------------------------------------|
| a) Does the study involve the use of any ionising radiation? | <input type="radio"/> Yes | <input checked="" type="radio"/> No |
| b) Will you be taking new human tissue samples? | <input type="radio"/> Yes | <input checked="" type="radio"/> No |
| c) Will you be using existing human tissue samples? | <input type="radio"/> Yes | <input checked="" type="radio"/> No |

3. Is your research confined to one site?

Yes No

4. Does your research involve work with prisoners?

Yes No

5. Does your research involve adults unable to consent for themselves through physical or mental incapacity?

Yes No

6. Is the study, or any part of the study, being undertaken as an educational project?

Yes No

NHS Research Ethics Committee **NHS**
Application form for a clinical investigation of a medical device

This form should be completed **by the Chief Investigator**, after reading the guidance notes. See glossary for clarification of different terms in the application form.

Short title and version number: (maximum 70 characters – this will be inserted as header on all forms)

Two Year Follow-up of KH3500 Intraocular Lens

Name of NHS Research Ethics Committee to which application for ethical review is being made:

Solihull Research Ethics Committee

Project reference number from above REC:

Submission date:

PART A: Introduction

A1. Title of the research

Full title: Follow-up Evaluation of Patients Implanted with the KH-3500 Accommodating Intraocular lens

Key words: intraocular lens, accommodating, presbyopia, complications

A2. Chief Investigator



Aston University

Content has been removed for copyright reasons

A copy of a current CV (maximum 2 pages of A4) for the Chief Investigator must be submitted with the application

A3. Proposed study dates and duration

Start date: 23/09/2006

End date: 01/06/2007

Duration: Years: ; Months: 8

A4. Primary purpose of the research: *(Tick as appropriate)*

- Commercial product development and/or licensing
- Publicly funded trial or scientific investigation
- Educational qualification
- Establishing a database/data storage facility
- Other

A6. Does this research require site-specific assessment (SSA)? *(Advice can be found in the guidance notes on this topic.)*

Yes No

If No, please justify:

Facilitating participant recruitment of patients implanted with the KH3500 intraocular lens at least 2 years ago. Patients will be identified from NHS lists by the Principal Investigator and appropriate patients will get a letter inviting them to attend an appointment to examine their visual function and the fit of the lens using non-invasive measures. This will take place outside the NHS and ethics approval has already been given by Aston University.

If Yes, Part C of the form will need to be completed for each research site and submitted for SSA to the relevant Local Research Ethics Committee. Do not submit Part Cs for other sites until the application has been booked for review and validated by the main Research Ethics Committee.

Management approval to proceed with the research will be required from the R&D Department for each NHS care organisation in which research procedures are undertaken. This applies whether or not the research is exempt from SSA.

PART A: Section 1**A7. What is the principal research question/objective?** *(Must be in language comprehensible to a lay person.)*

Whether two years after implantation, there have been any complications associated with the KH3500 intraocular lens

A8. What are the secondary research questions/objectives? *(If applicable, must be in language comprehensible to a lay person.)*

Whether the KH3500 intraocular lens allows any restoration of eye focus two years after implantation
Whether the KH3500 intraocular lens allows good visual function two years after implantation

A9. What is the scientific justification for the research? What is the background? Why is this an area of importance? *(Must be in language comprehensible to a lay person.)*

A cataract occurs when the natural lens of the eye, playing a major role in focusing light and producing sharp images, becomes cloudy and hardens, resulting in a loss of visual function. Left untreated, cataracts can cause preventable blindness.

During Cataract surgery the natural lens is removed and a man-made lens (IOL) is implanted in its place. Once placed the IOL has a set and fixed focal point, which in most cases requires the patient to use glasses either for near or for distance.

The KH3500 AIOL (Accommodating Intra Ocular Lens) is a lens implanted during Cataract surgery. The AIOL replaces a standard IOL and uses the same implant procedure. We have previously shown some improved ability of the eyes fitted with the AIOL to focus over a range of distance between distance and near without the use of spectacles or contact lenses, compared to eyes fitted with a conventional IOL over a 6 month period after surgery. However, it is important to assess whether there are any long-term complications associated with the AIOL and whether the focusing ability is maintained.

A10. Give a full summary of the purpose, design and methodology of the planned research, including a brief explanation of the theoretical framework that informs it. It should be clear exactly what will happen to the research participant, how many times and in what order. Describe any involvement of research participants, patient groups or communities in the design of the research.

This section must be completed in language comprehensible to the lay person. It must also be self-standing as it will be replicated in any applications for site-specific assessment on Part C. Do not simply reproduce or refer to the protocol. Further guidance is available in the guidance notes.

Purpose.

To assess whether any complications have occurred over 2 years since a patient had cataract surgery and implantation of the KH3500 accommodating intraocular lens, and whether this lens allows the patient to see or focus better than other lens types.

Design

Patients will be recruited from the NHS by letter, inviting them to have a free follow-up evaluation of their eye in which the KH3500 was implanted. A study information sheet will be enclosed highlighting that this will be a 30 minute appointment and travel expenses will be reimbursed.

Methodology

The patient will be asked about any complication that have occurred in the implanted eye since the cataract surgery. The lens will be imaged using non-contact devices based on photography. Visual function will be assessed with measurements of visual acuity, contrast sensitivity, autorefractometry (which measures the patient's refractive prescription and ability to focus), aberrometry (which measures the path of light as it passes through the eye) and a basic questionnaire.

Framework

Patients implanted with a KH3500 at least 2 years ago in the Solihull and Birmingham area will be recruited by letter. The measurements will take place outside the NHS at a private ophthalmology clinic (Midland Eye Institute) and ethical approval has been granted by Aston University.

A11. Will any intervention or procedure, which would normally be considered a part of routine care, be withheld from the research participants?

Yes No

A12. Give details of any clinical intervention(s) or procedure(s) to be received by research participants over and above those which would normally be considered a part of routine clinical care. (These include uses of medicinal products or devices, other medical treatments or assessments, mental health interventions, imaging investigations and taking samples of human biological material.)

Additional Intervention	Average number per participant		Average time taken (mins/hours/days)	Details of additional intervention or procedure, who will undertake it, and what training they have received.
	Routine Care	Research		
Other		1	30mins	Autorefracton, aberrometry/topography and Optical Coherence Tomography, all using commercially available, CE marked devices. Undertaken by UK qualified Optometrists who are experienced in using these techniques in clinical and research eye-care practice.

A13. Give details of any non-clinical research-related intervention(s) or procedure(s). (These include interviews, non-clinical observations and use of questionnaires.)

Additional Intervention	Average number per participant	Average time taken (mins/hours/days)	Details of additional intervention or procedure, who will undertake it, and what training they have received.
Other Questionnaire	1	5min	Questionnaire on near vision to assess well the patient feels the lens is performing

A14. Will individual or group interviews/questionnaires discuss any topics or issues that might be sensitive, embarrassing or upsetting, or is it possible that criminal or other disclosures requiring action could take place during the study (e.g. during interviews/group discussions, or use of screening tests for drugs)?

Yes No

The Information Sheet should make it clear under what circumstances action may be taken

A15. What is the expected total duration of participation in the study for each participant?

30 minutes

A16. What are the potential adverse effects, risks or hazards for research participants either from giving or withholding medications, devices, ionising radiation, or from other interventions (including non-clinical)?

None – non-interventional

A17. What is the potential for pain, discomfort, distress, inconvenience or changes to lifestyle for research participants?

None

A18. What is the potential for benefit to research participants?

A knowledge that their eye remains healthy or appropriate referral if this is not the case

A19. What is the potential for adverse effects, risks or hazards, pain, discomfort, distress, or inconvenience to the researchers themselves? (if any)

None

A20. How will potential participants in the study be (i) identified, (ii) approached and (iii) recruited?

Give details for cases and controls separately if appropriate:

Potential participants are known from NHS surgical lists. They will be written to by the Consultant Ophthalmologist principal investigator. Information on the study will be included. If they are interested in taking part, they can ring the number given in the letter and informed consent will be gained when they attend the appointment.

A21. Where research participants will be recruited via advertisement, give specific details.

Not Applicable

If applicable, enclose a copy of the advertisement/radio script/website/video for television (with a version number and date).

A22. What are the principal inclusion criteria? (Please justify)

Patients implanted with a KH3500 'accommodating' intraocular lens at least 2 years ago.

A23. What are the principal exclusion criteria? (Please justify)

None

A24. Will the participants be from any of the following groups? (Tick as appropriate)

- Children under 16
- Adults with learning disabilities
- Adults who are unconscious or very severely ill
- Adults who have a terminal illness
- Adults in emergency situations
- Adults with mental illness (particularly if detained under Mental Health Legislation)
- Adults with dementia
- Prisoners
- Young Offenders
- Adults in Scotland who are unable to consent for themselves
- Healthy Volunteers

- Those who could be considered to have a particularly dependent relationship with the investigator, e.g. those in care homes, medical students
- Other vulnerable groups

Justify their inclusion.

A25. Will any research participants be recruited who are involved in existing research or have recently been involved in any research prior to recruitment?

- Yes No Not Known

If Yes, give details and justify their inclusion. If Not Known, what steps will you take to find out?

A26. Will informed consent be obtained from the research participants?

- Yes No

If Yes, give details of who will take consent and how it will be done. Give details of any particular steps to provide information (in addition to a written information sheet) e.g. videos, interactive material.

If participants are to be recruited from any of the potentially vulnerable groups listed in A24, give details of extra steps taken to assure their protection. Describe any arrangements to be made for obtaining consent from a legal representative.

If consent is not to be obtained, please explain why not.

To be obtained by the Optometrist performing the measures after confirmation that they have understood the details on the information sheet sent to them by post.

Copies of the written information and all other explanatory material should accompany this application.

A27. Will a signed record of consent be obtained?

- Yes No

If Yes, attach a copy of the information sheet to be used, with a version number and date.

A28. How long will the participant have to decide whether to take part in the research?

At least 2 weeks

A29. What arrangements have been made for participants who might not adequately understand verbal explanations or written information given in English, or who have special communication needs? (e.g. translation, use of interpreters etc.)

The use of translators and interpreters. Patients will be excluded if informed consent is not possible.

A30. What arrangements are in place to ensure participants receive any information that becomes available during the course of the research that may be relevant to their continued participation?

Not applicable as only a single study visit which is non-interventional

A31. Does this study have or require approval of the Patient Information Advisory Group (PIAG) or other bodies with a similar remit? *(see the guidance notes)*

Yes No

A32a. Will the research participants' General Practitioner be informed that they are taking part in the study?

Yes No

If Yes, enclose a copy of the information sheet/letter for the GP with a version number and date.

A32b. Will permission be sought from the research participants to inform their GP before this is done?

Yes No

If No to either question, explain why not

It should be made clear in the patient information sheet if the research participant's GP will be informed.

A33. Will individual research participants receive any payments for taking part in this research?

Yes No

A34. Will individual research participants receive *reimbursement of expenses* or any other *incentives or benefits* for taking part in this research?

Yes No

*If Yes, indicate how much and on what basis this has been decided:
Travel expenses will be reimbursed.*

A35. What arrangements have been made to provide indemnity and/or compensation in the event of a claim by, or on behalf of, participants for negligent harm?

Private medical indemnity cover at the Midland Eye Institute.

Please forward copies of the relevant documents.

A36. What arrangements have been made to provide indemnity and/or compensation in the event of a claim by, or on behalf of, participants for non-negligent harm?

Private medical indemnity cover at the Midland Eye Institute.

Please forward copies of the relevant documents.

A37. How is it intended the results of the study will be reported and disseminated? (Tick as appropriate)

- Peer reviewed scientific journals
- Internal report
- Conference presentation
- Other publication
- Submission to regulatory authorities
- Access to raw data and right to publish freely by all investigators in study or by Independent Steering Committee on behalf of all investigators
- Written feedback to research participants
- Presentation to participants or relevant community groups
- Other/none e.g. Cochrane Review, University Library

A38. How will the results of research be made available to research participants and communities from which they are drawn?

By request

A39. Will the research involve any of the following activities at any stage (including identification of potential research participants)? (Tick as appropriate)

- Examination of medical records by those outside the NHS, or within the NHS by those who would not normally have access
- Electronic transfer by magnetic or optical media, e-mail or computer networks
- Sharing of data with other organisations
- Export of data outside the European Union
- Use of personal addresses, postcodes, faxes, e-mails or telephone numbers
- Publication of direct quotations from respondents
- Publication of data that might allow identification of individuals
- Use of audio/visual recording devices
- Storage of personal data on any of the following:
 - Manual files including X-rays
 - NHS computers
 - Home or other personal computers
 - University computers
 - Private company computers
 - Laptop computers

Further details:

Data will be stored in a spreadsheet managed by the Principal Investigator and identifying patients only by their initials and date of birth.

A40. What measures have been put in place to ensure confidentiality of personal data? Give details of whether any encryption or other anonymisation procedures have been used and at what stage:

The spreadsheet will instrument files will only identify the patient by initials and date of birth. The spreadsheet will be password protected (Microsoft encryption).

A41. Where will the analysis of the data from the study take place and by whom will it be undertaken?

By the listed investigators at Aston University

A42. Who will have control of and act as the custodian for the data generated by the study?

The Principal Investigator

A43. Who will have access to the data generated by the study?

Only the listed investigators

A44. For how long will data from the study be stored?

10 Years Months

Give details of where they will be stored, who will have access and the custodial arrangements for the data:
Stored at Aston University, with access only to the listed investigators and held by the Principal investigator

A45-1. How has the scientific quality of the research been assessed? (Tick as appropriate)

- Independent external review
- Review within a company
- Review within a multi-centre research group
- Internal review (e.g. involving colleagues, academic supervisor)
- None external to the investigator
- Other, e.g. methodological guidelines (*give details below*)

Justify and describe the review process and outcome. If the review has been undertaken but not seen by the researcher, give details of the body which has undertaken the review:
Review typical of non-interventional study

If you are in possession of any referees' comments or other scientific critique reports relevant to the proposed research, these must be enclosed with the application.

A45-2. Has the protocol submitted with this application been the subject of review by a statistician independent of the research team? (Select one of the following)

- Yes – copy of review enclosed
- Yes – details of review available from the following individual or organisation (give contact details below)
- No – justify below

Basic statistics only applicable (summary statistics and correlations). The research team has extensive research experience in similar studies and can access advice from the University statistical team

A48. What is the primary outcome measure for the study?

Complications reported post surgery

A49. What are the secondary outcome measures? (if any)

Range of eye focus and visual function.

A50. How many participants will be recruited?

If there is more than one group, state how many participants will be recruited in each group. For international studies, say how many participants will be recruited in the UK and in total.

100

A51. How was the number of participants decided upon?

This is approximately the number of patients implanted with a KH3500 'accommodative' intraocular lens at least 2 years ago.

If a formal sample size calculation was used, indicate how this was done, giving sufficient information to justify and reproduce the calculation.

A52. Will participants be allocated to groups at random?

Yes No

A53. Describe the methods of analysis (statistical or other appropriate methods, e.g. for qualitative research) by which the data will be evaluated to meet the study objectives.

Average and standard deviation summary statistics. Basic correlation of eye focus range and other eye characteristics.

A54. Where will the research take place? (Tick as appropriate)

- UK
 Other states in European Union
 Other countries in European Economic Area
 Other

If Other, give details:

A55. Has this or a similar application been previously rejected by a Research Ethics Committee in the UK, the European Union or the European Economic Area?

Yes No

A56. In how many and what type of host organisations (NHS or other) in the UK is it intended the proposed study will take place?

Indicate the type of organisation by ticking the box and give approximate numbers if known:

- | | Number of organisations |
|--|-------------------------|
| <input type="checkbox"/> Acute teaching NHS Trusts | |
| <input type="checkbox"/> Acute NHS Trusts | |
| <input type="checkbox"/> NHS Primary Care Trusts or Local Health Boards in Wales | |
| <input type="checkbox"/> NHS Trusts providing mental healthcare | |
| <input type="checkbox"/> NHS Health Boards in Scotland | |
| <input type="checkbox"/> HPSS Trusts in Northern Ireland | |
| <input type="checkbox"/> GP Practices | |
| <input type="checkbox"/> NHS Care Trusts | |
| <input type="checkbox"/> Social care organisations | |
| <input type="checkbox"/> Prisons | |
| <input checked="" type="checkbox"/> Independent hospitals | 1 |
| <input type="checkbox"/> Educational establishments | |
| <input type="checkbox"/> Independent research units | |
| <input type="checkbox"/> Other (give details) | |

Other:

A57. What arrangements are in place for monitoring and auditing the conduct of the research?

Journal peer review process

Will a data monitoring committee be convened?

Yes No

If Yes, details of membership of the data monitoring committee (DMC), its standard operating procedures and summaries of reports of interim analyses to the DMC must be forwarded to the NHS Research Ethics Committee which gives a favourable opinion of the study.

What are the criteria for electively stopping the trial or other research prematurely?

Not applicable as non-interventional study

A58. Has external funding for the research been secured?

Yes No

If Yes, give details of funding organisation(s) and amount secured and duration:

Content has been removed for copyright reasons

Organisation:

Address:

Post Code:

UK contact:

Telephone:

E-mail:

Amount (£):

A59. Has the funder of the research agreed to act as sponsor as set out in the Research Governance Framework?

Yes No

Has the employer of the Chief Investigator agreed to act as sponsor of the research?

Yes No

Sponsor (must be completed in all cases)

Name of organisation which will act as sponsor for the research:

Aston University

Status:

NHS or HPSS care organisation Academic Pharmaceutical industry Medical device industry Other

If Other, please specify:

Address: Aston Triangle
Birmingham
Post Code: B4 7ET
Telephone: 0121 204 4140
E-mail: j.s.w.wolffsohn@aston.ac.uk

Fax: 0121 204 4048

The responsibilities of the sponsor may be shared between co-sponsors. If this applies, name the lead sponsor for the REC application in this box and enclose a letter giving further details of co-sponsors and their responsibilities.

Sponsor's UK contact point for correspondence with the main REC

Title: Forename/Initials: Surname:
Address:
Post Code: Fax:
Telephone:
E-mail:

A60. Has any responsibility for the research been delegated to a subcontractor?

Yes No

A61. Will individual *researchers* receive any personal payment over and above normal salary for undertaking this research?

Yes No

A62. Will individual *researchers* receive any other benefits or incentives for taking part in this research?

Yes No

A63. Will the host organisation or the researcher's department(s) or institution(s) receive any payment or benefits in excess of the costs of undertaking the research?

Yes No

A64. Does the Chief Investigator or any other investigator/collaborator have any direct personal involvement (e.g. financial, share-holding, personal relationship etc.) in the organisation sponsoring or funding the research that may give rise to a possible conflict of interest?

Yes No

A65. Other relevant reference numbers if known*(give details and version numbers as appropriate):*

Applicant's/organisation's own reference number, e.g. R&D (if available): KH3500-2yr

Sponsor's/protocol number:

Funder's reference number:

International Standard Randomised Controlled Trial Number (ISRCTN):

European Clinical Trials Database (EudraCT) number:

Project website:

A66. Other key investigators/collaborators*(all grant co-applicants should be listed)*

Title:

Post:

Qualifications:

Organisation:

Address:

Postcode:

E-mail:

Title:



Aston University

Content has been removed for copyright reasons

Post:
Qualifications:
Organisation:
Address:

Postcode:
E-mail:

Title:

Post:
Qualifications:
Organisation:
Address:

Postcode:
E-mail:

Title:

Post:
Qualifications:
Organisation:
Address:

Postcode:
E-mail:

Title:

Post:
Qualifications:
Organisation:
Address:

Postcode:
E-mail:



Aston University

Content has been removed for copyright reasons



Aston University

Content has been removed for copyright reasons

A67. If the research involves a specific intervention, (e.g. a drug, medical device, dietary manipulation, lifestyle change etc.), what arrangements are being made for continued provision of this for the participant (if appropriate) once the research has finished?

Not Applicable

PART A: Summary of Ethical Issues

A68. What do you consider to be the main ethical issues which may arise with the proposed study and what steps will be taken to address these?

The main ethical issue is contacting the patient, but taking part is optional and past studies have shown patients to appreciate the option of further non-invasive follow up.

PART B: Section 2 – Investigation of medical devices**1. Give details of the medical device(s) to be used in the study**

Device description: KH3500 'accommodating' intracocular lens
 Manufacturer: Lenstec (Florida)
 Use: For crystalline lens replacement following cataract surgery
 Length of time since device came into use: 3 years * Does the device have a CE mark? Yes No

* For all products with CE mark please attach instructions for use.

2. Does the study involve the use of a *new* medical device or *new* implantable material or the use of an existing product outside the terms of its CE market intended purpose?

Yes No

In addition to the instructions for use, the following details should be provided where applicable:

- Description of new device, materials, method of use or operation and a summary of the intended purpose
- Composition of any new implantable materials, including summary of biocompatibility findings from studies to date
- If already CE marked, a summary of any proposed changes to the CE marked intended purpose

3. For electrical devices give summarised details of acceptance and safety testing**4. Is a medical device or other commercial company arranging this trial?**

Yes No

- a) Is this trial a clinical investigation requiring notification to the MHRA? Yes No
 b) Does the company have a Notice of No Objection from the MHRA? Yes No
 c) Has MHRA approval been applied for but not yet received? Yes No

Note: An application can be made prior to receipt of a valid Notice of No Objection from MHRA. The Notice will be issued subject to the sponsor subsequently receiving a favourable opinion. There is no requirement for a valid Notice of No Objection to be provided to relevant ethics committee before the research can be given a favourable opinion.

5. Have any of the medical devices been transferred from one organisation (legal entity) to another for the purpose of this trial?

Yes No

Give details:

6. In cases of equipment or medical devices, what arrangements have been made with the manufacturer to provide indemnity?

This is a CE marked product and on-label use. We are just evaluating the lens performance of already implanted lenses and the company has agreed to fund patient travel imbursement and staff costs, but has no say in the conduct of the study or dissemination of the results.

Enclose a copy of the relevant correspondence, with a version number and date.

PART B: Section 7 – Declaration

- The information in this form is accurate to the best of my knowledge and belief and I take full responsibility for it.
- I undertake to abide by the ethical principles underlying the Declaration of Helsinki and good practice guidelines on the proper conduct of research.
- If the research is approved I undertake to adhere to the study protocol, the terms of the full application of which the main REC has given a favourable opinion and any conditions set out by the main REC in giving its favourable opinion.
- I undertake to seek an ethical opinion from the main REC before implementing substantial amendments to the protocol or to the terms of the full application of which the main REC has given a favourable opinion.
- I undertake to submit annual progress reports setting out the progress of the research.
- I am aware of my responsibility to be up to date and comply with the requirements of the law and relevant guidelines relating to security and confidentiality of patient or other personal data, including the need to register when necessary with the appropriate Data Protection Officer.
- I understand that research records/data may be subject to inspection for audit purposes if required in future.
- I understand that personal data about me as a researcher in this application will be held by the relevant RECs and their operational managers and that this will be managed according to the principles established in the Data Protection Act.
- I understand that the information contained in this application, any supporting documentation and all correspondence with NHS Research Ethics Committees or their operational managers relating to the application, will be subject to the provisions of the Freedom of Information Acts. The information may be disclosed in response to requests made under the Acts except where statutory exemptions apply.

Signature:

Date: (dd/mm/yyyy)

Print Name: Mr Sunil Shah

APPENDIX 4

INFORMATION AND CONSENT FORMS FOR
EXPERIMENTAL PARTICIPANTS

The following documents are copies of the information and consent forms given to subjects participating in the study taking place in Chapter 6 of this thesis.

PATIENT INFORMATION SHEET

Solihull Hospital

Lode Lane, Solihull

West Midlands

B91 2JL

Tel: 0121 424 2000

Fax: 0121 424 5356

Minicom: 0121 424 1401

www.heartofengland.nhs.uk

Part 1.

Study title

“Follow-up Evaluation of Patients implanted with the KH-3500 Accommodating Intraocular Lens.”

Invitation paragraph

You are being invited to take part in a research study. Before you decide it is important for you to understand why the research is being done and what it will involve. Please take time to read the following information carefully. Talk to others about the study if you wish.

- Part 1 tells you the purpose of this study and what will happen to you if you take part.
- Part 2 gives you more detailed information about the conduct of the study.

Ask us if there is anything that is not clear or if you would like more information. Take time to decide whether or not you wish to take part.

What is the purpose of the study?

A cataract occurs when the natural lens of the eye, playing a major role in focusing light and producing sharp images, becomes cloudy and hardens, resulting in a loss of visual function. Left untreated, cataracts can cause preventable blindness.

You have had cataract surgery, where your natural lens was removed and a man-made intraocular lens (IOL) was implanted in its place. Your eye has been implanted with a newer type of intraocular lens and we want to know how well it is performing for you.

Why have I been chosen?

This is because you have had a certain type of special intraocular lens (KH-3500) implanted in your eye after cataract surgery a couple of years ago. We are looking to study 100 similar individuals over the next few months.

Do I have to take part?

‘No. It is up to you to decide whether or not to take part. This information sheet is yours to keep and you will be asked to sign the enclosed consent form. You are still free to withdraw at any time and without giving a reason. A decision to withdraw at any time, or a decision not to take part, will not affect the standard of care you receive’.

What will happen to me if I take part?

If you give your informed consent, we will invite you to attend an appointment. We will assess your vision and eye focus, ask you to complete a questionnaire on how you feel your vision is since the surgery and we will use some photographic techniques to image the intraocular lens in your eye. The procedures used to test your visual function are very similar to those used by opticians. The complete procedure should not take more than 30 minutes. In addition, your travel expenses will be paid with a £50 reimbursement.

Solihull Hospital

Lode Lane, Solihull

West Midlands

B91 2JL

Tel: 0121 424 2000

Fax: 0121 424 5356

Minicom: 0121 424 1401

www.heartofengland.nhs.uk

What are the possible adverse effects?

As this study does not involve any additional surgery, medication or invasive techniques, there are no known risks.

What are the possible benefits of taking part?

The study team will check your eyes to ensure that the implanted lens has remained healthy.

What if there is a problem?

If you have any problems with the conduct of the study, you can contact your surgeon on 0121 711 2020 or alternatively the hospital complaints department (0121 424 1212), either of which will arrange for your enquiry to be investigated.

Will my taking part in the study be kept confidential?

'Yes. All the information about your participation in this study will be kept confidential. See part 2.



Aston University

Content has been removed due to copyright restrictions

This completes Part 1 of the Information Sheet.

If the information in Part 1 has interested you and you are considering participation, please continue to read the additional information in Part 2 before making any decision.

Solihull Hospital

Lode Lane, Solihull

West Midlands

B91 2JL

Part 2

What will happen if I don't want to carry on with the study?

You may withdraw from the study at any time.

Tel: 0121 424 2000

Fax: 0121 424 5356

Minicom: 0121 424 1401

www.heartofengland.nhs.uk

Complaints:

If you have a concern about any aspect of this study, you should ask to speak with the researchers who will do their best to answer your questions (0121 711 2020). If you remain unhappy and wish to complain formally, you can do this through the NHS Complaints Procedure. Details can be obtained from the hospital.

Harm:

The study is covered by Midland Eye Institute insurance, in the exceptional circumstances that something should go wrong and you are harmed by the research study.

Will my taking part in this study be kept confidential?

All information which is collected about you during the course of the research will be kept strictly confidential. Any information about you which leaves the hospital/surgery will have your name and address removed so that you cannot be recognised from it. The data will be stored securely in a filing cabinet and on a computer, only accessible to the researchers. It will only be used for the purposes of the research study, being stored for the recommended 10 years following collection. The consent form seeks your permission to allow access to your medical records and to the information collected about you in the course of the study. Our procedures for handling, processing, storage and destruction of your data are compliant with the Data Protection Act 1998.

Involvement of the General Practitioner/Family doctor (GP)

Your own GP will be notified of your participation in this trial, if you give consent.

What will happen to the results of the research study?

The results from this study will be used to improve cataract surgery of the future and as such, the results will be presented and published to the academic community. You and your results will not be identifiable in any way. If you would like information on the results of the study, please let the researcher know.

Who is organising and funding the research?

This study has been organised by Aston University.

Who has reviewed the study?

This study was given a favourable ethical opinion for conduct in the NHS by the Solihull Research Ethics Committee.

This copy of the information sheet is yours to keep and a signed copy of the consent form will be returned to you. Thank you for considering taking part and taking the time to read this sheet.

CONSENT FORM

Patient Identification Number for this trial:

Title of Project: Follow-up Evaluation of Patients implanted with the KH-3500 Accommodating Intraocular Lens

Name of Researcher: Mr George Gibson

Please initial box

1. I confirm that I have read and understand the information sheet dated 22/10/2006 (version 3.0) for the above study. I have had the opportunity to consider the information, ask questions and have had these answered satisfactorily.
2. I understand that my participation is voluntary and that I am free to withdraw at any time, without giving any reason, without my medical care or legal rights being affected.
3. I understand that relevant sections of any of my medical notes and data collected during the study, may be looked at by responsible individuals from Aston University, from regulatory authorities or from the NHS Trust, where it is relevant to my taking part in this research. I give permission for these individuals to have access to my records.
4. I agree to my GP being informed of my participation in the study.
5. I agree to take part in the above study.

Name of Patient

Date

Signature

Researcher

Date

Signature

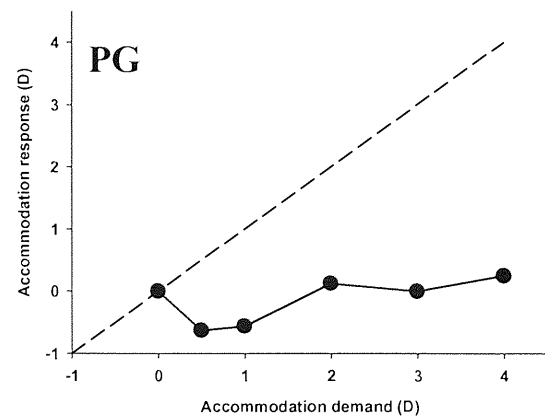
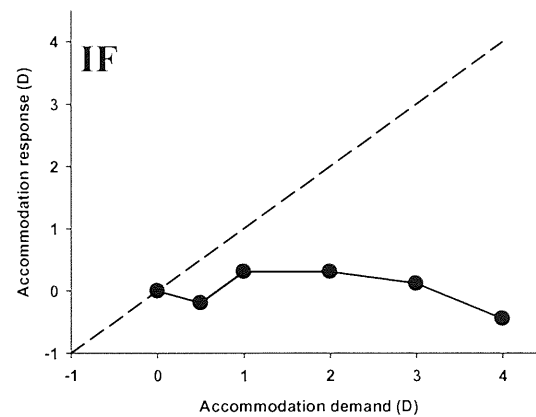
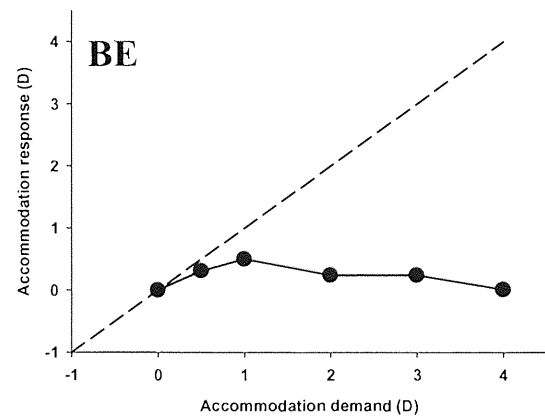
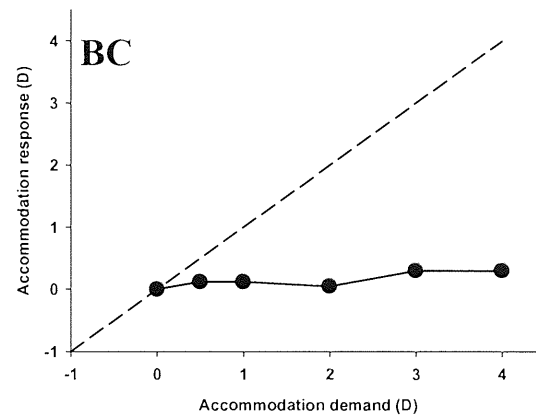
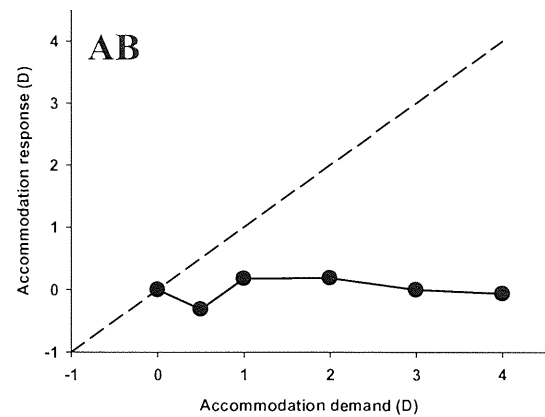
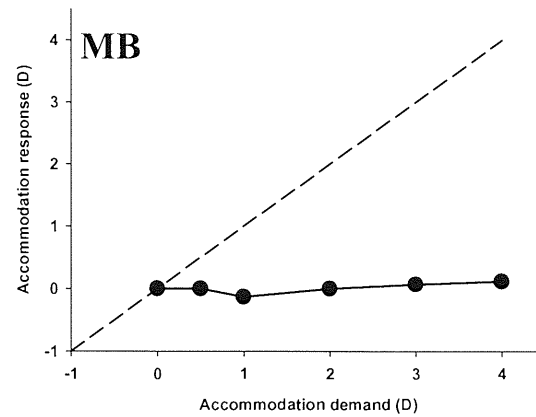
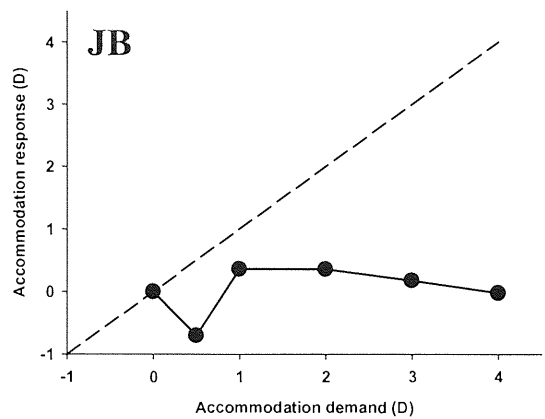
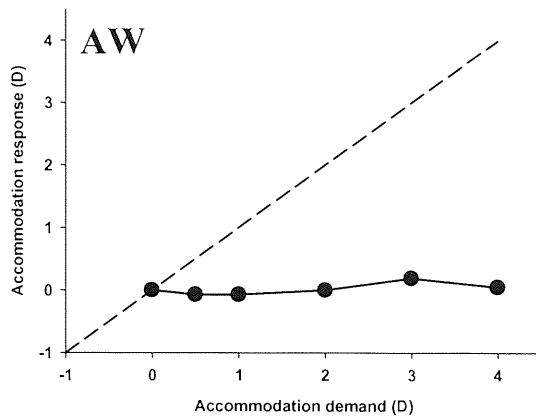
When completed, 1 copy for patient, 1 copy for researcher site file, 1 (original) to be kept in medical notes

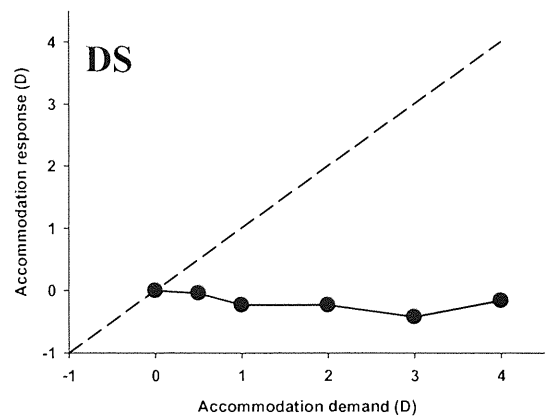
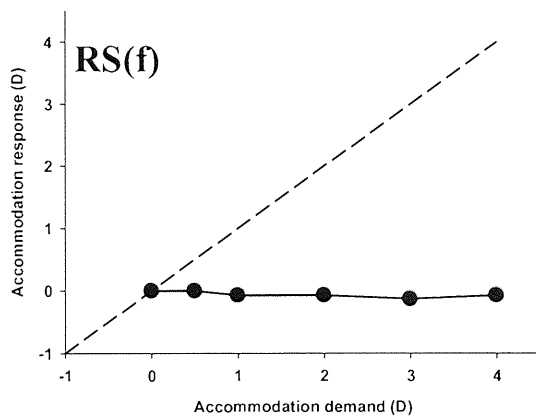
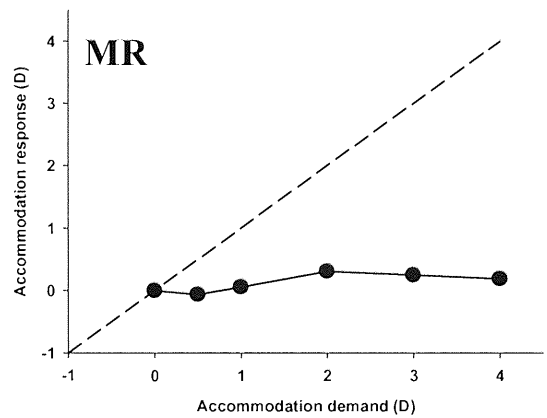
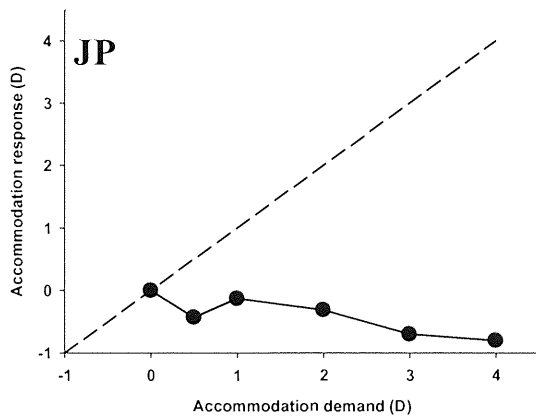
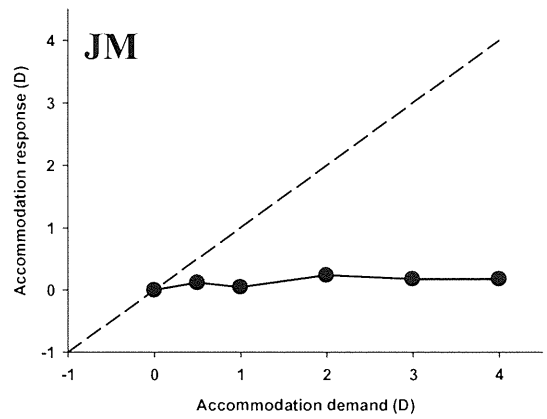
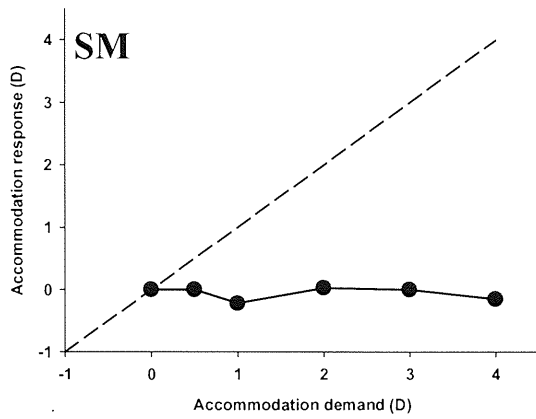
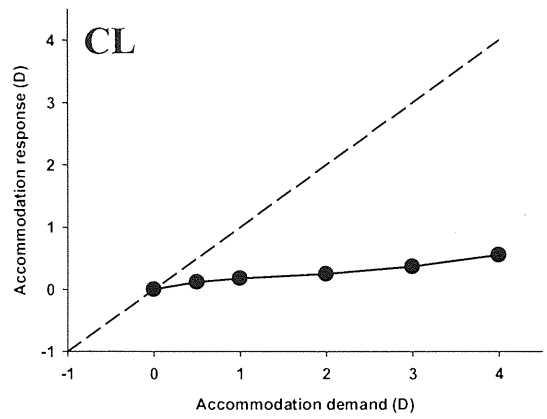
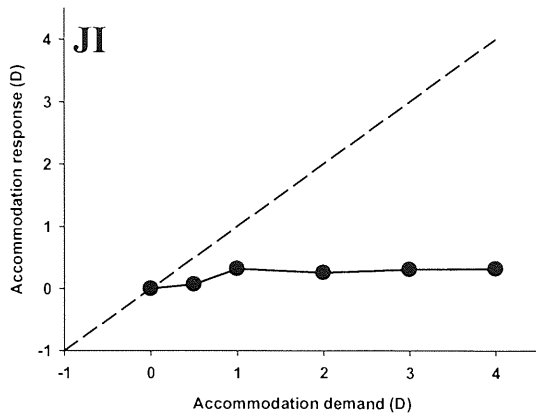
APPENDIX 5

STIMULUS-RESPONSE CURVES

Individual stimulus-response curves for 36 subjects in Chapter 6. Plots are categorised by eye measured: right ($n = 18$) and left ($n = 18$).

A5.1 Right eyes





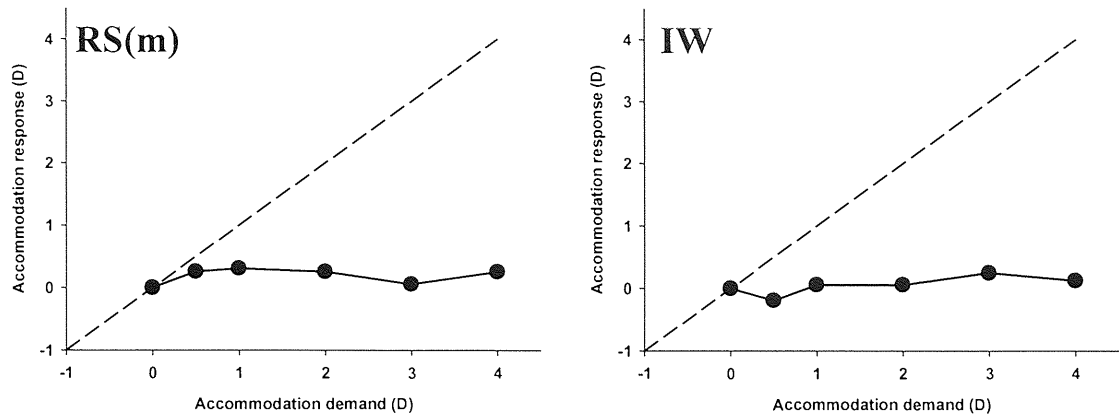
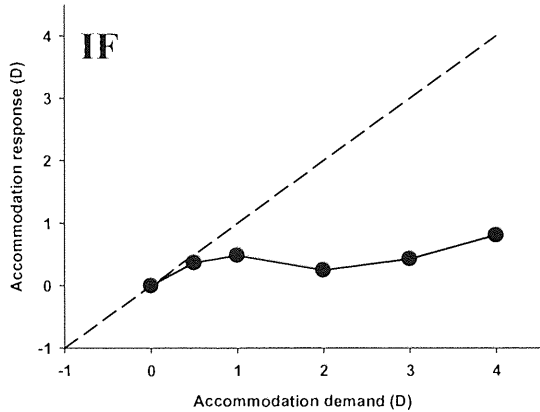
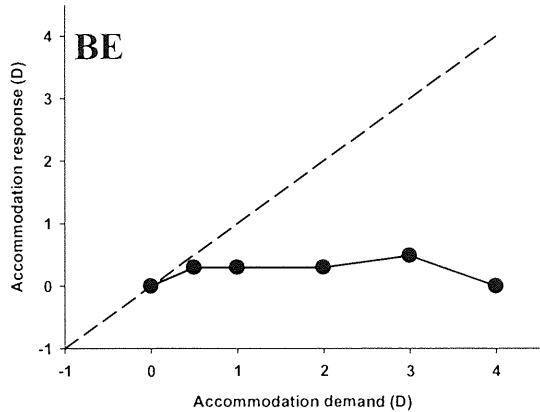
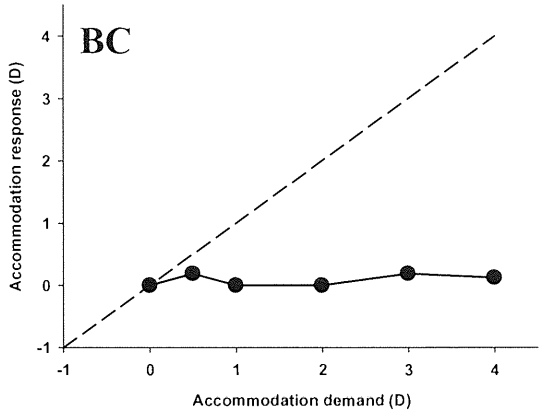
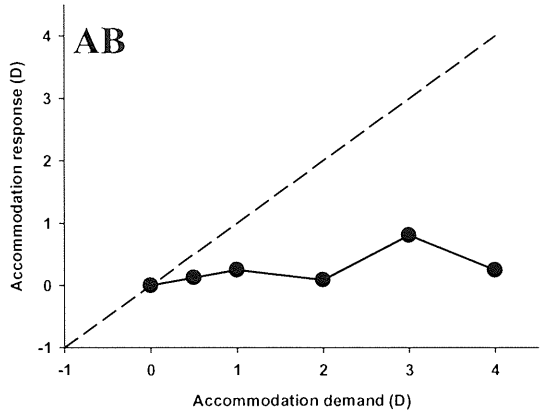
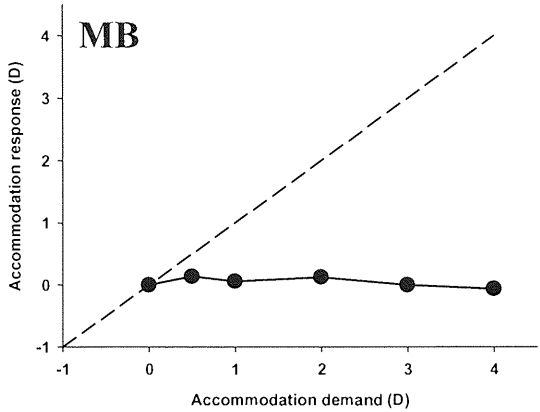
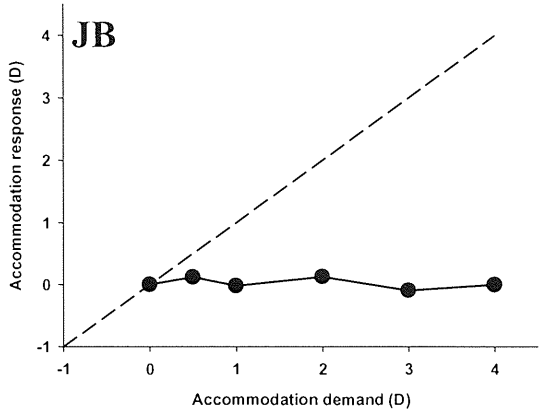
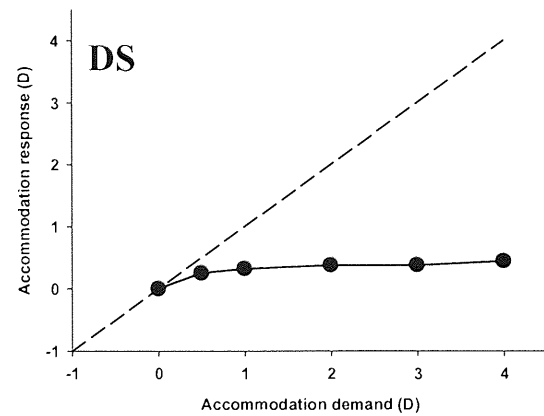
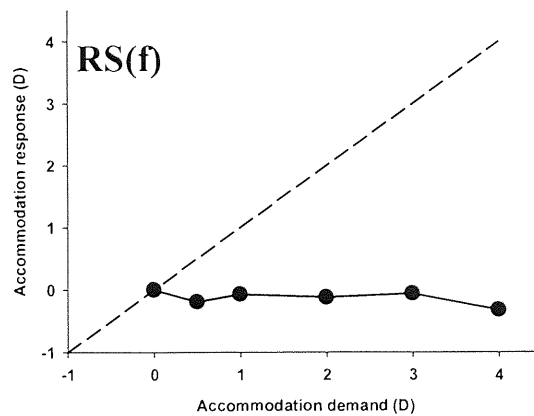
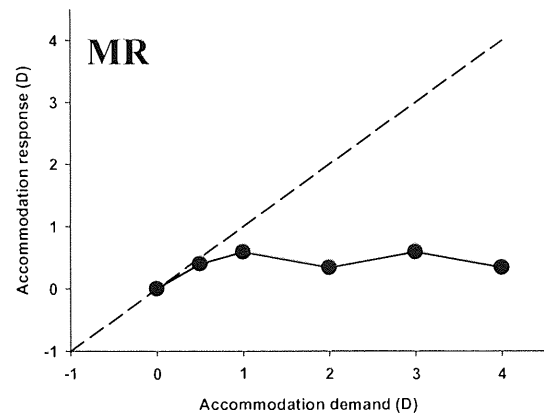
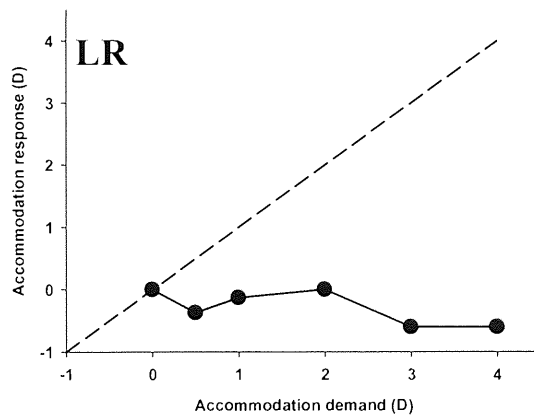
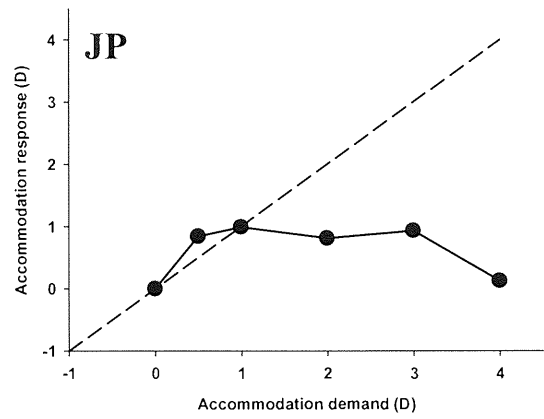
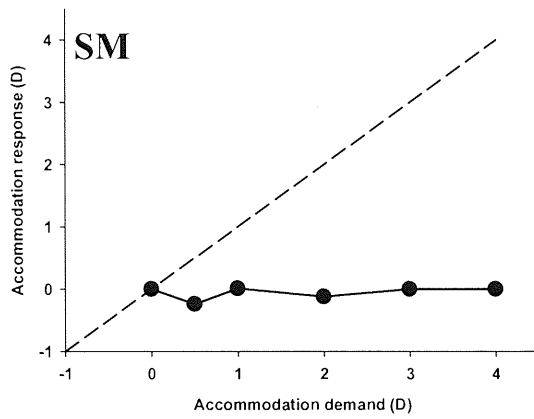
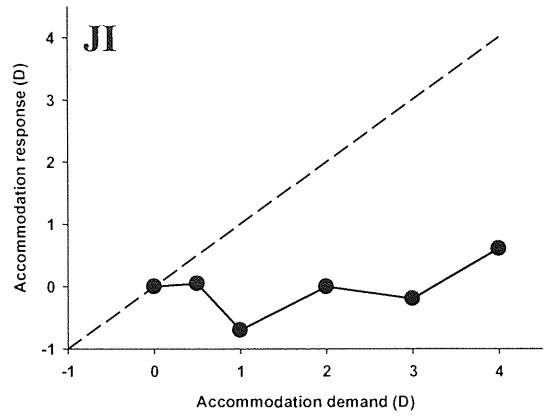
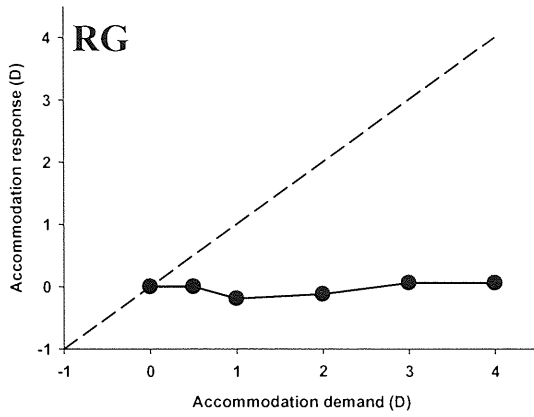


Figure A5.1 Normalised individual stimulus response curves for right eyes.

A5.2 Left eyes





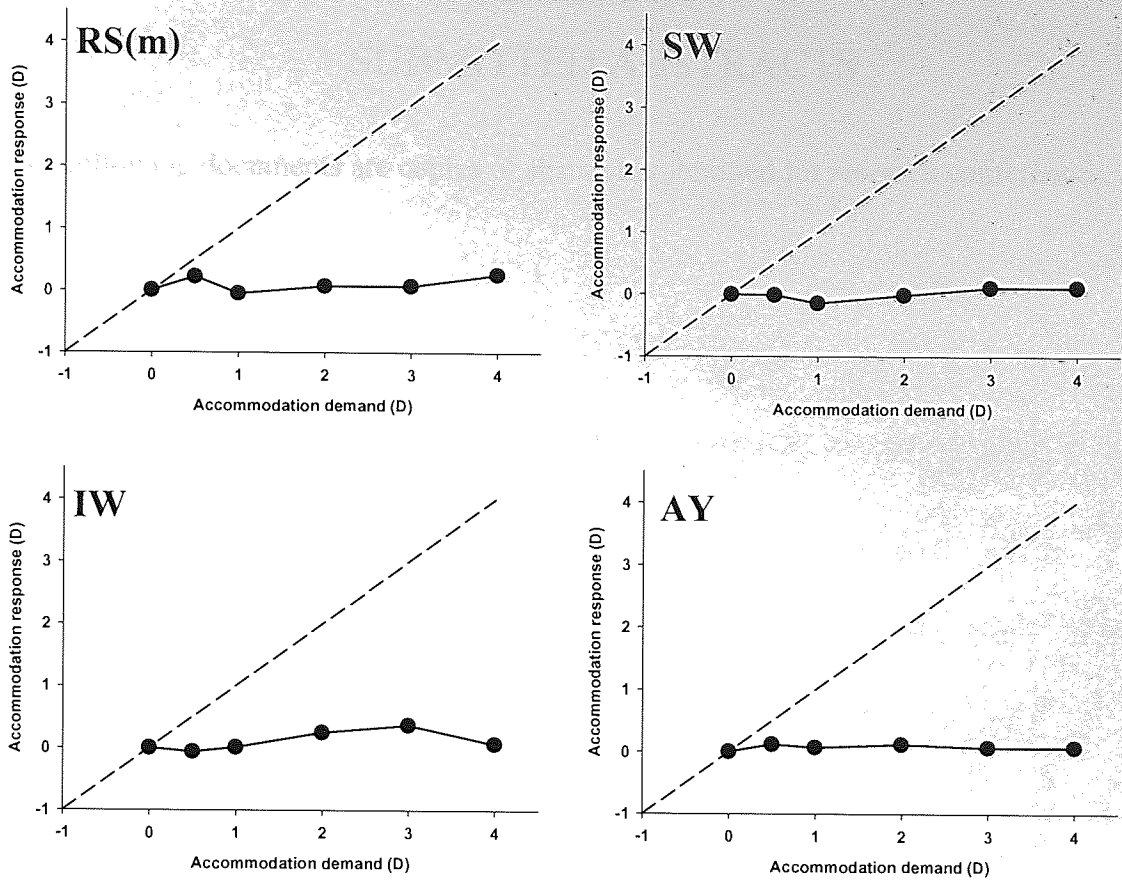


Figure A5.2 Normalised individual stimulus-response curves for left eyes.

APPENDIX 6

SUBMITTED ABSTRACTS

The following documents are copies of abstracts submitted for research conferences.

University of London

University of London

University of London

University of London

University of London

University of London

University of London

University of London

University of London

University of London

University of London

University of London

University of London

University of London

University of London

University of London

University of London

University of London

University of London

COMPARISON OF NEAR VISUAL ACUITY TESTS FOR PSEUDOPHAKES WITH ACCOMMODATING IOLS

Navneet Gupta, James S. Wolffsohn, Shehzad A. Naroo, Leon N. Davies, **George A. Gibson** and Sunil Shah*

Ophthalmic Research Group, School of Life and Health Sciences, Aston University, Birmingham, B4 7ET.

*Midland Eye Institute, Solihull, Heart of England Foundation Trust, Solihull, and Birmingham and Midland Eye Centre, Birmingham.

Purpose: To determine if there is a correlation between near visual acuity measurements obtained with uppercase single letter optotypes, lowercase single letter optotypes and lowercase words as used for assessment of near vision for patients with accommodating intraocular lenses (IOLs).

Methods: Near visual acuity was measured for uppercase single letter optotypes, lowercase single letter optotypes and lowercase words using the Logarithmic Visual Acuity Chart 2000 "New ETDRS", the Aston Near Visual Acuity (ANVA) Chart and the MNREAD Acuity Chart respectively, monocularly on 21 presbyopic subjects with accommodative intraocular lens implants at one month after implantation. All subjects wore their best-corrected spectacle prescription for distance together with a +2.50DS near addition and all measurements were taken at the same 40cm working distance, under the same viewing conditions, including light levels.

Results: Pearson Product Moment Correlation Coefficient (PPMCC) between uppercase letters and lowercase letters yielded an r-value of 0.91 (Linear Regression, $p < 0.0000001$). PPMCC between uppercase letters and lowercase words yielded an r-value of 0.91 (Linear Regression, $p < 0.0000001$). PPMCC between lowercase letters and words yielded an r-value of 0.90 (Linear Regression, $p < 0.0000001$).

Conclusion: All three methods of near visual acuity measurement are highly correlated to each other though the highest correlation is between uppercase letters and lowercase letters. The results suggest that each of these chart types would be suitable for assessing near visual acuity for patients with accommodating IOLs.

DEVELOPMENT OF A NEAR ACUITY VISION QUESTIONNAIRE FOR USE IN PRESBYOPIC CORRECTION

Navneet Gupta, Shehzad A. Naroo, James S. Wolffsohn, **George A. Gibson**, Leon N. Davies and Sunil Shah*

Ophthalmic Research Group, School of Life and Health Sciences, Aston University, Birmingham, B4 7ET, UK

*Midland Eye Institute, Solihull, Heart of England Foundation Trust, Solihull, and Birmingham and Midland Eye Centre, Birmingham, UK.

Purpose: To develop an instrument to subjectively assess near vision-related quality of life for presbyopic correction options.

Methods: A literature search identified all questions relating to near visual tasks from existing vision-related quality of life instruments. Questions were combined and re-worded if they were repeated in multiple instruments. Further relevant questions, including overall satisfaction, were added and a preliminary 19-item Near Activity and Vision Questionnaire (NAV-Q) was presented to 22 subjects at their one-month visit post first eye phacoemulsification with accommodative intraocular lens (IOL) implantation. The responses were analysed to assess Frequency of Endorsement (FE), Discrimination Ability Index (DAI), and Homogeneity (split-half reliability and internal consistency) of the NAV-Q items. Item and instrument test-retest reliabilities (Intraclass Correlation Coefficients) for the NAV-Q were assessed by repeat implementations of the instrument two weeks after the one-month visit (by post) and at the three-month visit. Final Construct Validity was obtained by comparing the NAV-Q score to reading speeds.

Results: Three items were eliminated due to little or no endorsement ($\geq 65\%$ FE). Three further items were removed due to poor item discrimination (DAI < 0.3). One final item was removed due to poor item test-retest reliability (Intraclass Correlation Coefficient, ICC < 0.4). The final 12 items were found to be internally consistent and reliable (Item-Total Correlation all > 0.6 , Guttman split-half reliability = 0.93, Cronbach's Alpha = 0.95, Test-retest reliability = 0.73).

Conclusion: The 12-item NAV-Q is a valid, internally consistent and reliable instrument for assessing near visual function.

PERFORMANCE OF THE KH3500 'ACCOMMODATING' INTRAOCULAR LENS 2 YEARS FOLLOWING IMPLANTATION

George A. Gibson, Leon N. Davies, James S. Wolffsohn, Shehzad A. Naroo, Navneet Gupta and Sunil Shah*

Ophthalmic Research Group, Life and Health Sciences, Aston University, Birmingham, B4 7ET, UK.

*Birmingham Midland Eye Centre; Midland Eye Institute, Solihull, Birmingham, UK

Purpose: To assess visual function at distance and near, and the occurrence of complications 2 years after implantation of the KH3500 'accommodative' intraocular lens (AIOL).

Methods: Twenty eyes of 12 patients (age 65.6 ± 10.4 years) implanted with a KH3500 AIOL 2.3 ± 0.2 years previously were assessed for uncorrected visual acuity at distance and near (40cm), subjective refractive error, contrast sensitivity (Pelli-Robson), subjective amplitude of accommodation (push-up), range of clear focus (defocus curve) and objective accommodative range (Shin-Nippon autorefractor). Post operative complications were assessed from the patient's medical record and posterior subcapsular opacification with a slit-lamp bio-microscope.

Results: Uncorrected visual acuity was 0.18 ± 0.24 logMAR at distance and 0.59 ± 0.16 logMAR at near. The residual mean spherical equivalent refractive error was -0.08 ± 0.97 D giving a best-corrected visual acuity of 0.04 ± 0.22 logMAR and contrast sensitivity of 1.43 ± 0.18 log-units. The subjective amplitude of accommodation was 1.5 ± 0.6 D, range of clear focus was 1.4 ± 0.5 D and the objective accommodative range was 0.59 ± 0.42 D. Seven eyes had had a YAG capsulotomy performed and 4 eyes had significant posterior subcapsular opacification.

Conclusion: Two years after implantation, the KH3500 AIOL give good distance and near unaided visual acuity, together with high contrast sensitivity. Objective accommodation was evident, but there was a limited subjective range of clear vision.

Financial interest: This study was sponsored by Lenstec.

COGNITIVE AND VISUAL FUNCTION IN PHAKIC AND PSEUDOPHAKIC EYES: AN INTRAOCULAR LENS FILTER STUDY

George A. Gibson, Leon N Davies, James S. Wolffsohn.

Ophthalmic Research Group, Life and Health Sciences, Aston University, Birmingham, B4 7ET, UK.
Email: gibsonga@aston.ac.uk

Purpose: To examine the effect of short-wavelength intraocular lens (IOL) filters on cognitive and visual function in phakic and pseudophakic eyes.

Methods: Twenty-four phakic eyes of 24 subjects (mean age 26.8 ± 6.0 years) and 22 eyes of 22 subjects fitted with a standard IOL (mean age 74.1 ± 9.1 years) were assessed. Measurements of visual acuity (logMAR), contrast sensitivity (Pelli-Robson and CSV 1000-E), colour discrimination (Farnsworth-Munsell 100-Hue), reading speed (MNRRead) and scotopic sensitivity (SST-1) were performed. In addition, the phakic cohort also performed a cognitive function test (two-alternative forced-choice paradigm) and short-wavelength automated perimetry (SWAP). Each phakic subject wore three tinted spectacle lenses in a randomised sequence; an additional short-wavelength filter was introduced for the pseudophakic group. Three of the four filters were matched to the transmission characteristics of the Alcon *AcrySof Natural*, Bausch & Lomb *VioletShield* and the AMO *OptiBlue* (pseudophakic only) violet-blocking IOLs. The control condition was a UV blocking filter.

Results: In the phakic cohort, mean defect scores for SWAP were found to be significantly higher with the *AcrySof Natural* tinted lens (-2.14 ± 1.85 dB) compared to the *VioletShield* (-1.34 ± 1.92 dB) and the control lens (-1.09 ± 1.65 db; $p < 0.01$). Further, cognitive function was attenuated with the *AcrySof Natural* lens compared to the *VioletShield*, and the control lens ($p < 0.05$). All other outcome measures were comparable between conditions. The different transmission characteristics of the filters, however, had no influence on the visual performance of the pseudophakic group.

Conclusion: Subjects' performance with the *AcrySof Natural*, *VioletShield* and *OptiBlue* filters were comparable to the UV blocking control for all measures, with the exception of SWAP and cognitive function in the phakic group. Here, the *AcrySof Natural* filter appeared to reduce the subjects' short-wavelength sensitivity, and cognitive ability.

OCULAR COMPONENT CONTRIBUTION TO OCULAR ACCOMMODATION BY VERGENCE ANALYSIS

George A. Gibson, Mark C.M. Dunne, Leon N. Davies.

Ophthalmic Research Group, Life and Health Sciences, Aston University, Birmingham, B4 7ET, UK.

Email: gibsonga@aston.ac.uk

Purpose: To examine ocular component contribution to ocular accommodation in terms of vergence analysis.

Methods: Utilising a recent schematic eye, a step-along reverse ray trace from the retina to the far point was created. The outcome refractive status and vergence contribution of each axial distance and surface radii were subsequently examined. The age of the model was varied between 20 and 50 years, and the accommodation level was modified from 0.0 to 4.0 D in 1.0 D steps. The results were displayed as physical biometric change (mm), vergence change (D) and Vergence Contribution Factor (VCF; D/mm) for each ocular component.

Results: The model behaves in a similar manner to published data with regard to axial distance and surface radii changes with accommodation. In terms of vergence changes, axial distance variations reduce the output refractive status (-1.8 D for 4.0 D of accommodation; 20 year old eye), whilst all surface changes enhance it (+6.3 D); the primary root for this is the anterior crystalline lens (+3.6 D). Anterior chamber depth and lens thickness alter in contrary directions to a similar magnitude; however, the negative vergence change exhibited by the anterior chamber (-1.2 D) is superior to the lens (-0.2 D). The posterior lens radius has the greatest VCF; it having a superior ability to modify outcome refraction per unit change of accommodation.

Conclusion: Analysing the human eye in terms of physical biometric changes taking place with accommodation provides insufficient information about the accommodative system. Using vergence change, however, highlights the role that each ocular component plays in the overall accommodative output and enhances our understanding of the mechanism of accommodation.

APPENDIX 7

REPORT PREPARED FOR BAUSCH & LOMB: THE UV+ VIOLET BLOCKING INTRAOCULAR LENS

The following document is a copy of the report prepared and sent to Bausch & Lomb detailing a literature review and clinical study comparing two intraocular lens tints.

1. Introduction

1.1 The Optical Spectrum and the Eye

The electromagnetic spectrum is the range of all possible electromagnetic radiation. The spectrum extends from just below the frequencies used for modern radio (at the long-wavelength end) to gamma radiation (at the short-wavelength end), covering wavelengths from thousands of kilometres down to fractions of the size of an atom. The visible or optical spectrum is only a small part of the electromagnetic spectrum.

Ultraviolet radiation (UVR) extends from 200 to 400 nm. This band is further divided into ultraviolet C (UVC; 200-280 nm), ultraviolet B (UVB; 280-315 nm) and ultraviolet A (UVA; 315-400 nm). UVC rays are usually blocked by the stratospheric ozone; however, in recent years holes have formed in this protective layer allowing increased levels of UVC radiation to reach the earth's surface (Bergmanson and Sheldon, 1997).

The ocular media absorb incoming UV radiation by varying degrees (Boettner and Wolter, 1962). The cornea protects the retina from UVR at wavelengths less than 300 nm. It has been shown that this corneal absorption can elicit structural damage to the corneal epithelial surface and stromal cells (Clarke *et al.*, 1990; Cullen *et al.*, 1984; Pitts *et al.*, 1977). The cornea, vitreous and aqueous humour transmit wavelengths above 300 nm, non the less, the crystalline lens blocks the majority of UVA and UVB spectra between 300 and 400 nm; up to 390 nm in the young eye and up to 400 nm in a 63 year old lens (Boettner and Wolter, 1962). Cortical cataract formation is linked to chronic exposure to UVB (Hiller *et al.*, 1977; Katoh *et al.*, 2001; Klein *et al.*, 1992; West, 1999; Taylor, 1995). The human retina is therefore exposed to the visible component of the electromagnetic spectrum from 400-760 nm and some short wavelength infra red (IR) (Margrain *et al.*, 2004).

There have been a number of studies which have considered the reduced ozone protection, longer life expectancy (i.e. increase UVR exposure) and increased exposure to the sun associated with modern lifestyles. These studies suggest we should advocate the use of tinted sunglasses, contact lenses and intraocular lenses (IOLs) which have chromophores to cut out

damaging UV rays (Bergmanson and Sheldon 1997; Lindstrom and Doddi, 1986; Hickson-Curran *et al.*, 1997; Sliney, 2001)

1.2 Retinal Phototoxicity

A few well documented papers have highlighted the phototoxic damage that short wavelength light can have on the eye. There are two types of phototoxicity; blue-green ('Noell-type' or class 1) photic retinopathy and UV-blue ('Ham-type' or class 2) photic retinopathy (Ham *et al.*, 1980; Mainster, 1987; Margrain *et al.*, 2004). The first type of phototoxicity is mediated by rhodopsin which has a peak sensitivity around 500 nm. The blue-green hazard therefore reduces in the blue/violet part of the spectrum below this peak (Noell *et al.*, 1966; Noell, 1980). Mainster (2006) suggests that any spectral filter which reduces blue-green phototoxicity causes an equivalent decrease in scotopic sensitivity.

Werner Noell (1966) showed that light could cause photochemical damage to the retina at irradiances which are too low to cause thermal effects (e.g. photocoagulation). Animal experiments (Ham, 1976) concluded that it was indeed a photochemical injury, and not a thermal mechanism. Ham also discovered that UVR caused acute retinal phototoxicity. In this case, he showed that UVR was more hazardous than violet or blue light. This can be explained by shorter wavelength light being more effective at generating harmful reactive oxygen species (ROS) in the retinal pigment epithelium (Ham *et al.*, 1980; Boulton *et al.*, 2001). Welder's, solar, and operating-microscope injuries can also be explained in this way (Mainster *et al.*, 1983; Mainster *et al.*, 2001). Of particular concern, is the damage associated with shorter wavelength visible light, namely violet and blue light (400-500 nm). Solar retinitis or 'eclipse blindness', resulting from staring at the sun, has only within recent decades been found to be a result of a photochemical injury mechanism following exposure of the retina to shorter wavelengths of the visible spectrum (Sliney, 2001). Blue light retinal injury, or 'photoretinitis', can result from viewing either a very bright light for a short interval, or a dimmer light for a prolonged exposure period (Sliney, 2001). UV-blue retinal phototoxicity requires shorter exposure but approximately 100 times more intensity than blue-green phototoxicity (Mainster, 1987; Kremers and van Norren, 1989; Mellerio, 1994).

1.3 The Aging Human Eye

Aging and a decline in retinal defences against phototoxicity are linked (Mainster, 1987; Beatty *et al.*, 2000; Bernstein *et al.*, 2002). Speculations have been made that environmental light exposure and photic retinopathy influence the development of age related macular degeneration (AMD) in susceptible individuals (Mainster, 1978; Mainster, 1987; Marshall, 1987; van der Hoeve, 1920).

The human crystalline lens yellows with age (Mellerio, 1987). This change leads to a greater absorption of the blue portion of the visible spectrum (Boettner and Wolter, 1962). The number of photons which subsequently reach the retina, and in particular the retinal pigment epithelium (RPE), will therefore diminish with age and lens brunescence. In 1920, a study by van der Hoeve noted a lower prevalence and severity of AMD in patients with cataracts. Gjessing backed this up in 1925 by reporting an inverse relationship between lens opacities and AMD. More recent studies concluded that cataract surgery, aphakia and pseudophakia are risk factors for late stage AMD (Klein *et al.*, 1992; Wang *et al.*, 2003; Sperduto *et al.*, 1981; Liu *et al.*, 1989). Mainster (2005) proposed a number of possible reasons for this. He suggested it may be due to intra or post operative light exposure, trauma or inflammation; which even from small incision surgery may adversely affect vulnerable maculae. Other studies have, however, found an increase risk of AMD in patients with cataracts (Liu *et al.*, 1989; Klein *et al.*, 2002; Freeman *et al.*, 2003).

1.4 Age Related Macular Degeneration (AMD)

Age related macular degeneration is the major cause of blindness among the elderly in the developed world, currently affecting 12.7 million people in Europe and North America (Klein *et al.*, 1995; 1999). It is generally considered to be a complex disorder, with a number of contributing factors including genetics, atherosclerosis, smoking and others (Hirvela *et al.*, 1996; McCarty *et al.*, 2001; van Leeuwen *et al.*, 2003).

Macular degeneration is a heterogeneous set of diseases characterised by the presence of soft and hard drusen (Figure 1), hyperpigmentation and hypopigmentation of the RPE, RPE

atrophy, geographic atrophy (GA), choroidal neovascularization (CNV) often with associated neurosensory detachment, and later fibrous scarring. It is usually classified into two forms, namely 'dry' and 'wet' AMD.

'Dry' or non-exudative AMD (Figure 2a) involves the accumulation of debris and deposits in the outer retina, along with atrophic and hypertrophic changes in the RPE, particularly underlying the central retina. 'Wet' or exudative AMD (Figure 2b) is a pathological process, secondary to angiogenic neovascular changes (CNV) that occur in about 20% of patients with AMD. At present, it is not proven whether the two forms ('wet' and 'dry') are the different manifestations of the same disorder, or if they are distinct diseases with diverse origins and pathologic mechanisms. Most cases of clinically diagnosed 'dry' AMD do not progress directly to CNV, the hallmark of 'wet' AMD. (Green and Enger, 1993; Bird *et al.*, 1995; Green, 1999; Sparrow and Boulton, 2005).

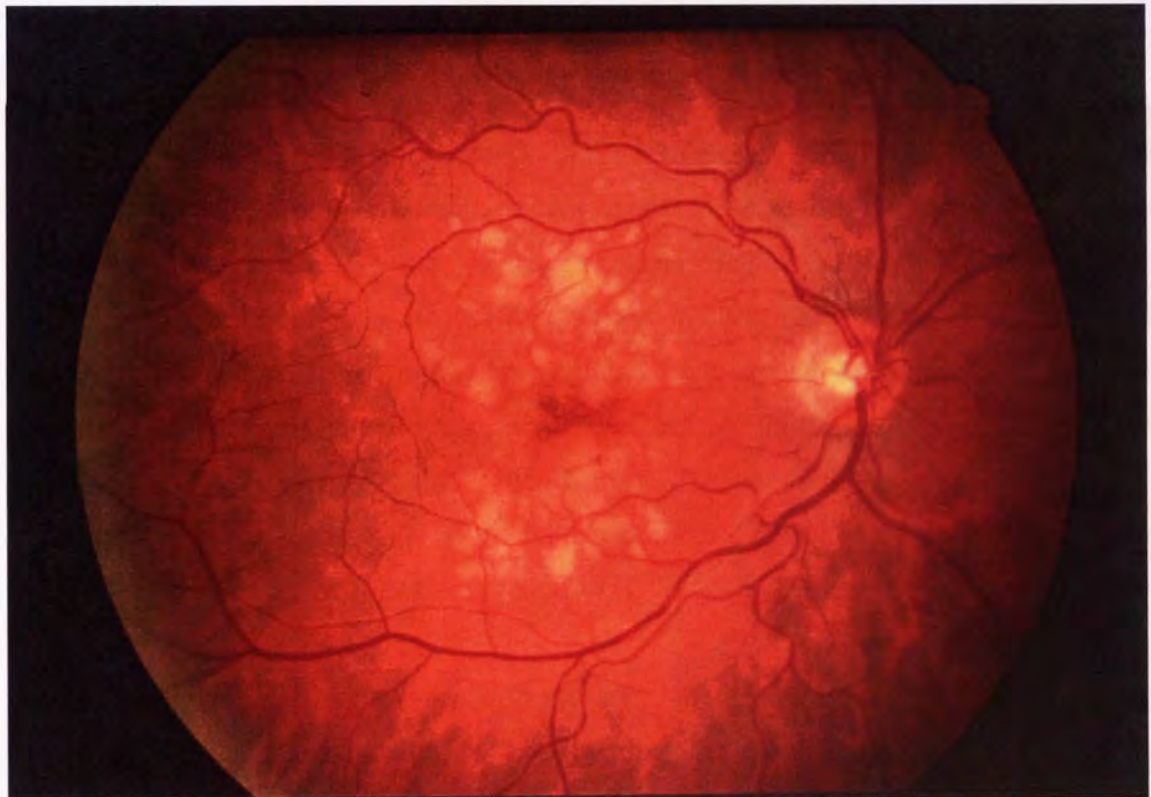


Figure 1: Fundus photograph showing drusen in the macular area (courtesy of Dr. H. Bartlett, Aston University, Birmingham, UK).

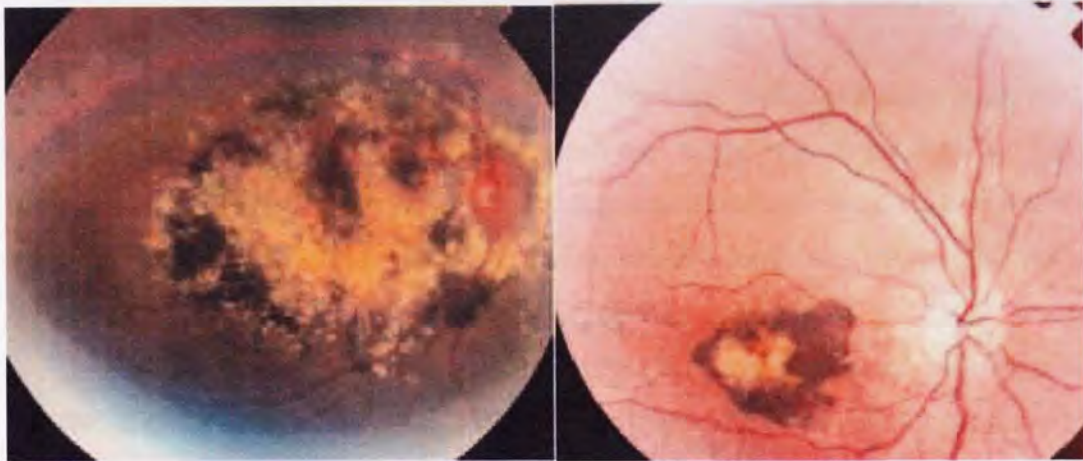


Figure 2a and 2b: Image of non-exudative (left) and exudative (right) AMD. The left hand picture shows geographic atrophy and pigment. The right hand picture illustrates CNV and scarring (courtesy of Dr. H. Bartlett, Aston University, Birmingham, UK)

1.5 Blue Light and AMD

Oxidative stress is a key factor in aging (Burkle, 2001). It potentially damages proteins, lipids and DNA (Burkle, 2001). High light and oxygen levels mean that the eye is a particularly susceptible organ for this oxidative stress. In order to remain in full working order, there must be a balance between the production and removal of harmful reactive oxygen species (Mainster, 1987). The eye's natural defences consist of absorption of optical radiation below 400 nm by the anterior ocular media (Boettner and Wolter, 1962). Retinal defences consist of shedding damaged photoreceptor outer segment discs, retinal antioxidants (e.g. superoxide dismutase, catalase and glutathione peroxidase), and retinal pigments. The latter potentially confer protection by absorbing light. They consist of xanthophyll in the macular region (peak absorption 460 nm) and melanin in the RPE and choroid (Boulton *et al.*, 2001; Mainster and Turner, 2001; Mainster, 1987; Pease *et al.*, 1987).

The role of chronic light exposure in AMD can be supported by solar retinopathy without direct solar observation (Gladstone and Tasman, 1978), the effects on vision of bright repetitive environmental exposures (Hecht *et al.*, 1948) and laboratory UV exposures (Wolf, 1946). Similarities between lesions and retinal abnormalities in AMD and repetitive acute phototoxicity (Borges *et al.*, 1990; Mainster, 1978) and loss of blue colour sensitivity in eyes

implanted with a clear IOL in bilateral pseudoaphakes with a UV blocking IOL in their contralateral eye also assist this hypothesis (Werner *et al.*, 1989).

It is extremely difficult to prove a link between light exposure and AMD on an epidemiological level. Mainster (2005) stated that acute experimental photic injuries don't stimulate retinal aging any more accurately than acute fractures simulate osteoporosis. To this end, it is also very difficult to determine an individual's total cumulative light exposure over a determined period of time. Several large studies have found a mixed response when comparing cumulative light exposure to AMD. Two large population based studies found a positive correlation (Taylor *et al.*, 1992; Tomany *et al.*, 2004), whilst three other trials found no relationship (Hirvela *et al.*, 1996; Delcourt *et al.*, 2001; McCarty *et al.*, 2001) as did two large AMD case-controlled studies (Darzins *et al.*, 1997; The Eye Disease Case-Control Study Group, 1992).

It has been hypothesized that increased exposure to light correlates to the occurrence of AMD, but epidemiological evidence for this connection is sparse (Hawkins *et al.*, 1999). Pollack and co-workers (1996) noted a correlation between the development of wet AMD post cataract extraction and implantation with a conventional intraocular lens (IOL). Taylor and co-authors (1990) suggested that blue (400-500nm) and visible (400-700nm) light were the causative factors. Van Norren & Vos (1990) considered that blue-green phototoxicity was a more likely candidate due to its occurrence at much lower light levels.

Retinal chromophores are central to this theory. It has been suggested that melanin (Gurrey *et al.*, 1985), protoporphyrin (Gottsch *et al.*, 1990), retinal (Delmelle, 1978), lipofuscin (Gaillard *et al.*, 1995; Reszka *et al.*, 1995; Wassel, 1999) and pyridinium bisretinoid (A2E), a lipofuscin component, (Gaillard *et al.*, 1995; Ragauskaite *et al.*, 2001) act as photosensitizers of damage. Other potentially harmful retinal photosensitisers include cytochrome oxidase and rhodopsin with its photoproducts (Noell *et al.*, 1980; Boulton *et al.*, 2001; Lawwill, 1982; Pautler *et al.*, 1990; Gorgels & van Norren, 1995, Grimm *et al.*, 2001). Most of these retinal photosensitizers, except for rhodopsin, are maximally excited in the violet-blue part of the

spectrum: porphyrins peak at 400 nm and cytochrome oxidase at 420 to 440 nm (Boulton *et al.*, 2001; Sparrow *et al.*, 2004).

Lipofuscin accumulates in the RPE with age, and is also found in a number of retinal disorders. It is a mixture of chromophores, and it has been shown to initiate photochemical processes that can lead to permanent damage to tissue (Gaillard *et al.*, 1995). One of the constituent chromophores, the major fluorescent component responsible for the blue light sensitivity of RPE cells (Sparrow *et al.*, 2000; Schütt *et al.*, 2000) is the fluorophore A2E (*N*-retinylidene-*N*-retinylethanolamine) (Eldred and Lasky, 1993; Parish *et al.*, 1998; Sakai *et al.*, 1996). A2E is unique to RPE cells, accumulating in human RPE cells throughout an individual's lifetime (Parish *et al.*, 1998). Lipofuscin is capable of generating reactive oxygen species (ROS) upon radiation with light (Wassel *et al.*, 1999). A2E is maximally excited by light in the blue region of the spectrum (Sparrow *et al.*, 2000) between 430 and 440nm (Reszka *et al.*, 1995). Studies have shown that A2E generates singlet oxygen that adds to carbon-carbon double bonds of A2E when irradiated; generating highly reactive epoxides (A2E-epoxides; Sparrow *et al.*, 2002; Ben-Shabat *et al.*, 2002). Ragauskaite and co-authors (2001) also observed A2E free radical reactions which were photo-initiated. Oxidative deoxyribonucleic acid (DNA) base changes have been included in the injury induced by the illumination of A2E laden RPE (Sparrow *et al.*, 2003) and the subsequent photochemical events provoked by this irradiation may result in the initiation of a cell death program (Sparrow *et al.*, 2004).

Numerous studies have linked atrophic AMD to both RPE lipofuscin (Weiter *et al.*, 1986; Wing *et al.*, 1978; Delori *et al.*, 1995, 2001; Holz *et al.*, 1999, 2001) and cumulative light exposure (Taylor *et al.*, 1992). Increasing lipofuscin content in the aging retinal pigment epithelium may therefore impair antioxidant activity, causing phototoxic damage, or compromise cell function mechanically (Boulton *et al.*, 2001; Sparrow *et al.*, 2000; Marshall, 1987; Shamsi and Boulton, 2001).

1.6 Aging and Scotopic Vision

Scotopic vision refers to vision in darkness. In terms of measured light levels, the scotopic range is below a luminance level of $-3.8 \log \text{ cd m}^{-2}$. It ranges from absolute threshold to a retinal illuminance of 0.3 trolands; about the maximum light levels encountered under natural conditions at night (Makous, 2004). Scotopic vision is mediated by rod photoreceptors only. However, scotopic and rod vision are not one and the same thing, as rods and cones overlap their range of sensitivity by approximately 3 log units; this range being referred to as mesopic vision (Werner, 2005). Scotopic sensitivity depends on the number of quanta absorbed by rhodopsin, the rod photopigment. Some wavelengths are more likely to be absorbed than others because of the chromophores in the photopigment and by pre-retinal filtering by the eye's media (mainly by the crystalline lens or IOL), however once absorbed, all wavelengths produce the same effects. This is known as univariance (Rushton, 1972). Once light photons have been absorbed, photochemical damage is wavelength dependant whereas scotopic vision is not (Werner, 2005).

The Purkinje shift, a well documented phenomenon, is the change in peak spectral sensitivity from longer to shorter wavelengths as illumination decreases (Wyszecki and Stiles, 1982). Scotopic luminous efficacy peaks at 507 nm (blue-green), while photopic peaks at 555 nm (green-yellow). Scotopic sensitivity declines faster with age than photopic sensitivity; almost twice as fast. This decline occurs in the absence of retinal disorders and media changes or ocular disease. It is mainly due to an age-related decline in the rod photoreceptor population; the cone population remaining largely stable (Makous, 2004; Curcio *et al.*, 1993; Curcio *et al.*, 2000; Jackson *et al.*, 1999; Jackson and Owsley, 2000; Jackson *et al.*, 2002). Aging not only affects scotopic sensitivity; scotopic contrast sensitivity (Scheffrin *et al.*, 1999) and dark adaptation (Jackson *et al.*, 1999) also decline with age. Age related macular degeneration and diabetic retinopathy have a negative effect on these and other measures of visual function (Jackson *et al.*, 2002; Greenstein *et al.*, 1993; Owsley *et al.*, 2000; Owsley *et al.*, 2001).

There is a concern that this reduction in rod photoreceptor sensitivity will have a depressing effect on human visual ability, especially at night. There are 18 times more rods than cones in the average human retina (90 million rods, 5 million cones) and 9 times more macular rods

than cones (Curcio *et al.*, 1990). Foveal contrast sensitivity under scotopic conditions declines with age (Mandel *et al.*, 2004) and pseudophakic patients have been found to have higher average scotopic thresholds than age-matched controls (Abraham *et al.*, 1988). There is evidence of rod mediated dark adaptation influencing cone mediated visual acuity (Naarendorp *et al.*, 1988).

Night vision is obviously very important to humans, but it appears to become a major problem for older adults. Research has suggested that older drivers limit night-time driving due to visual difficulties (Kline, 1991; Owsley and McGwin, 1999; Ball *et al.*, 1998; Brabyn *et al.*, 2005). Ivers (1998) and Lord (2001) with their co-workers reported a correlation between visual impairment and the risk of falling, and in particular, poor dark adaptation increases this risk (McMurdo and Gaskell, 1991). There is therefore an argument that older adults would benefit from blue, rod mediated, light; and that this could potentially increase sensitivity at night.

Scotopic sensitivity decreases with age due partly to decreasing pupil size and ocular media changes which reduce overall retinal illuminance. In some studies, it has been shown that the rod branch of the dark adaptation function is elevated with increasing age (Domey *et al.*, 1960; Jackson *et al.*, 1999; Pulos, 1989). However, it was not determined if pupil size and ocular media were causing an age-related decrease in retinal illuminance. Recent studies have taken these factors into account, and have demonstrated these age related losses in scotopic sensitivity (Sturr *et al.*, 1997; Scheffrin *et al.*, 1998). Pulos (1989) did not confirm these findings. Slowing photopigment regeneration may account for these changes, and 'in vivo' measurements of photopigment kinetics have gone some way to proving this (Coile and Baker, 1992; Keunen *et al.*, 1987). Rods are more prone to aging than cones (Jackson *et al.*, 2002). They lose their ability to capture quanta of light efficiently, and there are also significant losses in the number of rods with age; but it has been shown that the rod system may compensate for this to a degree, with surviving rods becoming larger to capture increased quanta of light (Curcio *et al.*, 1993). There is only a small decrease in the levels of rhodopsin in the retina with age (Plantner *et al.*, 1988), suggesting that the remaining rods actually contain more rhodopsin. Marshall (1987) showed that the aged rod outer segments deform and

become more convoluted. This change means that they are now not at the optimal orientation to absorb light, making them less effective; thus reducing scotopic sensitivity.

1.7 Filtering blue light: The use of yellow filters

Hitherto, it has been shown that UV radiation and short wavelength light have the potential to cause substantial retinal phototoxicity. Moreover, UV radiation and shorter wavelength light contribute little to rod mediated vision (Mainster and Sparrow, 2003; Mainster, 1986). The advantages of blocking UV light include decreased risk of pseudophakic erythropsia (Kamel and Parker, 1973; Bennett, 1994), blue-cone sensitivity loss (Werner *et al.*, 1989) and blood-retinal barrier disruption (Miyake *et al.*, 1999). Experiments using cultured human RPE cells concluded that absorbing blue light shields RPE cells that have accumulated the aging lipofuscin fluorophore A2E from the damaging effects of light (Sparrow *et al.*, 2004).

Hammer and co-authors (1986) speculated that the spectral transmission characteristics of the ideal IOL should mimic that of the adult crystalline lens. Since the natural human lens attenuates the absorption of blue light in the 400 to 500 nm range (Boettner and Wolter, 1962), it would seem sensible that an IOL should do the same.

The most common way to block blue light is to use a yellow filter. Yellow tinted lenses have been of interest to the clinician for a number of years. Yap (1984) showed that wearing a yellow tinted lens can improve the clarity of vision and reduce glare, and it is for these reasons that their use is popular in many outdoor activities including shooting and skiing; their use has even been suggested in the treatment of amblyopia (Fowler *et al.*, 1992). It has also been suggested that yellow tinted lenses absorb shorter wave energy such as in halogen lights which would be useful for reducing glare effects from oncoming car headlights, a significant problem for elderly drivers (Wolf, 1960; Weale, 1982; Vos, 1984; 1995). Previous data have demonstrated that the reaction time in normal subjects to grating stimuli, especially of low contrast targets at intermediate spatial frequencies, improved with the use of yellow filters (Kinney *et al.*, 1983). The contrast sensitivity of normal observers can be increased with the use of yellow tinted lenses (Yap, 1984) and intraocular lenses (Yuan *et al.*, 2004) although

some authors have disputed this (Kelly *et al.*, 1984). A study using tinted lenses found that compared with the no filter condition, yellow and orange lenses increased contrast sensitivity (Wolffsohn *et al.*, 2000). Kelly (1990) and Wolffsohn and colleagues (2000) showed that the apparent brightness of large targets under daylight conditions can be increased using yellow lenses. Zigman (1992) reported that in human vision, and in photography, elimination of environmental light with wavelengths shorter than 450 nm improves contrast and visual clarity.

Zigman (1982) proposed applying a yellow tint to intraocular lenses to enhance retinal protection after removal of the natural crystalline lens. Niwa and co-authors (1996) tested 'Ultraviolet absorbing IOLs' and 'Ultraviolet-cut and noncyanopsia IOLs' (UVCY IOL). They found that the yellow tinted IOL improved contrast sensitivity in the mid spatial frequencies under both photopic and mesopic conditions; this was corroborated by Yuan and colleagues (2004). Wolffsohn and co-workers (2000) proposed that the contrast of overlying objects is enhanced is due to the selective reduction of short-wavelength light by the yellow lenses.

Yellow filters reduce the transmittance of the visible spectrum and change colour perception to a greater or lesser degree depending on their spectral transmittance (Kuyk and Thomas, 1990; de Fez *et al.*, 2002). They cause a tritan-like defect with discrimination losses in the yellow-purplish region (de Fez *et al.*, 2002). Indeed, blue blocking sunglasses have been shown to cause moderate colour confusion (Thomas and Kuyk, 1988). A study with Hoya yellow tinted IOL blue blockers (UVCY IOL) compared with ultraviolet (UV) IOL and non-ultraviolet IOLs in individuals with normal colour vision (Ishida *et al.*, 1994) found that the yellow lens (UVCY IOL) best approximated the colour sensitivity of healthy eyes. The colour sensitivity was also found to be similar to phakic eyes without cataract (Shimizu *et al.*, 1993) and eyes with the UV IOL (Ohhama *et al.*, 1993; Yuan *et al.*, 2004). Colour vision was found to be relatively unaffected by the use of coloured lenses in subjects with AMD (Wolffsohn *et al.*, 2002). A similar study using young patients revealed a systematic detriment to colour vision with increasing cut-off wavelength of the yellow lenses (Wolffsohn *et al.*, 2000).

1.8 Yellow tinted intraocular lenses

A number of yellow tinted intraocular lenses have been used and assessed in previous studies (Table 3; p16-17). Many are currently under production and research. The Alcon AcrySof Natural SN60AT is commercially available.

1.8.1 Alcon AcrySof[®] Natural

The Alcon AcrySof Natural (SN60AT) tinted IOL was designed by Alcon Laboratories, Inc. It was approved for use by the U.S. Food and Drug Administration (FDA) in 2003, for the replacement of the human lens to achieve visual correction of aphakia in adult patients. The intraocular lens is a combination of acrylate and methacrylate material, and is identical to the original AcrySof single-piece IOL (SA60AT). The AcrySof Natural has, however, the addition of a 0.04% covalently bound yellow polymerizable chromophore. The chromophore most resembles the transmission curve of a 25 year old crystalline lens, according to Lerman and Borkman (1976).

Optic Diameter	6.0 mm
Overall Diameter	13.0 mm
Refractive Index	1.55
Suggested A-Constant	118.4
Dioptric Range	+6.0 to +30.0 (0.5 D increments) +31.0 to +34.0 (1.0 D increments)

Table 1: AcrySof Natural model SN60AT (Alcon Laboratories, Inc.)

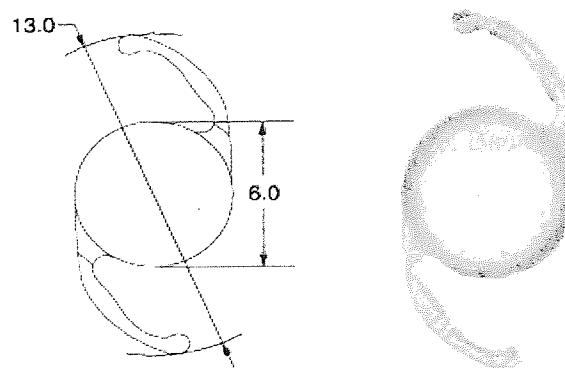


Figure 3a and 3b: A schematic and actual image of the AcrySof Natural IOL (Alcon Laboratories, Inc.)

The AcrySof Natural filters light in a manner that approximates the human crystalline lens in the 400 to 475 nm blue light wavelength range (Boettner and Wolter, 1962; Ernest, 2004). In addition to this, it reduces the transmittance of short wavelength light by 71% at 400 nm, 50% at 450 nm and 22% at 475 nm (Alcon Laboratories, 2003) (**Figure 3**).

The chromophore gives the lens a yellow tint, which initially raised some issues as to its effect on human visual function. There have been a number of studies which have compared the AcrySof Natural IOL (SN60AT) and the conventional AcrySof single piece IOL (SA60AT). No significant difference between the two lenses was found with regard to best corrected distance visual acuity, contrast sensitivity or colour vision (Marshall *et al.*, 2005; Raj *et al.*, 2005; Rodriguez-Galitero *et al.*, 2005a; 2005b; Cionni and Tsai, 2006). Espindle and colleagues (2005) compared the change in patient reported vision-related and health-related functioning and quality of life (HRQOL) following bilateral implantation with the AcrySof Natural and the standard AcrySof. Both IOLs improved most aspects of the patients' HRQOL including colour vision and driving. Espindle and co-authors found no significant differences with the HRQOL gains between the two IOLs.

1.8.2 Bausch & Lomb UV+

Bausch & Lomb have developed a prototype tinted IOL to cut out short wavelength light in much the same way as the Alcon AcrySof Natural. This lens is not currently commercially available. The Bausch and Lomb lens, the UV+, has a slighter tint than the Alcon lens. It is biconvex and made of UV absorbing silicone with PMMA "C" loop violet haptics. The intraocular lens has a more definite cut off than the SN60AT, reducing transmittance of short wavelength light by 99.5% at 400 nm, 36.8% at 425 nm, 11.2% at 450 nm and 9.2% at 475 nm (average for each point across the 0 to 30 D power range; Bausch & Lomb, 2005) (**Figure 4**; p16).

Optic Diameter	6.0 mm
Overall Diameter	13.0 mm
Refractive Index	1.429
Suggested A-Constant	118.0
Dioptric Range	+5.0 to +30.0 (0.5 D increments) +0.0 to +4.0 (1.0 D increments)

Table 2: Bausch & Lomb UV+ blue-light filtering intraocular lens

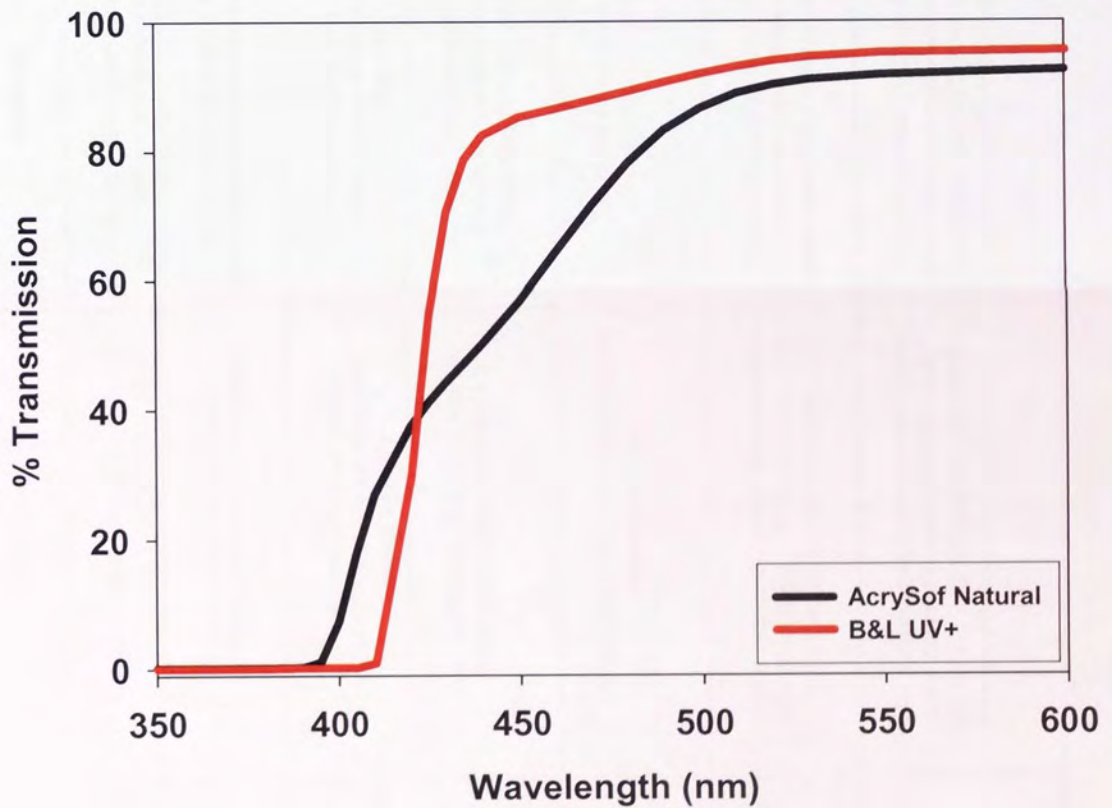


Figure 4: Transmission curves for the Alcon AcrySof Natural (SN60AT) and the Bausch & Lomb UV+ lens.

Author/s	N (eyes)	Compared	Methods	Conclusions
Hayashi and Hayashi 2006	148	Hoya YA60BB yellow IOL with non-tinted VA60BB IOL	VA with and without glare under photopic and scotopic conditions	No significant difference between either lens
Rodriguez-Galictero <i>et al.</i> 2005a	44	Yellow tinted AcrySof Natural (SN60AT) with UV blocking only AcrySof SA60AT	Contrast sensitivity with CSV 1000-E chart. Colour discrimination with FM-100	Better contrast sensitivity and colour vision on blue-yellow chromatic axis in diabetic eyes with AcrySof Natural.
Rodriguez-Galictero <i>et al.</i> 2005b	40	Yellow tinted AcrySof Natural (SN60AT) with UV blocking only AcrySof SA60AT	Contrast sensitivity with CSV 1000-E chart. Colour discrimination with FM-100	No statistical differences between the two lenses.
Cristobal <i>et al.</i> 2005	64	AcrySof Natural (SN60AT) with UV blocking only AcrySof SA60AT	Contrast sensitivity with CSV 1000-E chart. Colour discrimination with Farnsworth 25 test + patient survey	Improvement in CSF for 3, 6, 12 and 18 cpd for the AcrySof Natural compared to the SA60AT. No statistical difference in the Farnsworth test or patient survey.
Niwa <i>et al.</i> 1996	64	UV absorbing IOL with a noncyanopsia yellow-tinted IOL	Contrast sensitivity measured through a 3mm artificial pupil.	Yellow-tinted IOL showed increased CS in mid spatial frequencies (6 + 12 cpd) under mesopic and photopic conditions. Decreased effect of central glare on CSF with yellow lens.
Ishida <i>et al.</i> 1994	132	Aphakic eyes and pseudophakic eyes with UVCY IOL (Hoya). UV IOLs and non-UV IOLs were compared to normals.	Spectral sensitivity curve of normals measured. Colour distortion of pseudophakics and aphakes compared to this.	The UVCY and UV IOLs correspond to subjects in their 20's. Non-UV IOLs and aphakic eyes correspond to infants. The UVCY IOL best approximates the colour sensitivity of healthy eyes.
Cionni and Tsai 2006	54	Phakic patients, pseudophakics with Yellow tinted AcrySof Natural (SN60AT) and AcrySof UV only filtering IOL (SA60AT; with and without yellow clip-on lenses)	FM 100-hue test. Phakic and SN60AT group tested under photopic and mesopic conditions. SA60AT group tested with and without clip-on yellow lenses.	No difference in colour perception between AcrySof Natural IOLs and those in an age-matched phakic control group or in those with a UV only filtering AcrySof IOL with or without yellow clip-on lenses.

Mayer, Wirbelauer and Pham 2006	28	Yellow tinted AcrySof Natural (SN60AT) with UV blocking only AcrySof SA60AT	Contrast sensitivity under mesopic and high mesopic light conditions in a Ginsburg Box using the Functional Acuity Contrast Test (FACT). Visual perception also noted.	No statistical differences in CS. No reported differences in colour perception.
Marshall <i>et al.</i> 2005	297	Yellow tinted AcrySof Natural (SN60AT) with UV blocking only AcrySof SA60AT	Contrast sensitivity with the CSV-1000E unit and colour perception with the Farnsworth D-15 test.	The AcrySof Natural was equivalent to the conventional AcrySof lens with regard to postoperative visual performance.
Leibovitch <i>et al.</i> 2006	19	Yellow tinted AcrySof Natural (SN60AT) with UV blocking only AcrySof SA60AT	Pelli-Robson contrast sensitivity under photopic and mesopic conditions and colour perception with the Farnsworth D-15	No statistically significant differences between the both lenses with regard to CS. Postoperative colour perception improved with both lenses. No difference observed between the two groups. Both lenses comparable.
Vuori and Mantjarvi 2006	52	Yellow tinted AcrySof Natural (SN60AT) with UV blocking only AcrySof SA60AT	FM 100-hue colour test and retinal nerve fibre layer (RNFL) photographs	No statistically significant difference between the FM 100-hue total or box error scores. The yellow colour of the SN60AT did not affect the visibility of the RNFL photographs. AcrySof Natural can therefore be used in glaucoma patients.
Olson and Miller 2005	10	Yellow tinted AcrySof Natural (SN60AT) or SN60WF) with UV blocking only AcrySof SA60AT	Subjective colour comparison between eyes.	Many patients can tolerate the colour vision imbalance between the two eyes when given two different coloured IOLs.
Kara-Junior <i>et al.</i> 2006	54	Yellow tinted AcrySof Natural (SN60AT) with an Alcon MA30AC conventional IOL	Blue-yellow perimetry (SWAP)	No interference by the yellow filter of the AcrySof Natural in blue-yellow perception as determined by SWAP (therefore, early glaucoma still detected)
Raj <i>et al.</i> 2005	60	Yellow tinted AcrySof Natural (SN60AT) with UV blocking only AcrySof SA60AT	Ishihara pseudoisochromatic plates and the Farnsworth D-15 test in patients with congenital partial red-green colour deficiency (CPRG)	Implantation of the AcrySof Natural did not worsen any pre-existing severity of colour defect in CPRG individuals

Table 3: Studies which have compared and tested yellow tinted intraocular lenses under a variety of circumstances and conditions.

1.9 Do we need to filter out all short wavelength light?

Clearly, short wavelength light is potentially damaging to the retina. However, does blocking blue and violet light have detrimental effects on a person's quality of vision? It has been suggested that the filtering of blue light can help improve certain aspects of visual ability including clarity of vision, glare reduction, and contrast sensitivity to medium spatial frequencies under photopic and mesopic conditions (Yap, 1984), improve reaction time in response to stimuli (Kinney *et al.*, 1983) and increase in apparent brightness under daylight conditions (Kelly, 1990; Wolffsohn *et al.*, 2000).

Blue light dependant rod mediated vision of older adults' decreases markedly with aging (Mainster and Sparrow, 2003; Makous, 2004; Curcio *et al.*, 1993; Jackson *et al.*, 2000; 2002; Scheffrin *et al.*, 1999). Filtering blue light in addition to violet light can reduce scotopic sensitivity (Aarnisalo, 1988) and decrease the activity of retinal ganglion melanopsin photoreceptors involved in the timing of sleep and wakefulness (Van Gelder, 2004; Wee and Van Gelder 2004). Werner (2005) suggested that loss in scotopic sensitivity is far outweighed by the benefits of reducing the risk of photochemical damage for short wavelength light. The consequences for scotopic spectral sensitivity involved a reduction of 0.07 log units at absolute threshold when comparing the AcrySof Natural to a standard AcrySof lens. He also noted a loss of 0.01 log units in contrast sensitivity in the worst case, suggesting that this is insignificant considering measurement error, especially with inexperienced observers under scotopic conditions. Werner also suggested that this difference would not be detected with normal sampling using broadband illuminants (Werner, 2005)

In general, blocking UVR and violet light decreases the risk of acute UV-blue phototoxicity without significantly impairing vision (Mainster, 1986).

1.10 Aim

The aim of this study was to compare the new B&L UV+ lens with the existing AcrySof Natural (SN60AT) to see if one of the lenses has fewer effects on visual function compared to the level of retinal protection it affords the end user. To test this hypothesis, the subjects underwent a number of tests to assess visual function with a number of filtered lenses to mimic the tint of the IOL in question. The tint which has fewer effects on visual function but confers good retinal photo-protection would arguably be the most appropriate choice of IOL for cataract surgery.

2. Methods

2.1 Purpose and Subjects

The purpose of the study was to examine the visual performance of subjects wearing a variety of tinted UV-blocking lenses compared to control data using a range of tests. Eighteen right eyes of 18 subjects were recruited from Aston University (staff and students).

2.2 Exclusion criteria

Subjects were excluded from the study if the vision in their right eye was less than +0.20 logMAR, they reported any colour vision deficiency, they reported any ocular disease. A systematic anterior eye slit lamp and fundus examination was performed on all subjects to rule out any pathology.

2.3 Methods

To evaluate visual performance in the study participants, the subjects were tested using a Bailey-Lovie (90% contrast) logMAR chart at 3 m, a Pelli-Robson contrast sensitivity chart at 1 m, and a Farnsworth-Munsell 100-Hue colour discrimination test with standard illuminant daylight lamp (100 cd m^{-2}). They were also asked to perform an MNRead reading acuity/speed test at 40 cm and to complete a short wavelength automated perimetry (SWAP) program on the Humphrey Visual Field Analyser (24-2 Fastpac).

2.3.1 Lenses

Three plano CR39 lenses were used. One lens was matched to the colour and light transmission curves of the Alcon AcrySof Natural intra-ocular lens (IOL) (Lens A), one to the Bausch & Lomb (UV+) blue-light filtering IOL (Lens B), and the third lens was a clear CR39 blank as a control (Lens C; Cerium Visual Technologies, Kent, UK; **Figure 5**). Each lens was glazed to the shape of an eye-patch and drilled to accept a length of elastic.

The blank was then padded to provide an adequate distance between the eye and the lens thus aiding comfort. The left eye was occluded with a patch (Figure 6).

Each subject was required to attend four times. The first session enabled the subjects to practice the tests, to eliminate learning effects. At each subsequent session, subjects' visual function was assessed while wearing one of the three lenses. The order in which the lenses were tested was randomised. Each visit was separated by 5 to 7 days to avoid learning and fatigue. The SWAP was the last of the tests to be performed in the study due to the retinal adaptation involved which may have influenced subsequent colour vision testing.

2.3.2 Contrast Sensitivity Function

The performance index that most usefully documents human spatial vision is the contrast sensitivity function (CSF; Montés-Micó and Charman, 2001; Montés-Micó and Alió, 2003; Montés-Micó *et al.*, 2003; Montés-Micó *et al.*, 2004). There are a number of methods for measuring this index. In this study the CSF was measured with the Pelli-Robson chart (Clement Clarke UK) with the non-viewing (left) eye occluded for each measurement. The Pelli-Robson chart allows presentation of letters of a constant spatial frequency (1 cycle per degree at 1 m) in groups of 16 triplets; each triplet decreasing in contrast by 0.15 log units. The manufacturer's recommended testing procedures were followed with a testing distance of 1 m and room illumination of 85 cd m⁻². Means and standard deviations were calculated.

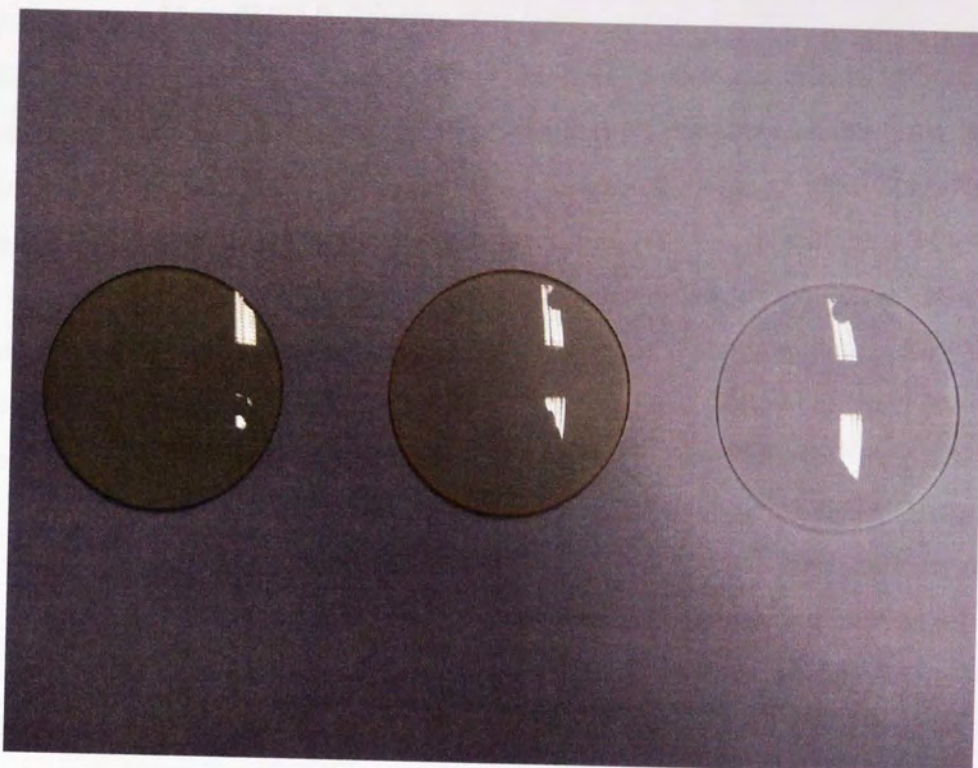


Figure 5: From the left; Alcon AcrySof Natural, Bausch & Lomb UV+, clear lens.



Figure 6: The position of the tinted patch and occluder.

2.3.3 Farnsworth-Munsell (FM) 100-Hue test

The FM 100-Hue test is a widely used tool to detect chromatic discrimination abnormalities and provide a non-invasive method to assess macular area damage (Kinnear and Sahraie, 2002). The test was performed monocularly. Coloured caps belonging to the first FM 100-Hue test box were removed and placed on a black table. Subjects were then asked to place the caps back into the box in the correct order. This procedure was repeated with the remaining three boxes. When completed, the examiner recorded the results without divulging them to the subject. Following previous studies, colour vision examination was performed under photopic conditions (85 cd m^{-2} ; Bowman and Cole, 1980). The results were then subjected to a Vingrys' Analysis (Vingrys and King-Smith, 1988), which produced an S-Index, C-Index, total error and an angle of deviation. 'Angle' indicates the axis of confusion and therefore the type of colour deficiency; 'C-Index' is the Confusion-Index, which is used to measure the severity of the colour deficit; 'S-Index' is the Scatter-Index, which assesses the degree of scatter, randomness or selectivity in the observer's arrangement (Vingrys and King-Smith, 1988). Vingrys and King-Smith claimed that these values are sufficient to discriminate between a variety of congenital or acquired colour vision deficiencies.

Type of Colour Vision	Angle	Major Radius	Minor Radius	Total Error	S-Index	C-Index
Normal	62.0	9.2	6.7	11.4	1.38	1.00
Minor Error	-12.1	9.8	9.2	13.4	1.07	1.06
Protanomalous	28.3	18.0	8.2	20.4	1.97	1.95
Protanope	8.8	38.8	6.6	39.4	6.16	4.20
Deuteranomalous	-5.8	25.4	9.6	27.5	2.99	2.75
Deuteranope	-7.4	37.9	6.3	38.4	6.19	4.10
Tritanomalous	-80.8	16.3	6.4	17.5	2.57	1.77
Tritanope	-82.8	24.0	6.4	24.9	3.94	2.60

Table 3: Colour vision deficiencies and their indices (Vingrys and King-Smith, 1988)

Blue-yellow dichromatopsy is indicated by scores in the ranges of 46 to 53 and 4 to 84 on the Farnsworth-Munsell test (Bowman and Cole, 1980).

2.3.4 The Minnesota Low-Vision Reading (MNRead) test

The MNRead test (Lighthouse Products by Optelec, New York, USA) has been developed at Minnesota Laboratory for Low-Vision Research (University of Minnesota, USA) to measure reading speed in low vision patients (Legge *et al.*, 1989; Ahn and Legge, 1995; Mansfield *et al.*, 1993; 1996). MNRead cards are 11x14-inch, white continuous-text reading acuity cards. The contrast is high (>85%). The chart was lit without shadows to a luminance of 100 cd m⁻² as per the manufacturer's guidelines.

MNRead cards use simple sentences with common vocabulary to minimise cognitive and linguistic demands. All sentences are matched in length (60 characters per sentence), and each sentence consists of three lines. The character count includes the spaces between words, at the end of the line, and an implied period at the end of the sentence. The lines of text are left and right justified with proportionally spaced *Times Roman* fonts (as are used commonly for newspapers and everyday printed material). Each sentence follows a 0.1 logarithmic progression from 1.3 logMAR to -0.5 logMAR (6/120 to 6/1.89) and should fit into a rectangular box of fixed aspect ratio. The testing distance for the card is 40 cm. During the study, the time taken for subjects to read each sentence was recorded until the subject's visual resolution limit was reached. The procedure was repeated for all three lenses.

Critical print size is the smallest print size at which patients can read at their maximum reading speed, and is often used in low vision patients to indicate the minimum magnification required for effortless reading. Reading acuity was calculated using the following formula.

$$\text{Acuity} = 1.4 - (\text{sentences read} \times 0.1) + (\text{errors} \times 0.01)$$

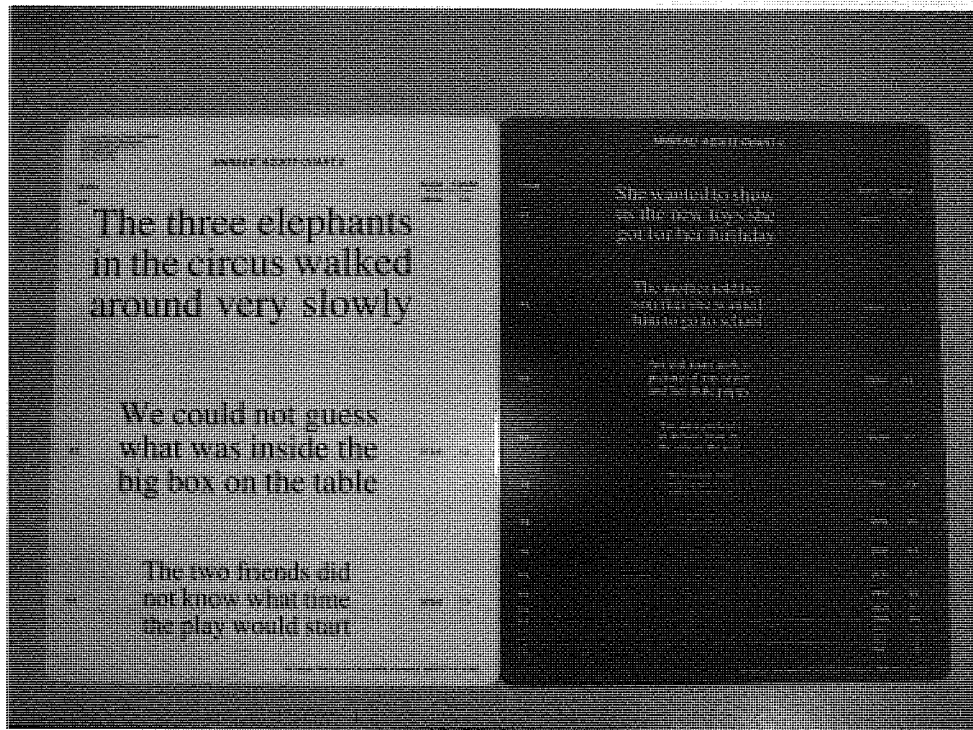


Figure 7: MNRead near acuity chart. On the right is the reversed contrast version. The chart on the left shows the larger type and therefore the starting point of the test; the text continuing to decrease in size on the reverse.

2.3.5 Short Wavelength Automated Perimetry

The retina contains three types of cones: cells sensitive to short wavelengths (400 to 440 nm; blue light), cells sensitive to medium wavelengths (530 to 540 nm; green light), and cells sensitive to long wavelengths (560 to 580 nm; red light). These cones transmit information to the ganglion cells of the retina, which process the information according to two colour mechanisms (blue–yellow and green–red) and one achromatic mechanism (black–white or luminance).

Short Wavelength Automated Perimetry (SWAP) utilizes a blue stimulus to preferentially stimulate the blue cones and a high luminance yellow background to adapt the green and red cones and to saturate, simultaneously, the activity of the rods. All testing was performed using the 24-2 full threshold (using the 3-3 step threshold FASTPAC strategy) program of the commercially available Humphrey Field Analyzer (HFA; Humphrey-Zeiss, Carl Zeiss Meditec AG, Jena, Germany). SWAP was performed using test conditions that have previously been reported to be optimal (Sample *et al.*, 1996) which

consists of a 100 cd m^{-2} yellow background (Schott OG 530 filter, BES Optics Inc., W. Warwick, Rhode Island, USA) and a Goldmann size V blue (Omega 440 nm interference filter, Omega Optical, Brattleboro, Vermont, USA) stimulus. Both the background and stimulus intensities of all HFA units used were calibrated prior to the initiation of the study. Rest periods were provided approximately halfway through a given test, as well as at the patient's request or technician's discretion. Reliability criteria included fixation losses $\leq 25\%$, false positive responses $\leq 25\%$ and false negative responses $\leq 25\%$ (Blumenthal *et al.*, 2003). Mean defect (MD) and Pattern Standard Deviation (PSD) were recorded; means and standard deviations were then calculated. Mean defect is classified as the mean value of the visual field damage averaged over the test locations. Mean defect is classified as normal if it is between zero and -2dB and becomes more negative as the visual field worsens. Pattern Standard Deviation is a measure of focal loss or variability within the field taking into account and generalised depression in the hill of vision. PSD is 'normal' if between zero and 2dB; any PSD greater than this will be assigned a probability value and will be classified as 'abnormal'.

2.3.6 Scotopic Sensitivity

To test the patients scotopic threshold (i.e. the point at which a light source becomes visible), the patient was dark adapted for 30 minutes in a completely darkened and sealed room. The patient was instructed to gaze directly ahead of them to a point identified before commencing the test. The illuminance of a light source, consisting of a white LED connected to a variable power unit, was gradually increased in intensity until the subject first reported it had been seen. This was recorded on a portable laptop personal computer using Instacal (Measurement Computing Corporation) for Windows. The process was repeated three times for each lens. Ten minutes was allowed to elapse between lens change over.

2.4 Statistical Analysis

For analysis, the data were split into three groups. The lenses were labelled A (Alcon AcrySof Natural), B (Bausch & Lomb UV+) and C (clear lens). Means and standard

deviations were calculated for all tests performed. A Shapiro-Wilk analysis of variance (ANOVA; Shapiro and Wilk, 1965) was conducted, with SPSS 12.0.1 for MS Windows.

The tinted lenses (A and B) were also normalised by subtracting the results or errors found whilst wearing the clear lens (lens C). The differences between each tinted lens and the clear lens were therefore calculated and a paired samples student t-test was performed; significance was achieved if $p < 0.05$.

3. Results

3.1 Visual Acuity

Figure 8a shows how LogMAR visual acuity varied between all three lenses tested. Mean visual acuity (\pm SD) was -0.02 ± 0.09 logMAR for the Alcon lens, -0.04 ± 0.09 logMAR for the B&L lens and -0.04 ± 0.08 logMAR for the clear lens. There was no significant difference between these acuities ($F_{(2,34)} = 2.249$; $p = 0.121$).

When the clear lens was taken into account and the results normalised, the difference between the AcrySof Natural and the clear lens (\pm SD) was $+0.02 \pm 0.04$ logMAR, and 0.00 ± 0.04 logMAR between the UV+ and clear lens. These differences were also found to be insignificant ($t = 1.490$; $p = 0.155$). This is illustrated in Figure 8b.

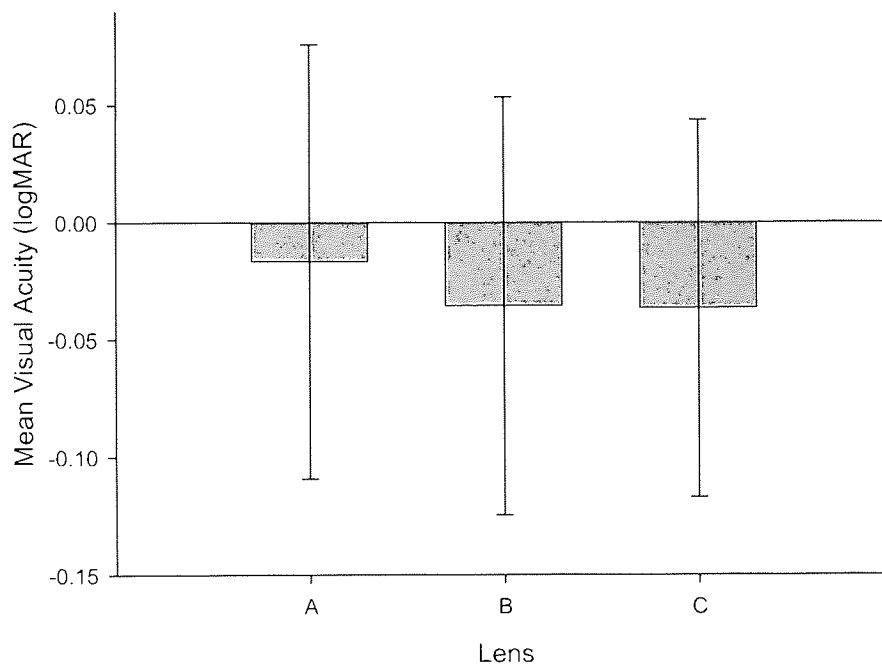


Figure 8a: Comparison of visual acuity between the Alcon AcrySof Natural (A), Bausch & Lomb UV+ (B) and clear lens (C). Error bars indicate \pm SD.

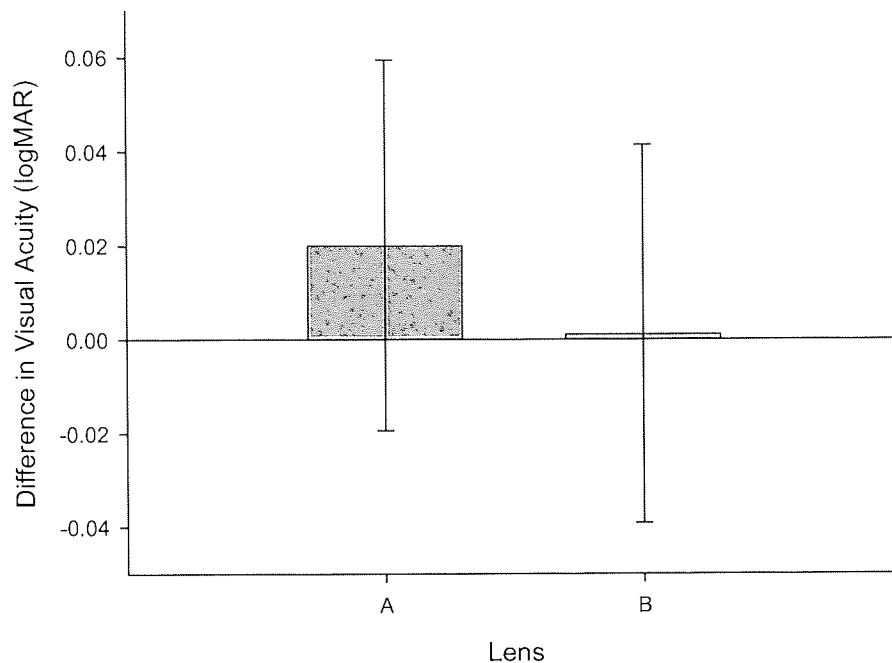


Figure 8b: Normalised data showing the mean difference in visual acuity between the Alcon AcrySof Natural (A) and the Bausch & Lomb UV+ (B) when compared to a clear lens. Error bars indicate \pm SD.

3.2 Contrast Sensitivity

Mean logCS (\pm SD) was 1.73 ± 0.11 logCS for the AcrySof Natural, 1.74 ± 0.13 logCS for the B&L UV+, and 1.76 ± 0.11 logCS for the clear lens. There was no significant statistical difference between these values ($F_{(2,34)} = 0.242$; $p = 0.786$). Normalised values (\pm SD) were -0.02 ± 0.14 logCS for the Alcon and -0.01 ± 0.15 logCS for the B&L lenses. These results were not significant ($p = 0.704$; $t = -0.387$). These results are illustrated by Figures 9a and 9b.

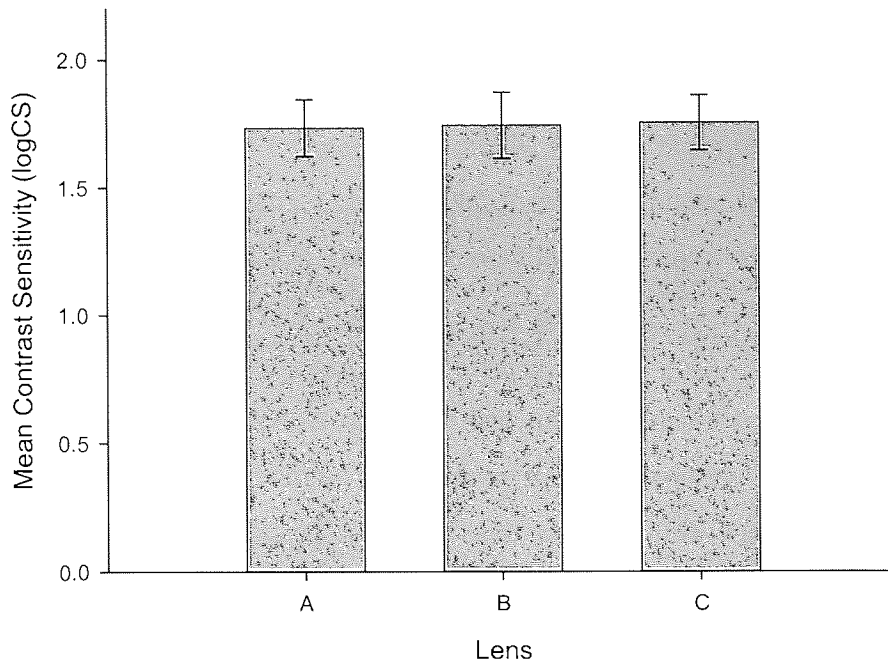


Figure 9a: Mean contrast sensitivity for the Alcon AcrySof Natural (A), Bausch & Lomb UV+ (B) and a clear lens (C). Error bars indicate \pm SD.

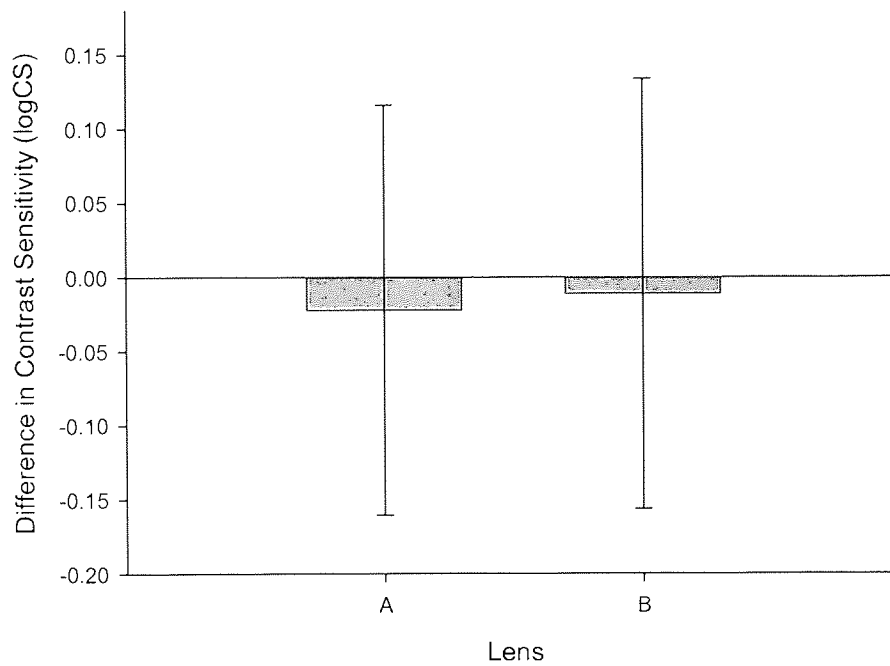


Figure 9b: Normalised data showing the mean difference in contrast sensitivity between the Alcon AcrySof Natural (A) and the B&L UV+ (B) compared to a clear lens. Error bars indicate \pm SD.

3.3 Farnsworth-Munsell 100-Hue

3.3.1 Total Error

Figure 10a expresses the mean total error (\pm SD) of the FM 100-Hue tests performed. The results were 67.11 ± 45.74 for the Alcon tint, 70.39 ± 45.09 for the B&L tint and 67.33 ± 40.75 for the clear lens. Although the B&L lens had a higher mean error, the standard deviation was high for all FM 100-Hue measures and there proved to be no significant relationship ($F_{(2,34)} = 0.200$; $p = 0.820$).

Figure 10b highlights the results when the two tinted lenses were normalised. The mean difference of the AcrySof Natural compared to the clear lens was $+0.03 \pm 24.10$, whereas the UV+ was $+2.71 \pm 21.62$. Paired t-test revealed this was also an insignificant difference ($t = -0.649$; $p = 0.525$)

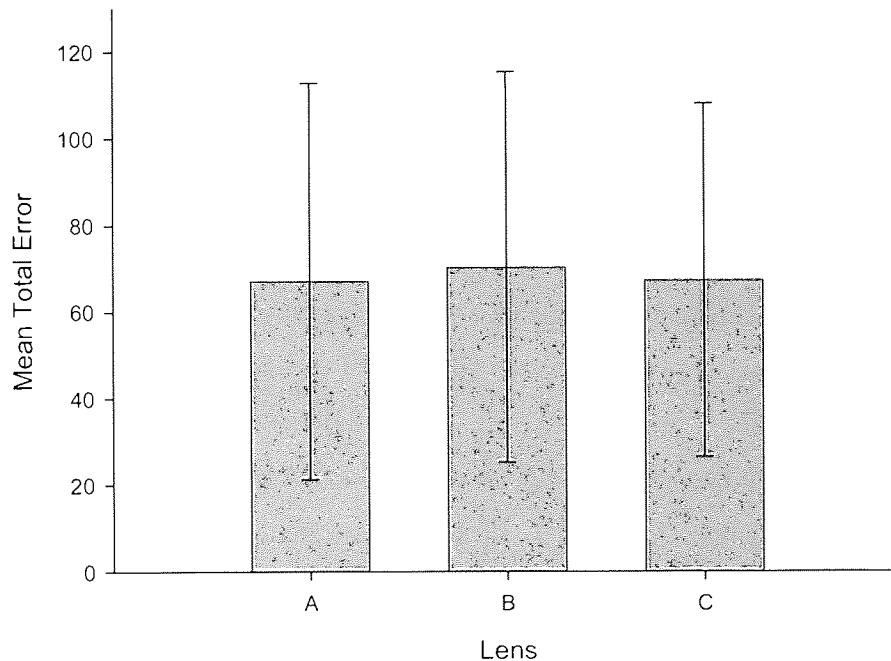


Figure 10a: Mean FM 100-Hue total error for the Alcon AcrySof Natural (A), Bausch & Lomb UV+ (B) and a clear lens (C). Error bars indicate \pm SD.

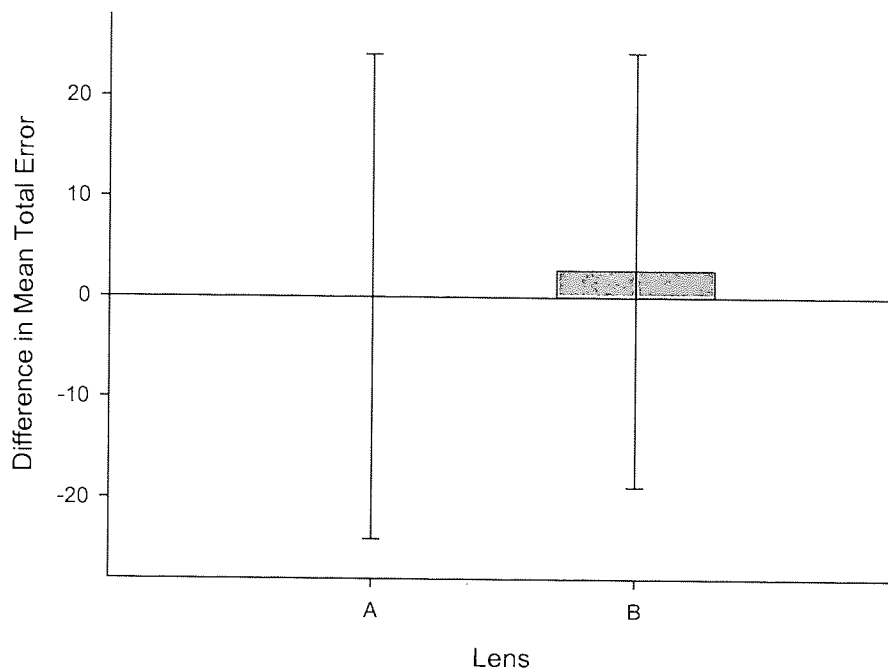


Figure 10b: Normalised data showing the mean difference in FM 100-Hue total error between the Alcon AcrySof Natural (A) and the Bausch & Lomb UV+ (B) when compared to a clear lens. Error bars indicate \pm SD.

3.3.2 Angle

The mean angle of confusion was 54.45 ± 9.47 for the Alcon, 50.09 ± 8.80 for the B&L and 55.99 ± 9.77 for the clear lens. There was no significant correlation between these results ($F_{(2,34)} = 1.874$; $p = 0.169$). This can be observed in **Figure 11a**.

Figure 11b represents the differences between the tinted lenses and the clear lens; showing that the mean difference in angle was -1.28 ± 13.10 for the AcrySof and -4.92 ± 10.92 for the UV+. These were again, not significant ($t = 1.418$; $p = 0.174$).

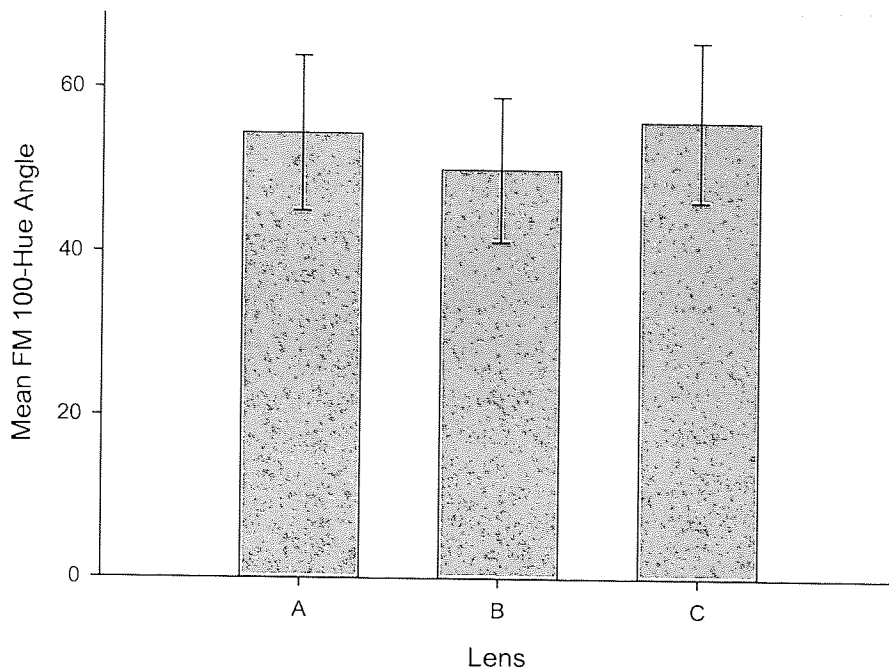


Figure 11a: Mean FM 100-Hue angle for the Alcon AcrySof Natural (A), Bausch & Lomb UV+ (B) and a clear lens (C). Error bars indicate \pm SD.

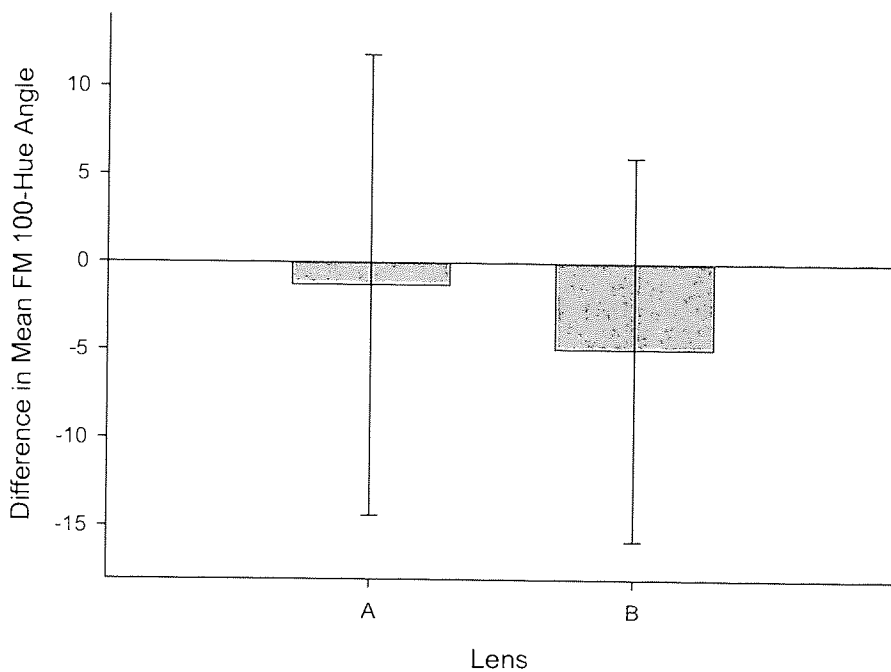


Figure 11b: Normalised data showing the mean difference in FM 100-Hue angle between the Alcon AcrySof Natural (A) and the B&L UV+ (B) compared to a clear lens. Error bars indicate \pm SD.

3.3.3 S Index

Figure 12a shows the mean S indices for lenses A, B and C. They were (\pm SD) 1.46 ± 0.16 for lens A, 1.47 ± 0.16 for lens B, and 1.46 ± 0.20 for the clear lens, C. When this data was normalised, the difference between lens A and C was 0.00 ± 0.22 and for lens B compared to the clear lens, $+0.01 \pm 0.26$. Figure 12b illustrates these results.

When this data was analysed, none of the results proved to be statistically significant ($F_{(2,34)} = 0.048$, $p = 0.953$; $t = -0.413$, $p = 0.685$).

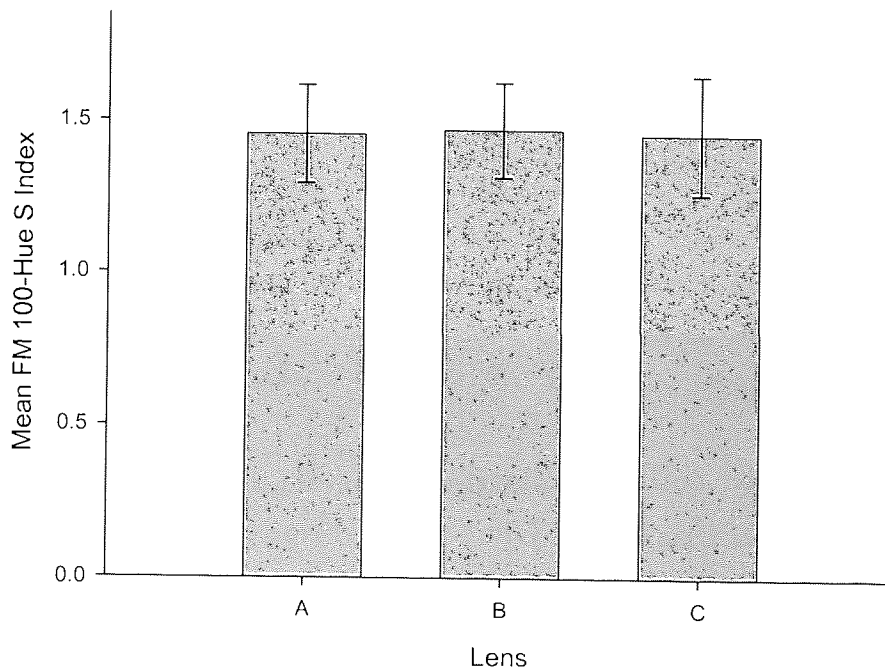


Figure 12a: Mean FM 100-Hue S Index for the Alcon AcrySof Natural (A), Bausch & Lomb UV+ (B) and a clear lens (C). Error bars indicate \pm SD.

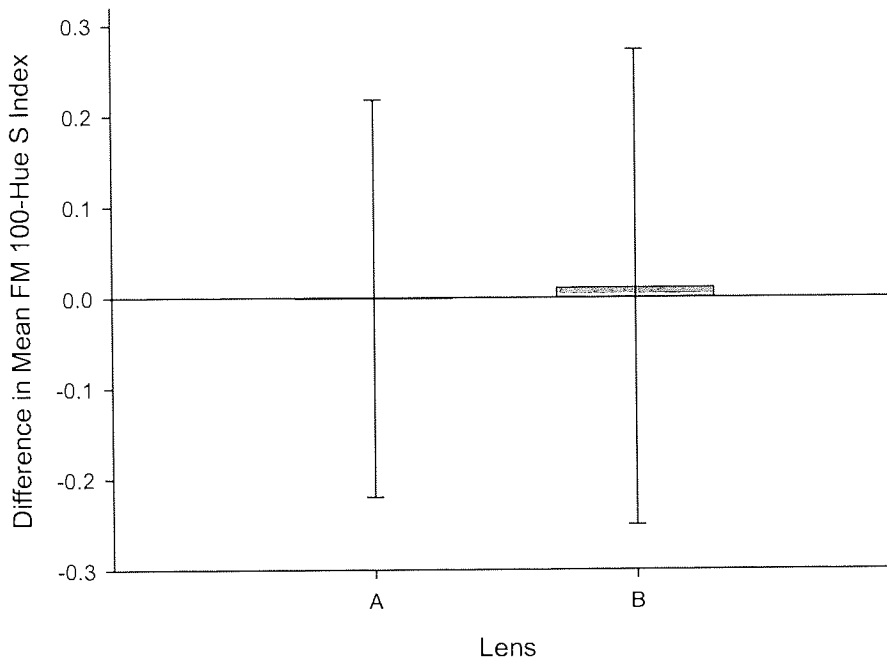


Figure 12b: Normalised data showing the mean difference in FM 100-Hue S Index between the Alcon AcrySof Natural (A) and the Bausch & Lomb UV+ (B) when compared to a clear lens. Error bars indicate \pm SD.

3.3.4 C Index

Figure 13a below represents the mean C indices for the Alcon, B&L and clear lens. These are (\pm SD) 1.50 ± 0.36 , 1.57 ± 0.37 and 1.53 ± 0.34 respectively. ANOVA revealed no statistical significance for these results ($F_{(2,34)} = 0.825$; $p = 0.447$).

When the results were compared to the clear lens (C), the mean differences (\pm SD) were -0.03 ± 0.20 for the Alcon tint, and $+0.03 \pm 0.33$ for the Bausch & Lomb tint. T-test revealed that these differences were also insignificant ($t = -1.641$; $p = 0.119$). These results are found in a graphical format in **Figure 13b**.

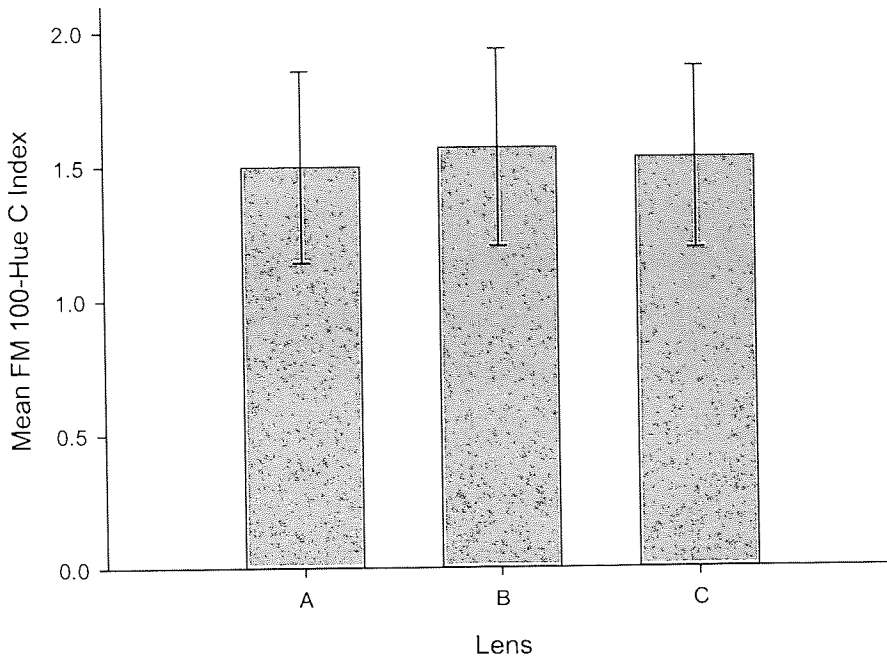


Figure 13a: Mean FM 100-Hue C Index for the Alcon AcrySof Natural (A), Bausch & Lomb UV+ (B) and a clear lens (C). Error bars indicate \pm SD.

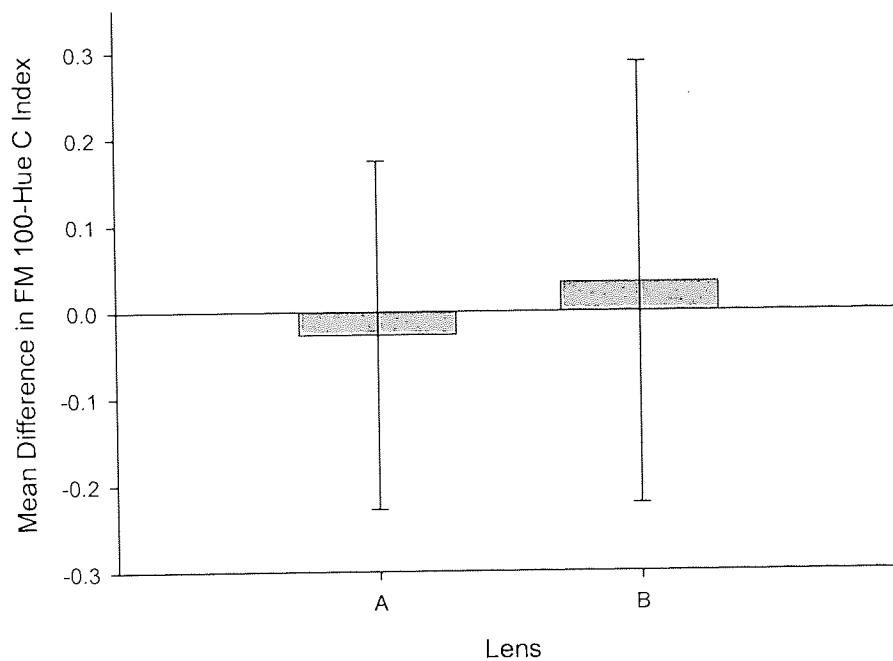


Figure 13b: Normalised data showing the mean difference in FM 100-Hue C Index between the Alcon AcrySof Natural (A) and the B&L UV+ (B) compared to a clear lens. Error bars indicate \pm SD.

3.4 Short Wavelength Automated Perimetry (SWAP)

3.4.1 Mean Defect (MD)

Average mean defect (\pm SD) for the three lenses tested was -2.08 ± 1.22 dB for lens A (Alcon), -1.41 ± 1.21 dB for lens B (B&L) and -1.26 ± 1.44 dB for lens C (clear). Statistical analysis showed that there was a significant difference between the three lenses tested, lens A having a higher MD than lens B, and this in turn higher than lens C ($F_{(2,34)} = 4.418$; $p = 0.020$). Therefore, the Alcon lens blocks more of the blue light stimulus than the B&L and this more than the clear lens. **Figure 14a** corresponds to this data.

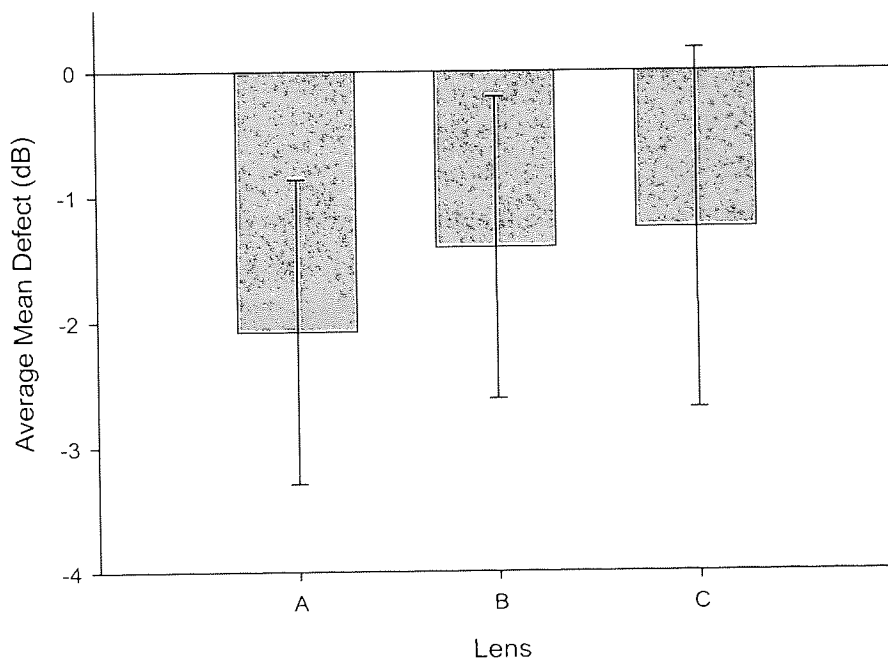


Figure 14a: Average mean defect (MD) for the Alcon AcrySof Natural (A), Bausch & Lomb UV+ (B) and a clear lens (C). Error bars indicate \pm SD.

Figure 14b illustrates the differences in MD between lenses A and C, and lenses B and C. These mean differences (\pm SD) were -0.82 ± 1.14 dB for lens A, and -0.15 ± 1.50 dB for lens B. These results were also found to be significant ($t = -2.651$; $p = 0.017$).

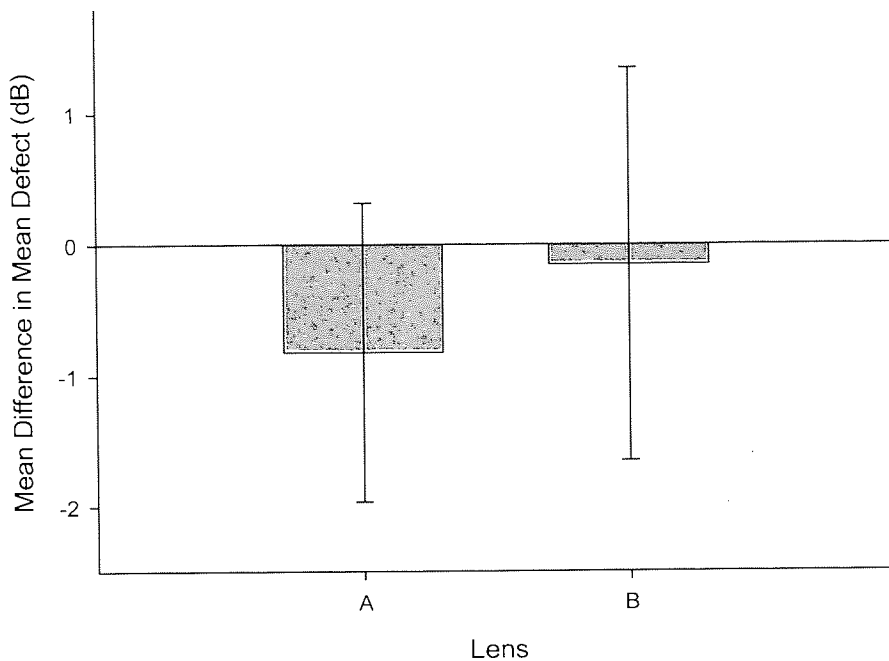


Figure 14b: Normalised data showing the mean difference in mean defect (MD) between the Alcon AcrySof Natural (A) and the Bausch & Lomb UV+ (B) when compared to a clear lens. Error bars indicate \pm SD.

3.4.2 Pattern Standard Deviation (PSD)

Mean pattern standard deviation varied little between the three lenses tested. They were (\pm SD), 2.18 ± 0.26 dB for the AcrySof tint, 2.18 ± 0.40 dB for the Bausch & Lomb tint, and 2.15 ± 0.22 dB for the clear lens. There was no statistical significance in these results ($F_{(2,34)} = 0.091$; $p = 0.913$). **Figure 15a** illustrates the mean PSD for the lenses.

When these results were normalised against the clear lens; the mean difference (\pm SD) of the AcrySof tint was $+0.03 \pm 0.27$ dB, whereas the B&L tint was $+0.03 \pm 0.33$ dB. T-test revealed that these results did not reach significance ($t = -0.016$; $p = 0.988$). This is illustrated by **Figure 15b**.

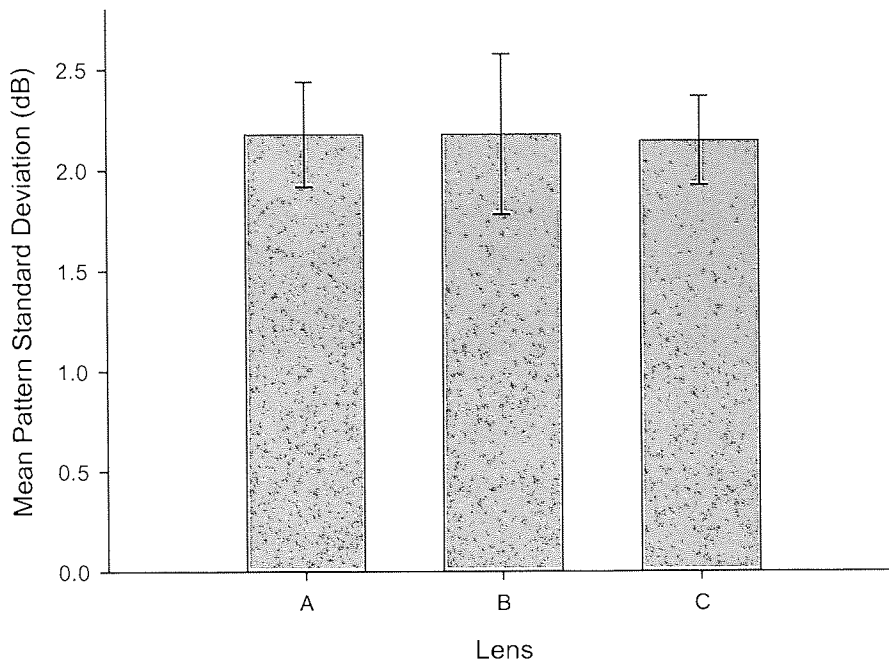


Figure 15a: Mean Pattern Standard Deviation (PSD) for the Alcon AcrySof Natural (A), Bausch & Lomb UV+ (B) and a clear lens (C). Error bars indicate \pm SD.

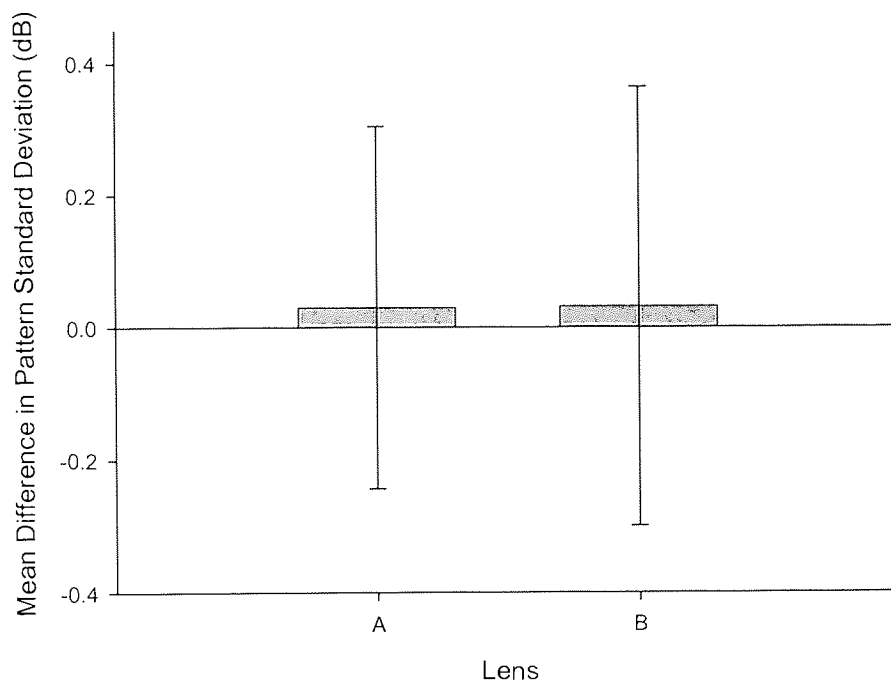


Figure 15b: Normalised data showing the mean difference in Pattern Standard Deviation (PSD) between the Alcon AcrySof Natural (A) and the Bausch & Lomb UV+ (B) when compared to a clear lens.

3.5 The Minnesota Low-Vision Reading (MNRead) test

3.5.1 Acuity

Mean logMAR acuities were calculated for each lens using the MNRead chart held at 40cm. The mean (\pm SD) for the AcrySof tint was -0.12 ± 0.09 logMAR, for the UV+ tint it was -0.14 ± 0.09 logMAR, and for the control lens -0.14 ± 0.07 logMAR. Statistical analysis revealed a probability score below significance ($F_{(2,34)} = 2.033$; $p = 0.147$; **Figure 16a**).

Figure 16b shows the mean differences in acuity for the tinted lenses against the control lens. These differences were 0.02 ± 0.05 logMAR for lens A, and 0.00 ± 0.05 for lens B.

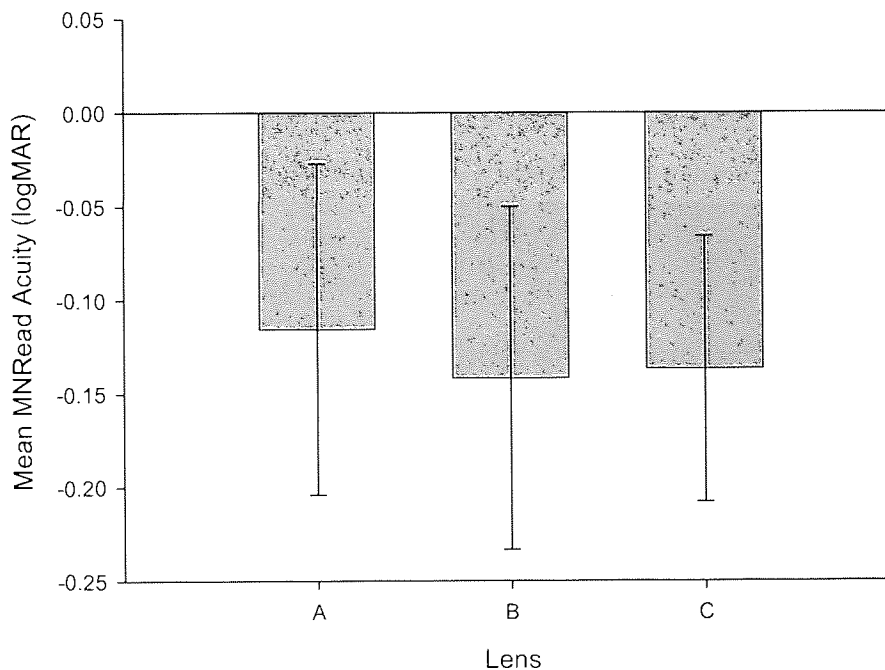


Figure 16a: Mean MNRead acuity for the Alcon AcrySof Natural (A), Bausch & Lomb UV+ (B) and a clear lens (C). Error bars indicate \pm SD.

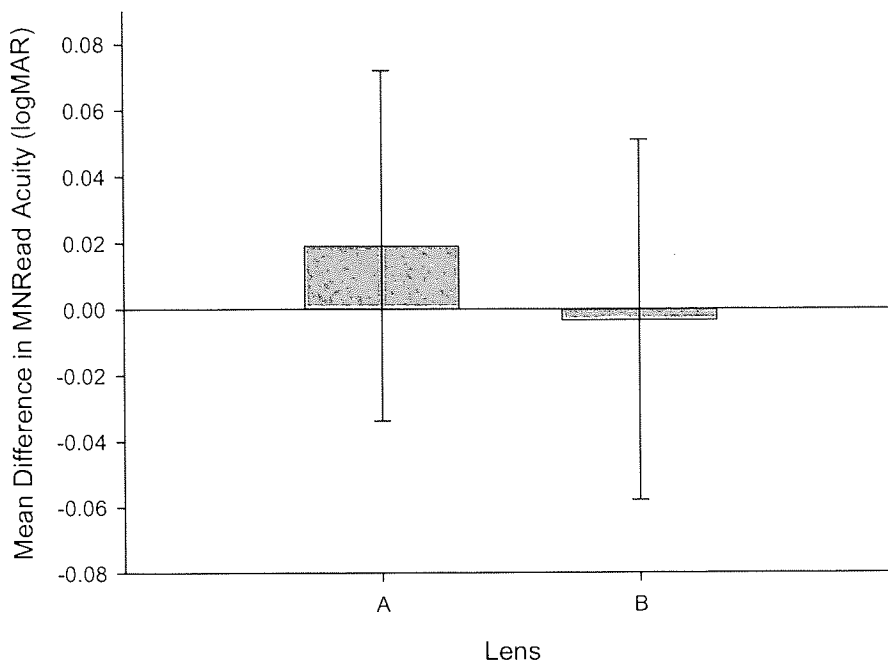


Figure 16b: Normalised data showing the mean difference in MNRead acuity between the Alcon AcrySof Natural (A) and the Bausch & Lomb UV+ (B) when compared to a clear lens. Error bars indicate \pm SD.

3.5.2 Critical Print Size (CPS)

Figure 17a details the differences in critical print size between the three lenses used. Mean CPS for lens A (\pm SD) was -0.03 ± 0.10 logMAR, for lens B it was -0.04 ± 0.09 logMAR, and for lens C, the clear lens, it was -0.02 ± 0.07 logMAR. The difference between these values was found to be below significance ($F_{(2,34)} = 0.749$; $p = 0.480$).

When normalised against the data for the clear lens, the mean difference for lens A was -0.01 ± 0.08 logMAR compared to -0.02 ± 0.08 logMAR for lens B. These results also fell below statistical significance ($t = 0.644$; $p = 0.528$; **Figure 17b**)

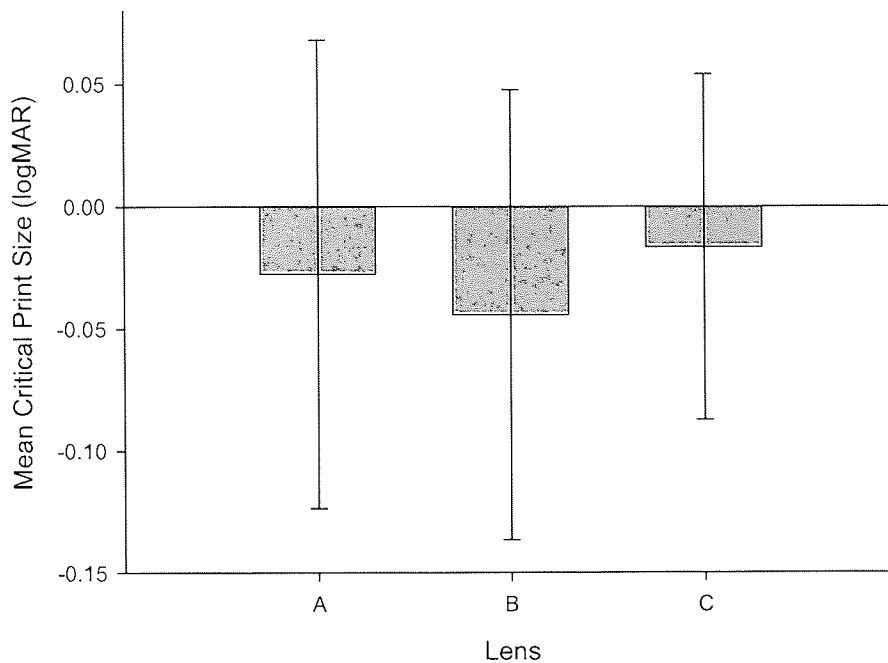


Figure 17a: Mean MNRead critical print size for the Alcon AcrySof Natural (A), Bausch & Lomb UV+ (B) and a clear lens (C). Error bars indicate \pm SD.

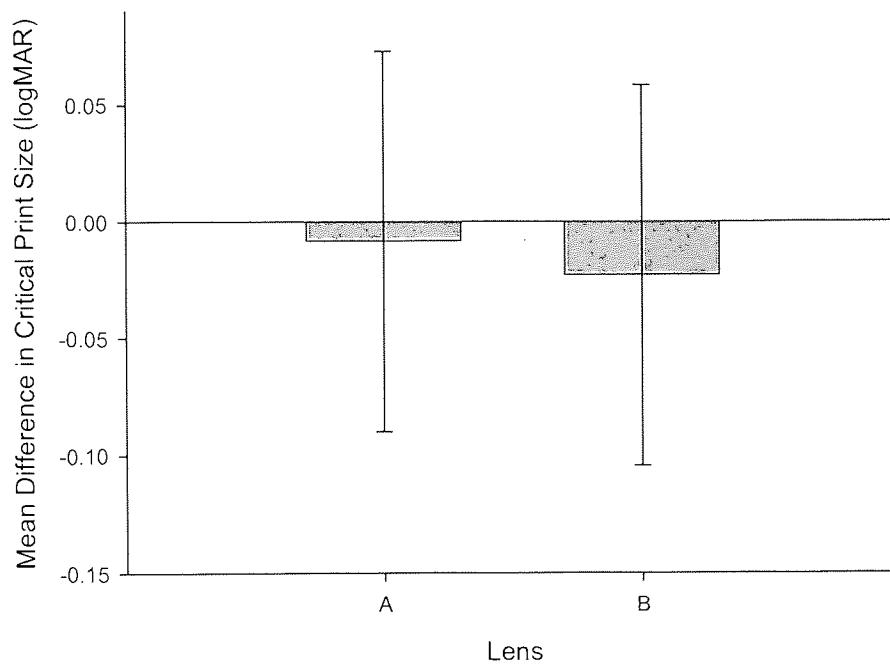


Figure 17b: Normalised data showing the mean difference in MNRead critical print size between the Alcon AcrySof Natural (A) and the B&L UV+ (B) compared to a clear lens. Error bars indicate \pm SD.

3.6 Scotopic Sensitivity

Of the three lenses tested, lens A (Alcon) had a slightly higher threshold for the light to be seen than any of the other lenses (B and C). The mean threshold (\pm SD) was 1.23 ± 0.18 for the Alcon lens, 1.19 ± 0.15 for the B&L lens, and 1.19 ± 0.11 for the clear lens. The results failed to reach a statistically significant level however ($F_{(2,34)} = 2.16$; $p = 0.120$).

When the results were normalised against the clear lens, the Alcon lens had a higher relative threshold of 0.05 ± 0.10 compared to the B&L value of 0.00 ± 0.08 . However, these results were not significant ($t = 1.76$; $p = 0.95$). All values are arbitrary and are shown graphically in figures 17a and 17b.

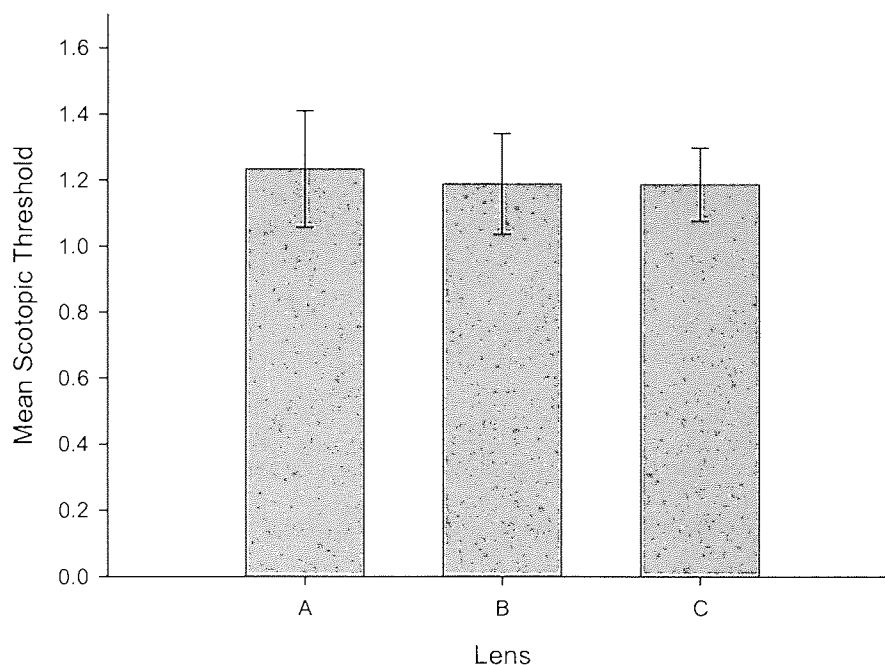


Figure 18a: Mean scotopic threshold for the Alcon AcrySof Natural (A), Bausch & Lomb UV+ (B) and a clear lens (C). Error bars indicate \pm SD.

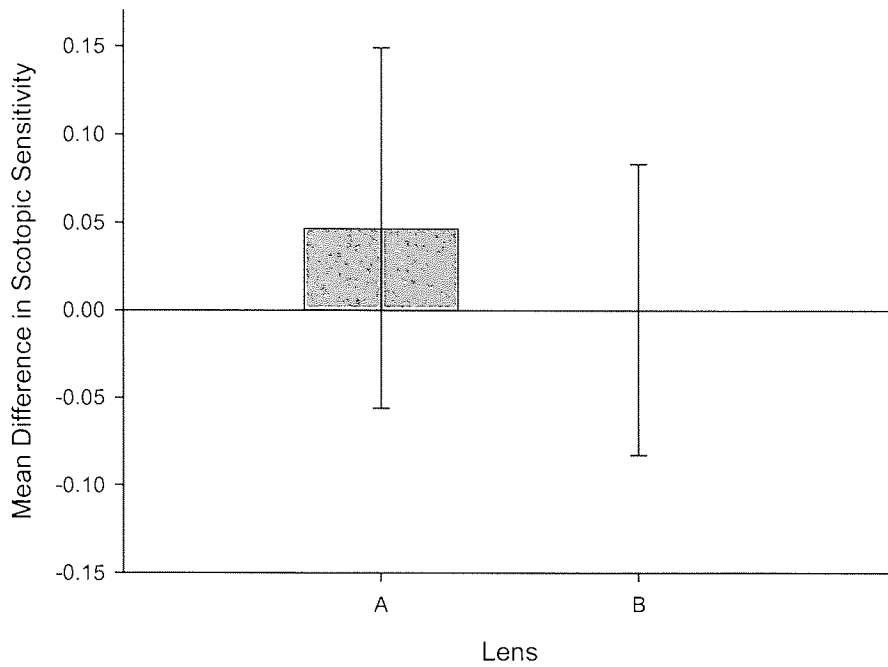


Figure 18b: Normalised data showing the mean difference in scotopic threshold between the Alcon AcrySof Natural (A) and the Bausch & Lomb UV+ (B) when compared to a clear lens. Error bars indicate \pm SD.

	Acrysof Natural	B&L UV+	Clear	F	p
Visual Acuity (logMAR)	-0.02	-0.04	-0.04	2.249	0.121
SD	0.09	0.09	0.08		
Contrast Sensitivity (logCS)	1.73	1.74	1.76	0.242	0.786
SD	0.11	0.13	0.11		
100 Hue Total Error	67.11	70.39	67.33	0.200	0.820
SD	45.74	45.09	40.75		
100 Hue Angle	54.45	50.09	55.99	1.874	0.169
SD	9.47	8.80	9.77		
100 Hue S Index	1.46	1.47	1.46	0.048	0.953
SD	0.16	0.16	0.20		
100 Hue C Index	1.50	1.57	1.53	0.825	0.447
SD	0.36	0.37	0.34		
SWAP MD (dB)	-2.08	-1.41	-1.26	4.418	0.020*
SD	1.22	1.21	1.44		
SWAP PSD (dB)	2.18	2.18	2.15	0.091	0.913
SD	0.26	0.40	0.22		
MNRead Acuity (logMAR)	-0.12	-0.14	-0.14	2.033	0.147
SD	0.09	0.09	0.07		
MNRead Critical Print Size (logMAR)	-0.03	-0.04	-0.02	0.749	0.480
SD	0.10	0.09	0.07		
Scotopic Sensitivity	1.23	1.19	1.19	2.16	0.120
SD	0.18	0.15	0.11		

Table 4: Table of mean results for all tests conducted. Standard deviations are shown below mean values.

* represents significance ($p < 0.05$).

	Acrysof Natural	B&L UV+	t	p
Visual Acuity (logMAR)	0.02	0.00	1.490	0.155
SD	0.04	0.04		
Contrast Sensitivity (logCS)	-0.02	-0.01	-0.387	0.704
SD	0.14	0.15		
100 Hue Total Error	0.03	2.71	-0.649	0.525
SD	24.10	21.62		
100 Hue Angle	-1.28	-4.92	1.418	0.174
SD	13.10	10.92		
100 Hue S Index	0.00	0.01	-0.413	0.685
SD	0.22	0.26		
100 Hue C Index	-0.03	0.03	-1.641	0.119
SD	0.20	0.26		
SWAP MD	-0.82	-0.15	-2.651	0.017*
SD	1.14	1.50		
SWAP PSD	0.03	0.03	-0.016	0.988
SD	0.27	0.33		
MNRead Acuity (logMAR)	0.02	0.00	1.965	0.066
SD	0.05	0.05		
MNRead Critical Print Size (logMAR)	-0.01	-0.02	0.644	0.528
SD	0.08	0.08		
Scotopic Sensitivity	0.05	0.00	1.76	0.95
SD	0.10	0.08		

Table 5: Table of normalised results indicating mean difference between the Alcon AcrySof Natural (A) and the Bausch & Lomb UV+ (B) when compared to a clear lens. Standard deviations are shown below mean values. * represents significance ($p < 0.05$).

4. Discussion

The results indicated that the two lenses were comparable to one another, and to the clear control lens. Visual acuity was not significantly affected in any of the three lenses tested. It was marginally lower for the Alcon tint, but this was not significant ($p = 0.121$). When comparing Alcon AcrySof (SN60AT) to the clear Alcon IOL (SA60AT), a great number of authors have also found no significant difference in VA (Marshall *et al.*, 2005; Raj *et al.*, 2005; Rodriguez-Galietero *et al.*, 2005a; 2005b; Cionni and Tsai, 2006).

Contrast sensitivity as performed with the Pelli-Robson chart was also found to be relatively unaffected by the choice of lens. The Alcon lens performed slightly better than the B&L lens and the clear lens respectively. This relationship was also found by other authors such as Yap (1984), Wolffsohn *et al.* (2000) and Yuan *et al.* (2004). It was disputed by Kelly *et al.* (1984). The results from this study were, however, below significance ($p = 0.786$).

The Farnsworth Munsell 100-Hue test showed that the colour discrimination of the observer was unaffected by the use of the tinted lenses. Of the two tinted lenses, the B&L tint did have a slightly higher total error. Interestingly, the Alcon lens had a slightly lower total error than the clear lens. Due to the difficult nature of the test, and the variability of the subjects' responses, none of the results reached statistical significance ($p = 0.820$). Rodriguez-Galietero *et al.* (2005a and 2005b), Cionni and Tsai (2006) and Vuori and Mantjarvi (2006) also compared the Alcon tinted IOL with a clear IOL and found no statistical difference in colour discrimination between the two lenses using the FM 100-hue test.

When the results were subjected to Vingrys' analysis, there was no significant difference in the *angle* (primary axis of colour confusion) between the lenses tested. According to Vingrys and King-Smith (1988), red-green colour defects tend to give horizontal axes with protans falling above the right horizontal (positive angles) and deutans below (negative angles); blue-yellow defects tend to give vertical angles. The authors also quote

normals with no error as having an angle of +62.0 (Table 3). The angles produced by the lenses were in the fifties, suggesting a near normal angle, with little difference between the angles ($p = 0.169$). When the clear lens was excluded, the UV+ was found to have a slightly more negative angle, perhaps suggesting a poorer colour discrimination, however, this also fell below significance ($p = 0.174$).

The *S Index* or 'scatter index' represents the selectivity or scatter in the cap arrangement. Random or non-polar arrangements (including normal arrangements) tend to have an S index in the region of 1.09-1.38. Polar arrangements of dichromatic observers have higher values (4.74-6.12; Vingrys and King-Smith, 1988). The mean S indices for the three lenses were between 1.46 and 1.47. This would suggest a mild deuteranomalous arrangement with an intermediate value of this index. There was little difference between the three lenses however ($p = 0.953$).

The final value derived from this analysis was the *C index* which can be used to estimate the severity of colour confusion and compare results obtained on different tests. The greater the C index, the greater the confusion. Vingrys & King-Smith (1988) suggest that a normal observer with no error would obtain a C index of 1.00 (Table 3) and an index greater than 1.77 would be classed as abnormal. The indices obtained were between 1.50 and 1.57; the Alcon lens having the lowest (1.50 ± 0.36) and the B&L the highest (1.57 ± 0.37). This would suggest a mild defect, but not outside of normal limits. There was no significant difference in the results however ($p = 0.447$). Interestingly, the clear lens had a C index between that of the two lenses (1.53 ± 0.37) which may suggest that any anomalies could be put down to subjective error as opposed to actual colour depreciation caused by the tint.

Short wavelength automated perimetry or 'blue-yellow perimetry' was performed for all lenses. Mean defect is average visual field loss and is 'normal' between zero and -2dB. The more negative the result obtained, the more visual field has been lost. The Alcon lens performed the worst out of all the lenses tested. It averaged -2.08 ± 1.22 dB, which would be classed as abnormal. The UV+ lens performed better (-1.41 ± 1.21 dB), but was still

more negative than the clear lens (-1.26 ± 1.44 dB); the latter two being within normal limits. I can conclude from these results, that the more heavily tinted Alcon AcrySof Natural tint blocks more shorter wavelength light than the B&L UV+ and the clear lens respectively. This is shown schematically in **Figure 4** in which the Natural tint has a lower initial cut off, whereas the UV+ has a higher cut off with a shorter progression to maximum transmittance. The Alcon lens has a transmittance of 50% at 450nm, whereas the B&L lens has a transmittance of 89.8% at 450nm; the blue stimulus of the perimeter is 440nm, so it would make sense that the Alcon lens should have a higher MD. These results were found to be statistically significant ($p = 0.020$).

There was no statistical difference between the lenses with regard to Pattern Standard Deviation (PSD) which is a measure of focal loss or variability within the field taking into account and generalised depression in the hill of vision. The PSD was slightly higher for the two tinted lenses compared to the clear lens (2.18 ± 0.26 dB AcrySof; 2.18 ± 0.40 dB B&L; 2.15 ± 0.22 dB clear) but all were just outside of the normal limits for PSD (zero to +2 dB) suggesting some areas of focal loss. There was no statistical difference between the three lenses ($p = 0.913$). Kara-Junior et al. (2006) used blue-yellow perimetry patients implanted with the Alcon AcrySof Natural (SN60AT) and a clear Alcon IOL (MA30AC). The authors determined the corrected pattern standard deviation (cPSD; difference between the patients' visual islands and a normal population's visual islands after adjusting for intra-test variability and short-term fluctuations). They found no statistically significant difference between both lenses, proving that glaucomatous differences can be detected even when the tinted lens is in situ. The authors concluded that the human crystalline lens accumulates yellow pigment as it ages and this naturally occurring yellowing partially blocks a portion of UV, violet, and blue radiation from reaching the retina. It does not, however, preclude accurate perimetry in detecting early glaucomatous changes, therefore the tinted lens should also not be problematic.

The MNRead test determines reading acuity and critical print size. The acuities for all three lenses were very good (mean = -0.12 to -0.14 logMAR). The Alcon lens performed very slightly worse (+0.02 mean logMAR) but there was no significant difference between the lenses ($p = 0.147$). Critical print size, the smallest print size at which patient's can read at their maximum reading speed, was also found to be very similar between the lenses, with mean values ranging from -0.02 logMAR for the clear lens, to -0.04 logMAR for the B&L tint ($p = 0.480$). All three lenses elicit a good level of reading ability, with little difference between the lenses.

Scotopic sensitivity proved to be slightly worse for the Alcon tint (1.23 ± 0.18) compared to the other tinted lens and the clear lens (1.19 ± 0.15 , 1.19 ± 0.11 respectively). However, this difference was not significant ($p = 0.120$), suggesting that both tinted lenses perform favourably with regard to scotopic light sensitivity.

5. Conclusion

From the experiment conducted, it can be concluded that there was little significant difference with regard to visual acuity, contrast sensitivity, colour discrimination or reading ability between the three tints used. There was, however, a significant difference with regard to SWAP/blue-yellow perimetry. The Alcon lens has a higher mean defect (i.e. blocks more blue light at 440 nm) compared to both the B&L and clear lenses. This relationship can be easily explained by examining the transmission spectra of both lenses and finding that the profile of the AcrySof Natural has a lower cut-off compared to the UV+ tint (Figure 4; p15). The question is, will this affect the visual function of the end-user?

There are two types of phototoxicity; blue-green ('Noell-type' or class 1) photic retinopathy and UV-blue ('Ham-type' or class 2) photic retinopathy (Ham *et al.*, 1980; Mainster, 1987; Margrain *et al.*, 2004). The first type of phototoxicity is mediated by rhodopsin which has a peak sensitivity around 500 nm. The blue-green hazard therefore reduces in the blue/violet part of the spectrum below this peak (Noell *et al.*, 1966; Noell, 1980). Mainster (2006) suggests that any spectral filter which reduces blue-green phototoxicity causes an equivalent decrease in scotopic sensitivity.

Violet (400-440 nm) and blue (440 – 500 nm) light compromise the shorter wavelength part of the visible spectrum (Mainster, 2005). UV-blue light hazard is well documented; its severity increases with decreasing wavelength. Lipofusin is one of the primary mediators of this phenomenon and shows a very similar trend (Margrain *et al.*, (2004); Rozanowska *et al.*, 1995). Studies have shown that protection of macular xanthophyll declines in the violet part of the spectrum (Werner *et al.*, 1987; Mainster, 1987). This is where the phototoxicity of cytochrome oxidase, porphyrin and A2E peak (Boulton *et al.*, 2001; Noell *et al.*, 1966).

There are three types of retinal photopigments: cone photoreceptor photopigments that provide photopic and mesopic vision (Stockman *et al.*, 2000), rhodopsin in rod

photoreceptors responsible for mesopic and scotopic vision (Griswold and Stark, 1992) and melanopsin in blue light sensitive retinal ganglion cells. The argument is, although a UV and visible light blocking IOL should potentially reduce the risk of UV-blue phototoxicity (Mainster 1978; 1986; 2005; Mainster and Sparrow 2003), it will also reduce the amount of light reaching the light sensitive retinal ganglions and the rod photoreceptors. Further work is required to determine how this will affect vision, especially under mesopic and photopic conditions.

6. Future Work

In order to test these tints further, the use of pseudophakic patients with UV blocking only IOLs (preferably all of the same design) should be advocated, to test the tints on the end-user, the pseudophakic patient. The inclusion of one or more advanced forms of dark adaptometry or scotopic sensitivity should also be advocated, to see if the relative loss of the blue-green end of the spectrum does affect scotopic vision in the Alcon AcrySof Natural tint.

To date, a study is being designed to include such criteria; this should be underway by the autumn of 2006.

The team at Aston University have enjoyed working with Bausch & Lomb and look forward to continuing collaboration.

Mr. G A Gibson

Dr. L N Davies

Dr. J S W Wolffsohn

7. References

- Aarnisalo, E. A. (1988). Effects of yellow filter glasses on the results of photopic and scotopic photometry. *Am J Ophthalmol.* **105**, 408-11.
- Abraham, F. A., Levartovsky, S., Blumenthal, M. (1988). Visual thresholds following posterior chamber lens implants. *Ophthalmic Res.* **20**, 117-120.
- Ahn, S. J., Legge, G. E. (1995). Psychophysics of reading--XIII. Predictors of magnifier-aided reading speed in low vision. *Vision Res.* **35**, 1931-8.
- Ball, K., Owsley, C., Stalvey, B., Roenker, D. L., Sloane, M. E., Graves, M. (1998). Driving avoidance and functional impairment in older drivers. *Accid Anal Prev.* **30**, 313-22.
- Beatty, S., Koh, H., Phil, M., Henson, D., Boulton, M. (2000). The role of oxidative stress in the pathogenesis of age-related macular degeneration. *Surv Ophthalmol.* **45**, 115-34.
- Ben-Shabat, S., Parish, C. A., Vollmer, H. R., Itagaki, Y., Fishkin, N., Nakanishi, K., Sparrow, J. R. (2002). Biosynthetic studies of A2E, a major fluorophore of retinal pigment epithelial lipofuscin. *J Biol Chem.* **277**, 7183-90.
- Bennett, L. W. (1994). Pseudophakic erythroptisia. *J Am Optom Assoc.* **65**, 273-6.
- Bergmanson, J. P., Sheldon, T. M. (1997). Ultraviolet radiation revisited. *CLAO J.* **23**, 196-204.
- Bernstein, P. S., Zhao, D. Y., Wintch, S. W., Ermakov, I. V., McClane, R. W., Gellermann, W. (2002). Resonance Raman measurement of macular carotenoids in normal subjects and in age-related macular degeneration patients. *Ophthalmology.* **109**, 1780-7.

- Bird, A. C., Bressler, N. M., Bressler, S. B., Chisholm, I. H., Coscas, G., Davis, M. D., de Jong, P. T., Klaver, C. C., Klein, B. E., Klein, R., et al. (1995). An international classification and grading system for age-related maculopathy and age-related macular degeneration. The International ARM Epidemiological Study Group. *Surv Ophthalmol.* **39**, 367-74.
- Blumenthal, E. Z., Sample, P. A., Berry, C. C., Lee, A. C., Girkin, C. A., Zangwill, L., Caprioli, J., and Weinreb, R. N. (2003). Evaluating several sources of variability for standard and SWAP visual fields in glaucoma patients, suspects, and normals. *Ophthalmology* **110**, 1895-1902.
- Boettner, E. A., Wolter, J. R. (1962). Transmission of the ocular media. *Invest. Ophthal. Vis. Sci.* **1**, 776-783.
- Borges, J., Li, Z. Y., Tso, M.O. (1990). Effects of repeated photic exposures on the monkey macula. *Arch Ophthalmol.* **108**, 727-33.
- Boulton, M., Rozanowska, M., Rozanowska, B. (2001). Retinal photodamage. *Photochem. Photobiol. B* **15**.
- Bowman, K. J., Cole, B. L. (1980). A recommendation for illumination of the Farnsworth-Munsell 100-hue test. *Am J Optom Physiol Opt.* **57**, 839-43.
- Brabyn, J. A., Schneck, M. E., Lott, L. A., Haegerstrom-Portnoy, G. (2005). Night driving self-restriction: vision function and gender differences. *Optom Vis Sci.* **2005** **82**, 755-64.
- Burke, A. (2001). Mechanisms of ageing. *Eye.* **15**, 371-5.
- Cionni, R. J., and Tsai, J. H. (2006). Color perception with AcrySof Natural and AcrySof single-piece intraocular lenses under photopic and mesopic conditions. *Journal of Cataract & Refractive Surgery* **32**, 236-242.

- Clarke, S. M., Doughty, M. J., Cullen, A. P. (1990). Acute effects of ultraviolet-B irradiation on the corneal surface of the pigmented rabbit studied by quantitative scanning electron microscopy. *Acta Ophthalmol (Copenh)* **68**, 639-650.
- Coile, D. C., Baker, H. D. (1992). Foveal dark adaptation, photopigment regeneration, and aging. *Vis Neurosci.* **8**, 27-39.
- Cristobal, J. A., Sierra, J., Martin, J., Rodriguez, N. A., Ascaso, J. (2005). [Intraocular lenses with blue light filter]. *Arch Soc Esp Oftalmol.* **80**, 245-49. Spanish.
- Cullen, A. P., Chou, B. R., Hall, M. G., Jany, S. E. (1984). Ultraviolet-B damages corneal endothelium. *Am J Optom Physiol Opt.* **61**, 473-478.
- Curcio, C. A. (2001). Photoreceptor topography in ageing and age-related maculopathy. *Eye.* **15**, 376-83.
- Curcio, C. A., Millican, C. L., Allen, K. A., Kalina, R. E. (1993). Aging of the human photoreceptor mosaic: evidence for selective vulnerability of rods in central retina. *Invest Ophthalmol Vis Sci.* **34**, 3278-96.
- Curcio, C. A., Owsley, C., Jackson, G. R. (2000). Spare the rods, save the cones in aging and age-related maculopathy. *Invest Ophthalmol Vis Sci.* **41**, 2015-8.
- Curcio, C. A., Sloan, K. R., Kalina, R. E., et al. (1990). Human photoreceptor topography. *J Comp Neurol.* **292**, 497-523.
- Darzins, P., Mitchell, P., Heller, R. F. (1997). Sun exposure and age-related macular degeneration. An Australian case-control study. *Ophthalmology.* **104**, 770-6.
- de Fez, M. D., Luque, M. J., Viqueira, V. (2002). Enhancement of contrast sensitivity and losses of chromatic discrimination with tinted lenses. *Optom Vis Sci* **79**, 590-7.
- Delcourt, C., Carriere, I., Ponton-Sanchez, A., et al. (2001). Light exposure and the risk of age-related macular degeneration: the Pathologies Oculaires Liees a l'Age (POLA) study. *Arch Ophthalmol.* **119**, 1463-8.

- Delmelle, N. (1978). Retinal sensitized photodynamic damage to liposomes. *Photochem Photobiol.* **28**, 357-60.
- Delori, F. C., Dorey, C. K., Staurenghi, G., Arend, O., Goger, D. G., Weiter, J. J. (1995). In vivo fluorescence of the ocular fundus exhibits retinal pigment epithelium lipofuscin characteristics. *Invest Ophthalmol Vis Sci.* **36**, 718-29.
- Dillon, J., Zheng, L., Merriam, J. C., and Gaillard, E. R. (2004). Transmission of light to the aging human retina: possible implications for age related macular degeneration. *Experimental Eye Research* **79**, 753-759.
- Domey, R. G., McFarland, R. A., Chadwick, E. (1960). Dark adaptation as a function of age and time. II. A derivation. *J Gerontol.* **15**, 267-79.
- Eldred, G. E., Lasky, M. R. (1993). Retinal age pigments generated by self-assembling lysosomotropic detergents. *Nature* **361**, 724-6.
- Ernest, P. H. (2004). Light-transmission-spectrum comparison of foldable intraocular lenses. *Journal of Cataract & Refractive Surgery* **30**, 1755-1758.
- Espindle, D., Crawford, B., Maxwell, A., Rajagopalan, K., Barnes, R., Harris, B., and Hileman, K. (2005). Quality-of-life improvements in cataract patients with bilateral blue light-filtering intraocular lenses: Clinical trial. *Journal of Cataract & Refractive Surgery* **31**, 1952-1959.
- Fowler, M. S., Mason, A. J., Stein, J. F. (1992). Binocular amblyopia improved by yellow spectacles. *Lancet.* **16; 339**, 1230.
- Freeman, E. E., Munoz, B., West, S. K., Tielsch, J. M., Schein, O. D. (2003). Is there an association between cataract surgery and age-related macular degeneration? Data from three population-based studies. *Am J Ophthalmol.* **135**, 849-56.
- Gaillard, E. R., Atherton, S. J., Eldred, G., Dillon, J. (1995). Photophysical studies on human retinal lipofuscin. *Photochem Photobiol.* **61**, 448-53.

- Gladstone, G. J., Tasman, W. (1978). Solar retinitis after minimal exposure. *Arch Ophthalmol.* **96**, 1368-9.
- Gorgels, T. G., van Norren, D. (1995). Ultraviolet and green light cause different types of damage in rat retina. *Invest Ophthalmol Vis Sci.* **36**, 851-63.
- Gottsch, J. D., Pou, S., Bynoe, L. A., Rosen, G. M. (1990). Hematogenous photosensitization. A mechanism for the development of age-related macular degeneration. *Invest Ophthalmol Vis Sci.* **31**, 1674-82.
- Green, W. R. (1999). Histopathology of age-related macular degeneration. *Mol Vis.* **5**, 27.
- Green, W. R., Enger, C. (1993). Age-related macular degeneration histopathologic studies. The 1992 Lorenz E. Zimmerman Lecture. *Ophthalmology.* **100**, 1519-35.
- Greenstein, V. C., Thomas, S. R., Blaustein, H., Koenig, K., Carr, R. E. (1993). Effects of early diabetic retinopathy on rod system sensitivity. *Optom Vis Sci* **70**, 18-23.
- Grimm, C., Wenzel, A., Williams, T., Rol, P., Hafezi, F., Reme, C. (2001). Rhodopsin-mediated blue-light damage to the rat retina: effect of photoreversal of bleaching. *Invest Ophthalmol Vis Sci.* **42**, 497-505.
- Griswold, M. S., Stark, W. S. (1992). Scotopic spectral sensitivity of phakic and aphakic observers extending into the near ultraviolet. *Vision Res.* **32**, 1739-43.
- Gurrey, R. K., Ham, W. T., Mueller, H. A. (1985). "Light toxicity in the posterior segment, in: Duane, T. D. (Ed.). Clinical Ophthalmology. Harper and Rowe, Philadelphia.."
- Ham, W. J., Mueller, HA, Sliney, DH. (1976). Retinal sensitivity to damage to short wavelength light. *Nature* **260**, 153-5.
- Ham, W. T. J., Ruffolo, J. J. Jr, Mueller H. A., *et al* (1980). The nature of retinal radiation damage: dependence on wavelegh, power level and exposure time. *Vis. Res.* **20**, 1105-11.

- Hammer, H. M., Yap, M., Weatherill, J. R. (1986). Visual performance in pseudophakia with standard and ultraviolet-absorbing intraocular lenses: a preliminary report. *Trans Ophthalmol Soc U K.* **105**, 441-6.
- Hawkins, S., Bird, A., Klein, R., West, S. (1999). Epidemiology of age-related macular degeneration. *Mol. Vis* **5**, 26.
- Hayashi, K., Hayashi, H. (2006). Visual function in patients with yellow tinted intraocular lenses compared with vision in patients with non-tinted intraocular lenses. *Br J Ophthalmol.* **2006** **90**, 1019-23.
- Hecht, S., Hendley, C. D., Ross, S., Richmond, P. N. (1948). The effect of exposure to sunlight on night vision. *Am J Ophthalmol.*
- Hickson-Curran S. B., Nason R. J., Becherer P. D., Davis R. A., Pfeifer J , and J., S. M. (1997). Clinical evaluation of Acuvue contact lenses with UV blocking characteristics. *Optom Vis Sci* **74**, 632-8.
- Hiller, R., Giacometti, L., Yuen, K. (1977). Sunlight and cataract: an epidemiologic investigation. *Am J Epidemiol.* **105**, 450-9.
- Hirvela, H., Luukinen, H., Laara, E., Sc, L., Laatikainen, L. (1996). Risk factors of age-related maculopathy in a population 70 years of age or older. *Ophthalmology.* **103**, 871-7.
- Holz, F. G., Bellman, C., Staudt, S., Schutt, F., Volcker, H. E. (2001). Fundus autofluorescence and development of geographic atrophy in age-related macular degeneration. *Invest Ophthalmol Vis Sci.* **42**, 1051-6.
- Holz, F. G., Schutt, F., Kopitz, J., Eldred, G. E., Kruse, F. E., Volcker, H. E., Cantz, M. (1999). Inhibition of lysosomal degradative functions in RPE cells by a retinoid component of lipofuscin. *Invest Ophthalmol Vis Sci.* **40**, 737-43.
- Ishida, M., Yanashima, K., Miwa, M., Hozumi, S., Okisaka, S. (1994). [Influence of the yellow-tinted intraocular lens on spectral sensitivity]. *Nippon Ganka Gakkai Zasshi.* **98**, 192-6. Japanese.

- Ivers, R. Q., Cumming, R. G., Mitchell, P., Attebo, K. (1998). Visual impairment and falls in older adults: the Blue Mountains Eye Study. *J Am Geriatr Soc.* **46**, 58-64.
- Jackson, G. R., Owsley, C. (2000). Scotopic sensitivity during adulthood. *Vision Res.* **40**, 2467-73.
- Jackson, G. R., Owsley, C., Curcio, C. A. (2002). Photoreceptor degeneration and dysfunction in aging and age-related maculopathy. *Ageing Res Rev.* **1**, 381-96.
- Jackson, G. R., Owsley, C., McGwin, G. (1999). Aging and dark adaptation. *Vis. Res.* **39**.
- Kamel, I. D., Parker, J. A. (1973). Protection from ultraviolet exposure in aphakic erythroptosis. *Can J Ophthalmol.* **8**, 563-5.
- Kara-Junior, N., Jardim, J. L., de Oliveira Leme, E., Dall'Col, M., and Junior, R. S. (2006). Effect of the AcrySof Natural intraocular lens on blue-yellow perimetry. *Journal of Cataract & Refractive Surgery* **32**, 1328-1330.
- Katoh, N., Jonasson, F., Sasaki, H., Kojima, M., Ono, M., Takahashi, N., Sasaki, K; Reykjavik Eye Study Group. (2001). Cortical lens opacification in Iceland. Risk factor analysis -- Reykjavik Eye Study. *Acta Ophthalmol Scand.* **79**, 154-9.
- Kelly, S. A. (1990). Effect of yellow-tinted lenses on brightness. *J Opt Soc Am A.* **7**, 1905-11.
- Kelly, S. A., Goldberg, S. E., Banton, T. A. (1984). Effect of yellow-tinted lenses on contrast sensitivity. *Am J Optom Physiol Opt.* **61**, 657-62.
- Keunen, J. E., van Norren, D., van Meel, G. J. (1987). Density of foveal cone pigments at older age. *Invest Ophthalmol Vis Sci.* **28**, 985-91.
- Kinnear, P. R., Sahraie, A. (2002). New Farnsworth-Munsell 100 hue test norms of normal observers for each year of age 5-22 and for age decades 30-70. *Br J Ophthalmol.* **86**, 1408-11.

- Kinney, J. A., Schlichting, C. L., Neri, D. F., Kindness, S. W. (1983). Reaction time to spatial frequencies using yellow and luminance-matched neutral goggles. *Am J Optom Physiol Opt.* **60**, 132-8.
- Klein, B. E., Klein, R., Linton, K. L. (1992). Prevalence of age-related lens opacities in a population. The Beaver Dam Eye Study. *Ophthalmology.* **99**, 546-52.
- Klein, R., Klein, B. E., Cruickshanks, K. J., (1999). The prevalence of age-related maculopathy by geographic region and ethnicity. *Prog Retin Eye Res* **18**.
- Klein, R., Klein, B. E., Moss, S. E. (1995). Age-related eye disease and survival. The Beaver Dam Eye Study. *Arch Ophthalmol.* **113**, 333-9.
- Klein, R., Klein, B. E., Wong, T. Y., Tomany, S. C., Cruickshanks, K. J. (2002). The association of cataract and cataract surgery with the long-term incidence of age-related maculopathy: the Beaver Dam eye study. *Arch Ophthalmol.* **120**, 1551-8.
- Kline, D. W. (1991). "Light, ageing and visual performance. In: *The Susceptible Visual Apparatus*," Macmillan Press, London, England.
- Kremers, J. J., van Norren, D. (1989). Retinal damage in macaque after white light exposures lasting ten minutes to twelve hours. *Invest Ophthalmol Vis Sci.* **30**, 1032-40.
- Kuyk, T. K., Thomas, S. R. (1990). Effect of short wavelength absorbing filters on Farnsworth-Munsell 100 Hue test and hue identification task performance. *Optom Vis Sci* **67**, 522-31.
- Lamb, L. E., Zareba, M., Plakoudas, S. N., Sarna, T., and Simon, J. D. (2001). Retinyl Palmitate and the Blue-Light-Induced Phototoxicity of Human Ocular Lipofuscin. *Archives of Biochemistry and Biophysics* **393**, 316-320.
- Lawwill, T. (1982). Three major pathologic processes caused by light in the primate retina: a search for mechanisms. *Trans Am Ophthalmol Soc.* **80**, 517-79.

- Legge, G. E., Ross, J. A., Luebker, A., LaMay, J. M. (1989). Psychophysics of reading. VIII. The Minnesota Low-Vision Reading Test. *Optom Vis Sci* **66**, 843-53.
- Leibovitch, I., Lai, T., Porter, N., Pietris, G., Newland, H., Selva, D. (2006). Visual outcomes with the yellow intraocular lens. *Acta Ophthalmol Scand.* **84**, 95-9.
- Lerman, S., Borkman, R. (1976). Spectroscopic evaluation of classification of the normal, aging and cataractous lens. *Ophthalmic Res.* **8**, 335-53.
- Lindstrom, R., Doddi, N. (1986). Ultraviolet light absorption in intraocular lenses. *J Cataract Refract Surg.* **12**, 285-9.
- Liu, I. Y., White, L., LaCroix, A. Z. (1989). The association of age-related macular degeneration and lens opacities in the aged. *Am J Public Health.* **79**, 765-9.
- Lord, S. R., Dayhew, J. (2001). Visual risk factors for falls in older people. *J Am Geriatr Soc.* **49**, 508-15.
- Mainster, M. A. (1978). Solar retinitis, photic maculopathy and the pseudophakic eye. *J Am Intraocul Implant Soc.* **4**, 84-6.
- Mainster, M. A. (1986). The spectra, classification, and rationale of ultraviolet-protective intraocular lenses. *Am J Ophthalmol.* **15**, 727-32.
- Mainster, M. A. (1987). Light and macular degeneration: a biophysical and clinical perspective. *Eye.* **1**, 304-10.
- Mainster, M. A. (2005). Intraocular lenses should block UV radiation and violet but not blue light. *Arch Ophthalmol.* **123**, 550-5.
- Mainster, M. A. (2006). Blue-blocking intraocular lenses and pseudophakic scotopic sensitivity. *J Cataract Refract Surg.* **32**, 1403-4.
- Mainster, M. A., Sparrow, J. R. (2003). How much blue light should an IOL transmit? *Br J Ophthalmol.* **87**, 1523-9.

- Mainster, M. A., Turner, P. L. (2001). "Photic retinal injury and safety," 3rd/Ed. Mosby Inc., St. Louis.
- Makous, W. (2004). "Scotopic vision. In: Chalupa, L. M., Werner, J. S., eds. The visual neurosciences. Cambridge, MA: The MIT Press."
- Mandel, Y., Belkin, M., Polat, U. (2004). Fast adaptation of foveal scotopic contrast sensitivity and effect of aging [ARVO abstract 5459]. *Invest Ophthalmol Vis Sci.* **45**.
- Mansfield, J. S., Ahn, S. J., Legge, G. E., and Luebker, A. (1993). A new reading-acuity chart for normal and low vision. . *Ophthalmic and Visual Optics/Noninvasive Assessment of the Visual System Technical Digest* **3**.
- Mansfield, J. S., Legge, G. E., Bane, M. C. (1996). Psychophysics of reading. XV: Font effects in normal and low vision. *Invest Ophthalmol Vis Sci.* **37**, 1492-501.
- Margrain, T. H., Boulton, M., Marshall, J., and Sliney, D. H. (2005). Do blue light filters confer protection against age-related macular degeneration? *American Journal of Ophthalmology* **139**, 398-398.
- Margrain, T. H., Boulton, M., Marshall, J., et al. (2004). Do blue light filters confer protection against age-related macular degeneration? *Prog Retin Eye Res* **23**, 523-31.
- Marshall, J. (1987). The ageing retina: physiology or pathology. *Eye.* **1**, 282-95.
- Marshall, J., Cionni, R. J., Davison, J., Ernest, P., Lehmann, R., Maxwell, W. A., and Solomon, K. (2005). Clinical results of the blue-light filtering AcrySof Natural foldable acrylic intraocular lens. *Journal of Cataract & Refractive Surgery* **31**, 2319-2323.
- Mayer, S., Wirbelauer, C., Pham, D. T. (2006). [Functional results after intraocular lens implantation with or without blue light filter: an intraindividual comparison]. *Klin Monatsbl Augenheilkd.* **223**, 142-6. German.

- McCarty, C. A., Mukesh, B. N., Fu, C. L., Mitchell, P., Wang, J. J., Taylor, H. R. (2001). Risk factors for age-related maculopathy: the Visual Impairment Project. *Arch Ophthalmol.* **119**, 1455-62.
- McMurdo, M. E., Gaskell, A. (1991). Dark adaptation and falls in the elderly. *Gerontology.* **37**, 221-4.
- Mellerio, J. (1987). Yellowing of the human lens: nuclear and cortical contributions. *Vis. Res.* **27**, 1581-7.
- Mellerio, J. (1994). Light effects on the retina. In: Albert DM, Jakobiec FA, eds. *Principles and practice of ophthalmology. Vol 1. Philadelphia: WB Saunders.*, 1326-45.
- Miyake, K., Ichihashi, S., Shibuya, Y., Ota, I., Miyake, S., Terasaki, H. (1999). Blood-retinal barrier and autofluorescence of the posterior polar retina in long-standing pseudophakia. *J Cataract Refract Surg.* **25**, 891-7.
- Montes-Mico, R., and Alio, J. L. (2003). Distance and near contrast sensitivity function after multifocal intraocular lens implantation. *Journal of Cataract & Refractive Surgery* **29**, 703-711.
- Montes-Mico, R., Alio, J. L., and Munoz, G. (2003). Contrast sensitivity and spatial-frequency spectrum after refractive surgery. *Journal of Cataract & Refractive Surgery* **29**, 1650-1651.
- Montes-Mico, R., Espana, E., Bueno, I., Charman, W. N., Menezo, J. L. (2004). Visual performance with multifocal intraocular lenses: mesopic contrast sensitivity under distance and near conditions. *Ophthalmology* **111**, 85-96.
- Montes-Mico, R., and Neil Charman, W. (2001). Intraocular pressure after excimer laser myopic refractive surgery. *Ophthalmic and Physiological Optics* **21**, 228-235.
- Naarendorp, F., Denny, N., Frumkes, T. E. (1988). Rod light and dark adaptation influence cone-mediated spatial acuity. *Vision Res.* **28**, 67-74.

- Niwa, K., Yoshino, Y., Okuyama, F., Tokoro, T. (1996). Effects of tinted intraocular lens on contrast sensitivity. *Ophthalmic Physiol Opt.* **16**, 297-302.
- Noell, W. K. (1980). Possible mechanisms of photoreceptor damage by light in mammalian eyes. *Vision Res.* **20**, 1163-71.
- Noell, W. K., Walker, V. S., Kang, B. S., Berman, S. (1966). Retinal damage by light in rats. *Ophthalmology.* **5**, 450-73.
- Olson, M. D., and Miller, K. M. (2006). Implanting a Clear Intraocular Lens in One Eye and a Yellow Lens in the Other Eye: A Case Series. *American Journal of Ophthalmology* **141**, 957-958.
- Owsley, C., Jackson, G. R., Cideciyan, A. V., et al. (2000). Psychophysical evidence for rod vulnerability in age-related macular degeneration. *Invest Ophthalmol Vis Sci.* **41**, 267-73.
- Owsley, C., Jackson, G. R., White, M., Feist, R., Edwards, D. (2001). Delays in rod-mediated dark adaptation in early age-related maculopathy. *Ophthalmology.* **108**, 1196-202.
- Owsley, C., McGwin, G. Jr. (1999). Vision impairment and driving. *Surv Ophthalmol.* **43**, 535-550.
- Parish, C. A., Hashimoto, M., Nakanishi, K., Dillon, J., Sparrow, J. (1998). Isolation and one-step preparation of A2E and iso-A2E, fluorophores from human retinal pigment epithelium. *Proc Natl Acad Sci U S A* **95**, 14609-13.
- Pautler, E. L., Morita, M., Beezley, D. (1990). Hemoprotein(s) mediate blue light damage in the retinal pigment epithelium. *Photochem Photobiol.* **51**, 599-605.
- Pease, P. L., Adams, A. J., Nuccio, E. (1987). Optical density of human macular pigment. *Vision Res.* **27**, 705-10.

- Pitts, D. G., Cullen, A. P., Hacker, P. D. (1977). Ocular effects of ultraviolet radiation from 295 to 365 nm. *Invest. Ophthalmol. Vis. Sci.* **16**, 932-9.
- Plantner, J. J., Barbour, H. L., Kean, E. L. (1988). The rhodopsin content of the human eye. *Curr Eye Res.* **7**, 1125-9.
- Pollack, A., Marcovich, A., Bukelman, A., Oliver, M. (1996). Age-related macular degeneration after extracapsular cataract extraction with intraocular lens implantation. *Ophthalmology.* **103**, 1546-54.
- Pulos, E. (1989). Changes in rod sensitivity through adulthood. *Invest Ophthalmol Vis Sci.* **30** 1738-42.
- Ragauskaite, L., Heckathorn, R. C., Gaillard, E. R. (2001). Environmental effects on the photochemistry of A2-E, a component of human retinal lipofuscin. *Photochem Photobiol.* **74**, 483-8.
- Raj, S. M., Vasavada, A. R., and Nanavaty, M. A. (2005). AcrySof Natural SN60AT versus AcrySof SA60AT intraocular lens in patients with color vision defects. *Journal of Cataract & Refractive Surgery* **31**, 2324-2328.
- Reszka, K., Eldred, G. E., Wang, R. H., Chignell, C., Dillon, J. (1995). The photochemistry of human retinal lipofuscin as studied by EPR. *Photochem Photobiol.* **62**, 1005-8.
- Rodriguez-Galitero, A., Montes-Mico, R., Munoz, G., and Albarran-Diego, C. (2005a). Blue-light filtering intraocular lens in patients with diabetes: Contrast sensitivity and chromatic discrimination. *Journal of Cataract & Refractive Surgery* **31**, 2088-2092.
- Rodriguez-Galitero, A., Montes-Mico, R., Munoz, G., and Albarran-Diego, C. (2005b). Comparison of contrast sensitivity and color discrimination after clear and yellow intraocular lens implantation. *Journal of Cataract & Refractive Surgery* **31**, 1736-1740.

- Rozanowska, M., Jarvis-Evans, J., Korytowski, W., Boulton, M. E., Burke, J. M., Sarna, T. (1995). Blue light-induced reactivity of retinal age pigment. In vitro generation of oxygen-reactive species. *J Biol Chem.* **270**, 18825-30.
- Rushton, W. A. H. (1972). Visual pigments in man. In: Dartnall, H. J. A., ed. *Photochemistry of vision Vol VII/1*, Berlin: Springer-Verlag, 364-94.
- Sakai, N., Decatur, J., Nakanishi, K., Eldred, G. E. (1996). Ocular age pigment A2-E an unprecedented pyridinium bis-retinoid. *J Am Chem Soc.* **118**, 1559-1560.
- Sample, P. A., Johnson, C. A., Haegerstrom-Portnoy, G., Adams, A. J. (1996). Optimum parameters for short-wavelength automated perimetry. *J Glaucoma.* **5**, 375-83.
- Scheffrin, B. E., Tregear, S. J., Harvey, L. O. Jr, Werner, J. S. (1999). Senescent changes in scotopic contrast sensitivity. *Vision Res.* **39**, 3728-36.
- Schutt, F., Davies, S., Kopitz, J., Holz, F. G., Boulton, M. E. (2000). Photodamage to human RPE cells by A2-E, a retinoid component of lipofuscin. *Invest Ophthalmol Vis Sci.* **41**, 2303-8.
- Schwiegerling, J. (2006). Blue-light-absorbing lenses and their effect on scotopic vision. *Journal of Cataract & Refractive Surgery* **32**, 141-144.
- Shamsi, F. A., Boulton, M. (2001). Inhibition of RPE lysosomal and antioxidant activity by the age pigment lipofuscin. *Invest Ophthalmol Vis Sci.* **42**, 3041-6.
- Shapiro, S. S., Wilk, M. B. (1965). Analysis of variance test for normality (complete samples). *Biometrika* **52**, 591-611.
- Sliney, D. (2001). Photoprotection of the eye - UV radiation and sunglasses. *Photochem. Photobiol. B* **64**, 166-75.
- Sparrow, J. R., Boulton, M. (2005). RPE lipofuscin and its role in retinal pathobiology. *Exp Eye Research* **80**, 595-606.

- Sparrow, J. R., Miller, A. S., and Zhou, J. (2004). Blue light-absorbing intraocular lens and retinal pigment epithelium protection in vitro. *Journal of Cataract & Refractive Surgery* **30**, 873-878.
- Sparrow, J. R., Nakanishi, K., Parish, C. A. (2000). The lipofuscin fluorophore A2E mediates blue light-induced damage to retinal pigmented epithelial cells. *Invest Ophthalmol Vis Sci.* **41**, 1981-9.
- Sparrow, J. R., Zhou, J., Ben-Shabat, S., Vollmer, H., Itagaki, Y., Nakanishi, K. (2002). Involvement of oxidative mechanisms in blue-light-induced damage to A2E-laden RPE. *Invest Ophthalmol Vis Sci.* **43**, 1222-7.
- Sparrow, J. R., Zhou, J., Cai, B. (2003). DNA is a target of the photodynamic effects elicited in A2E-laden RPE by blue-light illumination. *Invest Ophthalmol Vis Sci.* **44**, 2245-51.
- Sperduto, R. D., Hiller, R., Seigel, D. (1981). Lens opacities and senile maculopathy. *Arch Ophthalmol.* **99**, 1004-8.
- Stager, J. D. R., Weakley, J. D. R., Wang, X., Feliuss, J., and Beauchamp, C. L. (2006). AcrySof "Natural" Intraocular Lens Implantation in Children. *Journal of American Association for Pediatric Ophthalmology and Strabismus* **10**, 68-68.
- Stockman, A., Sharpe, L. T., Merbs, S., Nathans, J. (2000). Spectral sensitivities of human cone visual pigments determined in vivo and in vitro. *Methods Enzymol.* **316**, 626-50.
- Sturr, J. F., Zhang, L., Taub, H. A., Hannon, D. J., Jackowski, M. M. (1997). Psychophysical evidence for losses in rod sensitivity in the aging visual system. *Vision Res.* **37**, 475-81.
- Taylor, H. (1995). Ocular effects of UV-B exposure. *Doc Ophthalmol.* **88**, 285-93.

- Taylor, H. R., Munoz, B., West, S., Bressler, N. M., Bressler, S. B., Rosenthal, F. S. (1990). Visible light and risk of age-related macular degeneration. *Trans Am Ophthalmol Soc.* **88**, 163-73; discussion 173-8.
- Taylor, H. R., West, S., Munoz, B., Rosenthal, F. S., Bressler, S. B., Bressler, N. M. (1992). The long-term effects of visible light on the eye. *Arch Ophthalmol.* **110**, 99-104.
- The Eye Disease Case-Control Study Group (1992). Risk factors for neovascular age-related macular degeneration. *Arch Ophthalmol.* **110**, 1701-8.
- Thomas, S. R., Kuyk, T. K. (1988). D-15 performance with short wavelength absorbing filters in normals. *Am J Optom Physiol Opt.* **65**, 697-702.
- Tognetto, D., Toto, L., Sanguinetti, G., Cecchini, P., Vattovani, O., Filacorda, S., and Ravalico, G. (2003). Lens epithelial cell reaction after implantation of different intraocular lens materials: Two-year results of a randomized prospective trial. *Ophthalmology* **110**, 1935-1941.
- Tomany, S. C., Cruickshanks, K. J., Klein, R, et al. (2004). Sunlight and the 10-year incidence of age-related maculopathy: the Beaver Dam Eye Study. *Arch Ophthalmol.* **122**, 750-7.
- Van Gelder, R. N. (2004). Blue light and the circadian clock. *Br J Ophthalmol* **88**, 1353.
- van Leeuwen, R., Ikram, M. K., Vingerling, J. R., Witteman, J. C., Hofman, A., de Jong, P. T. (2003). Blood pressure, atherosclerosis, and the incidence of age-related maculopathy: the Rotterdam Study. *Invest Ophthalmol Vis Sci.* **44**, 3771-7.
- van Norren, D., Vos, H. (1990). Sunlight and age-related macular degeneration. *Arch Ophthalmol.* **108**, 1670-1.
- Vingrys, A. J., King-Smith, P. E. (1988). A quantitative scoring technique for panel tests of color vision. *Invest Ophthalmol Vis Sci.* **29**, 50-63.

- Vos, J. J. (1984). Disability glare—a state of the art report. . *Commission Internationale de l'Eclairage Journal* **3**, 39-53.
- Vos, J. J. (1995). Age dependence of glare effects and their significance in terms of visual ergonomics. . In: *Adrian, W., ed. Lighting for aging vision and health. New York: Lighting Research Institute, Inc.*, 11-25.
- Wang, J. J., Klein, R., Smith, W., Klein, B. E., Tomany, S., Mitchell, P. (2003). Cataract surgery and the 5-year incidence of late-stage age-related maculopathy: pooled findings from the Beaver Dam and Blue Mountains eye studies. *Ophthalmology*. **110**, 1960-7.
- Wassel, J., Davies, S., Bardsley, W., Boulton, B. (1999). The photoreactivity of the retinal age pigment lipofuscin. *J. Biol. Chem.* **274**.
- Weale, R. A. (1982). The age variation of "senile" cataract in various parts of the world. *Br J Ophthalmol* **66**, 31-4.
- Wee, R., Van Gelder, R. N. (2004). Sleep disturbances in young subjects with visual dysfunction. *Ophthalmology*. **111**, 297-302.
- Weiter, J. J., Delori, F. C., Wing, G. L., Fitch, K. A. (1986). Retinal pigment epithelial lipofuscin and melanin and choroidal melanin in human eyes. *Invest Ophthalmol Vis Sci*. **27**, 145-52.
- Werner, J. S. (2005). Night vision in the elderly: consequences for seeing through a "blue filtering" intraocular lens. *Br. J. Ophthalmol.* **89**, 1518-21.
- Werner, J. S., Donnelly, S. K., Kliegl, R. (1987). Aging and human macular pigment density. Appended with translations from the work of Max Schultze and Ewald Hering. *Vision Res.* **27**, 257-68.
- Werner, J. S., Spillmann, L. (1989a). UV-absorbing intraocular lenses: safety, efficacy, and consequences for the cataract patient. *Graefes Arch Clin Exp Ophthalmol.* **227**, 227-56.

- Werner, J. S., Steele, V. G., Pfoff, D. S. (1989b). Loss of human photoreceptor sensitivity associated with chronic exposure to ultraviolet radiation. *Ophthalmology*. **96**, 1552-8.
- West, S. (1999). Ocular ultraviolet B exposure and lens opacities: a review. *J Epidemiol*. **9**, S97-101.
- Wing, G. L., Blanchard, G. C., Weiter, J. J. (1978). The topography and age relationship of lipofuscin concentration in the retinal pigment epithelium. *Invest Ophthalmol Vis Sci*. **17**, 601-7.
- Wolf, E. (1946). Effects of exposure to ultra-violet light on human dark adaptation. *Proc Natl Acad Sci U S A* **32**, 219-26.
- Wolf, E. (1960). Glare and age. *Arch Ophthalmol*. **64**, 502-14.
- Wolffsohn, J. S., Cochrane, A. L., Khoo, H., Yoshimitsu, Y., Wu, S. (2000). Contrast is enhanced by yellow lenses because of selective reduction of short-wavelength light. *Optom Vis Sci* **77**, 73-81.
- Wolffsohn, J. S., Dinardo, C., Vingrys, A. J. (2002). Benefit of coloured lenses for age-related macular degeneration. *Ophthalmic and Physiological Optics* **22**, 300-311.
- Wyszecki, G., Stiles, W. S. (1982). "Color Science," 2nd/Ed. John Wiley & Sons, New York.
- Yap, M. (1984). The effect of a yellow filter on contrast sensitivity. *Ophthalmic Physiol Opt*. **4**, 227-32.
- Yuan, Z., Reinach, P., Yuan, J. (2004). Contrast sensitivity and color vision with a yellow intraocular len. *Am J Ophthalmol*. **138**, 138-40.
- Zigman, S. (1992). Light filters to improve vision.. *Optom Vis Sci* **69**, 325-8.

SUPPORTING PUBLICATIONS

The following documents are copies of supporting publications.



Development of a near activity visual questionnaire to assess accommodating intraocular lenses[☆]

Navneet Gupta^a, James S Wolffsohn^a, Shehzad A. Naroo^{a,*}, Leon N. Davies^a,
George A. Gibson^a, Sunil Shah^b

^a Ophthalmic Research Group, School of Life and Health Sciences, Aston University, Birmingham, B4 7ET, UK
^b Midland Eye Institute, 50 Lode Lane, Solihull B91 2AW, UK



Content has been removed for copyright reasons

includes attributes such as intelligence, depression and social functioning. It cannot be measured by a mechanical

human sensations are measured by various stimuli. The measurement of latent traits however replaces stimuli with questions forming the field of psychometrics [2].



Content has been removed due to copyright restrictions

Corresponding author. Tel.: +44 (0)121 359 3211.
E-mail address: s.a.naroo@aston.ac.uk (S.A. Naroo).

commonest example of this, surgical techniques including

Clinical Evaluation of the Nidek ARK-530A Auto Refractor/Keratometer

George A Gibson BSc, MCOptom and Leon N Davies PhD, MCOptom, FAAO

Aim



Aston University

Content has been removed for copyright reasons



Aston University

Content has been removed for copyright reasons

used to increase alignment and observation.

The ARK 530A has a measurement range between -30 and +25 D; it can also measure pupils as small as 2 mm in diameter, allowing wider application, particularly in an elderly population. The characteristics of the Nidek ARK-530A are summarised in Table 1.

and keratometry with the Nidek ARK-530A autorefractor/keratometer on all subjects. Subjective refraction and manual keratometry was performed prior to autorefraction/keratometry, which allowed the optometrist to be masked from the objective results, thus avoiding any operator bias. Subjects were asked to view the image inside the